



*The Proceedings*  
OF  
THE INSTITUTION OF  
ELECTRICAL ENGINEERS

FOUNDED 1871; INCORPORATED BY ROYAL CHARTER 1921

PART B  
ELECTRONIC AND COMMUNICATION ENGINEERING  
(INCLUDING RADIO ENGINEERING)

*Price Ten Shillings and Sixpence*



# THE INSTITUTION OF ELECTRICAL ENGINEERS

FOUNDED 1871 INCORPORATED BY ROYAL CHARTER 1921

PATRON: HER MAJESTY THE QUEEN

## COUNCIL 1961-1962

### President

G. S. C. LUCAS, O.B.E., F.C.G.I.

### Past-Presidents

W. H. ECCLES, D.Sc., F.R.S.  
THE RT. HON. THE EARL OF MOUNT  
EDGUMBE, T.D.  
J. M. DONALDSON, M.C.  
PROF. E. W. MARCHANT, D.Sc.  
H. T. YOUNG.  
SIR GEORGE LEE, O.B.E., M.C.  
J. R. BEARD, C.B.E., M.Sc.

SIR NOEL ASHBRIDGE, B.Sc.(Eng.).  
SIR HARRY RAILING, D.Eng.  
P. DUNSHEATH, C.B.E., M.A., D.Sc.  
(Eng.), LL.D.  
SIR VINCENT Z. DE FERRANTI, M.C.  
T. G. N. HALDANE, M.A.  
PROF. E. B. MOULLIN, M.A., Sc.D.,  
LL.D.

SIR ARCHIBALD J. GILL, B.Sc.(Eng.).  
SIR JOHN HACKING.  
COL. B. H. LEESON, C.B.E., T.D.  
SIR HAROLD BISHOP, C.B.E., B.Sc.(Eng.),  
F.C.G.I.  
SIR JOSIAH ECCLES, C.B.E., D.Sc.  
THE RT. HON. THE LORD NELSON OF  
STAFFORD.

SIR W. GORDON RADLEY, K.C.B., C.B.E.,  
Ph.D.(Eng.).  
S. E. GOODALL, M.Sc.(Eng.), F.Q.M.C.  
SIR WILLIS JACKSON, D.Sc., D.Eng.  
LL.D., F.R.S.  
SIR HAMISH D. MACLAREN, K.B.E.,  
C.B., D.F.C.\*, LL.D., B.Sc.

B. DONKIN, B.A.

O. W. HUMPHREYS, C.B.E., B.Sc.  
R. L. SMITH-ROSE, C.B.E., D.Sc., Ph.D., F.C.G.I.

A. H. MUMFORD, O.B.E., B.Sc.(Eng.).

### Vice-Presidents

### Honorary Treasurer

C. E. STRONG, O.B.E., B.A., B.A.I.

### Ordinary Members of Council

J. C. ARKLESS, B.Sc.  
PROF. H. E. M. BARLOW, Ph.D., B.Sc.  
(Eng.), F.R.S.  
D. A. BARRON, M.Sc.  
C. O. BOYSE, B.Sc.(Eng.).  
F. H. S. BROWN, C.B.E., B.Sc.

J. BROWN, M.A., Ph.D., D.Sc.(Eng.).  
SIR ROBERT COCKBURN, K.B.E., C.B.,  
M.Sc., Ph.D.  
L. DRUCQUER.  
THE RT. HON. THE VISCOUNT FALMOUTH.  
R. A. HORE, M.A., B.Sc., Ph.D.

J. S. MCCULLOCH.  
J. S. MCPETRIE, C.B., Ph.D., D.Sc.  
PROF. J. M. MEEK, D.Eng.  
G. MILLINGTON, M.A., B.Sc.  
THE HON. H. G. NELSON, M.A.  
PROF. C. W. OATLEY, O.B.E., M.A., M.Sc.

J. R. RYLANDS, M.Sc., J.P.  
G. A. V. SOWTER, Ph.D., B.Sc.(Eng.).  
H. G. TAYLOR, D.Sc.(Eng.).  
P. L. TAYLOR, M.A.  
H. WEST, M.Sc.

### Chairmen and Past-Chairmen of Sections

*Electronics and Communications:*  
R. J. HALSEY, C.M.G., B.Sc.(Eng.),  
F.C.G.I.  
†T. B. D. TERRONI, B.Sc.

*Measurement and Control:*  
W. S. ELLIOTT, M.A.  
†C. G. GARTON.

*Supply:*  
J. S. FORREST, D.Sc., M.A.  
†J. E. L. ROBINSON, M.Sc.

*Utilization:*  
H. G. TAYLOR, D.Sc.(Eng.).  
†J. M. FERGUSON, B.Sc.(Eng.).

### Chairmen and Past-Chairmen of Local Centres

*East Midland Centre:*  
PROF. J. E. PARTON, B.Sc., Ph.D.  
†LT.-COL. W. E. GILL, T.D.  
*North-Western Centre:*  
C. H. FLURSCHEIM, B.A.  
†F. LINLEY.

*Mersey and North Wales Centre:*  
R. N. PEGG.  
†D. A. PICKEN.  
*Northern Ireland Centre:*  
W. SZWANDER, Dipl.-Ing.  
†J. MCA. IRONS.  
*Southern Centre:*  
T. G. C. HARROP, M.B.E., B.E.M.  
†R. GOFORD.

*North-Eastern Centre:*  
P. RICHARDSON.  
†D. H. THOMAS, M.Sc.Tech., B.Sc.(Eng.).  
*Scottish Centre:*  
PROF. E. C. CULLWICK, O.B.E., M.A.,  
D.Sc., F.R.S.E.  
†R. B. ANDERSON.  
*Western Centre:*  
T. GILL, B.Sc.  
†A. C. THIRTL.

*North Midland Centre:*  
W. J. A. PAINTER, A.C.G.I., D.I.C.  
†F. W. FLETCHER.  
*South Midland Centre:*  
C. F. FREEMAN, B.Sc.(Eng.).  
†BRIGADIER F. JONES, C.B.E., M.Sc.

† Past Chairman.

## ELECTRONICS AND COMMUNICATIONS SECTION COMMITTEE 1961-1962

### Chairman

R. J. HALSEY, C.M.G., B.Sc.(Eng.), F.C.G.I.

### Vice-Chairman

J. A. RATCLIFFE, C.B.E., M.A., F.R.S.

### Past-Chairmen

M. J. L. PULLING, C.B.E., M.A.

T. B. D. TERRONI, B.Sc.

### Ordinary Members of Committee

W. H. ALDOUS, B.Sc., D.I.C.  
F. S. BARTON, C.B.E., M.A., B.Sc.  
P. A. T. BEVAN, C.B.E., B.Sc.  
J. BROWN, M.A., Ph.D., D.Sc.(Eng.).  
V. J. COOPER, B.Sc.(Eng.), A.C.G.I.  
H. DAVIES, M.Eng.

G. W. A. DUMMER, M.B.E.  
R. FEINBERG, Dr.-Ing., M.Sc.  
C. A. MARSHALL, B.Sc.  
L. J. I. NICKELS, B.Sc.(Eng.).  
W. J. PERKINS.  
N. C. ROLFE, B.Sc.(Eng.).

K. F. SANDER, M.A., Ph.D., B.Sc.  
T. R. SCOTT, D.F.C., B.Sc.  
F. J. D. TAYLOR, O.B.E., B.Sc.(Eng.).  
C. WILLIAMS, B.Sc.(Eng.).  
R. C. G. WILLIAMS, Ph.D., B.Sc.(Eng.).  
R. C. WINTON, B.Sc.

The President (*ex officio*).

The Chairman of the Papers Committee.

PROFESSOR H. E. M. BARLOW, Ph.D., B.Sc.(Eng.), F.R.S. (representing the Council).

E. H. COOKE-YARBOROUGH, M.A. (Co-opted Member).

A. J. COLGAN (representing the North-Eastern Measurement and Electronics Group).

A. H. W. BECK, M.A., B.Sc.(Eng.) (representing the Cambridge Electronics and Measurement Group).

C. HEYS (representing the North-Western Electronics and Communications Group).

J. R. POLLARD, M.A. (representing the East Midland Electronics and Control Group).

J. A. BENNETT, B.Sc., Ph.D. (representing the Scottish Electronics and Measurement Group).

and

R. E. YOUNG, B.Sc.(Eng.) (representing the South Midland Electronics and Measurement Group).

G. B. B. CHAPLIN, M.Sc., Ph.D. (representing the Southern Electronics and Control Group).

The following nominees:

Royal Navy: CAPTAIN J. S. RAVEN, B.Sc., R.N.

Army: COL. R. G. MILLER, M.A.

Royal Air Force: AIR COMMODORE A. FODEN, C.B.E., B.Sc.Tech., R.A.F.

## MEASUREMENT AND CONTROL SECTION COMMITTEE 1961-1962

### Chairman

W. S. ELLIOTT, M.A.

### Vice-Chairmen

A. C. LYNCH, M.A., B.Sc.; A. J. MADDOCK, D.Sc.

### Past-Chairmen

PROFESSOR A. TUSTIN, M.Sc.; C. G. GARTON.

### Ordinary Members of Committee

S. S. CARLISLE, M.Sc.  
W. H. DEVENISH.  
H. M. GALE, B.Sc.(Eng.).

E. J. R. HARDY, B.Sc.(Eng.).  
W. J. JEFFERSON.  
C. A. LAWS.

S. N. POCOCH.  
G. H. RAYNER, B.A.  
W. RENWICK, M.A., B.Sc.

R. D. TROTTER, B.Sc.(Eng.).  
J. H. WESTCOTT, B.Sc.(Eng.), Ph.D.  
F. C. WIDDIS, B.Sc.(Eng.), Ph.D.

And

The President (*ex officio*).

The Chairman of the Papers Committee.

G. A. V. SOWTER, Ph.D., B.Sc.(Eng.) (representing the Council).

A. J. COLGAN (representing the North-Eastern Measurement and Electronics Group).

R. BARRASS (representing the Cambridge Electronics and Measurement Group).

E. C. SMITH (representing the North-Western Measurement and Control Group).

H. M. GALE, B.Sc.(Eng.) (representing the South Midland Electronics and Measurement Group).

D. R. HARDY, Ph.D., M.Sc.(Eng.) (representing the East Midland Electronics and Control Group).

W. H. P. LESLIE, B.Sc. (representing the Scottish Electronics and Measurement Group).

C. E. TATE (representing the Southern Electronics and Control Group).

A. FELTON, B.Sc.(Eng.) (nominated by the National Physical Laboratory).

### Secretary

W. K. BRASHER, C.B.E., M.A., M.I.E.E.

### Principal Assistant Secretary

F. C. HARRIS.

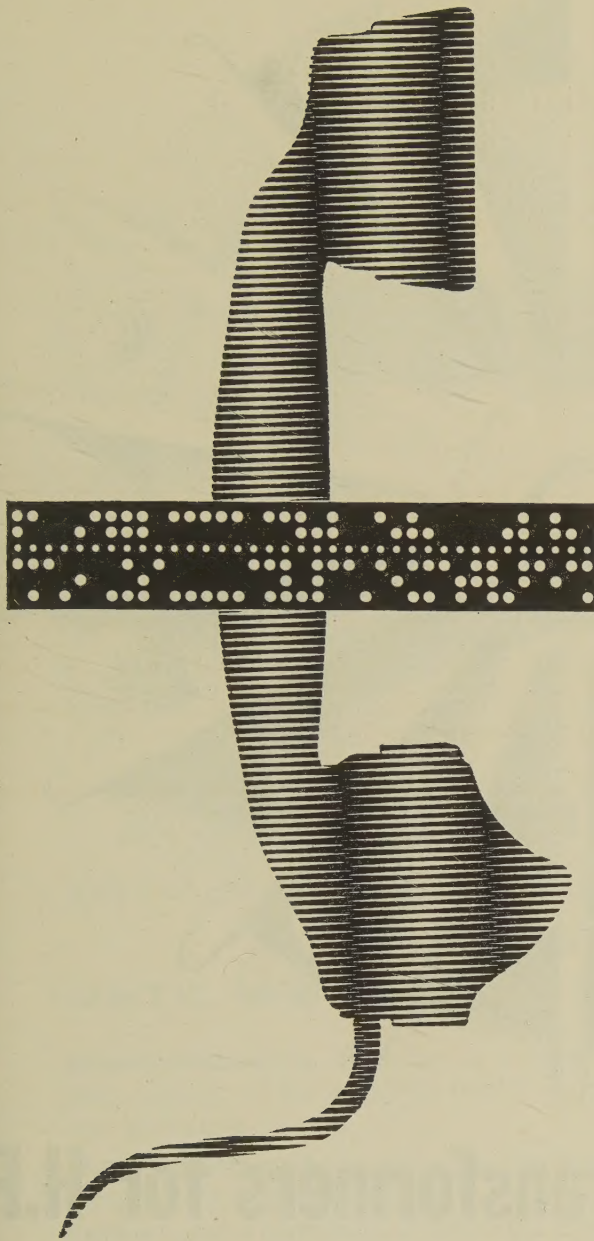
### Editor-in-Chief

G. E. WILLIAMS, B.Sc.(Eng.), M.I.E.E.

### Deputy Secretary

F. JERVIS SMITH, M.I.E.E.





# FIRST RAILWAY MICROWAVE RADIO TELEPHONE SYSTEM IN BRITAIN

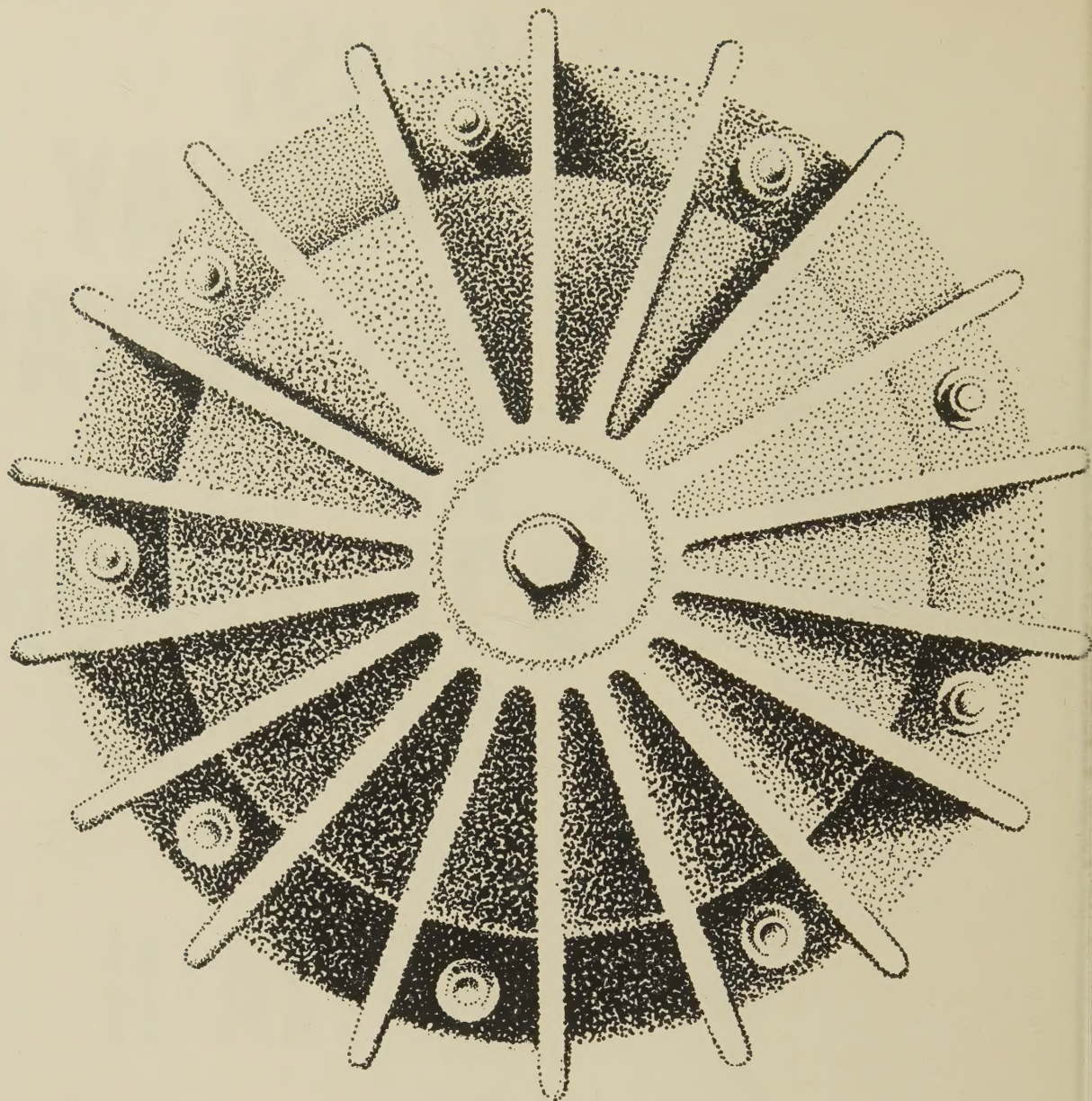
**300 Channels  
between  
Newcastle and York**

British Railways first microwave multichannel system from Newcastle to York via Darlington will have a 300 telephone channel capacity. The system allows for channels to be dropped off at intermediate points and can accommodate high speed data transmission.

## MARCONI

COMPLETE COMMUNICATION SYSTEMS  
SURVEYED • PLANNED • INSTALLED • MAINTAINED





## Wide Band Matching Transformers for H.F.

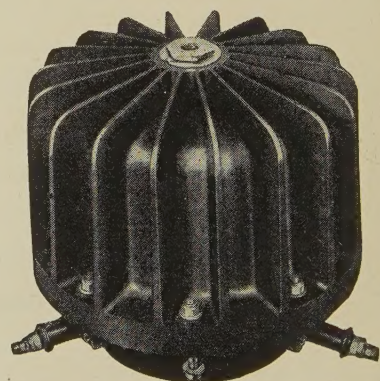
- Power Capacities 1 kW & 5 kW
- Impedance ratios 600 ohms balanced to 75/50/60 ohms unbalanced

*Compact • no tuning • low loss • weather-proof*

Write for data sheets and further technical details quoting reference K/687/11 to:—

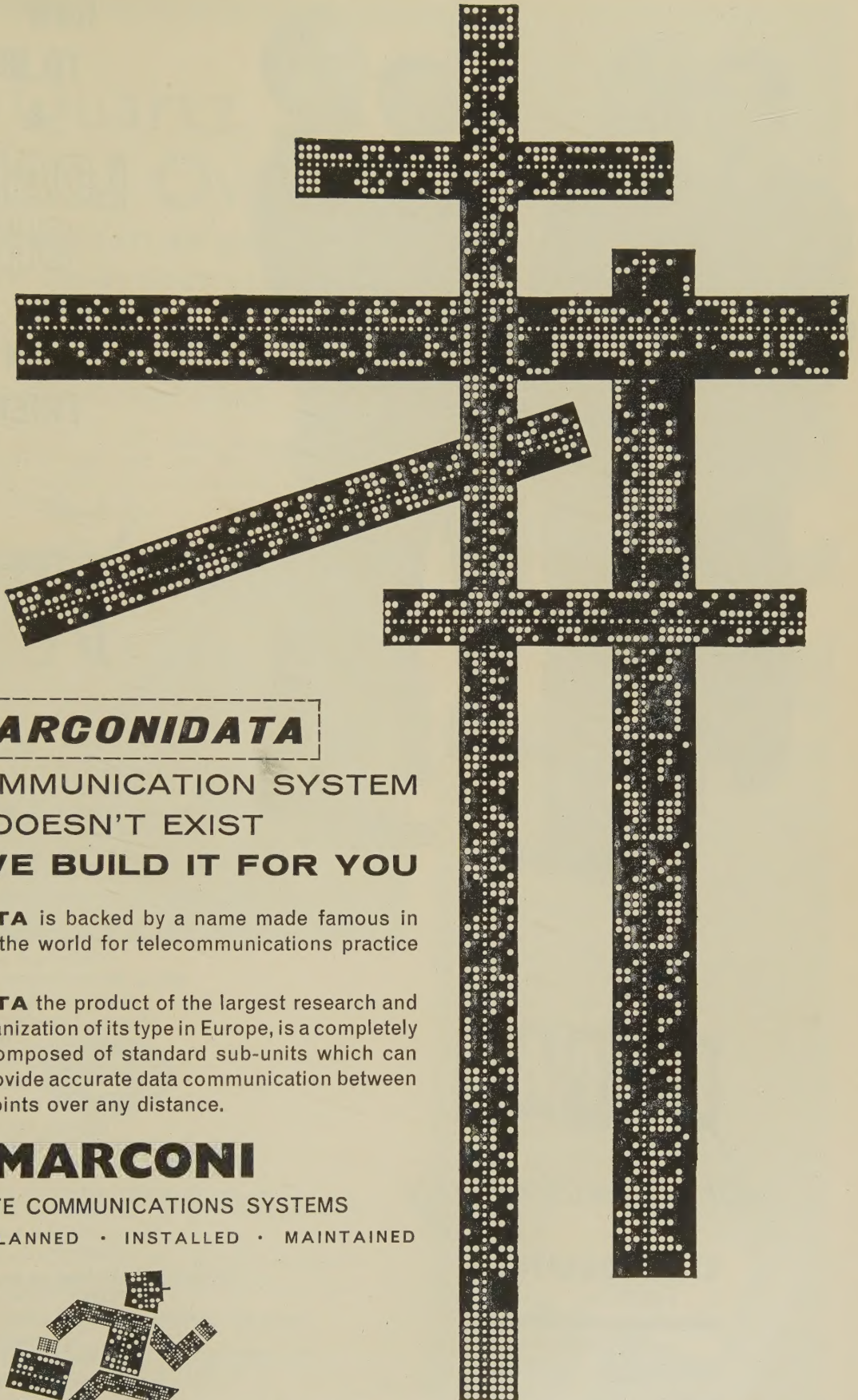
**MULLARD EQUIPMENT LIMITED**

MANOR ROYAL, CRAWLEY, SUSSEX • Telephone Crawley 28787



5 kW Type L.382 in cast aluminium.  
Frequency range 1.5–30 Mc/s,  
with VSWR better than 1.5





A

**MARCONIDATA**

**DATA COMMUNICATION SYSTEM  
DOESN'T EXIST  
UNTIL WE BUILD IT FOR YOU**

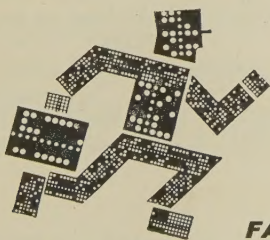
**MARCONIDATA** is backed by a name made famous in every country of the world for telecommunications practice and technique.

**MARCONIDATA** the product of the largest research and development organization of its type in Europe, is a completely flexible system composed of standard sub-units which can be arranged to provide accurate data communication between any number of points over any distance.

**MARCONI**

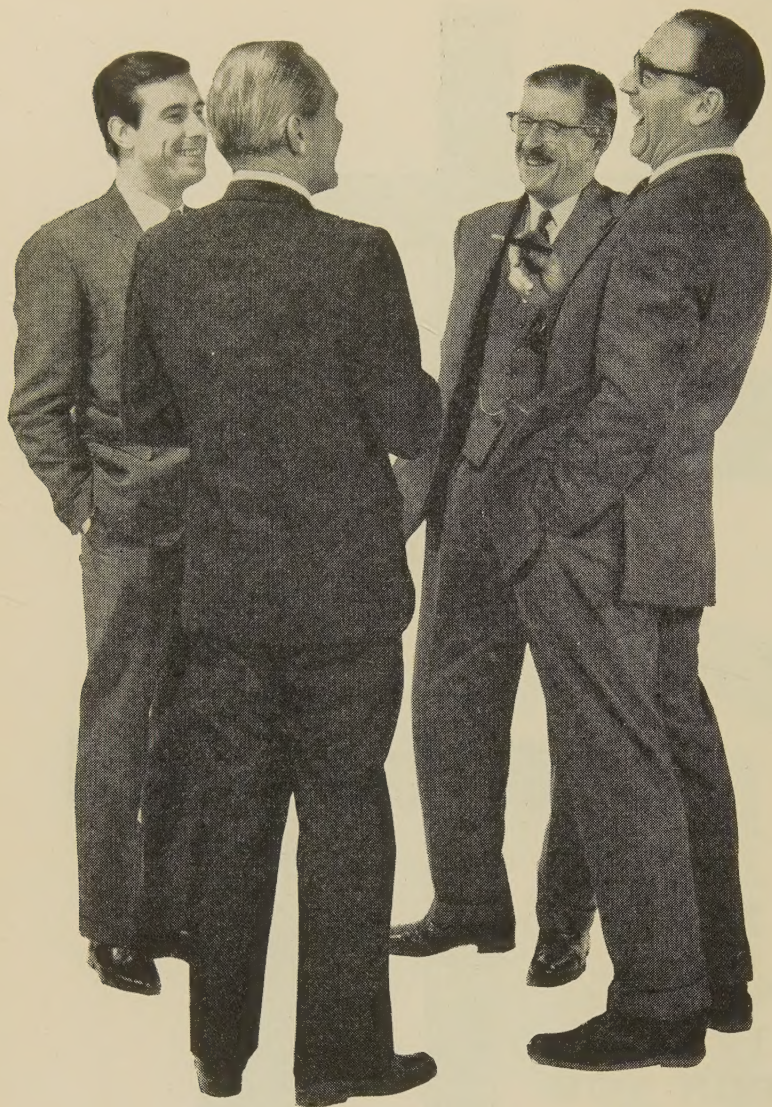
COMPLETE COMMUNICATIONS SYSTEMS

SURVEYED • PLANNED • INSTALLED • MAINTAINED

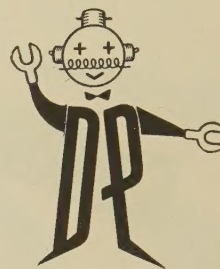
**FAST ACCURATE DATA COMMUNICATION SYSTEMS**

MARCONI'S WIRELESS TELEGRAPH COMPANY LIMITED, CHELMSFORD, ESSEX, ENGLAND





# HOW TO BE A LOAD SHOVER AND WIN FRIENDS



The subject is load-shoving.  
More particularly, load-shoving relating to  
motor control problems. Right,  
so you've got problems.

Pushbuttons, timers, isolators,  
electric motors for pumping rooms,  
casting rooms, plating shops,  
betting shops.

Forget betting shops.

Don't take a gamble.

You've got problems. *Breakdown.*

Blame the electrician,

blame the foreman,

blame a dreaming apprentice,

blame the government,

blame the weather (sun-spots).

No, no, no.

This is *not* the way to be a load-shover.

Strictly old hat.

Won't make friends that way.

Won't stop breakdowns, either.

So how come the load-shover in the picture is so popular?

Simple.

He's a DUPAR load-shover.

DUPAR . . . that's it.

He's shoved the load on to DUPAR . . .

DUPAR Technical Advisory Service . . .

DUPAR Control Gear.

No wonder he's so popular.

They haven't had a breakdown in years.

Nor likely to either.

## DUPAR

*for dependability*

### DEWHURST

& PARTNER LIMITED

INVERNESS WORKS  
HOUNSLOW · MIDDLESEX

Telephone: HOUnslow 7791 (12 lines)  
Telegrams: DEWHURST HOUNSLOW

Field Offices at:-

BIRMINGHAM, GLASGOW,  
GLOUCESTER, LEEDS, MANCHESTER,  
NEWCASTLE, NOTTINGHAM

There is DUPAR electric motor control gear for all branches of Engineering.



# Quartz Crystal Ovens

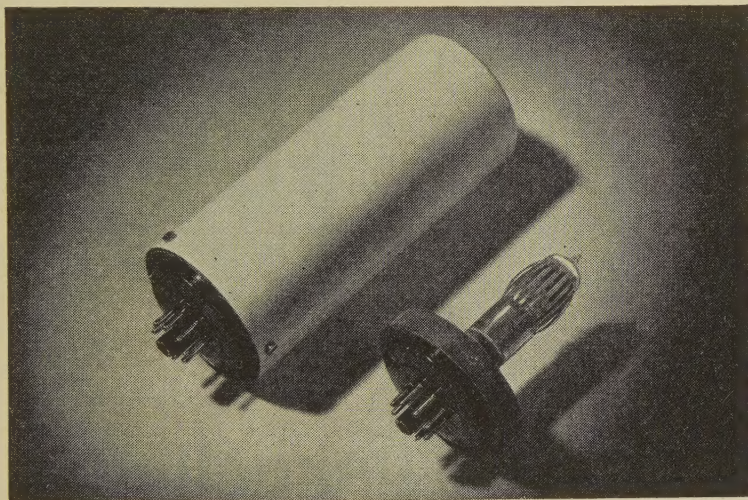
**STABLE TEMPERATURE ENSURING  
MAXIMUM FREQUENCY STABILITY**

Switching differential  $0.0014^{\circ}\text{C}$ .

No thermostat

No thermometer switch

Orthodox crystal ovens, using thermostats or thermometer switches, are available for applications where wider temperature variations are acceptable.



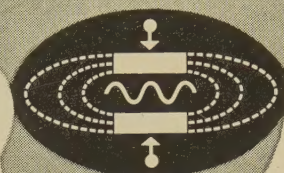
## MARCONI

**SPECIALIZED RADIO COMPONENTS**

*Write for details of crystal ovens and other specialized components  
in the Marconi range, and address your enquiries to:*

**SPECIALIZED COMPONENTS GROUP**

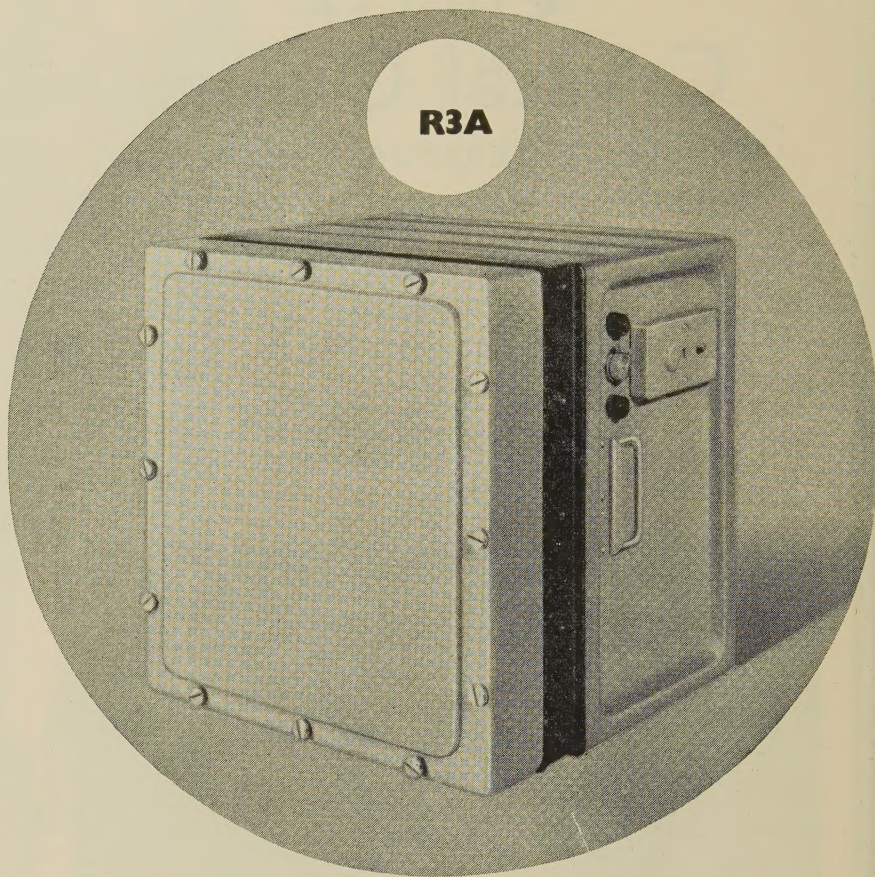
MARCONI'S WIRELESS TELEGRAPH COMPANY LTD.,  
CHELMSFORD, ESSEX, ENGLAND



This symbol has been adopted by the Marconi Specialized Components Group. The Marconi Company undertakes the design and manufacture of specialized components only when no suitable alternative is available; and in almost every case, Marconi specialized components are designed to more exacting standards and built to closer tolerances than any similar components. A preliminary catalogue is available, listing ferrite isolators and circulators, coaxial connectors, attenuators, terminations and switches; waveguide filters terminations, and bends; crystal filters and ovens.







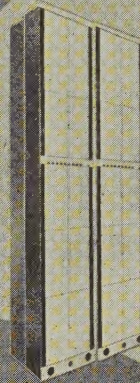
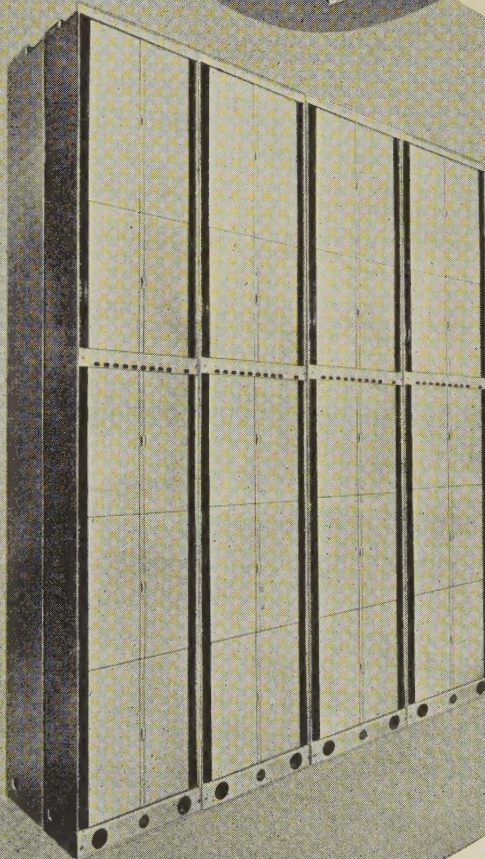
## **A.T.E. "Packaged" Radio Channelling in Fully-transistorised Basic Units for 3 to 300 Circuits**

Economical, reliable, completely self-contained, these terminals are ideal for rapid installation at any microwave or VHF radio terminal. They meet relevant Services and C.C.I.T.T. requirements.

All terminals include inbuilt, outband, signalling facilities suitable for dialling. Simple ringdown relay sets can also be inbuilt when required. Racksides may be mounted back to back or side by side.

**AUTOMATIC TELEPHONE & ELECTRIC CO LTD**  
STROWGER HOUSE · ARUNDEL STREET · LONDON · W.C.2 TEL. TEMPLE BAR 9262



**R24B****R60B****RI20A****R300A**

**R3A** A transportable 3 channel terminal designed for field or Service use. Write for Bulletin TEB. 3303

**R24B** A 12/24 channel terminal in the 6-108 Kc/s spectrum, complete on one rackside. Write for Bulletin TEB. 3301

**R60B** A 60 channel terminal (12-252 or 60-300 Kc/s), complete on two rackside. Write for Bulletin TEB. 3302

**RI20A** A 120 channel terminal (12-552 Kc/s), complete on four rackside. Write for Bulletin TEB. 3304

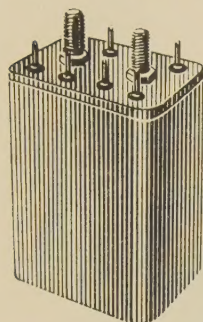
**R300A** A 300 channel terminal (60-1300 Kc/s), complete on eight rackside. Write for Bulletin TEB. 3305





# Plessey relays

## for the electrical industry



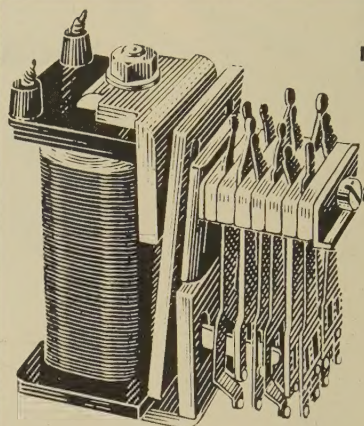
### MINIATURE TYPE CA

Fully Type Approved to RCS 165 and 166.

Light and medium duty types have two changeover contacts.

Heavy duty types single make or break.

Available sealed, or unsealed with dustcover.



### MINIATURE TYPE CB

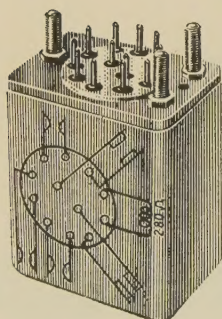
Based on Type CA with heavier magnetic circuit.

All versions fully Type Approved.

Available with up to twelve contact springs.

Twinned platinum contacts on light duty versions.

Available sealed, or unsealed with dustcover.



### MINIATURE TYPE CC

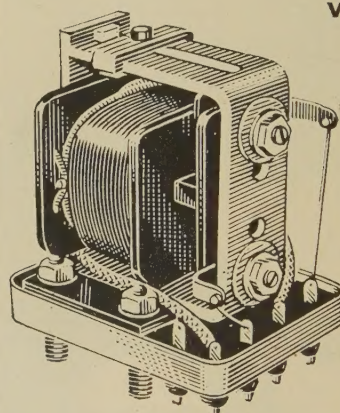
Meets RCS 165 and MIL-R-5757 Specifications.

Based on Type CA magnetic circuit, providing up to four light or medium-duty contact sets.

Available sealed, or unsealed with dustcover.

Printed circuit versions available.

*Contact loadings up to 10A d.c., non-inductive, can be arranged for Types CA, CB, and CC.*



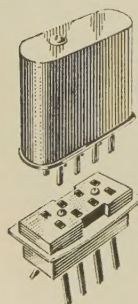
### VOLTAGE REGULATING TYPE XC 269

Fully Approved to S.R.D.E. Spec. 166/1.

Temperature compensated in range  $-40^{\circ}\text{C}$  to  $+85^{\circ}\text{C}$ .

Available for 6, 12 or 24 V operation.

Typical changeover voltage differential 1 V in 24 V.



### SUB-MINIATURE TYPE CE

Occupies less than  $\frac{1}{4}$  square inch of chassis area.

Two changeover contacts rated 0.25A at 28 V d.c.

Insulation proof against 500 V a.c., r.m.s. between coil and contact stack.

$-55^{\circ}\text{C}$  to  $+100^{\circ}\text{C}$  operational temperature range.

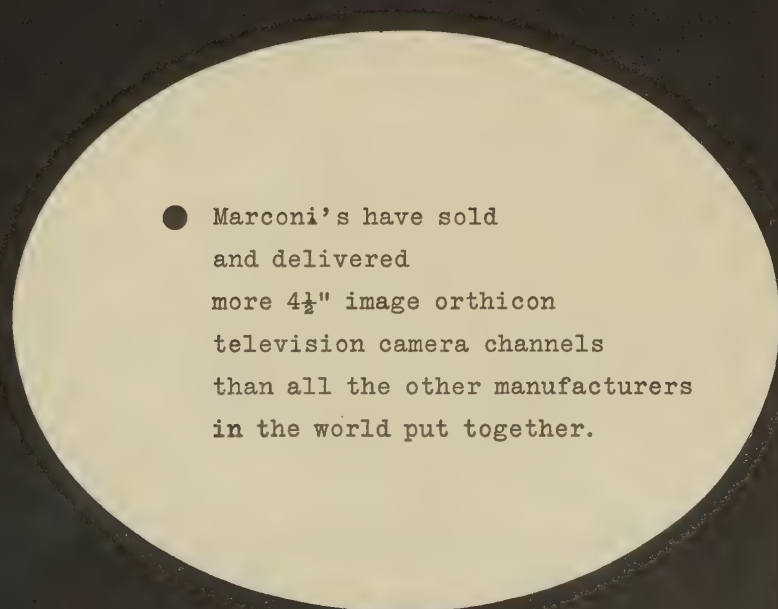
# Plessey

**THE PLESSEY COMPANY LIMITED**  
(Relays and Control Systems Unit)

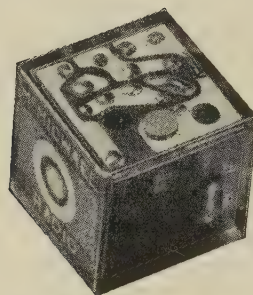
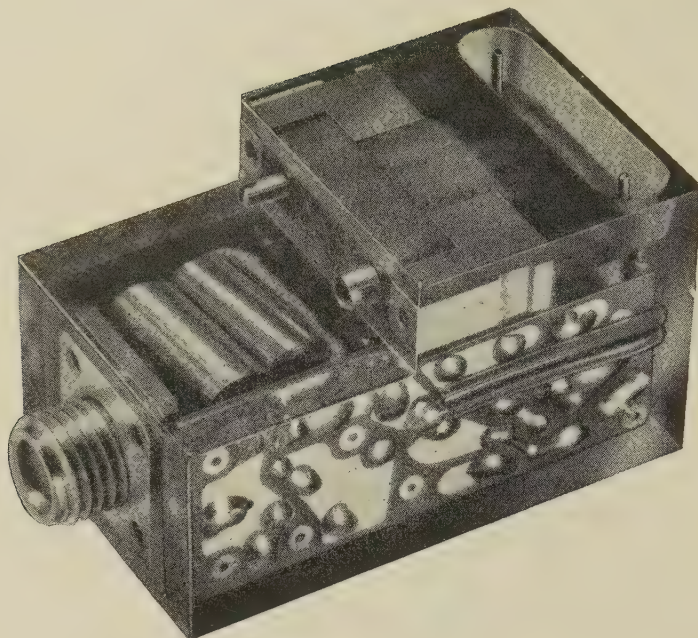
Eddes House, Eastern Avenue West, Romford, Essex  
Telephone: Seven Kings 6050

Overseas Sales Organisation: Plessey International Limited,  
Ilford, Essex. Telephone: Ilford 3040



- 
- Marconi's have sold and delivered more  $4\frac{1}{2}$ " image orthicon television camera channels than all the other manufacturers in the world put together.





actual size

## After the miniature, the microminiature

## EPOXY RESINS

Araldite is a registered trade mark

This pre-amplifier unit, encapsulated in a half-inch cube of Araldite, is produced by McMichael Radio Ltd. to replace the larger unit shown. From the photograph it is not only apparent that the new unit needs a fraction of the Araldite used in the earlier type; it is also a striking illustration of the manner in which Araldite epoxy resins permit the use of very small and fragile components, completely protected and forming a compact assembly. The unit has a higher input impedance and lower input capacitance than are provided by normal manufacturing techniques. Many uses of Araldite are described in our booklet, 'Araldite Resins in the Electrical Industry'. May we send you a copy?

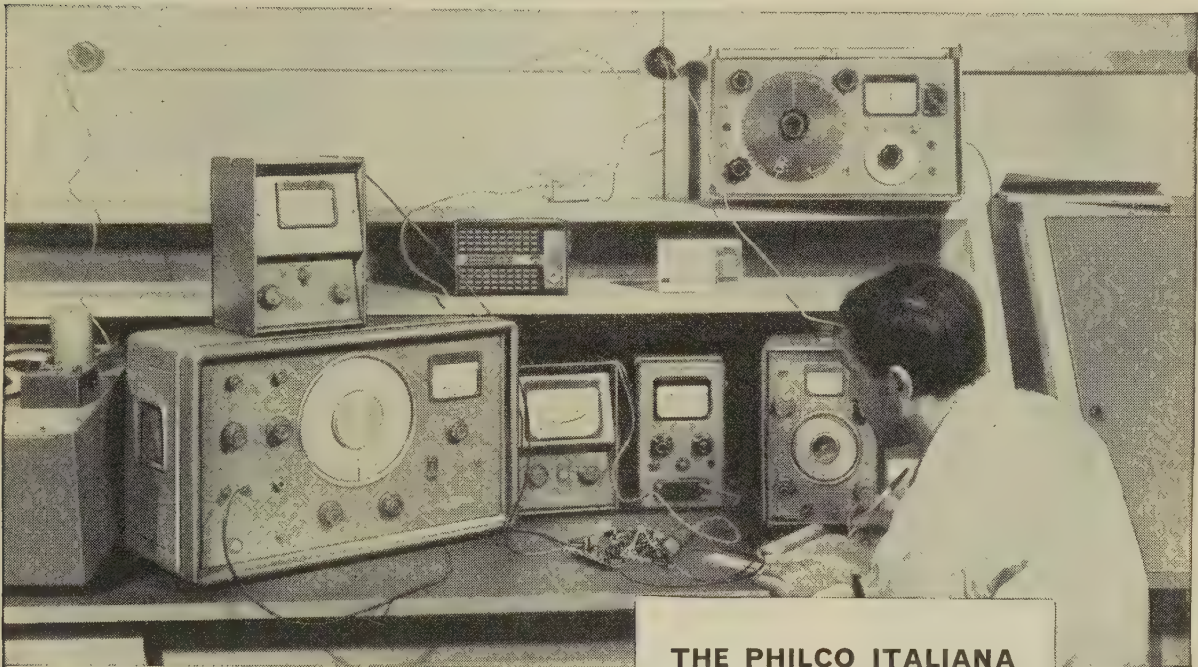


In Design and Production

**PHILCO** italiana

use

## MARCONI TEST EQUIPMENT



### THE PHILCO ITALIANA LABORATORIES, MILAN

In Italy, people happily go home to their Philco radio and television receivers. For Philco realise that the continued success of their products is due to a rigorous adherence to quality standards. It follows naturally that this leading Italian company employs a wide variety of Marconi instruments. Prominent in this picture is the Wave Analyser TF 455E, a highly selective and sensitive Analyser for the accurate evaluation of both absolute and relative levels of individual components of a complex waveform. It covers the frequency range 20 c/s to 16 kc/s.

*For full details of Wave Analyser TF 455E, an instrument which has many uses in testing audio equipment, write for Leaflet K193. Please mention any other fields of electronic measurement in which you are interested.*

Marconi test equipment, including the Wave Analyser TF 455E (at left), being used to test the distortion of the low-frequency amplifier of a transistored receiver undergoing development.

## MARCONI INSTRUMENTS

### THE INTERNATIONAL CHOICE FOR ELECTRONIC MEASUREMENT

AM & FM SIGNAL GENERATORS · AUDIO AND VIDEO OSCILLATORS · FREQUENCY METERS · VOLTMETERS · POWER METERS · DISTORTION METERS  
TRANSMISSION MONITORS · DEVIATION METERS · OSCILLOSCOPES, SPECTRUM & RESPONSE ANALYSERS · Q METERS AND BRIDGES

London and the South :

English Electric House, Strand, London, W.C.2.  
Telephone: COVent Garden 1234.

Midlands :

Marconi House, 24 The Parade, Leamington Spa.  
Telephone: 1408

North :

23/25 Station Square, Harrogate.  
Telephone: 67455

Export Department: Marconi Instruments Limited, St. Albans, Herts. England. Telephone: St. Albans 59292.

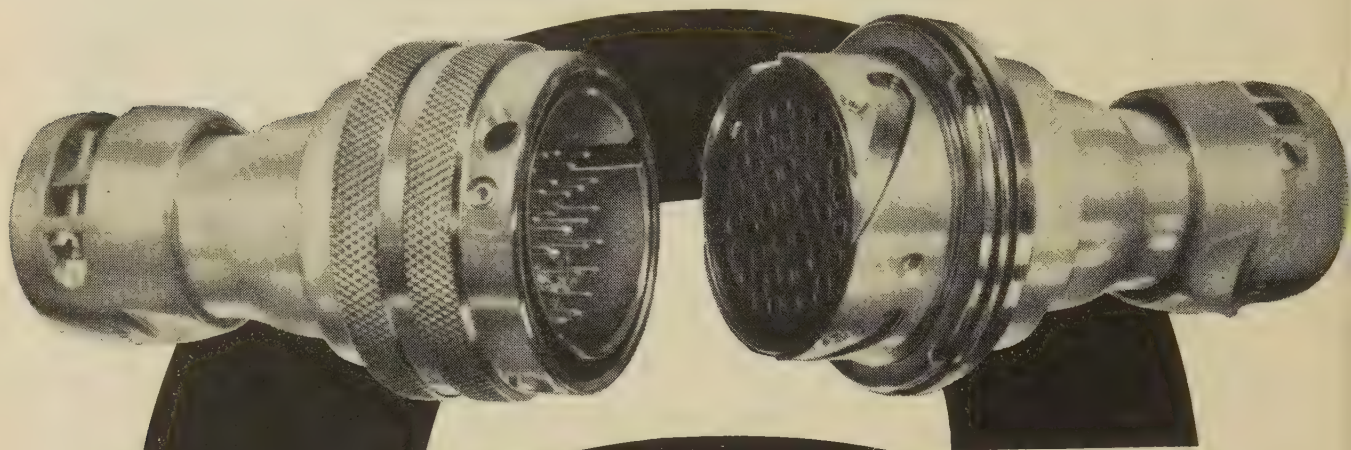
REPRESENTATION IN 68 COUNTRIES

TC193



**Plessey****MARK 6**

A new conception in high performance connectors  
with 6 outstanding features \*



- \* Crimped connections
- \*  $-55^{\circ}\text{c}$  to  $+155^{\circ}\text{c}$
- \* Bayonet Coupling
- \* 6 to 55 contacts
- \* Pressure sealed
- \* 1kV. all contacts

The new Plessey Aluminium Mark 6 is an entirely new conception in electrical connectors — offering a greater number of contacts than the ubiquitous Mark 4 plus other singular features introduced to meet the exacting requirements of this modern age.

To the aircraft and missile designer, it offers a considerable saving in weight plus efficient operation and dependable service over an extremely extensive temperature range. To the designer of electronic equipment it offers a high standard of performance with valuable space-saving dimensions.

To all users of electrical connectors, the Plessey Mark 6 Connector constitutes the latest example of forward thinking design and unsurpassable efficiency from a Company recognised throughout the world as one of the leading manufacturers of high quality, reliable electrical connectors.

WIRING & CONNECTORS DIVISION

**THE PLESSEY COMPANY LIMITED • CHENEY MANOR • SWINDON • WILTS • SWINDON 6251**

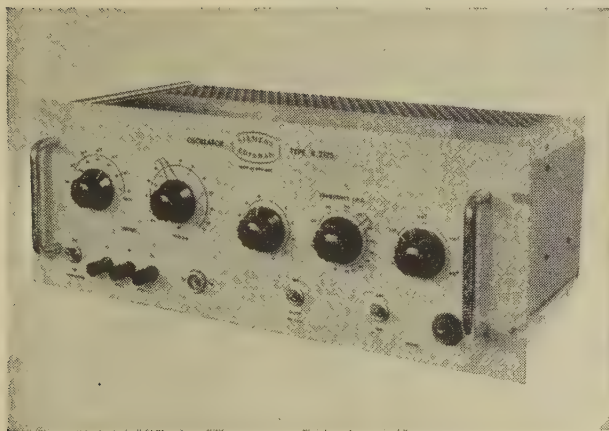
Overseas Sales Organisation: Plessey International Limited • Ilford • Essex • Ilford 3040



# Oscillographic recording and testing equipment from Siemens Ediswan

If your work involves the study of fluctuating or intermittent phenomena, you should know more about these instruments.

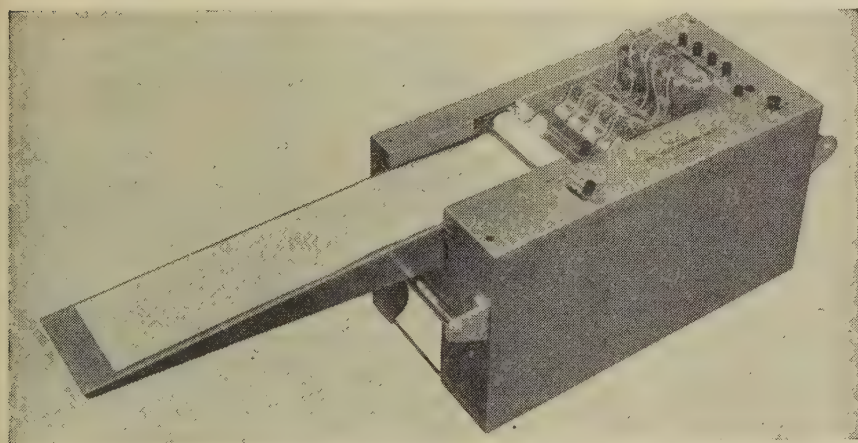
The versatile High Speed Pen Recorder unit can be supplied singly or grouped in multiples of four up to a maximum of 16 channels and suitable amplifiers having a sensitivity of  $1\mu\text{V}/\text{mm}$  a.c. or  $10\text{ mV}/\text{mm}$  d.c. can also be supplied. These combinations are already making permanent economical records in industrial, physiological and physical research.



## LOW FREQUENCY OSCILLATOR TYPE R.2125

The Low Frequency Oscillator is a general purpose R.C. instrument designed for testing, calibrating and setting up amplifiers, recorders, and low frequency wave analysers.

Frequency Range	1 c/s to 132 Kc/s
Frequency accuracy	2%
Output	Balanced push pull, 50 volts p.p. maximum on open circuit.
Attenuator	5 x 20 dB steps plus 0—20 dB continuously variable.
Output Impedance	600 $\Omega$ —0—600 $\Omega$



## PORTABLE RECORDER TYPE EPR

The Siemens Ediswan pen oscillograph is a portable 1 to 4 channel, high speed, direct ink writing, recorder.

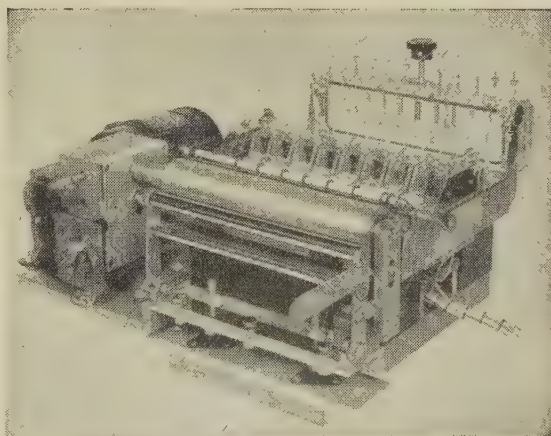
The pen motor coil is 1450 ohms centre tapped. Frequency response within 10% from 0–70 c.p.s. Pen motors can be supplied with coil resistances of 230 ohms for use with transistors. Maximum deflection of pen tip 4 cms peak to peak. An electrical time and event marker is provided, writing on the lower edge of the paper. The 4" wide paper is driven by a rubber covered capstan roller and speeds of 0.75 cms/sec. to 12 cms/sec. can be obtained.

## 8 CHANNEL PEN RECORDER UNIT

The pen motors incorporated in this unit are identical to those used in the 4 channel pen oscillograph. The unit includes 8 pen motors fitted into a magnet block, two time markers, ink system and paper drive mechanism.

Three speeds of 1.5, 3 and 6 cms/sec. are available.

The unit is offered as shown in the photograph and is intended for incorporation into the users own equipment. A 16 channel version of the above unit is also available.



We shall be pleased to send you particulars of these products

**Associated Electrical Industries Ltd**

Radio and Electronic Components Division

PD 17, 155 Charing Cross Road, London WC2

Tel: GERrard 9797. Telegrams: Sieswan Westcent London

**AEI**





# ERIE<sup>★</sup> Transcaps<sup>★</sup>

Pat. App. for

## for all Transistor Circuits

### SPECIFICATION

	811T	831T
CAPACITANCE	: 0.5 $\mu$ F	0.1 $\mu$ F
TOLERANCE	: -20% +50%	-20% +50%
DIAMETER	: 0.594" max.	0.312" max.
THICKNESS	: 0.156" max.	0.156" max.
WORKING VOLTS	: 3 d.c.	3 d.c.

In line with the Erie policy of anticipating the component requirements of the future, the Erie Transcap capacitor is now added to our ever-increasing range of components for use with transistors.

Designed specifically as a small, reliable, high capacitance, low voltage, coupling, and by-pass capacitor, the Erie developed Transcap is manufactured entirely at our Great Yarmouth factory.

Styles 811T and 831T shown here in their actual physical sizes are only forerunners of the wide range in differing values and voltages which will ultimately emerge.

# ERIE<sup>★</sup>

R E S I S T O R  
L I M I T E D

1, HEDDON STREET, LONDON, W.1  
Telephone: REGent 6432

#### FACTORIES

Great Yarmouth and Tunbridge Wells, England; Trenton, Ont., Canada; Erie, Pa., Holly Springs, Miss., and Hawthorne, Cal., U.S.A.

<sup>★</sup> Registered Trade Marks

*Photograph of miniature by courtesy of Victoria & Albert Museum*



# right-angle

exclusive to



## CONTACTORS

The RIGHT-ANGLE mechanism saves space and therefore cost

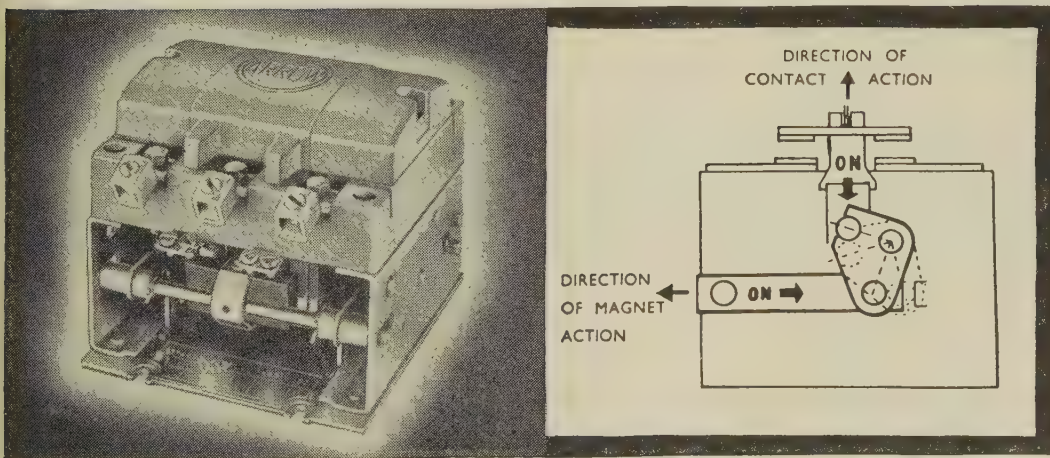
It makes coil changing rapid and simple

Three sizes 30, 50 and 100 amps

Available as INTERLOCKED pairs

Comply with BSS.775 and NEMA sizes 1, 2 and 3

CSA approved



*Make sure you get full details . . . write for our MS11 Catalogue today.*

**ARROW ELECTRIC SWITCHES LIMITED**

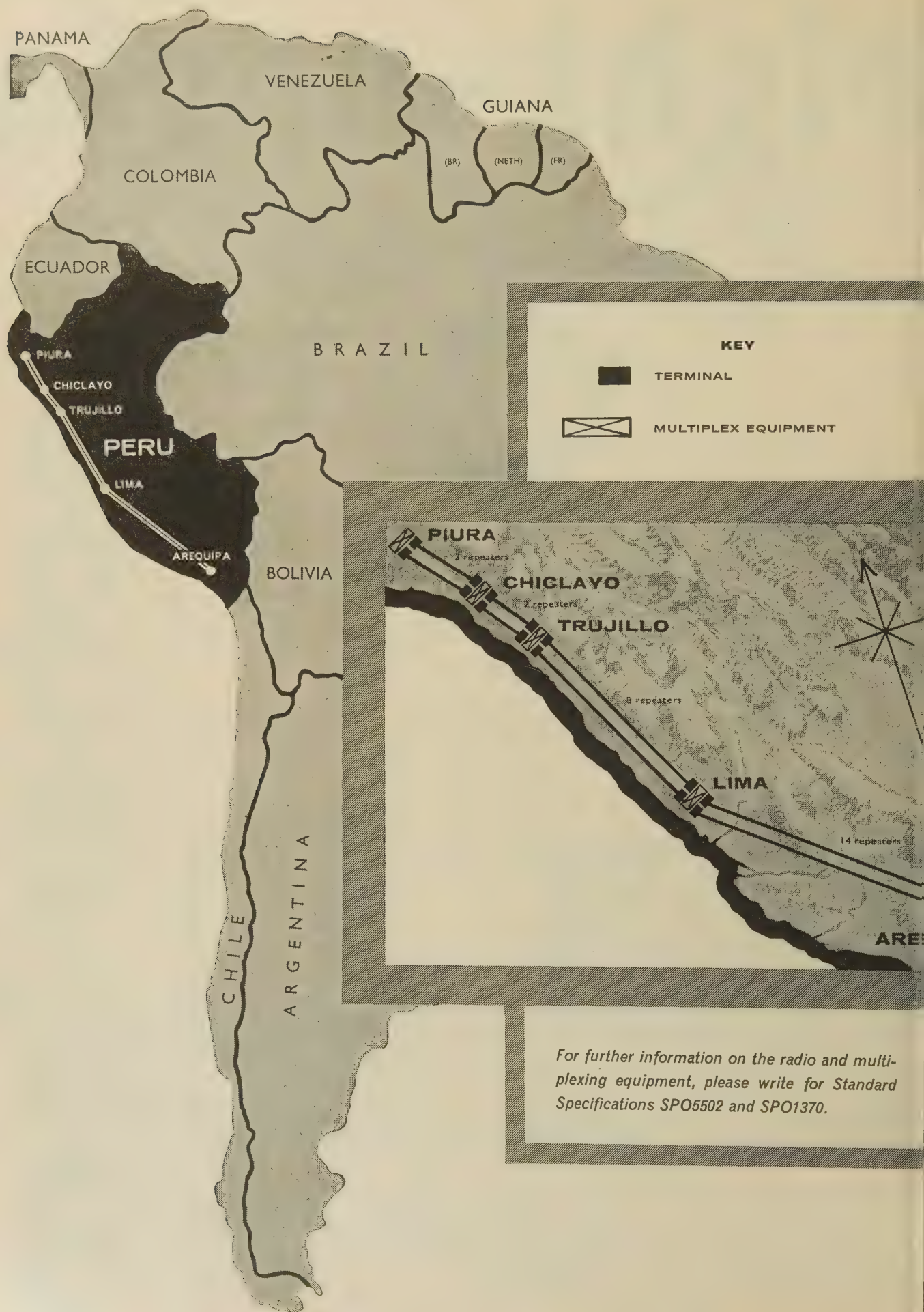
**BRENT ROAD**

**SOUTHALL**

**MIDDLESEX**

mechanism





*For further information on the radio and multiplexing equipment, please write for Standard Specifications SPO5502 and SPO1370.*



The General Electric Company Limited of England has been awarded the contract by the Compañía Nacional de Teléfonos del Perú to supply the radio and multiplexing equipment for a microwave system linking the towns of Arequipa, Lima, Trujillo, Chiclayo and Piura in Peru.

The network comprising five terminal and twenty-seven bothway repeater stations will be the longest in South America extending

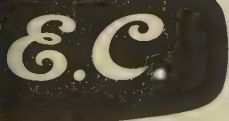
for 1,100 miles along the Pacific seaboard.

The network will employ GEC's well proven 2000Mc/s radio relay equipment.

A main and standby (protection) radio frequency channel will be provided on all routes. In the event of failure or degradation of the working radio channel change-over to the standby is automatic.

Each radio channel has a capacity of 240 speech channels.

# **G.E.C. provides nationwide microwave network in Peru**



**EVERYTHING FOR TELECOMMUNICATIONS**

Transmission Division

**THE GENERAL ELECTRIC COMPANY LIMITED OF ENGLAND**


**TELEPHONE WORKS • COVENTRY • ENGLAND**

*Works at Coventry • London • Middlesbrough • Portsmouth*



Presenting  
the  
new

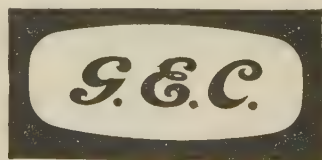
# VerSatile



transistors  
—at the  
new  
lower prices !

The GET 88/89 range of r.f. and switching transistors mounted in the JEDEC TO-5 can is now released. And prices are low! These germanium p-n-p alloy transistors come in 3 groups—for use in switching circuits, radio frequency amplifier and oscillator applications, and radio receivers. And here are some of their advantages:

- By virtue of their low price these transistors can economically be used in audio and i.f. circuits as well as r.f.
- Device outlines are internationally standard and conform to K 1007, VASCA and IEC specifications.
- Electrically interchangeable with the well-known GET 87 series.
- 20 volt ratings available.
- Controlled gain range—2 to 1 spread simplifies circuit design.
- Radio 'packages' available.



## SEMICONDUCTORS

For further details please contact

The General Electric Co Ltd Semiconductor Division  
School Street Hazel Grove Stockport Cheshire.  
Or, in the London area, ring TEMple Bar 8000 Ext. 10



# Cable carrier systems by A.T.E.

The A.T.E. Range of Cable Carrier Systems features equipment for large and small capacity routes. All systems meet the internationally recognised C.C.I.T.T. requirements for trunk circuits, are of high quality and advanced design.

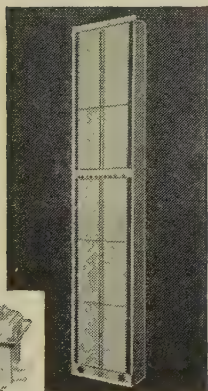
Write for further details to:—

**AUTOMATIC TELEPHONE & ELECTRIC CO LTD**

Strowger House, Arundel Street, London, W.C.2. Phone: TEMple Bar 9262



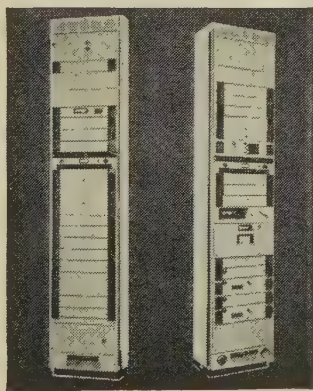
## A.T.E. TRANSMISSION EQUIPMENT TYPE CM FOR LINE, CABLE AND RADIO SYSTEMS



Right: Terminal Repeater  
Left: Intermediate Buried Repeater

### C300A Small Core Coaxial System

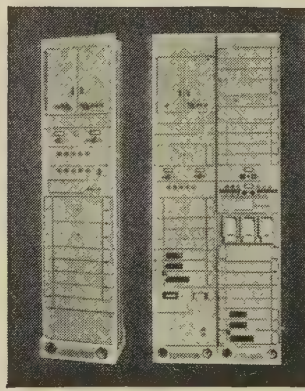
- Fully Transistorised.
- 300 channel system for small core coaxial cables.
- Intermediate power fed repeaters in sealed buried boxes.
- Automatic pilot regulation, suitable for buried or aerial cable.
- Power feeding stations may be up to 60 miles apart.
- Inbuilt maintenance and fault location facilities.



Left: Terminal Repeater (Receive)  
Right: Terminal Repeater (Transmit)

### C960A 4 Mc/s Coaxial System

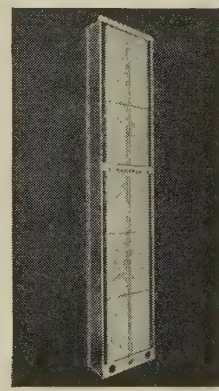
- Up to 960 high-grade telephone circuits on each pair of conventional coaxial tubes.
- Power fed dependent repeaters at 6 mile spacing.
- Main power feed stations up to 100 miles apart.
- Comprehensive maintenance and test facilities.
- Conforms to C.C.I.T.T. recommendations.



Left: Dependent Repeater—6 ft.  
Right: Terminal Repeater—9 ft.

### CX12A 12.5 Mc/s Coaxial System

- Up to 2,700 high grade telephone circuits or transmission of mixed traffic on a pair of conventional .375 inch dia. coaxial tubes.
- Conforms to C.C.I.T.T. recommendations and G.P.O. specifications.
- Dependent repeaters power fed from terminal equipment, with automatic transfer to local mains supply in case of failure.
- Comprehensive maintenance and test facilities.



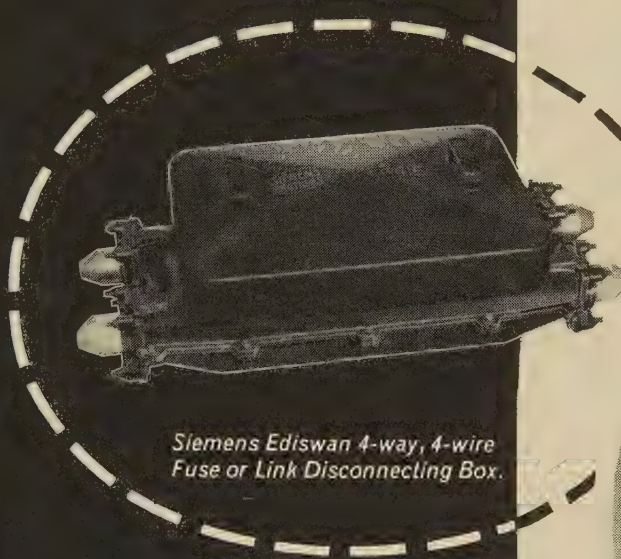
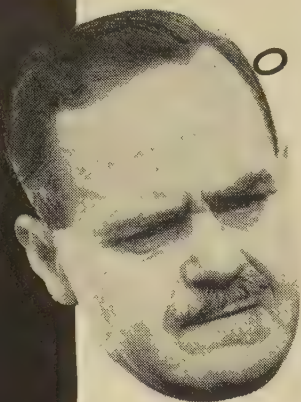
Terminal Rackside

### C12G Cable Carrier System

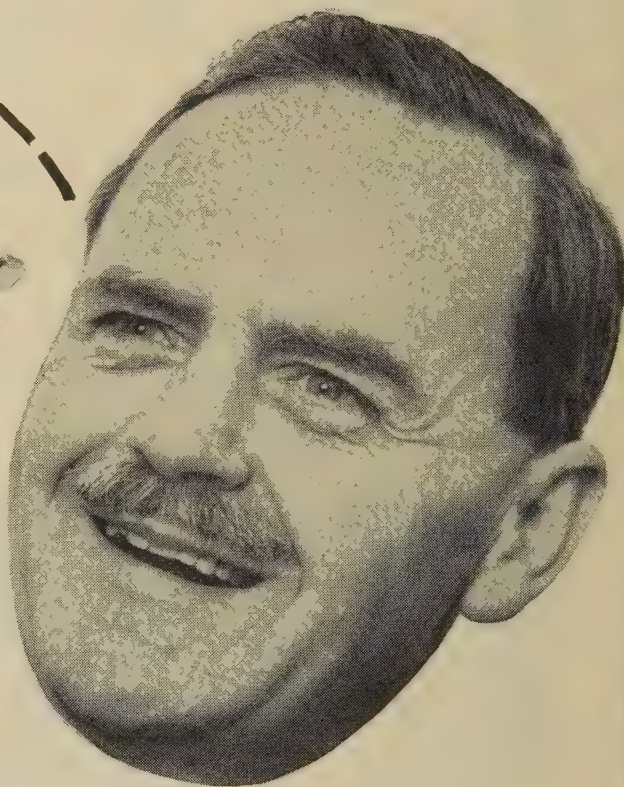
- Fully Transistorised.
- 12 Channels on a single cable pair. (6-54 Kc/s and 60-108 Kc/s 'go' and 'return').
- Automatic pilot regulation, suitable for aerial or buried cables.
- Straight or 'frogging' repeaters.
- Terminal for 2 complete systems with signalling and frequency generating equipment on one 9 ft. rackside.



# Distribution Problem?



*Siemens Ediswan 4-way, 4-wire  
Fuse or Link Disconnecting Box.*



**Just think of the  
equipment  
with the**

**AEI name  
behind it!**

Distribution pillars and panels—Underground disconnecting boxes, branch boxes, service boxes and straight-through joints—Indoor and outdoor terminal boxes—Indoor and outdoor service fuses—H.T. and super-tension joints and sealing ends—Overhead service accessories—Rising mains systems—House service fuses and consumers' control units—Jointing materials and accessories of every description.

**AEI CABLE DIVISION**

**Associated Electrical Industries Limited**

**DISTRIBUTION EQUIPMENT SALES DEPARTMENT**

145 Charing Cross Road, London, W.C.2 Tel: GERrard 9797



Before  
specifying  
magnetic  
materials  
consult  
this record

**HIGHEST  $\mu$  OBTAINABLE**

... is in nickel-iron alloys--  
available in all forms down  
to ultra-thin strip.

**SQUARE HYSTERESIS LOOP**

... nickel-iron alloys are the best  
materials for magnetic amplifiers  
and saturable reactors.

**LOW CURIE POINT**

associated with certain nickel alloys  
provides a temperature dependant  
permeability—a valuable  
characteristic for compensating  
and control devices.

**HIGH MAGNETOSTRICTION**

Nickel and nickel alloys make the most  
rugged and efficient transducers  
for ultrasonic equipment.

**HIGH B H. MAX**

Nickel-cobalt-aluminium-iron  
permanent magnets provide the  
maximum energy per unit volume,  
extreme stability and the greatest  
resistance to the effects of  
temperature change and vibration.

Design with Nickel-containing **MAGNETIC MATERIALS**

Send for a free publication 'Nickel-containing Magnetic Materials'



THE INTERNATIONAL NICKEL COMPANY (MOND) LIMITED THAMES HOUSE MILLBANK LONDON SW1

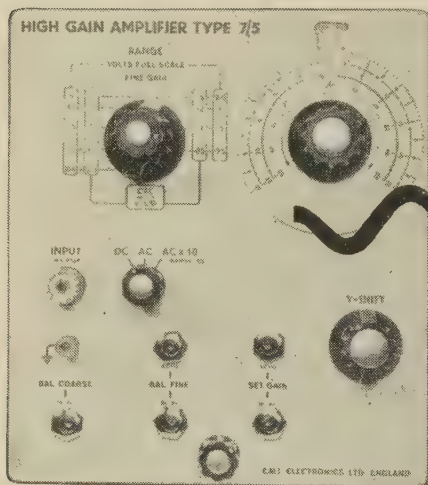
TGA GN/6



Still more versatility for the WM16! Even before this, no other oscilloscope in the same price range could equal its performance. Proved in action for over a year in government establishments, universities and industrial laboratories, the WM16 has shown itself ideal for radar, television, computers and millimicro-second oscillography, as well as for general laboratory electronic work.

Now the WM16 is given even greater versatility by the addition of 2 new plug-in units, which establish it even more firmly in a class of its own.

# 2 NEW UNITS FOR THIS HIGH PERFORMANCE 'SCOPE

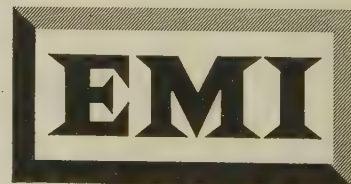
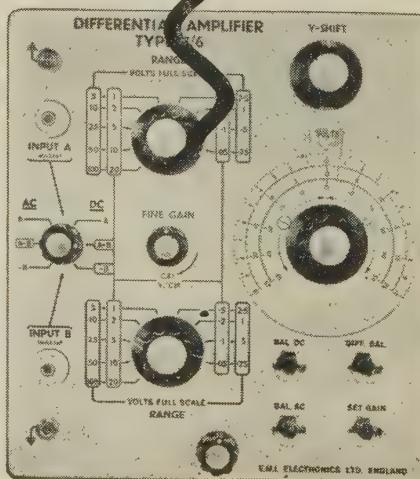
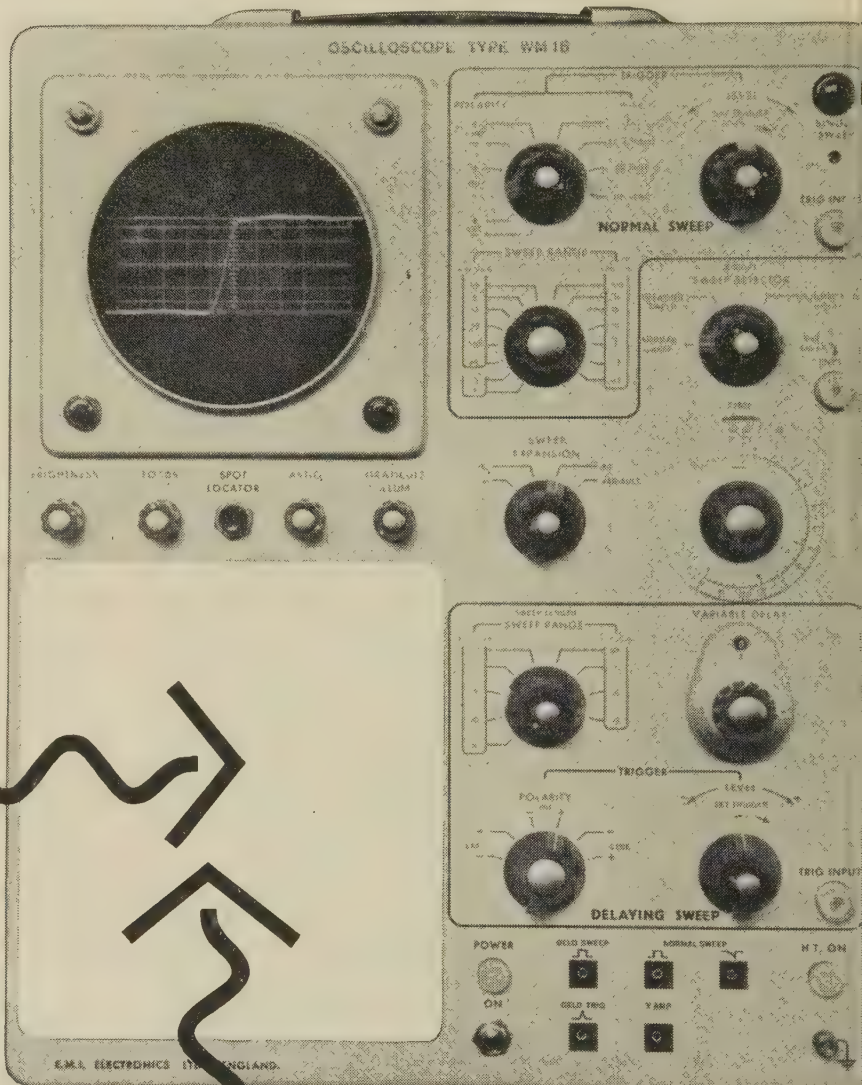


**High Gain Amplifier Type 7/5 (above)**  
High Gain, 5 mV/cm, 5 c/s - 25 Mc/s  
Normal Gain, 50 mV/cm, DC - 40 Mc/s

**Differential Amplifier Type 7/6 (right)**  
Two inputs can be displayed either separately or differentially.  
Bandwidth DC - 25 Mc/s  
Max. sensitivity 50 mV/cm  
Rejection ratio greater than 100 : 1

## General features of the WM16

Measurement accuracy 3%  
Sweep delay 1  $\mu$ sec - 150 m sec  
Normal Sweep rate 12.5 m  $\mu$ sec/cm - 0.5 sec/cm



Ask now for technical information or a demonstration of the WM16 and its new plug-in units.

**EMI ELECTRONICS LTD**

INSTRUMENT DIVISION, HAYES, MIDDYX  
TELEPHONE: HAYES 3888 EXT. 2223



# STC MICROWAVE OSCILLATORS

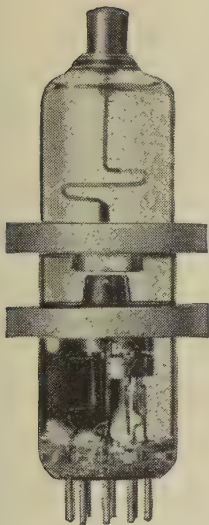
**Coaxial Line Oscillators V types**

**H-wave Oscillators V types**

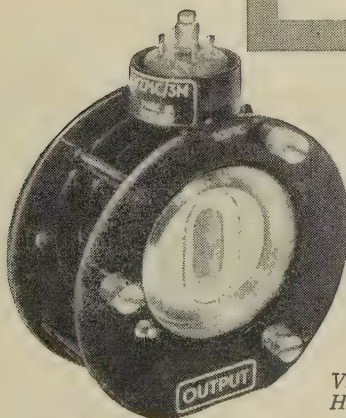
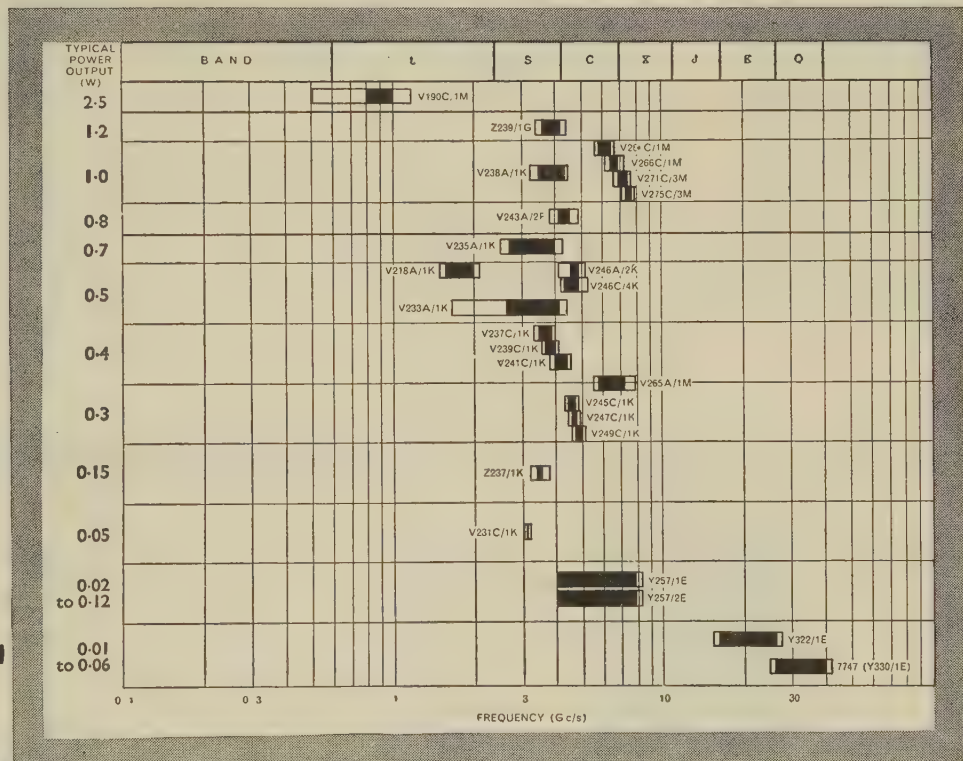
**Backward Wave Oscillators Y types**

**Reflex Klystrons Z types**

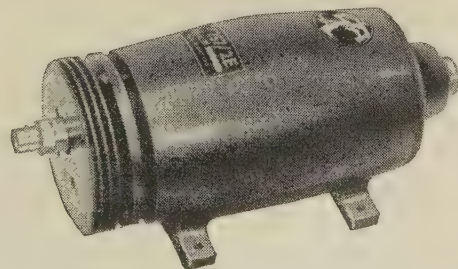
Excellent frequency stability.  
High degree of modulation linearity.  
Low working voltage.  
No forced air cooling.  
Very wide electronic frequency coverage.  
Wide electronic tuning range.  
High degree of modulation linearity.



Z237/1K



V271C/3M  
H-wave Oscillator



Y257/2E

Send for a copy  
of the new edition  
of the illustrated  
brochure "STC  
Microwave Tubes"  
MS/113.



**Standard Telephones and Cables Limited**

VALVE DIVISION: FOOTSCRAY • SIDCUP • KENT



# ALLSCOTT

## E.H.T POWER

with close regulation & ultra-smooth output



### E.H.T Power unit TYPE 1112

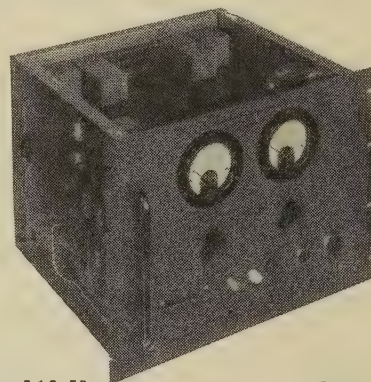
Specially designed to operate low noise Klystrons requiring up to 50 mA D.C. Adjustable from 2 to 8 kv negative to earth. D.C. heater supply included.

Fan cooled cabinet, castor mounted. Safety interlocks on all access points. Additional external safety circuits provided by jack inputs.

#### ELECTRICAL SPECIFICATION

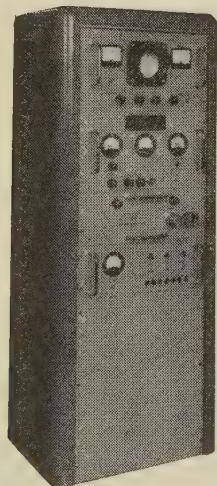
##### E.H.T. SUPPLY

Output Voltage:	2 to 8 kv negative to earth.
Output Current:	Max. 50 mA.
Regulation (no load to full load):	Better than 0.02% per mA.
Stabilisation against mains voltage variations:	Better than 0.01% per 1% mains voltage change.
Ripple:	Less than 10 mV between 50 c/s and 1 kc/s: less than 30 $\mu$ V at 1 kc/s decreasing at 3 db/octave upwards.
D.C. heater supply	0-6 volts 0-10 amps.
Mains input	50 c/s, 3 phase star.



### Multi-line power unit TYPE 244

- Eleven stabilised D.C. lines at various positive and negative voltage levels.
  - Two separate 6.4 volt heater supplies.
  - Operated from 400 c/s, 3-phase 200 volt mains. (50 c/s single-phase alternative available.)
- 19" rack mounting. Weight 67 lb.



### R.F. Spectrum analyser TYPE 306

#### analysis of fine microwave spectra

The Allscott Microwave Spectrum Analyser Type 306 represents a valuable aid to the experimenter concerned with the analysis of fine microwave spectra. It can be used over a wide video spectrum range and enables noise and line sideband components to be determined unambiguously.

The instrument has a resolution of 1 kc/s or 25 kc/s and can be used for the accurate determination of low level sideband amplitudes or noise powers in terms of the carrier power.

Full information and specifications on request.

**James Scott ELECTRONIC ENGINEERING Ltd**

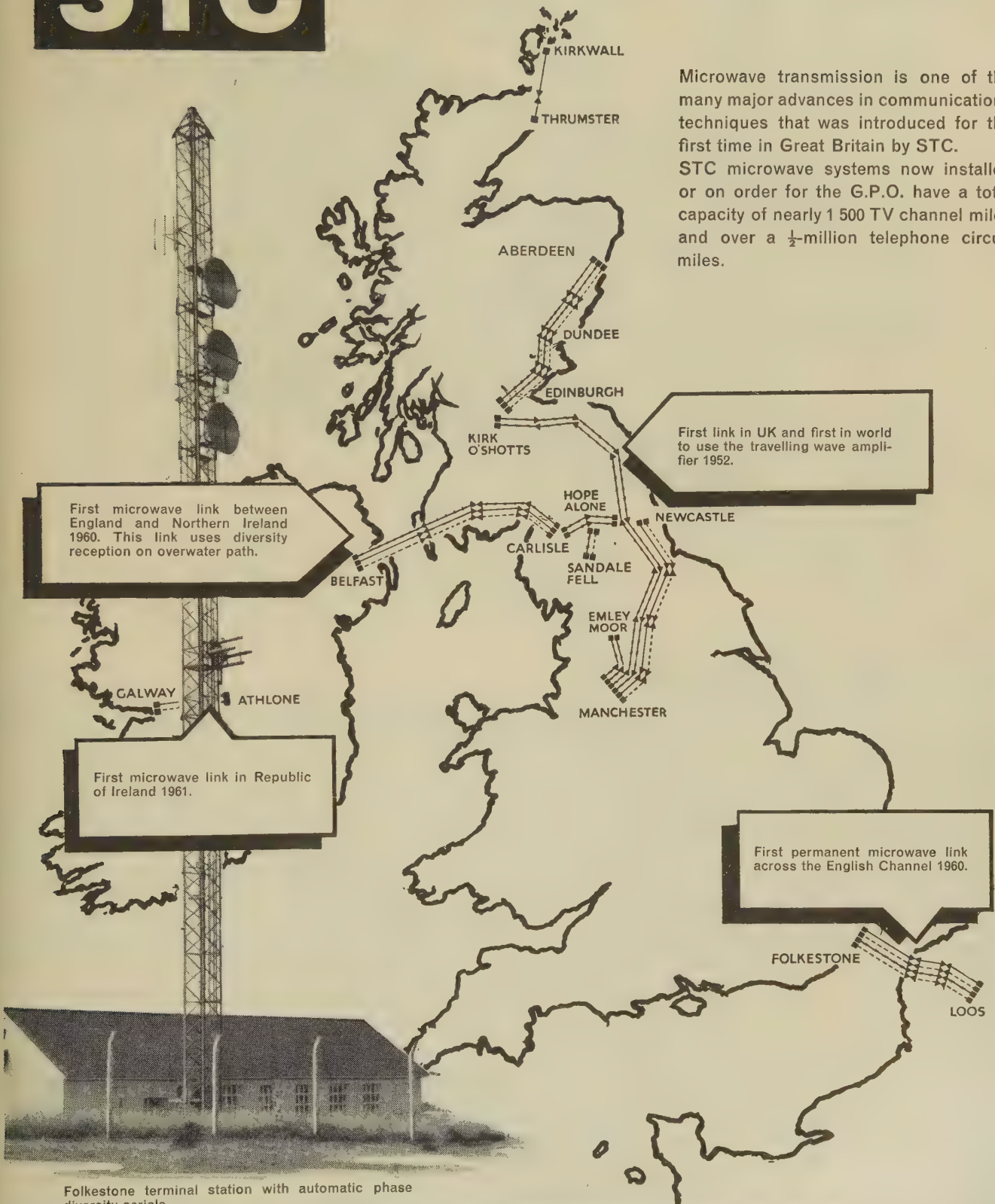
68 Brockville Street,  
Carntyne Industrial Estate, Glasgow, E.2.,  
Tel: Shettleston 4206



**STC****PIONEERS OF MICROWAVE**

Microwave transmission is one of the many major advances in communications techniques that was introduced for the first time in Great Britain by STC.

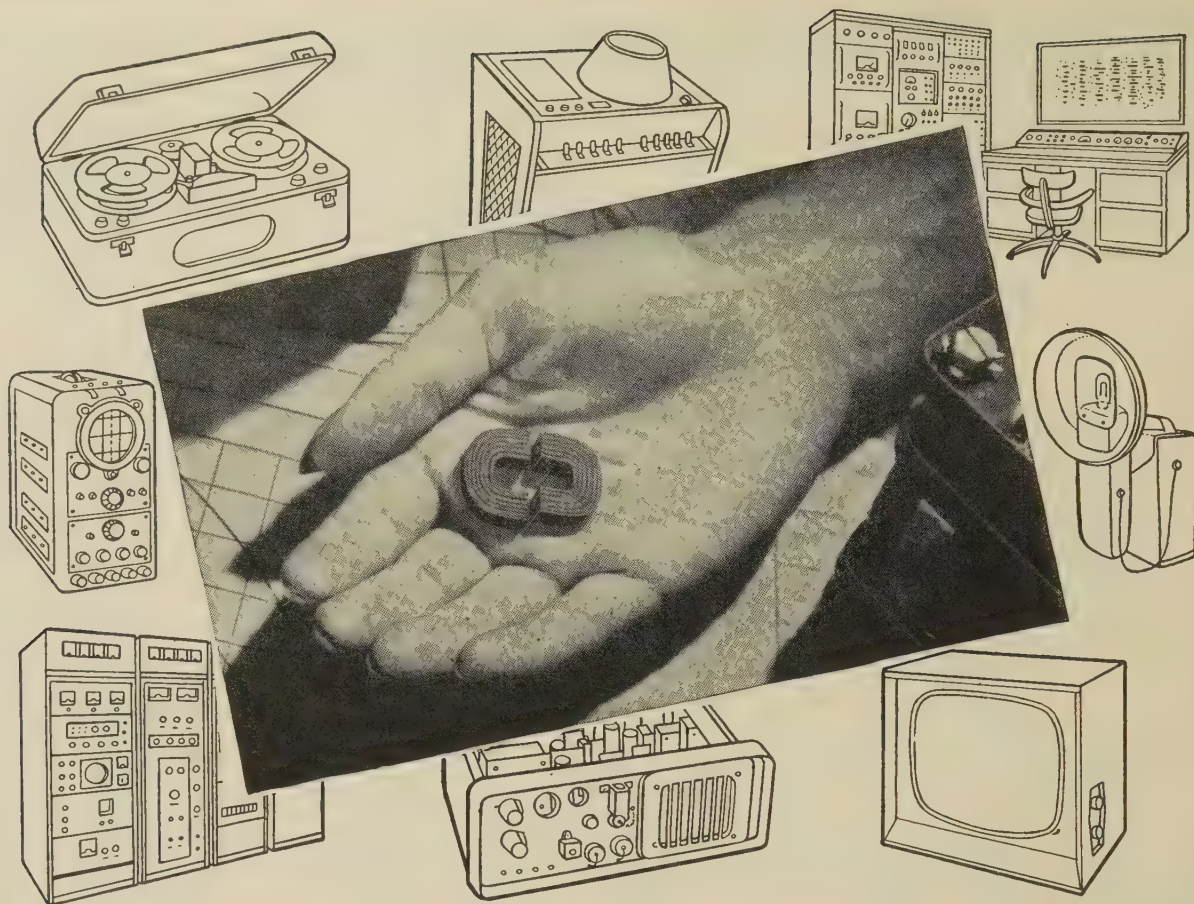
STC microwave systems now installed or on order for the G.P.O. have a total capacity of nearly 1 500 TV channel miles and over a  $\frac{1}{2}$ -million telephone circuit miles.



**Standard Telephones and Cables Limited**

TRANSMISSION SYSTEMS DIVISION: NORTH WOOLWICH · LONDON E.16





## 'C' CORES for open-type transformers

'ENGLISH ELECTRIC' 'C' cores, developed specifically to meet the exacting standards of the electronic industry, provide smaller, lighter and more efficient transformers and chokes for interservice, industrial and commercial applications. The full range of 'C' cores in .013", .004" and .002" grain-oriented steel strip complies with the requirements of the Standard Interservice range (RCL.193). Special cores can also be supplied on request.

'ENGLISH ELECTRIC' 'C' cores are suitable for use in oil filled, open type, or resin cast transformers. Clamping frames and other accessories are available and manufacturers can obtain many of their component requirements from 'ENGLISH ELECTRIC'.

*Send enquiries, or for Publication TF/239 to:  
The ENGLISH ELECTRIC Company Limited,  
Transformer Sales & Contracts Section,  
East Lancashire Road, Liverpool, 10.  
Telephone: Aintree 3641.*

**'ENGLISH ELECTRIC'**  
**'C' and 'E' cores**

THE ENGLISH ELECTRIC COMPANY LIMITED, ENGLISH ELECTRIC HOUSE, STRAND, LONDON, W.C.2  
WORKS: STAFFORD • PRESTON • RUGBY • BRADFORD LIVERPOOL • ACCRINGTON





# STANTELUM TANTALUM ELECTROLYTIC CAPACITORS

## HIGH TEMPERATURE FOIL TYPE

(POLAR & NON-POLAR)

Designed to withstand conditions of high temperature and high vibration.

Temperature Range:  
-40°C to +125°C.

Voltage Range: 6 to 100V d.c.

Capacitance Range:  
0.2 to 200  $\mu$ F.

## STANDARD FOIL TYPE

(POLAR & NON-POLAR)

Type approved to RCS 134B

Temperature Range:  
-40°C to +85°C

Voltage Range: 6 to 150V d.c.

Capacitance Range:  
0.15 to 200  $\mu$ F.

## SOLID TYPE

(POLAR)

Sintered Slug and solid electrolyte construction.

Temperature Range:  
-55°C to +85°C (to +125°C with voltage derating)

Voltage Range: 6 to 35V d.c.

Capacitance Range: 1 to 330  $\mu$ F.

## MINIATURE FOIL TYPE

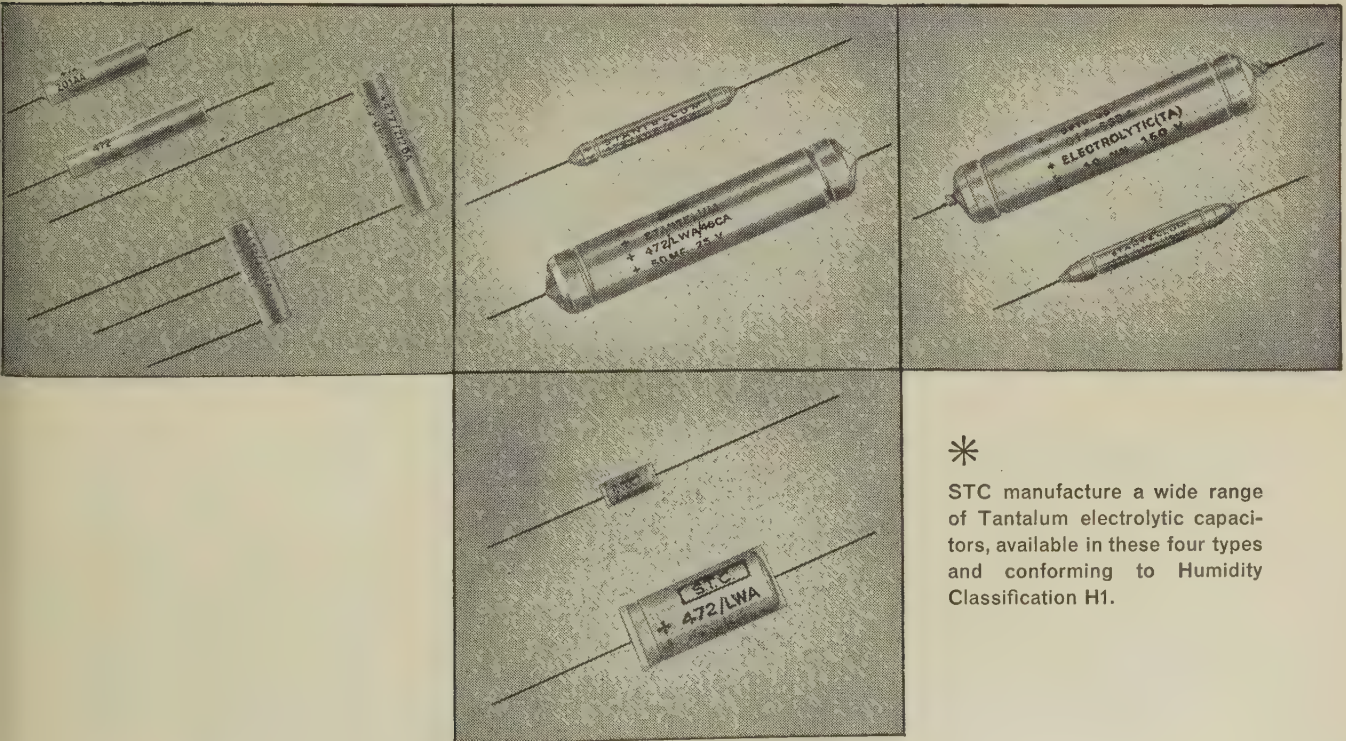
(POLAR)

A foil type tantalum capacitor in its most economical form. Available with axial or radial terminal wires.

Temperature Range:  
-25°C to +85°C.

Voltage Range: 3 to 25V d.c.

Capacitance Range: 1.5 to 16  $\mu$ F.



STC manufacture a wide range of Tantalum electrolytic capacitors, available in these four types and conforming to Humidity Classification H1.

Write for Data Sheets to:

**Standard Telephones and Cables Limited**

CAPACITOR DIVISION: BRIXHAM ROAD · PAIGNTON · DEVON



61/8MC



# CINTEL DELAYED PULS

This versatile instrument has four main outputs generating true +ve or -ve going pulses with a rise time of less than 10µsec at an output of 5V in 75Ω. Variable amplitude, width and delay are provided and the instrument is capable of either single or double pulse modes of operation.

The four main outputs of the generator are (1) a pre-pulse of fixed amplitude and width. (2) A single or double main pulse of variable width and amplitude. (3) A single or double negative going sawtooth (sweep) pulse coinciding with the main pulse. (4) A single or double cable pulse derived from the main pulse.

APPLICATIONS of this instrument can be made in many fields of research and measurement. Its comprehensive specification makes it particularly suitable for use in radio navigation, radar, television, electronics, nucleonics, computers, telemetering and physiological research. Other uses will be apparent and the more common applications are listed in a comprehensive leaflet available on written request.

## BRIEF SPECIFICATION

**PERIOD:** Continuously variable from 0.9µsec to 1.05sec corresponding with a frequency range 0.95c/s to 1.1Mc/s. Accuracy is within  $\pm 5\%$ .

**PRE-PULSE:** Fixed amplitude 8V peak in 75Ω positive going. Fixed width 60µsec.

**DELAY:** The time between the peak of the pre-pulse and the advent of the main pulse is variable from 0.9µsec to 105msec. Accuracy is within  $\pm 5\%$ .

**MAIN OUTPUT PULSE:** Continuously variable in width from 0.09µsec to 105msec with a calibration accuracy of  $\pm 5\%$ . The amplitude and impedance is controlled by a four position switch and a fine control giving a 4:1 attenuation of each maximum as follows

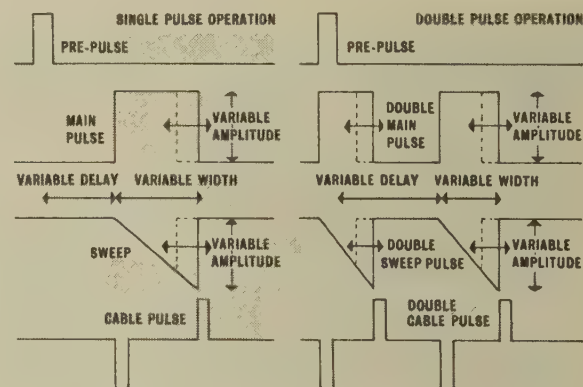
AMPLITUDE	IMPEDANCE	RISE TIME
5V max	75Ω	<10µsec
10V max	150Ω	>25µsec
25V max	600Ω	>40µsec
50V max	1000Ω	>50µsec

**POLARITY** of the output pulse can be positive or negative going with respect to earth as required. Accuracy of calibration is within  $\pm 2\%$  on all ranges except the 50V range where it is within  $\pm 5\%$ .

**THE SWEEP** waveform is a direct coupled negative going sawtooth with the same width and delay as the main pulse. The amplitude of this waveform is 15V peak at maximum width. Linearity is maintained to within  $\pm 2\%$ . Output impedance approximately 300Ω.

**CABLE PULSE** is obtained from a short circuited pure line. Two narrow output pulses are obtained, one positive and one negative going, coincident with the leading and trailing edges of the main pulse. The width of both pulses is 25µsec. The maximum amplitude is 3V peak in 75Ω and rise time 8µsec.

**DOUBLE PULSE** operation can be obtained by a setting on the front panel. Two pulses are produced, the first coincident with the pre-pulse and the second delayed on it by a selected amount.



**SYNC/TRIGGER** The generator can be synchronised or triggered by almost any externally applied waveform. The minimum amplitude levels for a sine wave being: SYNC operation 0.5V peak to peak 2Mc/s max., and TRIGGER operation 1.0V peak to peak 2Mc/s max.

SINGLE SHOT operation obtained by a push-button switch

**POWER SUPPLY** . . . 110-120V and 200-250V a.c. in 10V steps 40 to 60 c/s

**POWER CONSUMPTION** . . . 200W

**DIMENSIONS** . . . 22½" wide x 15" deep x 21" high (57 x 38 x 53 cm.)

**WEIGHT** . . . . . 90 lbs. (41 kilos).

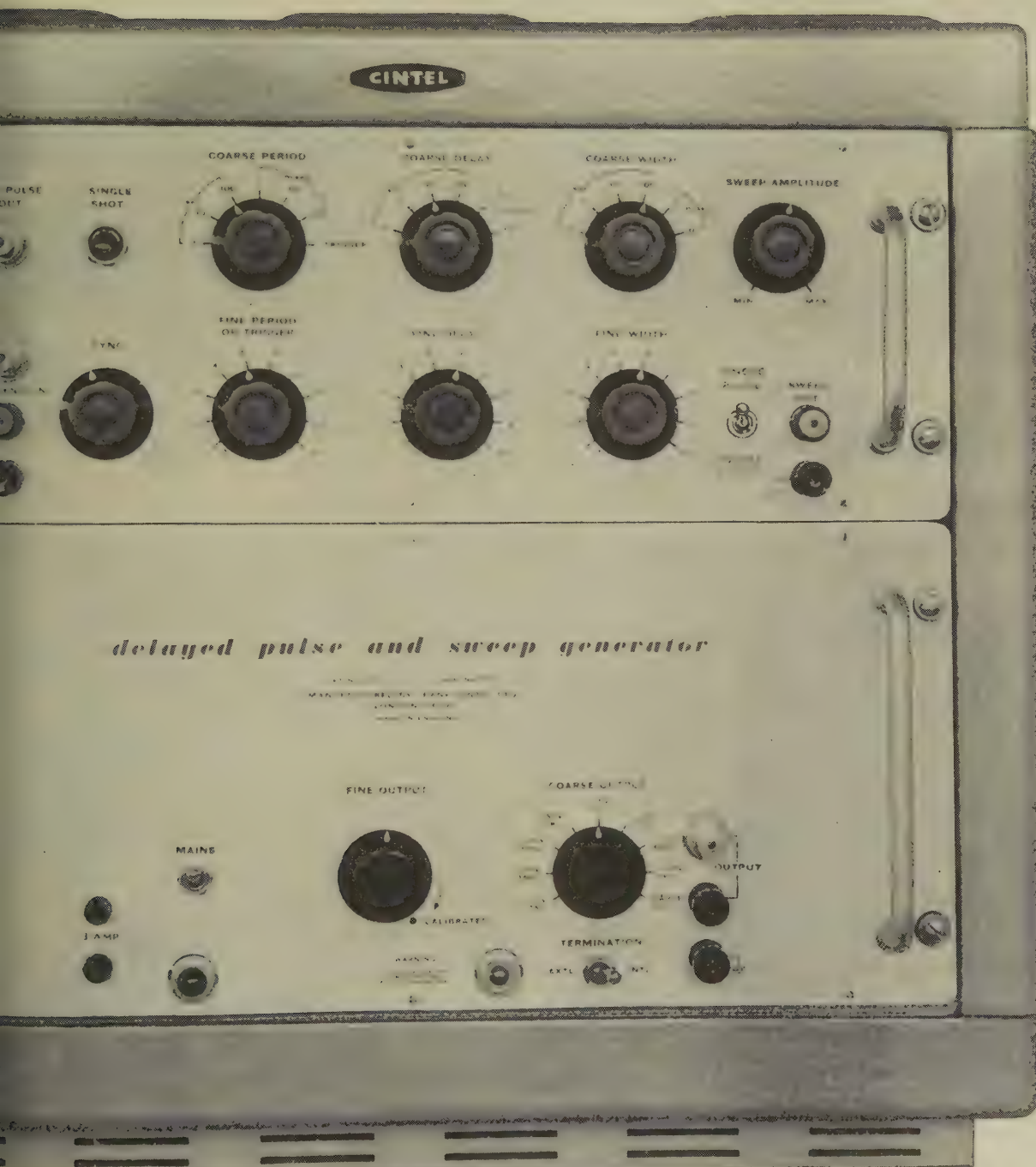


# RANK CINTEL LIMITED

Worsley Bridge Road, Lower Sydenham, S.E.26. Hither Green 4600

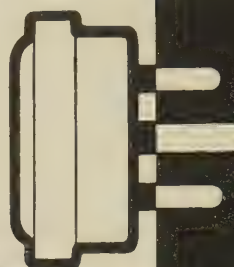


# SWEEP GENERATOR

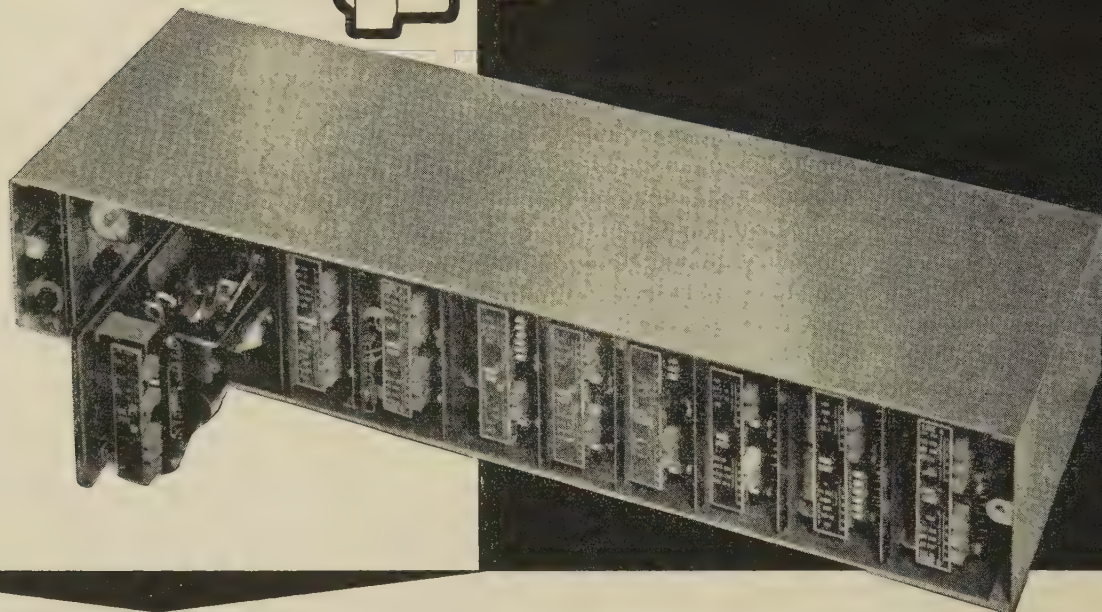




# As simple as



# ...plugging in the light!



## THE ERICSSON RURAL CARRIER TELEPHONE SYSTEM TYPE R.C.101

- LOWER POWER CONSUMPTION
- BATTERY OR OPTIONAL MAINS OPERATION
- TRANSMITTED CARRIER FOR AUTOMATIC GAIN CONTROL AND SIGNALLING
- INTERCHANGEABLE SIGNALLING UNITS
- TRANSISTOR CIRCUITS
- COMPANDOR UNITS OPTIONAL
- AMPLE TEST POINTS
- ONE 10 CHANNEL TERMINAL ACCOMMODATED ON A WALL MOUNTING RACK 3' 3" HIGH
- SIMPLE INSTALLATION
- PORTABLE TEST SET AVAILABLE

Designed to combine ease of maintenance with small physical size and low power consumption, it is particularly suitable for use in remote areas where personnel trained to service carrier equipment may be limited. A fault may be cleared by substituting a spare for each plug-in unit in turn until the service is restored.

The system will provide up to ten additional speech circuits on an open wire line. The circuits are stackable and thus extra circuits may be added as demand increases. This feature together with a wide range of pole mounted "drop-off" filter units offers a high degree of system flexibility. Channel re-allocation is easily achieved with this system of plug-in sub-units.

Illustrated above is a **SINGLE CHANNEL TERMINAL** (less panel cover) with mains power unit and compandor units fitted.

For further information please write to:—



## ERICSSON TELEPHONES LIMITED • ETELCO LIMITED





**GLASS-METAL SEALS**  
SIEMENS EDISON SWAN LTD

*introducing*

**TRANSISTOR HEADERS**  
AND ENCLOSURES

**SIEMENS EDISON SWAN**

SIEMENS EDISON SWAN LIMITED

**WRITE FOR THEM!**

Do you make hermetically sealed devices involving electrical connections? If you do send for these two booklets about "Ediswan" Transistor Headers and Glass to Metal Seals. You need this information at your finger tips when you're buying seals or headers because a lot of seal-making experience that you don't get anywhere else goes into both these "Ediswan" product ranges.

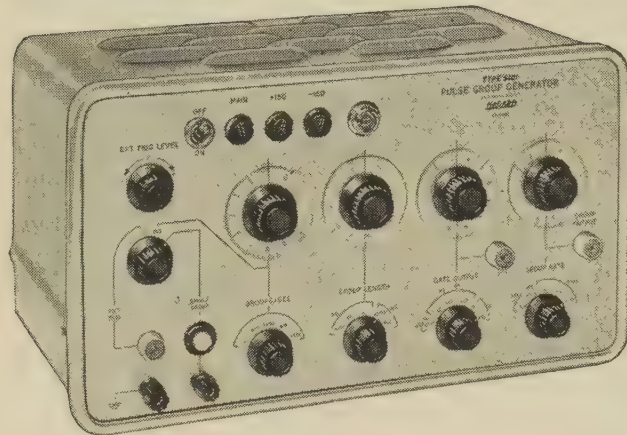
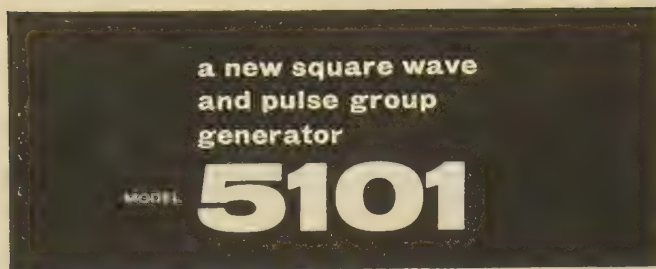
**Associated Electrical Industries Ltd**

Radio and Electronic Components Division

PD 16, 155 Charing Cross Road, London, W.C.2

Telephone GERRard 9797. Telegrams Sieswan Westcent London





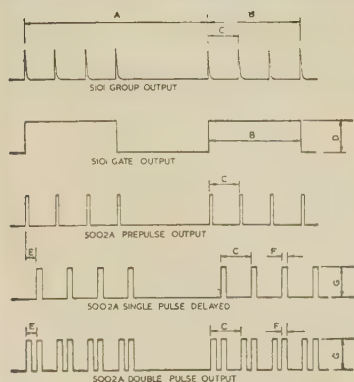
A study of the diagram may suggest how this instrument can be of use in your specific problem.

Calibrated and continuously variable groups of pulses, plus square wave output of continuously variable amplitude 100  $\mu$ V to 100 volts. Versatile triggering system, external or internal. Single groups of pulses by push button. For use with the NAGARD 5002 Double Pulse Generator or any other generator capable of being externally triggered.

IDEAL FOR COMPUTER TESTING by providing a simulated programme of pulses controllable in a great variety of ways.

If you already have a Nagard 5002 Pulse Generator the 5101 will extend its usefulness, besides being a good square wave generator and triggering device when used by itself.

Ask for data sheet No. 6610.



A - 1-100,000 GROUPS PER SEC.  
B - 5 $\mu$  SEC. TO 0.5 SEC. GROUP LENGTH  
C - 10Hz - 1MHz FREQUENCY IN GROUP  
D - SQUARE PULSE 100V-100V POSITIVE GOING  
E - 0.2 $\mu$  SEC. TO 2 SEC. DELAY  
F - 0.1 $\mu$  SEC. TO 1 SEC. PULSE WIDTH  
G - 200 $\mu$ V - 50V POSITIVE OR NEGATIVE

18 AVENUE ROAD,  
BELMONT, SURREY  
Tel: VIGilant 9161-2

**NAGARD**  
LTD

**ADCOLA**  
(Regd. Trade Mark)

**Soldering  
Instruments**

ILLUSTRATED

$\frac{3}{16}$  DETACHABLE BIT  
MODEL, List 64  
IN PROTECTIVE SHIELD  
WITH ACCESSORIES,  
List 700

THE WIPING PAD REDUCES  
THE DESTRUCTIVE PRACTICE  
OF BIT FILING

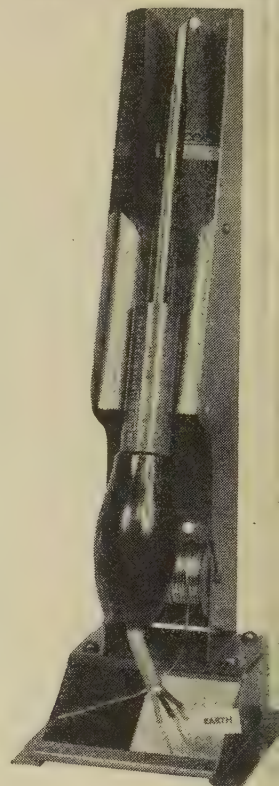
British and Foreign Pats.  
Reg. design, etc.

For further information apply Head Office:

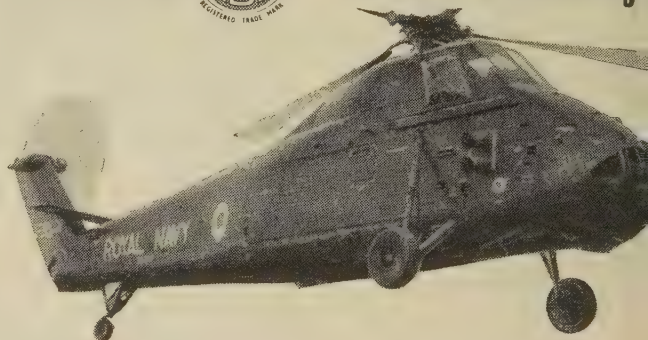
**ADCOLA PRODUCTS LTD.**  
**ADCOLA HOUSE**  
**GAUDEN ROAD**  
**CLAPHAM**  
**LONDON S.W.4**

Tel: MAC 4272 & 3101

Telegrams: SOLJOINT, LONDON S.W.

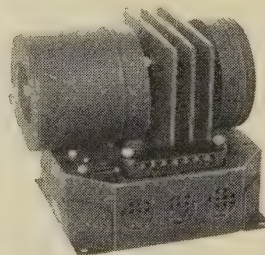


When does "take off" vertically



... when the Westland Wessex 1 rises from the ground.

Newton Derby Voltage Regulators are a vital part of the electrical system in this turbine-driven machine which is in quantity production for the Royal Navy and which is fitted with automatic equipment to allow operation by day and by night, in all weathers, from ship or from shore.



- Motor Generator Sets
- Permanent Magnet Alternators
- Transistor Converters
- High Frequency Alternators (400 to 3,000 c.p.s.)
- Automatic Voltage Regulators
- Servo Motors
- Rotary Transformers and Converters

**NEWTON  
DERBY**

**NEWTON BROS. (DERBY) LIMITED**  
**ALFRETON ROAD, DERBY**

Telephone : Derby 47676 (4 lines). Grams : DYNAMO DERB  
London Office: IMPERIAL BUILDINGS, 56 KINGSWAY, W.C.



# AEI NEW SOLID STATE MICROWAVE SWITCH

R MICROWAVE SWITCHING, MICROWAVE DIODE PROTECTION, CW AERIAL SWITCHING AND CW SIGNAL MODULATION AT BANDS FROM S TO X INCLUSIVE

## ADVANCE INFORMATION

### OUTSTANDING FEATURES

★ LOW VOLTAGE OPERATION ★ LOW POWER CONSUMPTION  
SMALL SIZE AND LOW WEIGHT ★ EXCELLENT FORWARD TO BACK ATTENUATION RATIO

### FEATURES

operation for 25 db of attenuation. High voltage supplies not required. Its lightness and ruggedness lends itself to applications where weight and space are at a premium.

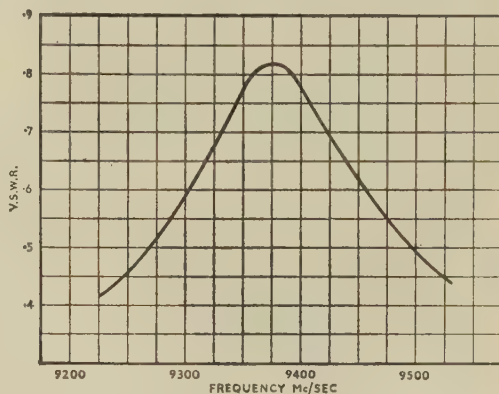
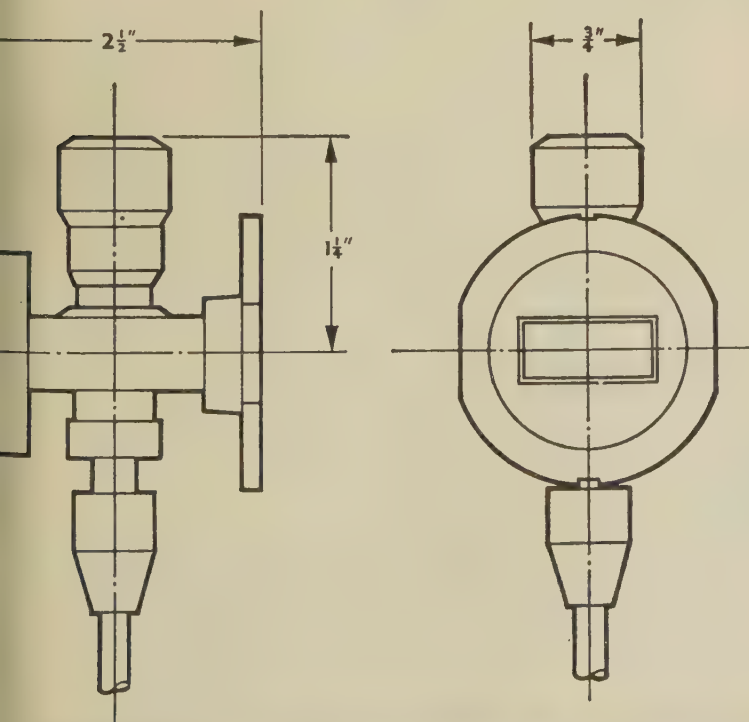
### TYPICAL SPECIFICATION

Operating Voltage:—	1.5 volt max.
Operating Current:—	20 mA max.
Insertion Loss:—	1 db max.
Attenuation range:—	1 db to 25 db*
Power Handling Capacity	
a) pulsed line power:—	500 watts peak max.
b) CW line power	10 watts max.
Bandwidth (fixed mount)†:—	100 mc/s
Minimum switching time:—	0.5 microseconds max.°

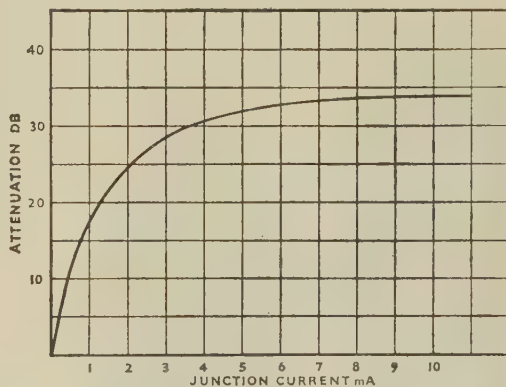
\* corresponds to varying the applied voltage between 0 and 1.5 volts.

† available mounts will be available shortly to cover S and X bands respectively.

° depending on power level.



V.S.W.R. Frequency Response for P-N Switch Type BS.336



Attenuation—Junction Current Graph for P-N Switch Type BS.336

### PLEASE DON'T TEAR OUT THIS ADVERTISEMENT—

Others will want to see it. If you would like to have full details of these or any other AEI electronic components for that matter, all you have to do is write to AEI at the address below. Data sheets with detailed information will be sent to you without charge.

**DON'T DELAY—**write now and be sure of receiving latest news of these and other AEI components as they become available.



**AEI**

**Associated Electrical Industries Limited**

ELECTRONIC APPARATUS DIVISION, VALVE & SEMI CONDUCTOR SALES DEPT.  
CARHOLME ROAD • LINCOLN • TEL: LINCOLN 26435

A 5686

SOLID STATE MICROWAVE SWITCH





ENGLISH ELECTRIC



NATURAL COOLED

# TETRODES

FOR COMMUNICATIONS & INDUSTRY

The English Electric Valve Co. Ltd. offers a range of natural cooled tetrodes for the lower power communication and industrial application. The majority of the types in this range, comprising both single and double tetrodes, are capable of operation, at full ratings, well into the V.H.F. band—up to 250 Mc/s in the case of the C178A/5894. Even higher frequencies may be attained with suitable de-ratings. All are equivalents or near equivalents to American and CV types.

For full details of these valves please write to the address below.

	E.E.V. Type	American Type	British Services Type	Operating Frequency Mc/s	Max. Anode Dissipation (W)
FOR NEW EQUIPMENTS	4D32	4D32	CV3543	60	50
	C178A/5894	5894	CV2797	250	20+20
	C1108	4-125A*	CV2130	120	125
	C1112	4-250A*	CV2131	75	250
	C1134	6252 *	CV2799	150	10+10
MAINTENANCE	813	813	CV26	30	100
	829B	829B	CV2666	200	20+20
	832A	832A	CV788	200	7.5+7.5

\* Near equivalent

ENGLISH ELECTRIC VALVE COMPANY LIMITED

AGENTS THROUGHOUT THE WORLD

Chelmsford, England. Telephone: Chelmsford 3491



# STATIC FIELDS in ELECTRICITY and MAGNETISM

D. H. Trevena

268 pages

Price 35s.

Based on lectures the author has delivered over the past eight years to students at the University College of Wales, Aberystwyth, the book is concerned with the three main topics of electrostatics, magnetism and the magnetic fields of steady electric currents. The use of such concepts as the magnetic pole and the magnetic shell have been included, the latter because the author feels that all students should be aware of the elegance of this method. The problematic question of units, including M.K.S. units, is fully discussed and worked examples have been included throughout.

# AUTOMATIC and REMOTE CONTROL

Proceedings of the First International Congress  
of the International Federation of Automatic Control  
(I.F.A.C.) Moscow 1960

Editor: J. F. Coales

Co-Editors: J. R. Ragazzini and A. T. Fuller

Four Volumes

Price £45 the set

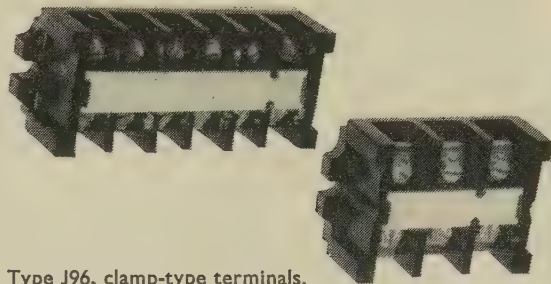
Individual Volumes £12 each

These volumes which are expected to be published in October 1961 contain the papers read at the First International IFAC Conference (Moscow 1960) together with the ensuing discussions. The Russian papers have been translated into English and are published in full. The papers reflect the most recent work in many countries and are divided into three principal sections. 1—Theory. 2—Components. 3—Applications. The first section contains papers dealing with the present state of the theory of continuous and discrete systems, the theory of structures, stochastic and special mathematical problems of automatic control. In the second section the papers are devoted to the theory and practical work of designing electric, magnetic and pneumatic elements of control systems, programming and computing devices, controlling computers and systems of automatic control. The final section deals with design principles and the practical industrial application of automatization in machine-building; metallurgical and chemical industries amongst others.

**BUTTERWORTHS**  
**4-5 BELL YARD,**  
**LONDON, W.C.2**

# Decide on Donovan

## TERMINAL BLOCKS



Type J96, clamp-type terminals.

White marker strip, generous clearance between phases and to earth. Sizes available: 15-amp. 550-volt, 3, 4, and 6-way. 30-amp. 550-volt, 3 and 4-way. C.S.A. approved. As standard without alteration.

## A.C. POWER RELAYS



Type A.11. Available 2, 4, or 8-pole (with one or two coil circuit change-over contacts), fine silver double-break main contacts rated at 15-amp. 550-volt. Any pole can be N.O. or N.C. Available C.S.A. approved. Illustrated is a 4-pole enclosed relay.



# DONOVAN

Manufacturers of Industrial Contactor Gear & Allied Equipment

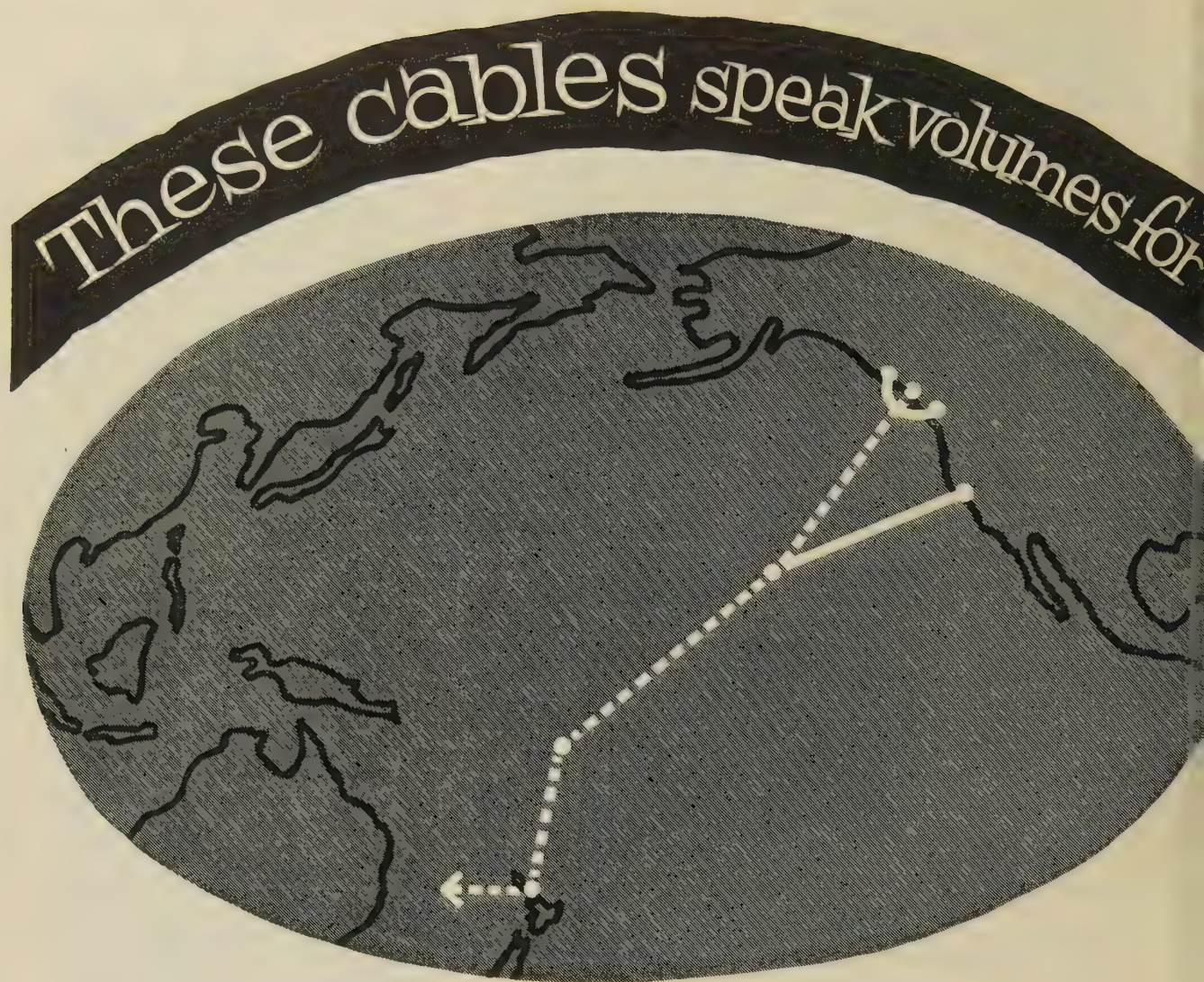
**THE DONOVAN ELECTRICAL CO. LTD.**

Granville Street, Birmingham 1

Depots: LONDON, 149-151 YORK WAY, N.7.  
GLASGOW, 22 PITT STREET, C.2.

Sales Engineers available in LONDON — BIRMINGHAM  
MANCHESTER — GLASGOW — BELFAST — BOURNEMOUTH





Fathoms below the Atlantic and the Pacific, mighty cables carry myriads of voices from wind-swept shores to palm-fringed islands ... from ice-bound ports to sun-scorched cities. Unseen, but playing a vitally important part is TMC CARRIER TELEPHONE EQUIPMENT, helping to narrow the distance between continents that were once, communicationally speaking, far apart.

*Full information about TMC 2 kc/s, 3 kc/s and 4 kc/s Spaced Carrier Telephone Equipment can be obtained simply by writing to the address below.*



**TELEPHONE MANUFACTURING COMPANY LIMITED**

Transmission Division: Cray Works, Sevenoaks Way,  
St. Mary Cray, Orpington, Kent. Telephone: Orpington 26611





Connects Seattle to Ketchikan (Alaska).

Extending from San Francisco to Hawaii.

From Vancouver to Hawaii, Fiji and New Zealand (to be extended to Australia), known as COMPAC.

From Oban (Scotland) to Clarenville (Newfoundland) extending to Sydney Mines (Nova Scotia). This system is known as TAT1.

From Oban to Cornerbrook (Newfoundland), known as CANTAT.

Begins at Gairloch on the west coast of Scotland and extends to Torshavn (Faroes). Thence to Reykjavik (Iceland), known as SCOTICE.

Linking Vestmannaeyjar in Iceland with Frederiksdal (Greenland) and Cornerbrook, Newfoundland — called ICECAN.

Starts at Manahawkin (U.S.A.) terminating at Bermuda.

From Florida to Jamaica, Curacao and Venezuela.

From Widemouth (Cornwall) to Manahawkin (U.S.A.) known as TAT3.

## SELLING AGENTS

**Australia and New Zealand:**  
Telephone Manufacturing Company (A'sia) Proprietary Limited, Sydney, New South Wales.

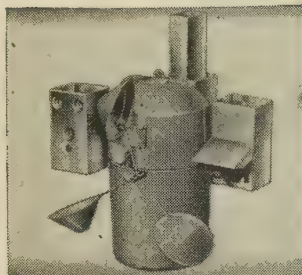
**Canada and U.S.A.**  
Telephone Manufacturing Company Limited, Toronto, Ontario.

Also represented in other countries.



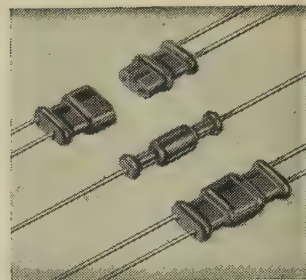


# Radio Sonde and electronic equipment

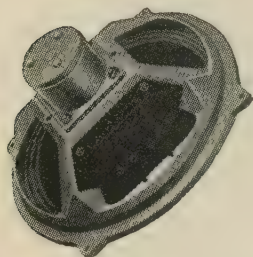


Radio Sonde Transmitter, supplied to British meteorological Office and foreign governments.

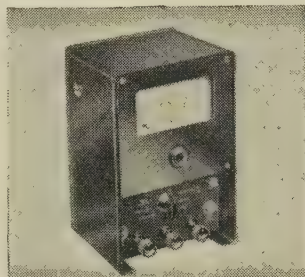
The items shown here are representative of the extensive variety of products manufactured by the Whiteley organisation. Our technical resources are available for the development and production of specialised components for the electronic industry.



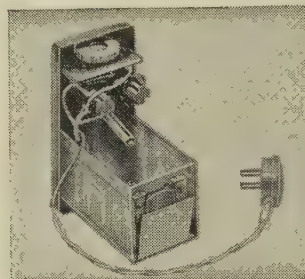
Waterproof plugs and sockets moulded in Polythene for underwater or outdoor installation.



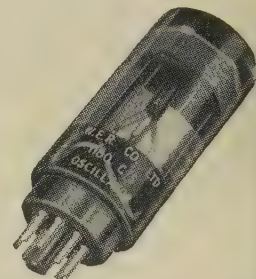
Stentorian Cambric Cone Units, recognised throughout the world as the greatest value in High Fidelity.



The Post Office Tester is a multi-range meter used for making tests on subscribers' apparatus and lines.



Potted components and assemblies in epoxy, Polyester resins and Polythene.



This fixed frequency oscillator constructed on a standard octal base and encapsulated in epoxy resin.

**WHITELEY ELECTRICAL RADIO CO. LTD • Mansfield • Nottingham**

## PAPERS FOR THE PROCEEDINGS

**Handbook for Authors** Anyone who is thinking of submitting a Paper to The Institution should apply to the Secretary for a copy of the **Handbook for Authors**. The price is 3s. (post free), but a copy will be supplied free of charge if the application is accompanied by a summary of the Paper. The following are some of the main points considered in the Handbook.

**Acceptability** To be acceptable, a Paper should normally contribute to the advancement of electrical science or technology. The Institution does not accept Papers which have been published elsewhere.

**Length** No Paper should occupy more than 10 pages in the *Proceedings*. Authors can generally keep well within this limit. For example, the average Paper published in 1960 consisted of 6 000 words (5 pages) and, with its illustrations and mathematics, occupied a total of 8 pages.

**Summary** An essential part of a Paper is the **Summary**, which should not exceed 200 words.

**Text** The Text should begin with sufficient introductory matter to enable the Paper to be understood without undue reference to other publications.

The Text should include no more mathematics than is essential. Extended mathematical treatment and lengthy digressions—if they must be included—should be put in **Appendices**.

Proprietary articles should not be mentioned by name unless this is unavoidable.

The rationalized M.K.S. system of units is preferred.

**Acknowledgments** Assistance in the preparation of the Paper, and sources of information, should be acknowledged. References to manufacturers should be made only under **Acknowledgments**.

**Bibliographical References** should be numbered and listed in a special section, and indicated in the Text by means of 'indices'.

The Text should be appropriately sectionalized, the sections and their subdivisions being numbered according to the 'decimal' system. Acknowledgments, References and Appendices should be numbered as though they were sections of the Text.

Typing should be on one side of the paper only, with double spacing between lines and a 1½ inch margin on the left. Besides the original typescript, two carbon copies are required by The Institution.

Advice on the typing of mathematics is given in the **Handbook for Authors**, which includes a facsimile of a typewritten page containing mathematics.

Illustrations should not be drawn or pasted on the typewritten pages. They are of no use to the printer, but he does need a complete list of captions, again with double spacing. The list should be attached to the typescript.

Three sets of drawings, which may be in the form of dye-line prints, should accompany the typescript. Tracings, which will be required later, should be in indian ink with the lettering in pencil. The reduction in the size of the drawings, and therefore the size of lettering required, is not settled before the Paper has been accepted.

The typescript and illustrations should be packed flat, not rolled, and addressed to *The Secretary, The Institution of Electrical Engineers, Savoy Place, London, W.C.2.*

**References**

**Numbering**

**Typing**

**Drawings**

**Dispatch**

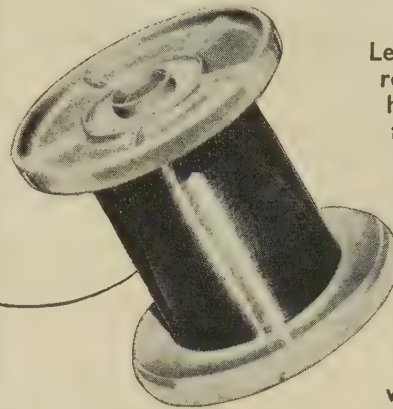


# LEWCOS

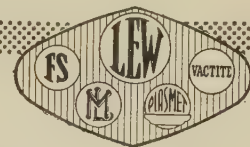
*insulated  
resistance  
wires*

## FOR ALL RESISTORS

Supplied with standard coverings of  
cotton, silk, rayon, enamel and glass.



Lewcos insulated resistance wires have been used for many years for winding resistances for instruments, radio, control apparatus, etc. These fine and superfine wires meet the demands of the Electrical Industry for high precision and exceptional properties.



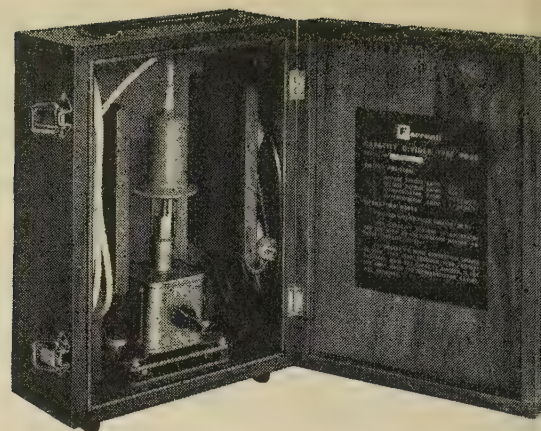
THE LONDON ELECTRIC WIRE CO. & SMITHS LIMITED LEYTON LONDON • E.10

### INDEX OF ADVERTISERS

Acicola Products Ltd.	ad 32	International Nickel Co. (Mond) Ltd.	ad 21
Arrow Electric Switches Ltd.	ad 15	London Electric Wire Co. and Smiths Ltd.	ad 39
Associated Electrical Industries Ltd.	ad 13, 20, 31 and 33	Marconi Instruments Ltd.	ad 11
Automatic Telephone and Electric Co. Ltd.	ad 6, 7 and 19	Marconi's Wireless Telegraph Co. Ltd.	ad 1, 3, 5 and 9
Batterworths	ad 35	Mullard Equipment Ltd.	ad 2
BA (A.R.L.) Ltd.	ad 10	Nagard Ltd.	ad 32
Bewhurst and Partner Ltd.	ad 4	Newton Bros. (Derby) Ltd.	ad 32
Bonovan Electrical Co. Ltd.	ad 35	Plannair Ltd.	IBC
EMI Electronics Ltd.	ad 22	Plessey Co. Ltd.	ad 8 and 12
English Electric Co. Ltd.	ad 26	Rank Cintel Ltd.	ad 28 and 29
English Electric Valve Co. Ltd.	ad 34	James Scott Electronic Engineering Ltd.	ad 24
Ericsson Telephones Ltd.	ad 30	Standard Telephones and Cables Ltd.	ad. 23, 25 and 27
Electric Resistor Ltd.	ad 14	Telephone Manufacturing Co. Ltd.	ad 36 and 37
Eranti Ltd.	ad 40	Whiteley Electrical Radio Co. Ltd.	ad 38
General Electric Co. Ltd.	ad 16, 17 and 18		



# FERRANTI CAPACITY DIVIDER



## TYPE PD30

- \* Measures accurately high voltage pulses up to 30 kV.
- \* Incorporates differentiation circuits for measuring rate of rise.
- \* Suitable for laboratory use or for permanent installation.



### Specification and Ratings :

Top Capacitance :	$3.4 \pm 0.2$ pf
Total Load Capacitance :	6 pf. max.
Applied Voltage :	30 kV. max.

### Ratios :

Position 1 :	250:1
Position 2 :	500:1
Position 3 :	7.5kV/μs/V.
Position 4 :	5.0kV/μs/V.

**FERRANTI**  
*First into the Future*



The Institution is not, as a body, responsible for the opinions expressed by individual authors or speakers. An example of the preferred form of bibliographical references will be found beneath the list of contents.

# THE PROCEEDINGS OF THE INSTITUTION OF ELECTRICAL ENGINEERS

EDITED UNDER THE SUPERINTENDENCE OF W. K. BRASHER, C.B.E., M.A., M.I.E.E., SECRETARY

VOL. 108. PART B. No. 42.

NOVEMBER 1961

621.397.621

The Institution of Electrical Engineers  
Paper No. 3564 E  
May 1961  
©

## THE BANANA-TUBE DISPLAY SYSTEM

A New Approach to the Display of Colour-Television Pictures

By P. SCHAGEN, Ph.D.

(The paper was first received 17th November, 1960, and in revised form 10th February, 1961. It was published in May, 1961, and was read before the ELECTRONICS AND COMMUNICATIONS SECTION 15th May, 1961.)

### SUMMARY

An introduction is given to the concept of colour-display systems with mechanical field-scan. The optical elements are of fundamental importance to this kind of display and various optical aspects are discussed, including the advantages of direct-viewing systems over projection, the application of cylindrical optical elements and the size of moving optical elements in relation to the required picture size. This discussion leads to the basic concept of a rotating mirror—or lens drum with a magnifying cylindrical mirror.

The fundamental properties of these two solutions are compared and the favoured system with the banana tube is described in detail. The basic requirements of this system with respect to the design of the tube, the optical elements and the mechanical components are dealt with. Finally, some inherent advantages of the present system are discussed and possible further improvements are mentioned.

### (1) INTRODUCTION

A typical feature of the post-war era has been the rapid expansion in the field of electronic devices. The most spectacular example of this expansion has been the establishment of television as a means of mass entertainment. In nearly every case the introduction of television in a country has been followed by an extremely rapid build-up of receivers in the homes. It might therefore be considered rather surprising that the growth of colour television has been comparatively slow, even in a country like the United States, where colour programmes have now been transmitted for a number of years.

The main reason for this reluctance on the part of the public to buy a receiver with the added attraction of colour is undoubtedly an economic one. Whereas the price of a monochrome receiver is by no means low for a person of average means, its possession does mean the difference between being able to view and not to view. The addition of colour, on the other hand, can only enhance the pleasure of viewing a programme which could be seen anyway in monochrome on an ordinary receiver, and therefore may not warrant a receiver

price which is two to three times as high. It is, however, generally accepted that this is not the only reason, since a proportion of the public always appears to be prepared to pay a higher price for additional features, even where they are only of secondary importance from a utilitarian point of view.

Apart from the economic aspect, the slow advance of colour television can probably be traced to a general distrust on the part of the public of the level of technical perfection achieved in present-day colour receivers. Owing to the much more complex nature of the cathode-ray tube and the electrical signals to be handled, it is more likely that slight maladjustments in the receiver will deteriorate the picture quality and lead to serious colour errors, which can be far more objectionable than the picture deterioration due to maladjustments in a monochrome receiver. Reports of early colour receivers needing a 'resident engineer' to maintain picture quality have probably created a bad impression which may have survived subsequent improvements. The fact remains, however, that even the later colour receivers are much more critical in this respect than monochrome receivers.

Some additional unfavourable features of colour receivers are mainly due to the display element which is now generally used, the shadow-mask tube. The maximum scanning angle achieved up to the present in these tubes does not exceed  $70^\circ$ , which leads to a large depth of cabinet, as in the earlier monochrome receivers. With these the trend has been to increase the scanning angle and reduce the depth of cabinet, leading to an aesthetically more acceptable design of cabinet. A colour picture of high quality can only be maintained on these tubes at comparatively low levels of ambient illumination owing to the limited picture brightness obtainable, which is still below that of a monochrome tube, and owing to the loss of colour saturation as a result of the reflected white light. Finally, the complex nature of the shadow-mask tube leads to a high manufacturing price and therefore the tube-replacement cost is well above that of a monochrome cathode-ray tube.

In view of this situation a programme was started in 1955 to investigate a possible alternative method of colour-television

Dr. Schagen is at the Mullard Research Laboratories.



display. A critical survey was made of the existing and proposed devices. In nearly every case the picture is presented on the screen of a cathode-ray tube containing a 2-dimensional array of phosphor elements luminescing in the three primary colours under electron bombardment. For a picture with high definition, the size of the phosphor elements, in at least one dimension for a line pattern and in both dimensions for a dot pattern, must be considerably smaller than the size of a picture element to enable the generation of the three primary colours within each element. The problem of striking the correct phosphors with the appropriate intensities of the scanning electron beam necessitates the use of masks, grids or reflex elements which must be located with a very high degree of accuracy in relation to the screen.<sup>1-4</sup>

The alternative approach, of a projection system employing three small tubes, each with a screen luminescing in one of the primary colours, appeared to be at least as expensive and has other deficiencies with respect to picture quality.

It was therefore decided to investigate the possibility of using a cathode-ray tube where a single repetitive line scan was produced in the three primary colours, combined with auxiliary means outside the tube for shifting the apparent position of the line to produce the required field scan. A cathode-ray tube of this kind could obviously be manufactured at only a fraction of the cost of any of the proposed 2-dimensional types of display tube, thus leaving a generous margin for the cost of the additional equipment to produce the field scan. Such a system seemed to offer at least the possibility of a reduction in manufacturing price of the receiver combined with a much lower cost of tube replacement.

A widely ranging study of auxiliary field-scan methods<sup>5</sup> finally led to the development of what has been termed the 'banana-tube' display system,<sup>6</sup> which in its present form is discussed in detail in companion papers. It may be useful to point out at this stage that this display system is still in a purely experimental phase and that the preliminary results given in these papers are not intended to serve as proposals for a fully developed domestic receiver.

## (2) OPTICAL SYSTEM

### (2.1) General Discussion of the Optical System

Various methods of effecting the vertical displacement of the line in order to constitute the picture can be visualized. In general, however, the picture can be presented in either of two basically different ways.

#### (2.1.1) Projection.

In the first method the line as displayed on the narrow screen in the tube is projected on to a diffusing viewing screen, whilst the vertical movement of the line during the field period is effected with the aid of moving parts in the optical system. In this case, the light emitted from each picture element of the line screen in the tube must be brought into a corresponding sharp focus on the viewing screen. This system has the following two important disadvantages:

(a) The light-collecting power of such an optical system is always comparatively low and the brightness of the picture suffers accordingly.

(b) The geometrical accuracy of the reflecting or refracting surfaces in the optical elements must be very high to avoid loss of resolution in the picture. This will make the manufacture of these elements difficult and therefore expensive.

#### (2.1.2) Direct Viewing.

The second method consists of producing a virtual image of the line with the aid of optical elements where, once again, moving parts produce the vertical displacement of the apparent position of the line. The advantages of this way of presentation,

which might be termed a 'direct-viewing' method, are the following:

(a) Since the observer looks directly at a virtual image of the line produced in the tube, its apparent brightness, apart from absorption and reflection losses in the optical elements, will be the same as on the screen in the tube. The picture brightness is then determined by the apparent line-width in the final picture and the distance between adjacent lines.

(b) From each picture element only a narrow beam of light rays, determined by the observer's pupil, is used for a certain position of the observer. This means that only a very small part of the optical elements contributes to the image formation for each picture element. The requirements on the geometrical accuracy of the optical elements are therefore far less stringent than in the case of a projected picture. Large area deviations of accuracy in these elements produce distortions in the picture without loss of resolution.

(c) The length of the line as scanned in the cathode-ray tube can be the same as the width required for the final picture. The optical elements can therefore be cylindrical, which facilitates their manufacture, and the picture resolution in the line direction will be purely determined by the resolution in the line direction in the tube.

For these reasons the direct-viewing method of presentation with the aid of cylindrical optical elements was chosen.

### (2.2) Cylindrical Optics

It is necessary at this point to recall some of the properties of cylindrical optical elements in more detail.

#### (2.2.1) Astigmatism: Point Image and Slit Image.

A cylindrical mirror or lens has a certain finite focal length in a plane at right angles to its cylindrical axis, whereas in a plane parallel to its axis the focal length is infinite. Such an element will form an astigmatic image of a point object. This is illustrated in Fig. 1, where a point object O is observed through

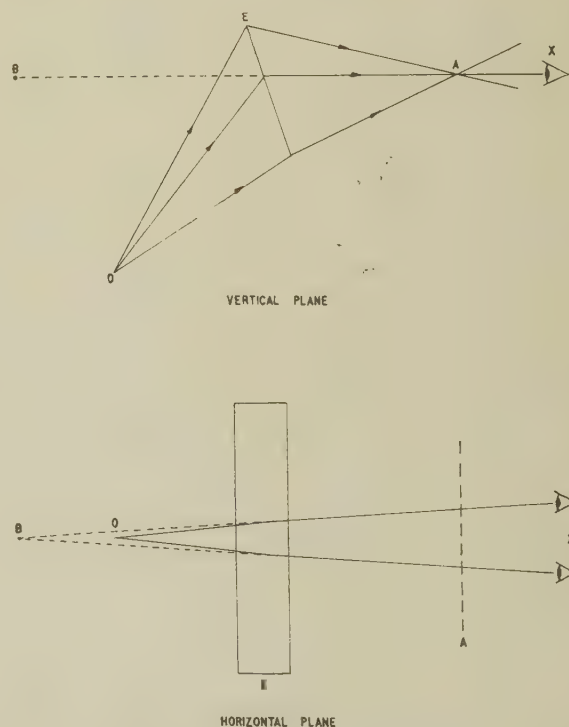


Fig. 1.—Slit image, A, and picture image, B, formed by a cylindrical optical element, E, when observing a point object, O.

cylindrical lens E, with its cylindrical axis located horizontally. In a vertical plane the rays appear to diverge from an image on the axis, A, parallel to the cylindrical axis. The position of A depends on the characteristics of the element E and its distance from the observer.



position relative to the eye and the object. In the plane containing the eye and the image axis the rays appear to diverge from a point image, B. This lies at a distance from the eye which is equal to the total optical path from the object to the eye.

Viewing O through E with one eye only, it is not possible to determine whether the image is at A or B. Convergence of the two eyes, however, is a far better guide to the position of an object than the focusing of each individual eye, and consequently, provided that the observer's head is upright, the image appears to lie at B. Axis A is like a slit through which B is observed and has therefore been termed the 'slit image'.

### (2.2.2) Travelling-Slit Image and Picture Image.

An auxiliary field scan can be achieved by the appropriate movement of a cylindrical element parallel to its axis. This displaces the slit image of the line in the tube through a raster, thus forming a 'travelling-slit image'. The line can be observed in successive positions, building up the 'picture image' on an image surface, of which B is a part, through this travelling-slit image. The shape of the image surface is determined by the optical path lengths from the line screen in the tube to the eye in the various positions of the optical element. The picture image is always virtual, whereas the slit image can be either real or virtual.

The apparent height of the picture image is given by the projection of the travelling-slit image from the eye on to the image surface, and so depends on the position of the observer. The width of the picture, on the other hand, remains equal to the length of the line scanned in the tube. Consequently, some variation in the aspect ratio of the picture image will occur as the observer approaches or withdraws from the display. This distortion, and some possible eye-strain, can be minimized if slit image and picture image are close together.

### (2.2.3) Line Brightness, Angle of View and Magnification.

The brightness of a stationary virtual image produced by an optical element is equal to the brightness of the object, provided that the pupil of the observer's eye is completely filled with rays from the image, and neglecting absorption and reflection losses in the element. The element, however, can only collect a limited fraction of the light emitted by the object, which is determined by the geometrical conditions. This apparent contradiction is explained by the reduction in angle of view.

Consider a cylindrical element of which the useful area subtends an angle  $\alpha$  to a small area of the object in a plane at right angles to its axis (see Fig. 2). If the useful area of the optical

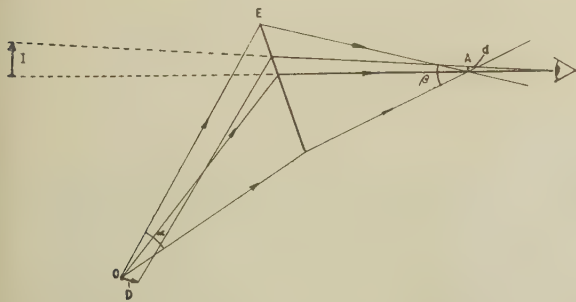


Fig. 2.—Angle of view and magnification obtained when observing an object O through a cylindrical optical element E.

element subtends an angle  $\beta$  to the slit image, then an observer can only view the picture within an angle  $\beta$  diverging from the slit image. In the case of a line object with width  $D$ , the slit

image will show a line width  $d$ , which is roughly related to  $D$  by  $d/D \simeq \alpha/\beta$ .

Owing to aberrations in the optical element, the value of  $d$  may vary considerably as the observer moves to catch different rays in the eye within the angle of view  $\beta$ . The apparent line width in the picture image I is determined by the projection of  $d$  from the eye on to the picture-image surface, and hence depends on the distance of the observer from the slit image. In cases where slit image and picture image are close together compared with the distance of the observer, the line width of I is almost equal to  $d$ .

In a plane parallel to the cylindrical axis, the magnification is unity and the angle of view is purely determined by the length of the cylindrical element and its distance to the object.

In the case of a rotationally symmetrical projection element, the angle it subtends to the object is equally limited in the horizontal and vertical directions, and the limitation in viewing angle applies in the same way to both directions. In this case, however, the diffusing screen is employed as a means to increase the angle of view, but at the expense of the brightness, without further affecting the magnification, which has already been determined by the focal length of the element and its distance from the object.

### (2.3) Moving Element

It has already been indicated that an auxiliary field scan can be obtained by the appropriate movement of a cylindrical element parallel to its horizontally placed axis. The slit image of the line in the tube can thus be moved through a raster and the picture image consists of the virtual images of the successive lines on the image surface, as observed through the travelling-slit image.

The simplest mechanical movement which will shift the apparent position of the line is a rotation of the cylindrical element about an axis parallel to its cylindrical axis and to the line scanned in the tube. The mechanical problems would be very great if every field had to be generated completely by one single element, since this would require a rapid fly-back after the completion of each field. A continuous motion at constant speed can, however, be employed by using a drum which carries a number of identical elements that come into play successively as the drum rotates.

#### (2.3.1) Mirror Drum.

A comparatively straightforward system employs a mirror drum which carries a number of identical cylindrical mirror elements, combined with a cathode-ray tube with more or less conventional design characteristics, to produce a repetitive line scan on a triplet of phosphor lines, each fluorescing in a primary colour. A cross-section of such an arrangement in a vertical plane is illustrated in Fig. 3.

Several difficulties arise with this system as a result of the asymmetry in the set-up for top and bottom of the picture. These will be discussed in more detail in Section 4.

#### (2.3.2) Lens Drum.

A very attractive symmetrical solution can be conceived in the form of a drum which carries a number of identical cylindrical lenses, combined with a cathode-ray tube inside the drum, which generates the repetitive line scan, again on a triplet of phosphor stripes (see Fig. 4). The main problems in this arrangement will arise in the design of the required cathode-ray tube.

### (2.4) The Magnifying Element

It has been pointed out in Section 2.2.3 that the vertical angle of view is increased with larger demagnification by the cylindrical element in a vertical plane. A reasonable vertical angle of view



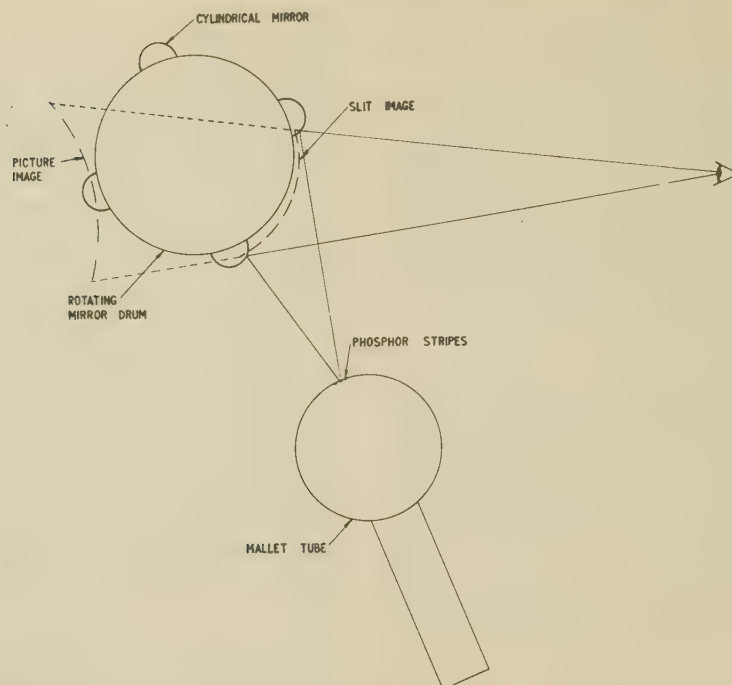


Fig. 3.—Schematic of a line-scan tube observed in a rotating-mirror drum.

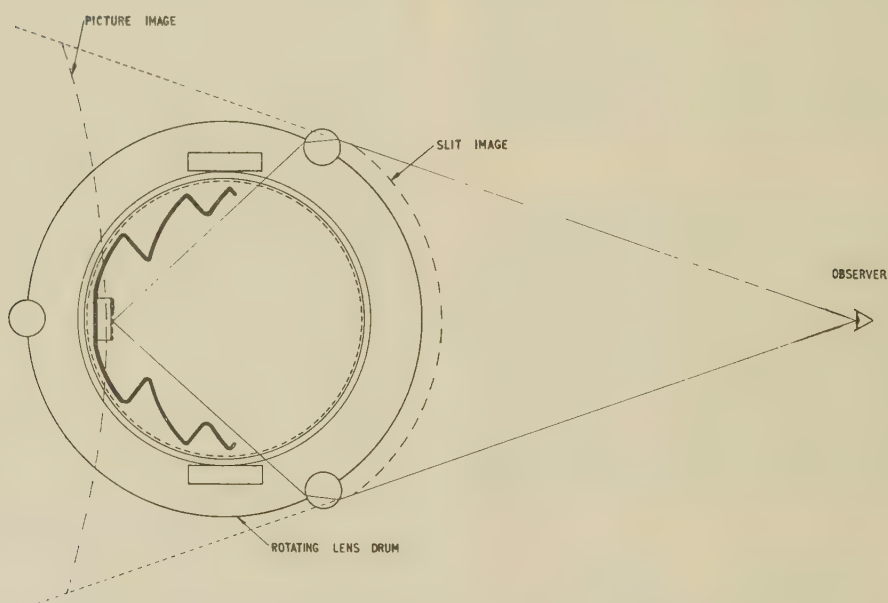


Fig. 4.—Schematic of a line-scan tube observed through a rotating-lens drum.

can be obtained if the slit image is close to the element. This implies that the distance covered by each optical element during its operative period is of the same order as the picture height. For a sufficiently large picture size the drum then becomes very bulky, with associated problems of wear and noise. For this reason it was considered necessary to limit the diameter of the rotating drum producing the field deflection and to add a stationary cylindrical optical element to magnify the slit image to its required size. The requirements for such a magnifying element are that the picture must be upright with little curvature in the picture image surface and, to the observer, should be apparently free from aberrations.

Various types of cylindrical magnifying mirrors were considered. The main problem was to satisfy the condition that the mirror must produce a uniform image which does not distort with a limited vertical movement of the observer. This condition was particularly difficult to satisfy, since the mirror must be used in an off-axis position to avoid interruption of the reflected rays by the drum.

Under these conditions a cylindrical mirror with a hyperbolic cross-section finally appeared to give satisfactory results. Such a mirror can be mounted with its cylindrical axis parallel to that of the rotating drum. In the vertical plane, the rays diverging from the travelling-slit image formed by the rotating drum were



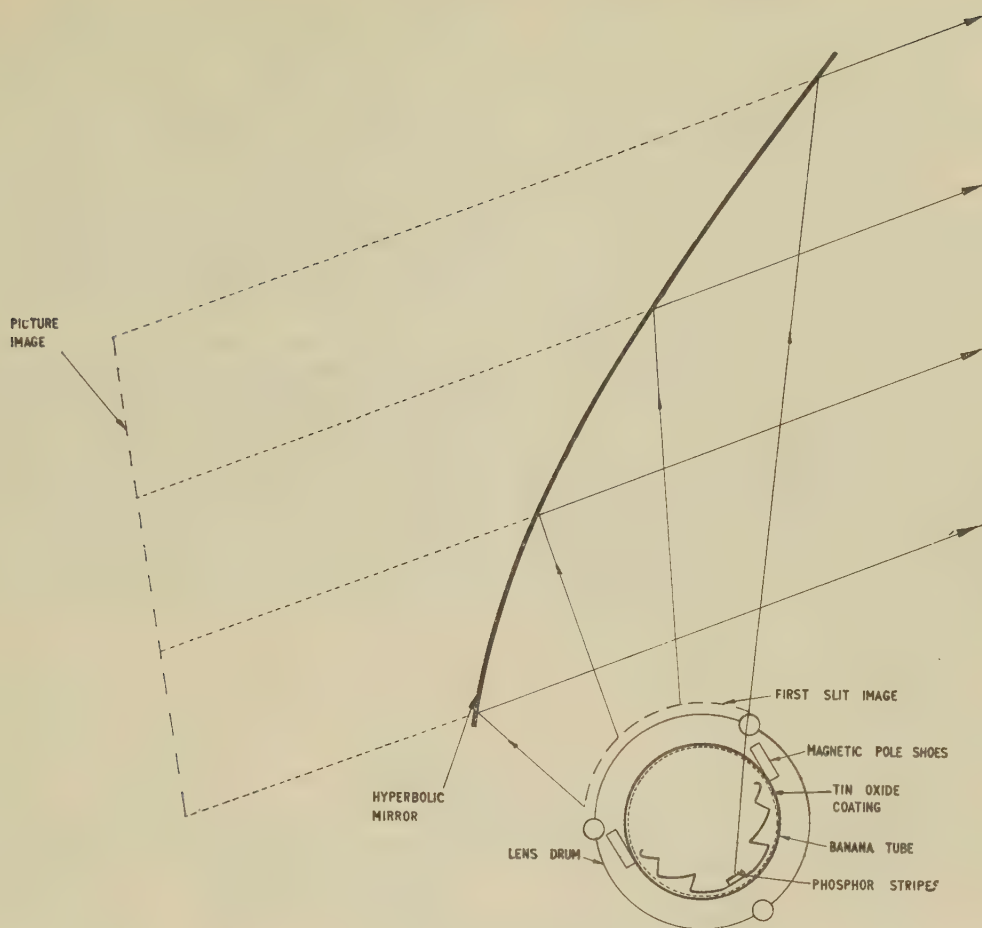


Fig. 5.—Picture formation in the banana-tube display system.

then be focused in a second travelling-slit image. An observer with his head in the upright position again sees a picture image through or against this second travelling-slit image on a final virtual-image surface. This surface is determined once again by the total optical path lengths for each position of the rotating drum. This is illustrated in Fig. 5, where a stationary cylindrical mirror of hyperbolic cross-section has been added to the arrangement with a lens drum shown in Fig. 4.

The magnification of the stationary mirror reduces the vertical angle of view correspondingly. The aberrations also increase with the magnification, but it was found experimentally that a linear magnification of approximately two can still provide a satisfactory solution. This allows a reasonable vertical movement of the observer at a normal viewing distance without causing disturbing picture distortion. The horizontal angle of view of the system is still completely determined by the length of the cylindrical elements and the distance from the screen in the cathode-ray tube to the magnifying mirror.

The line width in the final picture image is determined by the overall demagnification in the vertical plane. For maximum picture brightness the width of a line should be as large as is compatible with satisfactory resolution in the frame direction. Since the lines will normally consist of colour triplets, it was found that a good resolution can still be obtained when the triplets of adjacent lines in the picture overlap to a certain extent. The width of the line scanned in the tube can thus be chosen accordingly.

### (3) THE CATHODE-RAY TUBE

#### (3.1) Basic Concept

An important element of the type of display system under discussion is the cathode-ray tube. The design of this tube depends very largely on the optical system adopted. In each case, however, the tube will contain at least one electron gun and a narrow phosphor screen on which each successive colour line can be generated.

The simplest method of producing a single colour line with a dot-sequential system is to scan the electron beam along three narrow parallel phosphor stripes fluorescing in the primary colours. The colour selection can then take place by applying spot-wobble, where a high-frequency lateral deflection of the electron spot is introduced. If phase and amplitude of the spot-wobble deflection are correctly adjusted, the electron beam should always strike the correct phosphor at the time when the corresponding colour signal is applied to the electron gun of the tube. This method of colour presentation does, however, require a high degree of accuracy in the tracking of the scanning beam along the phosphor stripes, and is discussed in greater detail elsewhere.<sup>7</sup>

#### (3.2) Mallet Tube

A mirror drum, as described in Section 2.3.1, imposes few restrictions on the design of the cathode-ray tube. Consequently, a tube can be conceived which makes full use of conventional



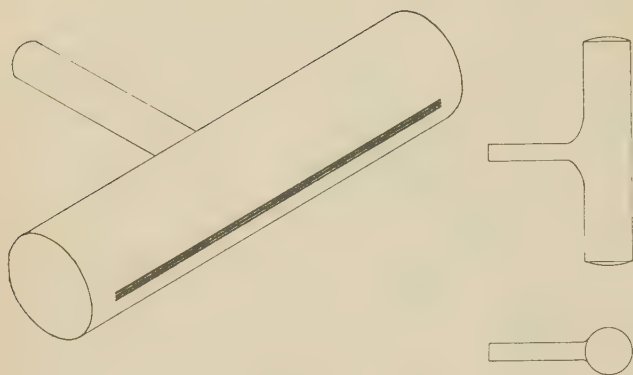


Fig. 6.—Mallet tube.

cathode-ray-tube techniques, taking into account that the screen has substantially only one dimension. Fig. 6 illustrates an example of such a tube, which in essence consists of a tubular body containing the screen parallel to its axis, and a thinner tubular neck at right angles to the main body containing the electron gun; hence the name 'mallet' tube. The neck can be

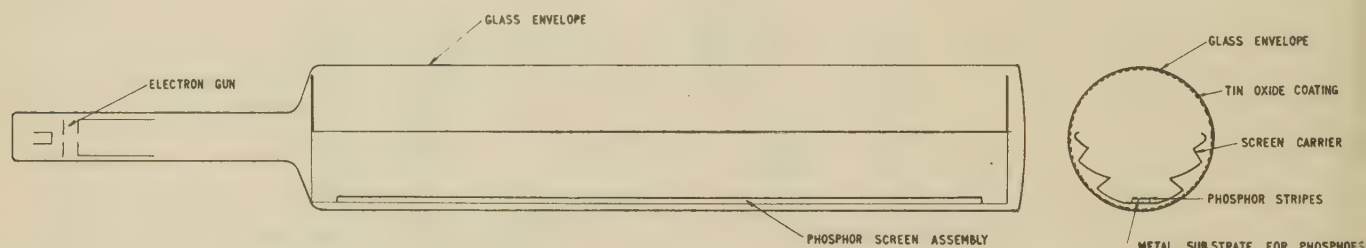


Fig. 7.—Banana tube.

flared in the direction of the line scan to allow a large deflection angle.

The line deflection can be effected by conventional scanning coils around the neck and is symmetrical. Usual methods may be employed to improve the spot size at both ends of the line if required. No particular difficulties are encountered in adjusting beam-centring and deflection coils in order to achieve correct tracking of the spot along the phosphor strips. Spot wobble can also be achieved with conventional means and a symmetrical amplitude correction may be added if necessary. The three phosphor lines can be applied directly to the glass wall of the tube and backed with a thin metal coating in the usual manner, thus avoiding light reflections inside the tube.

### (3.3) Banana Tube

#### (3.3.1) Geometrical Design.

A cathode-ray tube which can be employed with a lens drum must be of unconventional design to fit inside the rotating drum. A logical design, which also seems very attractive from a production point of view, is where the main body of the tube consists of a tubular glass envelope which contains the phosphor stripes parallel to its axis. One end of this tube is sealed and the other end is joined to a tubular neck of smaller diameter containing the electron gun. The neck of the tube can project through an opening in one of the end plates of the drum, thus providing easy access to deflection and focusing arrangements around the neck of the tube, if these are required.

The distance from the phosphor stripes to the rotating lenses

of the drum in their operative positions should be as large as possible to avoid excessive vertical brightness variations in the picture due to oblique viewing of the stripes in the extreme positions of the lenses. This implies that the stripes should be viewed from the side where the electron beam is incident. An additional advantage of this way of viewing is the possibility of applying the phosphor stripes to a separate metal carrier. This can be processed and coated outside the tube, and also provides better cooling of the screen at high electron-beam currents.

Fig. 7 shows a diagrammatic cross-section of such a tube, which, because of its geometry and by analogy with the American 'apple' tube for colour display,<sup>4</sup> has been called the 'banana' tube.

#### (3.3.2) The Deflection System.

Normal line-deflection coils around the neck of the tube can provide a line scan along the phosphor stripes. Owing to the very small angle of approach of the electron beam towards the far end of the screen (see Fig. 8), the resulting elliptical spot will then be so much elongated that the resolution in the line direction is completely inadequate. With the tube geometry as described, it is clear that a substantial increase in the angle of incidence of the electron beam at the far end of the phosphor screen can be obtained only by introducing a deflecting field along the main body of the tube.

Early experiments with electrostatic deflecting fields inside the tube were disappointing as a result of wall charges building up between electrode surfaces, leading to instabilities in the deflection. This effect could be avoided by providing the tube wall with a continuous conductive coating at screen potential and



Fig. 8.—Schematic of electron paths in a banana tube without permanent magnetic deflecting field.

introducing a magnetic field at right angles to the trajectory plane of the electron beam to deflect this beam on to the screen. A complete line could in this way be scanned with the aid of deflection coils alongside the main body of the tube, but the deflection energy required to energize the comparatively large coils was considered to be prohibitive. For this reason the deflection system is now being used which consists of conventional line-deflection coils around the neck of the tube, combined with a constant magnetic field across the main body of the tube provided by a permanent-magnet system.

A further increase in the angle of approach at the far end of the screen has been obtained by providing a suitable gradient in the magnetic field strength, which increases towards the end



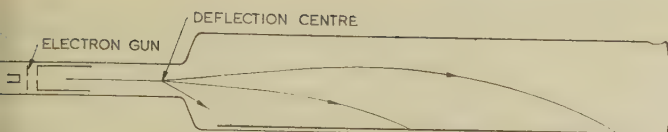


Fig. 9.—Schematic of electron paths in a banana tube with a permanent magnetic deflecting field.

of the tube. Fig. 9 shows a diagram of some electron paths for different deflection currents through the line coils.

The permanent-magnet assembly must satisfy the following two geometrical requirements:

(a) The assembly, including pole shoes, must allow an unobstructed view of the screen by the lenses in their operative positions.

(b) Since a maximum diameter of the cathode-ray tube inside the drum is desirable for a good spot size, the components of the assembly should extend as little as possible beyond the diameter of the tube.

Fig. 10 shows a schematic of the magnet assembly as it is applied at present. Two pole shoes in the form of flat mild-steel

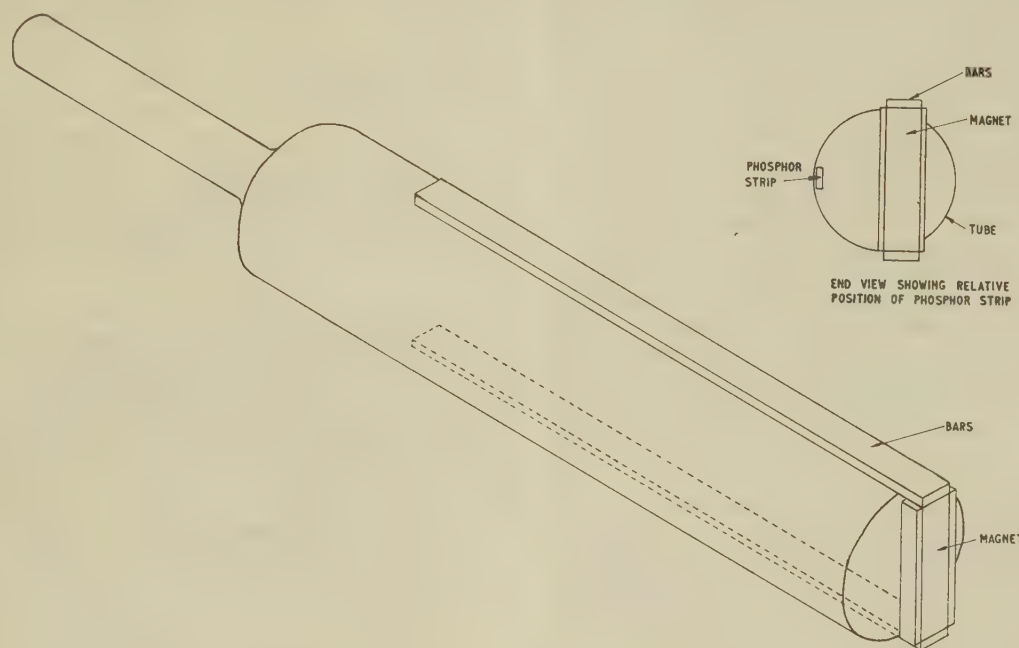


Fig. 10.—Permanent-magnet assembly used with the banana tube.

bars extend along the major part of the tube. They are interconnected at the far end of the tube by a permanent magnet which has been magnetized in the direction at right angles to the screen to deflect the electron beam towards the strips.

A more detailed discussion of the present method of beam deflection and its effect on beam focus is given in a paper<sup>8</sup> which deals specifically with the banana tube.

### (3.3.3) Phosphor Requirements.

The phosphor screen consists of three closely-spaced phosphor strips luminescing under electron bombardment in the three primary colours, red, green and blue. The main requirements which the phosphors must meet are:

(a) The decay of the luminescence, after the excitation ceases, must be sufficiently short to avoid vertical streaking in the picture.

(b) Because every line is scanned on the same phosphor

strips, the phosphors must be able to withstand a high average loading without a serious loss of efficiency. Small flaws in the narrow strips must also be avoided, since they would give rise to dark vertical lines in the picture.

(c) The phosphors must be of sufficiently high efficiencies, and correctly matched in efficiencies and colour points to allow a high-quality colour rendering.

### (3.3.4) Dimensions of the Screen.

For a picture width of 40 cm, as used at present, the length of the phosphor strips should also be 40 cm. The height of the final picture must then be 30 cm and the width of one triplet of colour lines in this picture is limited by the required vertical resolution. Taking a field blanking of 7% into account with a 405-line standard, 377 lines should be resolved.

It has been found experimentally that the line triplets in the picture may overlap to a certain extent without impairing the vertical resolution. This should be expected, since the lines in each colour are much narrower than the triplet itself and can therefore still be completely separated when the triplets start to overlap. The only result is that the three colour pictures are

slightly displaced with respect to each other in the vertical direction. A line triplet occupying just over one-and-a-half line widths in the final picture does not appear to cause a noticeable loss of vertical resolution. This means that in our case (405 lines, picture size 30 × 40 cm) the width of one triplet in the picture may be approximately 1.4 mm.

The width of the screen triplet in the tube is then determined by the overall demagnification in the optical elements. In the present system this is approximately a factor 5 for the centre of the picture, increasing slightly towards top and bottom. The width of the line triplet scanned in the cathode-ray tube may therefore be approximately 7 mm. Each colour stripe has been given a width of 2 mm, with gaps of 1 mm between the stripes.

Wide gaps and stripes are advantageous from the point of view of avoiding colour pollution due to finite spot size<sup>9</sup> and of minimizing the effect of small flaws in the screen. They also facilitate the problem of tracking but, on the other hand, require



a higher electron-beam current to produce the same brightness over the wider phosphor area.

#### (4) COMPARISON OF MIRROR-DRUM AND LENS-DRUM SYSTEMS

It has been pointed out in Section 2 that a lens drum has significant advantages over a mirror drum when considering their optical merits. On the other hand, it became evident in Section 3 that the cathode-ray tube required for a mirror drum presents fewer difficulties.

The various advantages and disadvantages of the complete systems can now be compared to allow a choice between the two. Consequently, only those features are considered which are different for the two approaches and other colour-display devices are not included at this stage.

##### (4.1) Advantages of the Mirror-Drum System

The main advantage of the mirror-drum system is the possibility of employing more or less conventional methods to generate a symmetrical line scan. This eases the problems of setting-up for correct tracking, achieving the desired spot wobble and obtaining a good resolution with the best spot size in the central area of the picture. It also makes the system somewhat less vulnerable to extraneous magnetic fields, such as the earth's field, since the path lengths of the electron beam from gun to screen are shorter and vary less during the line scan.

The second advantage is of a mechanical nature. A mirror drum can be mounted on a central shaft, and this is more satisfactory from the point of view of bearings than a lens drum with one open end through which a cathode-ray tube protrudes.

A minor point in favour of the mirror-drum system is that the length of the mallet tube is only determined by the length of its screen. The cabinet does not, therefore, require a greater width than the length of the optical elements. With the banana tube, on the other hand, the neck of the tube adds to the length of the screen as well as to the distance from deflection centre to screen stripes. This increases the minimum width of the cabinet.

##### (4.2) Advantages of the Lens-Drum System

A very important feature in favour of the lens drum is the symmetrical nature of the first travelling-slit image. The distance of the screen in the tube to the cylindrical lenses in their operative positions does not vary unduly, in contrast to the system with the mirror drum where this distance will vary considerably and is also larger.

The first result of this is that the demagnification of the line width is much more uniform with the lens drum, thus avoiding noticeable brightness variations in the picture image. Secondly, it is much easier to obtain a final picture image which appears vertical to an observer in the normal viewing position. Thirdly, the final picture image will appear closer behind the stationary magnifying mirror in the lens-drum system, thus increasing the useful angle of view for the same size of mirror.

A mirror drum combined with a stationary cylindrical mirror will always reflect a considerable proportion of any incident light received from the observer's surroundings. This proportion can be reduced by a decrease in the reflecting area of the drum. The areas between the cylindrical mirrors can be made highly light-absorbing and could be extended at the expense of the width of the mirror surfaces. In order to maintain the vertical angle of view, this implies that the optical demagnification of these elements should then be further increased, necessitating an excessively high beam current in the tube to maintain the correct line width, and therefore the brightness, in the final

picture. An additional cylindrical magnifying lens in close proximity to the screen in the tube can only partly overcome the last objection. The situation with a lens drum is much more favourable in this respect, since the lenses will reflect only a very small proportion of any incident light.

Whereas the width of the cabinet required for a lens drum system may be somewhat larger than for a system employing a mirror drum (see Section 4.1), the depth of the cabinet can be considerably smaller. This is due to the much more compact arrangement with the lens drum, where the tube is placed inside the drum and consequently does not take up additional space.

#### (4.3) Conclusion

After some initial experiments with both systems a complete experimental model with a mirror drum and mallet tube was constructed, and also a model of the lens-drum system. The respective merits of the two systems were completely confirmed on the experimental models, and it was concluded that, in particular, the implications of the symmetrical nature of the first travelling-slit image formed by the lens drum, as discussed in Section 4.2, were sufficiently important to decide in favour of this system.

The following Sections are therefore concerned only with the banana-tube display system.

#### (5) PRELIMINARY DISCUSSION OF THE DISPLAY DEVICE

The significant features of the display system in its present form are fully dealt with elsewhere.<sup>7-11</sup> It should therefore suffice in this more general survey of the system to mention some of the most important ones and to discuss them briefly.

##### (5.1) Economic Aspects

The banana tube itself will obviously be cheaper to manufacture than any of the proposed colour tubes, and may even prove to compare favourably with an ordinary monochrome tube for the same picture size. The amount of raw material involved alone is only a fraction of that required for a standard tube. This is illustrated by comparing the weights of various tubes:

17 in monochrome tube (110° deflection)	12 lb
21 in monochrome tube (110° deflection)	22 lb
Shadow-mask tube	36.5 lb
Banana tube	2.5 lb

The lower cost of the tube is off-set by the requirement for additional components for the optical system, of which the magnifying mirror, the lens drum and the driving gear are the major items. For a domestic receiver the circuits required to operate a single-gun colour tube and the cabinet design also play an important part.

Preliminary estimates for these items lead to the conclusion that it seems likely that a receiver based on the present system can compare favourably with a shadow-mask-tube receiver.

##### (5.2) Picture Contrast

A very important feature of the banana-tube display system as described is its unique characteristic of maintaining a high contrast ratio in the picture with ambient illumination. This is due to the fact that the segments of the drum between the lenses can be made matt black, thus presenting the picture against a highly non-reflective background.

Any light reflections inside the drum must be avoided as much as possible to increase the basic contrast ratio on the picture. With present tubes a ratio in the picture of 40 to 1 can easily be



obtained. The decrease in this contrast ratio with increasing ambient illumination levels will then be far smaller than for any domestic display system.

### (5.3) Picture Brightness and Beam Current

The picture brightness is determined by the beam current in the tube. This is ultimately limited by the characteristics of the electron gun and the maximum permissible screen loading. It is possible to derive some theoretical values of the beam current required to obtain a picture brightness comparable to that which can be obtained with a 21 in shadow-mask tube by the following considerations.

According to the published data for this tube a white raster with an average brightness of 10ft-L can be obtained at 25kV screen potential with the following beam currents:

			$\mu\text{A}$
Red gun	..	..	350
Green gun	..	..	217
Blue gun	..	..	133
			—
			700

If phosphors with the same lumen efficiencies were used in the banana tube, also operating at 25kV, the same picture brightness could be obtained for different average beam currents on each of the phosphor stripes, which can be deduced from the following considerations:

(a) A beam current,  $I$ , in the shadow-mask tube leads to 0.15  $I$  effective screen current due to the interception of current by the shadow-mask.

(b) The glass face of the shadow-mask tube has a transparency of 72% to increase the contrast ratio with ambient illumination. This further reduces the effective beam current in the tube by a factor 0.72.

(c) The glass wall of the banana tube, the cylindrical lenses and the magnifying mirror will each absorb about 8% of the light. The combined effect is that the required beam current for each colour will be higher by a factor of about 1.3 than in the shadow-mask tube.

(d) The line width in the banana tube is demagnified in the optical system by a factor of about 5. Consequently, the tube requires 5 times as much beam current on each phosphor stripe.

(e) The area scanned by the electron beam in the shadow-mask tube, including the invisible corners of the picture, is approximately 300 in<sup>2</sup>. With the banana tube the displayed picture area is  $12 \times 16 = 192 \text{ in}^2$ . This reduces the required beam current by a factor  $192/300 = 0.64$ .

The combined effect of these factors is that the average currents in the banana tube on each of the three phosphor stripes, necessary to produce a white raster of the same brightness, should be approximately  $0.15 \times 0.72 \times 1.3 \times 5 \times 0.64 \approx 0.45$  times as high as in the shadow-mask tube.

In practice, the efficiencies of the green and blue phosphors are somewhat reduced in the banana tube in order to produce a white raster when the unmodulated spot is wobbled across the phosphor triplet. When the amplitude is adjusted to obtain a duty cycle of approximately 110° on the red phosphor, 110° on blue and 70° on green, a white raster is generated. With an unmodulated electron beam, this means that the average beam current required to produce a white raster should be 360/110 times the beam current on the red phosphor. The value of such a beam current is then  $0.45 \times 360/110 \times 350 \approx 510 \mu\text{A}$  for a brightness of 10ft-L.

Actual measurements of the beam current in a tube, with the picture brightness at 10ft-L, yielded values of approximately 500  $\mu\text{A}$ , and this completely confirmed the theoretical value.

### (5.4) Picture Size and Cabinet Design

During the initial stage of investigating the general characteristics of the display system, the final picture size was only of

secondary importance. The present picture size of  $12 \times 16$  in with a diagonal of 20 in has therefore been chosen quite arbitrarily. Any other picture size, if desired, could be obtained in future by scaling the present dimensions of the components up or down.

Alternatively, it would be possible to increase the picture size by a limited amount by lengthening the tube and the optical elements and increasing the magnification in the mirror, or by scaling up the drum and increasing the length of the tube but leaving the magnification in the mirror, and consequently the vertical angle of view, unchanged. The final choice of the dimensions of the various components can therefore also be influenced by other factors concerned, for instance, with the design of the cabinet.

With regard to the cabinet design, there is one other aspect of the system which is worth mentioning. The horizontal angle of view is determined by the width of the mirrors. This leads to a certain minimum cabinet width which is larger than that required for an orthodox cathode-ray tube. The minimum depth of the cabinet, on the other hand, is determined by the diameter of the drum and its distance in front of the mirror, and can be considerably smaller than that for the present shadow-mask tube. Consequently, the cabinet for a banana-tube display device can be designed in a more contemporary style.

### (5.5) Possible Further Improvements in the Display Device

If the final aim is to produce a successful domestic receiver, further development of the present display device should have two objectives. In the first place, cheap mass-production methods should be investigated for the optical and mechanical components of the system,<sup>11</sup> whilst establishing how much various components can be simplified without undue sacrifice in picture quality. This could further reduce the price of a receiver and make this even more attractive from an economic point of view. Secondly, the present design of the banana tube itself can not yet be regarded as providing the best solution possible. In particular, its sensitivity to extraneous magnetic fields may well be considered to be a serious disadvantage, whereas a simplification in the setting-up procedure for correct tracking of the scanning electron beam along the phosphor stripes is also desirable.

It may be possible to avoid these difficulties with a modified type of banana tube in which the principle of 'positive guidance' is applied to the electron beam. This might, for instance, be achieved by introducing an electrostatic field inside the tube, with the property that it corrects small sideways deviations of the electron beam from its correct trajectory plane, due to slight misalignments of the focus and deflection units or to extraneous magnetic fields.

### (6) CONCLUSION

The banana-tube display system as described here has not yet outgrown the laboratory stage. Whether it will ever be applied in domestic colour receivers in competition with the now well-established shadow-mask tube is still very much an open question. The answer to it must depend to a large extent on a realistic assessment of its present performance and its potential advantages.

When considering the possible future of the device the fact has to be borne in mind that an unconventional alternative to an already established technique must offer some clear advantages. In the case of the banana tube the possible advantages to aim at are a lower receiver cost, lower cost of tube replacement, and the ease of setting-up and maintaining a good colour picture. It must also be taken into account that the shadow-mask tube in its present form is the result of a major research



and engineering effort over a considerable period of time, whereas the banana-tube display device is still in an early stage of development and therefore more likely to be subject to further significant improvements.

The most unconventional features of the display device are the picture presentation in the form of a virtual image suspended in space behind the viewing mirror, and the introduction of mechanically moving components in the system. It is difficult to predict the psychological reaction of the viewing public to this type of picture presentation. The limited number of observers who have seen the pictures certainly did not object to the virtual image, whilst the flatness of the picture plane and the absence of corner cutting were considered to be a clear advantage.

The introduction of moving parts with the inherent problems of wear and noise raises a more fundamental objection. This can be overcome in a domestic receiver only if their presence is sufficiently concealed, and if the rotating elements are properly engineered to reduce the wear and noise problems to a minimum. Other favourable features of the receiver, either of an economic nature or from the point of view of being able to obtain consistently good picture quality without a very complicated adjustment procedure, must then compensate for this fundamental objection.

#### (7) ACKNOWLEDGMENTS

A project of the kind described can only progress beyond the stage of an interesting idea by the enthusiasm of everyone concerned with its realization.

It is therefore a pleasure to acknowledge the wholehearted support given to the project by Mr. P. E. Trier, Director of the Mullard Research Laboratories, and the skill and effort put into it by many members of the laboratory staff, not only in the Special Tubes and Applications Divisions, but also in the various workshops, glass shop, drawing and design offices.

An important contribution to the original concept of a colour-display system with mechanical field scan was made by Mr. N. D. R. Calder, who has since left our Laboratories and is now Science Editor of *The New Scientist*.

The active support of Dr. E. F. de Haan and Mr. J. Kaashoek of the Philips Research Laboratories, Eindhoven, who built and

investigated an experimental model of the mirror-drum system employing a mallet tube, is gratefully acknowledged, as well as the numerous discussions with other members of the laboratories.

The present demonstrations would not have been possible without the valuable contributions made to the technology of the banana tube by Mr. F. G. Blackler and his staff, in particular Mr. D. Maskell, of the Cathode-Ray Tube Development Department of the Mullard Radio Valve Co. at Mitcham, where the tubes used at present have been manufactured.

Finally, the author wishes to thank the Directors of Mullard Limited for permission to publish the paper.

#### (8) REFERENCES

- (1) ZWORYKIN, V. K., and MORTON, G. A.: 'Television Engineering' (John Wiley, 1954), 2nd edition.
- (2) Colour Television Issue, *Proceedings of the Institution of Radio Engineers*, October, 1951, **39**, No. 10.
- (3) Second Colour Television Issue, *ibid.*, January, 1954, **42**, No. 1.
- (4) CLAPP, R. G., CREAMER, E. M., MOULTON, S. W., PARTER, M. E., and BRYAN, J. S.: 'A New Beam-Indexing Colour Television Display System', *ibid.*, 1956, **44**, p. 1108.
- (5) CALDER, N. D. R.: 'Auxiliary Frame-Scans for Colour Television Display', V.P.L. Report 158, October, 1955.
- (6) SCHAGEN, P., and EASTWELL, B. A.: 'The Banana Tube Colour Television Display System', V.P.L. Report 159, November, 1957.
- (7) FREEMAN, K. G.: 'Circuits for the Banana-Tube Colour Television Display System' (see page 604).
- (8) EASTWELL, B. A., and SCHAGEN, P.: 'Development of the Banana Tube' (see next page).
- (9) JACKSON, R. N.: 'Colorimetry of the Banana-Tube Colour Television Display System' (see page 613).
- (10) FREEMAN, K. G., and OVERTON, B. R.: 'Appraisal of the Banana-Tube Colour-Television Display System' (see page 624).
- (11) HOWDEN, H.: 'Mechanical and Manufacturing Aspects of the Banana-Tube Colour-Television Display System' (see page 596).

[The discussion on the above paper will be found on page 630.]



## DEVELOPMENT OF THE BANANA TUBE

By B. A. EASTWELL, B.Sc., and P. SCHAGEN, Ph.D.

(The paper was first received 17th November, 1960, and in revised form 10th February, 1961. It was published in May, 1961, and was read before the ELECTRONICS AND COMMUNICATIONS SECTION 15th May, 1961.)

### SUMMARY

The unconventional system of beam deflection and spot formation in the banana tube is considered in detail. The discussion of electron optics includes a formulation of the requirements for the permanent-magnetic deflecting field, with a detailed description of the effect of this field on the electron spot, as well as the scanning and focusing means employed.

The tube technology is considered in broad outline, including certain aspects of manufacture.

### (1) INTRODUCTION

A colour-television display system, where the field scan of the raster is effected by means of a rotating lens drum, requires an unconventional type of cathode-ray tube. The 'banana' tube has been developed for this application.

The tube must satisfy the special requirements imposed by the display system which are, basically,

- (a) The tube must contain a phosphor screen, consisting of three narrow parallel phosphor stripes, each fluorescing in one of the primary colours when bombarded by a scanning electron beam.
- (b) It must be possible to locate the tube inside a lens drum with its screen parallel to the axis of the drum and at a maximum distance from the operative positions of the rotating cylindrical lenses.
- (c) An unobstructed view of the screen must be provided along its entire length with a viewing angle of at least  $85^\circ$  at right angles to the axis of the drum.

The simplest tube geometry, suggested by the combination of these three requirements, is that of the banana tube. The main body of this tube consists of a tubular glass envelope, in which the phosphor screen is located parallel to the axis of the tube and close to its wall. The tube is sealed at one end and joined at the other to a tubular neck of smaller diameter, containing the electron gun (see Fig. 1).

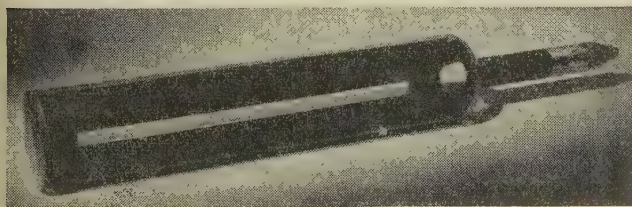


Fig. 1.—The banana tube.

This construction provides mechanical strength, as well as cheap and easy manufacture. A serious disadvantage is that the electron beam enters the main body of the tube near one end of the screen and at only a short distance above it. This makes it difficult to obtain a sufficiently small spot size along the entire length of the screen. Unconventional methods must therefore be employed to deflect and focus the electron beam on to the screen.

### (2) ELECTRON OPTICS OF THE BANANA TUBE

#### (2.1) Formation of the Electron Beam

Every cathode-ray tube must satisfy the basic requirement that it should be capable of producing sufficiently bright pictures while maintaining an acceptable resolution. Greater brightness can be obtained by an increase in beam current, which normally implies an increase in spot size and therefore a reduction in picture resolution. The result is that, in practice, a reasonable compromise is usually established between picture brightness and resolution.

In colour display tubes this problem is further aggravated by the fact that the average luminous efficiency of the three phosphors is lower than that of the white phosphor in a monochrome tube, and that not all the electrons in the scanning beam necessarily strike phosphor particles. It is therefore necessary to design the electron gun and the deflection and focusing means even more carefully.

A considerable improvement can be expected from the use of three separate electron guns, producing electron beams which scan the three phosphors simultaneously. This method, which is employed in the shadowmask tube, does, however, create other problems, such as the correct positioning of the three spots at any moment. For this reason a single electron gun has been preferred for the banana tube.

An improvement in spot size can be achieved by increasing the velocity of the electrons in the beam, i.e. by applying the maximum tolerable potential to the tube. This decreases aberrations in the electron optics of the electron gun, and reduces space-charge effects in the beam, while at the same time increasing the light output of the phosphor screen for the same beam current.

A higher working potential does, of course, introduce more severe insulation and X-ray problems, and 25 kV appears to be a reasonable compromise, in practice, for a domestic receiver.

#### (2.1.1) The Electron Gun.

An analysis of the optical design characteristics of the display system as employed at present<sup>1</sup> indicates that adequate picture brightness can be obtained with peak beam currents in the banana tube not exceeding 3 mA, for a working potential of 25 kV across the tube.

With a conventional gun design, the required drive voltage for this operation can be limited to an amplitude of approximately 100 V, which is a reasonable value from a circuitry point of view.

For a given angle of divergence of the electron beam emerging from the gun, the dimensions of the crossover inside the gun should be as small as possible to ensure a minimum spot size on the screen.

The best type of electron gun for this purpose appears to be a triode. The dimensions can be adjusted to obtain a cut-off potential of approximately 100 V for a final-anode potential of 25 kV. With an average cathode loading of just over  $1 \text{ A/cm}^2$ , a reasonably small crossover is obtainable.



### (2.1.2) The Focus Lens.

The purpose of the focus lens is to provide an image of the crossover on the phosphor screen. Ignoring aberrations in the lens and beam widening as a result of space-charge repulsion, the spot size is determined by the image magnification produced by the lens. The magnification is approximately equal to the ratio of the distances of the image (spot) and the object (crossover) from this lens.

As the lens is moved away from the crossover, the resulting magnification decreases and a smaller spot size should be obtained. For a given angle of divergence of the electron beam, however, the diameter of the beam inside the lens increases with the object distance. This leads to a deterioration in spot size due to lens aberrations, and in the banana tube it also increases the aberrations in the deflecting field, which are discussed in Section 2.2. Consequently, there will be a maximum distance for optimum results.

In the initial stage of the project a high-quality electro-magnetic focusing lens has been used to facilitate experimental variations in the strength of the lens. It has been established, however, that comparable results can be obtained with permanent-magnet focusing which would be preferred on economic grounds and for simplicity.

## (2.2) Deflection of the Electron Beam

The spot-size problem of a colour display tube in general is more acute in the banana tube, due to the unusual geometry which creates two further complications.

If normal line-deflection coils are used round the neck of the tube to scan the electron beam along the phosphor stripes, the angle of incidence of this beam becomes progressively smaller as the beam approaches the far end of the screen (see Fig. 2).

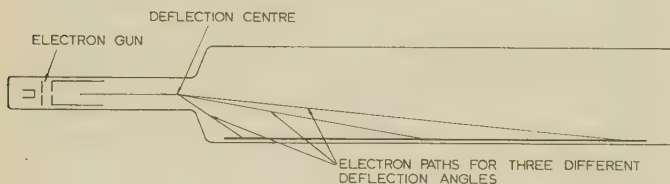


Fig. 2.—The electron paths in a banana tube without a permanent-magnet deflection field.

The resulting elliptical spot thus becomes so elongated that the resolution in the line direction is completely inadequate.

Secondly, the difference in path lengths for the electron beam to the near and the far end of the screen is such that the required amounts of beam focusing are substantially different in the two cases.

An attempt must be made to reduce both these effects as much as possible by the method of beam deflection employed.

### (2.2.1) The Line-Deflection System.

Obtaining a suitable spot size at the gun end of the screen does not present any fundamental difficulties, since the angle of approach is moderately large (approximately  $25^\circ$ ), and the distance to the focus lens is comparatively small, thus yielding a favourable object-to-image ratio for the spot. The main improvement, therefore, must take place towards the far end of the screen.

The first and major improvement there can be achieved by an increased angle of incidence. This can be obtained by causing the electron trajectories to deviate from a straight line. In

other words, the main body of the tube should not be a field-free space, but must contain deflecting fields, either electrostatic or magnetic, or a combination of both which curves the electron paths towards the screen.

The initial approach has been along the lines of an electrostatic deflecting field. It was soon apparent that instabilities in the deflection were difficult to avoid. These were caused by breakdown of insulation between electrodes and the building up of wall charges between electrode surfaces. Experimental variations in the field configuration were also difficult to realize. Because of these technological difficulties the effort was subsequently concentrated on magnetic fields. This has two important advantages:

(a) The optimum configuration of the magnetic deflecting field could be investigated without altering the design of the tube for each experiment.

(b) Since the main body of the tube was free from electric field insulation problems were avoided.

Magnetic fields acting on the electron beam in the main body of the tube can be generated by coils or by permanent magnets with suitable pole-shoes. With a tube diameter of 10 cm, the distance from deflecting coils along the side of the tube to the electron beam is much larger than in the normal case of beam deflection in the neck of a cathode-ray tube. This, combined with the necessarily large dimensions of the coils, would lead to abnormally high deflection powers if the complete line scan of the electron beam were to be achieved with these coils.

It was therefore decided to generate the line scan in the normal way with the aid of scanning coils round the neck of the tube, and to set up a constant magnetic field in the main body of the tube to curve the electron trajectories in an appropriate manner.

### (2.2.2) The Permanent-Magnet Deflecting Field.

A trajectory plane can be considered through the axis of the tube and cutting the phosphor screen along the line which must be scanned.

The line deflection in the neck of the tube varies the angle of entry of the electron beam into the main body of the tube. The magnetic field must then be perpendicular to this plane in order to bend the electron trajectories towards the screen.

The effect will now be considered of the magnetic field on the spot size in the line direction, which is the dimension of the spot affected by the small angle of incidence.

A homogeneous magnetic field along the entire length of the tube would result in electron trajectories with a constant radius of curvature. With the main body of the tube about five times as long as its diameter, this would allow only a limited increase in the angle of incidence at the far end of the screen, where the increase is most needed. If, on the other hand, the magnetic field strength increases along the tube, the curvature of the trajectories will be increased as the electrons penetrate deeper into the tube, and larger angles of incidence can be obtained (see Fig. 3).

An increasing field strength along the length of the tube can also have a second beneficial effect on the spot size in the line direction. This is due to the fact that the electrons near the top edge of the beam will strike the screen farther away from the neck of the tube than the electrons near the opposite edge of the beam. Since these electrons penetrate deeper into the tube, where the deflecting field is stronger, they are deflected to a greater extent. In this way the field provides an additional focusing action in the line direction. This leads to a further improvement of the spot size in the line direction, since the extra focusing action takes place towards the end of the



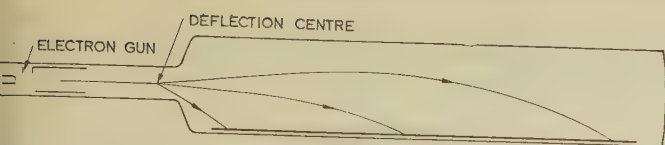


Fig. 3.—The electron paths in a banana tube with a permanent-magnet deflection field.

trajectories, resulting in an advantageous object-to-image ratio for the spot.

### 2.2.3) Astigmatism.

In the previous Section the effect was considered of the permanent deflecting field on the spot size in the line direction only. If the field in each cross-section of the tube perpendicular to its axis were homogeneous, then the spot size in the field direction would not be affected and some astigmatism would result from the additional focusing action of the field in the line direction.

Since no obstruction can be tolerated in the required viewing angle of the screen, the magnetic components must be located along the sides and/or bottom of the tube. This means that the field in a cross-section of the tube cannot be made homogeneous and an even more complicated form of astigmatism will result. With the magnetic components along the sides, the field in the top section of the tube, where the electrons pass on their way to the far end of the screen, will be curved in such a way that some defocusing of the beam takes place in the line direction and some additional focusing in the direction of the field scan. This effect can lead to severe astigmatism in the spot at the far end of the screen. It was found in practice that this astigmatism could be considerably reduced by curving the field in the lower half of the tube in the opposite direction.

A satisfactory arrangement for the magnetic deflecting field was achieved by placing a flat permanent magnet at the end of the tube, perpendicular to the trajectory plane, and extending the pole-pieces of mild steel in the shape of flat bars parallel to the axis of the tube along approximately two-thirds of the length of the main body towards the gun (see Fig. 4). The magnetic-

field gradient along the axis of the tube thus increases roughly as shown in Fig. 5, while the field in a cross-section of the tube at right angles to the axis is illustrated in Fig. 6.

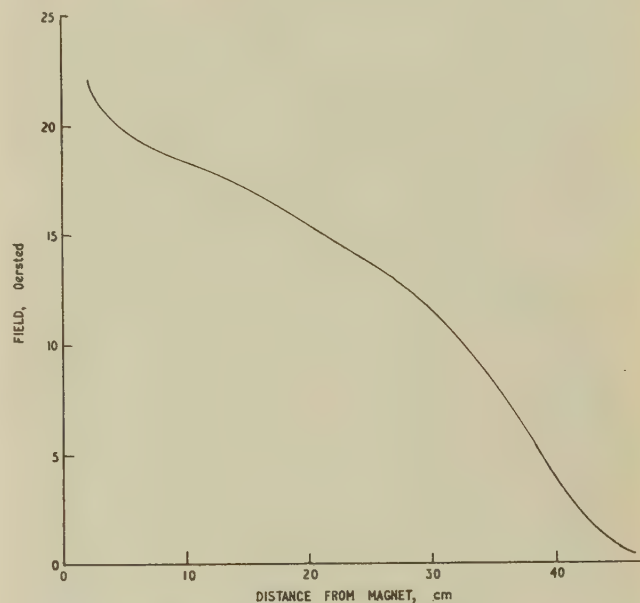


Fig. 5.—The permanent-magnetic-field gradient along the axis of a banana tube.

With this arrangement a small nearly-round spot on the screen can be obtained for the unscanned position of the spot, which, with the field strength applied in practice, appears at approximately two-thirds of the distance along the screen from the gun.

At a beam current of  $400\mu\text{A}$  the dimensions of the spot in the line and field directions are approximately 0.6 and 0.5 mm, which appear to be adequate for good resolution.

The astigmatism in the spot at the far end of the screen,

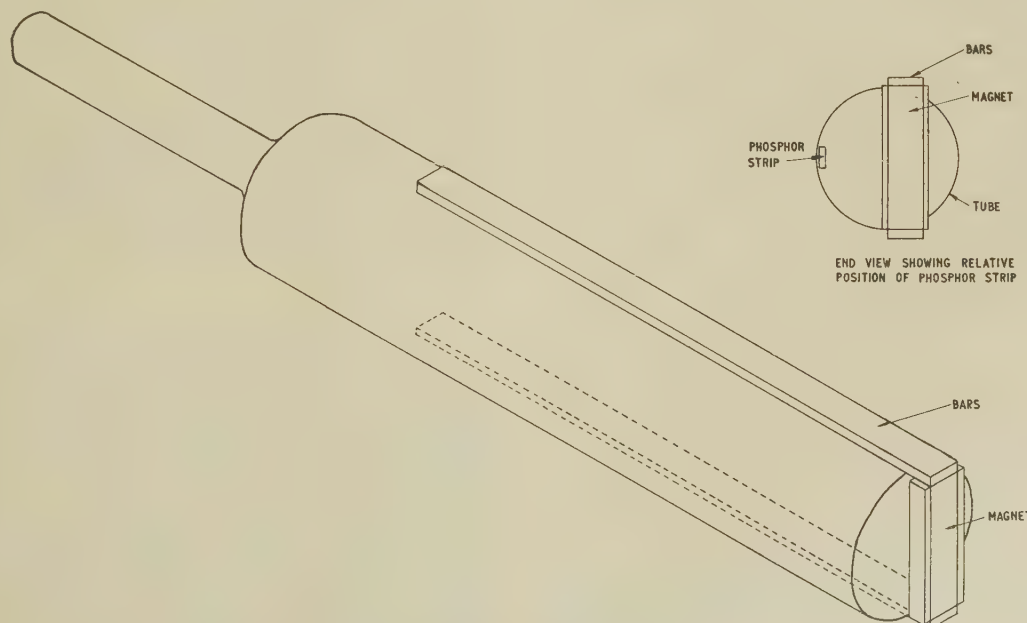


Fig. 4.—The permanent-magnet assembly used with a banana tube.





Fig. 6.—Cross-section of the permanent-magnetic field at right angles to the axis of a banana tube.

introduced by the deflecting field, can be further reduced by a modification of the line-deflection coils, which normally generate a homogeneous field. Insertion of narrower coils inside the normal ones, mounted on the same yoke and connected in series with them, will modify the deflection field in such a way that with increasing deflection to either side an increasing amount of focusing in the line direction and defocusing in the direction of the field scan is introduced. This will counteract the astigmatism in the spot towards the far end of the screen, but introduce some astigmatism towards the gun end. A reasonable compromise can then be found by adjusting the number of turns on the inserted line coils for best overall results.

With this deflection system, a reasonably good spot size can be obtained for any position of the spot along the line. A further improvement is, however, possible by applying a small amount of dynamic focusing.

The spot at the gun end of the screen could be made considerably smaller than in the centre, owing to the more favourable image-to-object ratio. This would result in a much better resolution at one side of the picture only, and is therefore not desirable. A more limited amount of dynamic focusing at line frequency is sufficient to obtain a spot size at the gun end which is at least as small as that obtainable towards the far end. The waveform required to modulate the focus current is then not critical and can, in fact, be made equal to that of the current through the line-deflection coils.

It was found in practice that satisfactory results could be obtained by adding a small subsidiary coil to the normal focus coil, and connecting this separate coil in series with the line-deflection coils.

Table 1 shows a series of actual spot sizes achieved with such

an arrangement. The beam current was  $400\text{ }\mu\text{A}$ . 'Spot size' refers to the dimensions of the area where the brightness is at least half the maximum brightness in the spot.

Table 1  
SPOT SIZE

Distance from gun end of screen (cm)	0	7	14	20	26	33	40
Spot length (mm)	0.5	0.6	0.8	0.8	0.6	0.7	1.0
Spot width (mm)	0.5	0.5	0.5	0.6	0.5	0.8	0.6

### (2.3) Colour Selection

The phosphor screen in the banana tube consists of thin narrow parallel stripes of phosphor, each fluorescing under electron bombardment in one of the primary colours, red, green and blue. As the electron beam scans along this screen at line frequency, the phosphors can be sequentially excited by applying a high-frequency lateral deflection to the beam.

With an N.T.S.C. type of colour-transmission signal, a suitable frequency for the spot wobble is that of the colour sub-carrier, since this leads to a simplification of the circuit. The circuitry aspects of this method of colour selection are fully dealt with in a separate paper.<sup>2</sup>

The main problem is to ensure that phase and amplitude of the spot-wobble deflection are correctly adjusted. This will then satisfy the requirement that the electron beam should always strike the correct phosphor when the appropriate colour signal is applied to the electron gun.

The transverse displacement of the spot can be generated by a pair of coils placed round the neck of the tube. Owing to the difference in length of the electron trajectories during the line scan, a constant amplitude of the spot-wobble deflection current would normally result in a gradual increase of the spot-wobble amplitude along the screen. As a result of its focusing properties in the direction of the field scan, the permanent-magnet deflection field adds to this effect for a large part of the scanned line where the beam remains in the lower half of the tube, but counteracts it when the spot scans the far end of the screen. Consequently the amplitude of the current through the spot-wobble coils must be modulated at line frequency in an appropriate manner to be correct for these two effects.

Minor modifications in the strength and gradient of the permanent-magnetic field can affect substantially the amplitude of the spot wobble at the far end of the screen without unduly affecting the spot size. This made it possible to modify the field in such a way that the required modulation waveform for the current through the spot-wobble coils could be generated with the aid of passive circuit-elements.

### (2.4) Influence of Extraneous Magnetic Fields

In order to obtain satisfactory colour rendering, it is essential that the tracking of the electron beam along the phosphor stripes should be correct. Small transverse deviations of the spot from the central phosphor stripe, apart from those caused by the spot-wobble action, easily lead to noticeable colour errors in the picture.

Provided that the initial setting-up procedure has been carried out correctly, and that the complete assembly of the tube and its accessories has sufficient mechanical rigidity, subsequent transverse spot displacements can be caused by an extraneous magnetic field with a component in the plane of the electron trajectories. This displacement will be proportional to



length of the electron trajectories over which such a field acts on the beam, and is therefore most serious at the far end of the screen.

A constant field, such as the earth's magnetic field, can be compensated for by applying a small direct current through a large coil placed round the main body of the tube. This coil should then generate a magnetic field in the trajectory plane, with a field strength equal and opposite to that of the disturbing component of the extraneous field.

It was found in practice that a coil round the tube, consisting of 650 turns, needed approximately 10 mA to give a first-order compensation for the harmful component of the earth's magnetic field when the axis of the tube was in the N-S direction. If the display unit is subsequently rotated round a vertical axis, however, a different value of the compensating current is required.

Other extraneous fields, e.g. from the motor which drives the drum or from transformers in the receiver, should be avoided by shielding the appropriate components.

### (2.5) Setting-Up Procedure

Correct tracking of the electron beam along the screen can be achieved by a careful setting-up procedure of the complete tube assembly.

The drum has been provided with a transparent window, through which the screen is observed during this operation with the drum stationary, and which is subsequently obscured with a strip of black tape.

The following sequence of operations can be carried out:

(a) The tube is located in its magnetic cradle inside the drum, with the screen in an approximately symmetrical position in relation to the cradle, and the various connections are made.

(b) Depending upon the orientation of the tube in relation to the earth's magnetic field, the appropriate current is applied to the corrector coil.

(c) A focused stationary spot of low intensity is generated on the screen, with zero current through the line-deflection coils. This spot is moved to its prescribed 'zero position', in the centre of the central phosphor stripe and 5 in from the far end of the screen, by adjusting the alignment of the focus coil.

(d) Line deflection is applied and the beam current is increased until the complete line can be observed easily. The line-deflection coils are then rotated until the line passes through the centre of the central phosphor strip at the gun end of the screen.

(e) The line will now be correctly located for at least two points on the screen: in the 'zero position' and at the gun end of the screen. If the central phosphor strip is not located symmetrically with respect to the magnetic deflecting field, the line will be curved towards left or right at the far end of the screen. In that case, the tube must be rotated in its cradle in the same direction, and the sequence of setting-up operations repeated from (c) onwards.

(f) If the line cannot be made completely straight, the current flowing in the coil round the tube should be changed to move the line in the direction in which it is curved, and the operations again repeated from (c) onwards until optimum tracking has been obtained.

## (3) PHOSPHORS AND SCREEN ASSEMBLY

### (3.1) The Phosphors

#### (3.1.1) Colour Co-ordinates and Decay Time.

The phosphor triplet is scanned at 10 kc/s. Each phosphor element must therefore be able to accept new video information every 100  $\mu$ s. If the phosphor is still fluorescing from the previous excitation, small-area contrast will be diminished and vertical streaks will result owing to the downward movement of the virtual image caused by the rotating lens rods.

An investigation into the decay characteristics of phosphors soon showed that the decay rates are initially exponential, but it was apparent from the pictures that there can be a very long tail. It is therefore necessary not only to specify the time limit

for the light to fall to  $1/\epsilon$  of the initial output, but also to limit the amount remaining after several line periods. The specification requires this to be below 10% of the initial emission after 100  $\mu$ s and less than 1% after 200  $\mu$ s. Neither the blue nor the green phosphors appear to meet these requirements. In practice, it is found that the blue is not objectionable owing to its low luminance contribution to the normal picture, while the green gives some unpleasant streaking effects in certain pictures. Work is in hand to reduce the afterglow to comply with the target.

The short decay characteristics required by the system limit the choice of phosphors to sulphide materials. Unfortunately, the loci of colour points obtainable from this group of phosphors (Fig. 7) fall short of the N.T.S.C. requirement in the green region.

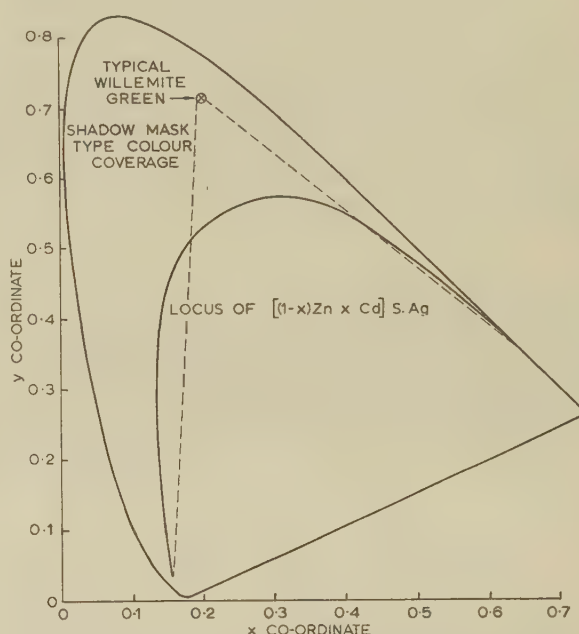


Fig. 7.—Locus of the colour points obtainable from sulphide phosphors.

The full implications of this are dealt with in the paper on colorimetry.<sup>3</sup> Table 2 compares the colour points of the phosphors used at present with the N.T.S.C. specification.

Table 2  
COLOUR POINTS OF PHOSPHORS

	Sulphide phosphors	N.T.S.C. specification
Red .. ..	$x = 0.625$ $y = 0.365$	$x = 0.670$ $y = 0.330$
Green .. ..	$x = 0.260$ $y = 0.570$	$x = 0.210$ $y = 0.710$
Blue .. ..	$x = 0.140$ $y = 0.120$	$x = 0.140$ $y = 0.080$

#### (3.1.2) Phosphor Loading and Saturation.

Each phosphor stripe is 400 mm long and 2 mm wide. The loading,  $p$ , of the stripe at 25 kV with a mean current of  $i$  microamperes is



$$p = \frac{25 \times 10^3 \times i \times 10^{-6}}{40 \times 0.2}$$

$$= 31.3 \times 10^{-4} i \text{ watts per square centimetre.}$$

Because the banana tube is a one-gun device, each stripe will be activated for only about one-third of the active scanning period. Therefore the actual loading is  $31.3 \times 10^{-4}/3 i$  watts per square centimetre. The average current corresponding to a brightness of 10 ft-L is approximately  $500 \mu\text{A}$ . The resultant loading of the phosphors is  $0.5 \text{ W/cm}^2$ . This is very similar to the MW6/2 black-and-white projection tube, which has a loading of about  $0.3 \text{ W/cm}^2$ . In the latter case the limit is set by the highest temperature the face-plate is able to withstand, a condition which does not apply to the banana tube. There the limit will be set by the characteristics of the phosphors.

Although the average phosphor loading of the banana tube and the projection tube are about equal, the instantaneous peak current densities to which the relative phosphors are subjected differ by almost two orders of magnitude. The projection tube at  $0.8 \text{ mA}$  is subjected to a peak current density of  $9 \text{ A/cm}^2$ , while in the banana tube at about  $2.5 \text{ mA}$  it amounts to about  $0.16 \text{ A/cm}^2$ . This is only twice as large as in a normal black-and-white tube.

### (3.1.3) Temperature Dependence.

In general, the efficiency of a phosphor decreases with an increase in its temperature.<sup>4</sup> The rate of change, within certain limits, is influenced in the manufacturing stage by the quantity of nickel present to control the afterglow.

It can be seen from Fig. 8 that the efficiency of the phosphors

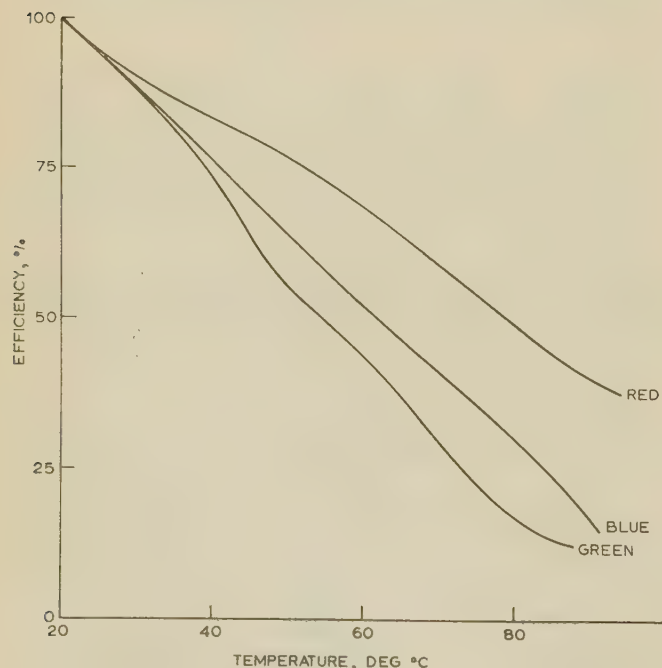


Fig. 8.—The temperature dependence of certain sulphide phosphors.

falls considerably with a relatively small temperature rise. It is therefore apparent that, since the phosphors of the banana tube are contained on a screen inside the vacuum, special precautions will be necessary to radiate the dissipated energy efficiently. This problem is considered in Section 3.2.2.

## (3.2) Screen Assembly

The phosphor triplet is deposited on a material which termed the 'phosphor substrate'. This in turn is fixed to much larger metal surface known as the 'screen carrier'.

### (3.2.1) Phosphor Substrate.

The phosphor substrate must be stable throughout all the necessary processing, be free from local impurities, and undergo no reaction with any of the phosphors. In order for it to leave the path of the electron beam uninfluenced, it must be of a non-magnetic material and have either surface or bulk electrical conductivity. Finally, to maintain its shape throughout the many stages of screen processing, it must be rigid.

In addition, the substrate must be in adequate thermal contact with a screen carrier which has good thermal-emissivity properties, combined with a sufficiently large surface area to keep the phosphors near ambient temperature under working conditions. The screen carrier is designed also to trap stray light.

The most practicable materials which fulfil the requirements are certain metals, possibly coated with a thin glass layer to seal in possible contaminants.

Thin glass layers were successfully applied to stainless-steel and aluminium strips, but on test in banana tubes the efficiency of the phosphors deposited on them was observed to be about an order lower than the best on uncoated metal strips. The low efficiency was caused by the 'sticking potential' of the glass. To overcome this the glass would need to be made conductive or to have a conductive layer, such as tin oxide, applied to it. In view of promising results being obtained by parallel work on uncoated metals, work on coated surfaces was stopped.

The metals considered as possible substrates for the phosphors were aluminium, magnesium silicide aluminium alloy (NS3), stainless steel, molybdenum, silver and gold.

Silver and gold could be used economically only when plated on a base metal. Doubts about the porosity of plated surfaces and the difficulties incurred in achieving a consistent high-clad plating soon eliminated this method. Molybdenum was not used on account of poor adhesion between the phosphor and the base material. Stainless steel was eventually considered unsatisfactory because of its poor thermal conductivity.

As a result of a series of tests it was decided to use commercially pure aluminium as the substrate material. This is the only metal found to give consistent surface conditions following rigorous cleaning schedules. A difficulty in using pure aluminium is its diminished rigidity following a high-temperature bake during the phosphor processing. From this stage onward the strip has to be handled with extreme care.

### (3.2.2) Screen Carrier.

Fortunately, the essential requirements called for by the dual role of the screen carrier are not only very similar but also never in conflict. This component must not intercept direct light from the phosphors to the window area. The surface must be made black both for good non-reflectivity and good thermal emissivity. The material should be cheap, be easily worked, fulfil all the vacuum requirements and be of similar expansion coefficient to the substrate with which it will be in good thermal contact. NS3, an aluminium alloy, is found to fulfil all these requirements. The final design is shown in Fig. 9.

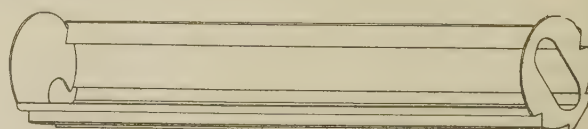


Fig. 9.—The screen carrier.



The corrugations in the screen carrier are necessary to prevent any light emitted by the phosphors striking its surface at glancing incidence. It has been found with all the matt-black surfaces investigated that considerable reflectivity is apparent at low angles of incidence if the adhesion of the black surface to the NS3 is good. Until steps were taken to prevent light striking the screen carrier at glancing incidence, unpleasant horizontal streaks were apparent in high-light areas of the picture.

The screen carrier is mounted inside the glass bulb in such a manner that it will retain the phosphor stripes parallel to the axis of the bulb. It cannot be fixed rigidly at both ends, owing to the differential expansion between the NS3 and the glass. At the highest temperature reached during tube processing it expands more than 2 mm in excess of the glass.

Contact springs between one end of the carrier and the flare of the bulb ensure electrical continuity with the final anode of the electron gun. The e.h.t. connector, mounted in the end plate of the bulb, is connected to the carrier by a flexible wire.

The most satisfactory surface coating to date is obtained with matt black enamel AMX548.

### (3.3) Screen Processing

In the early stages of the project the quality of the screen was important. All that was needed was an emissive layer which would permit spot-size measurements to be made while the electron optics of the tube were being investigated. During this stage it was noticed that the complete surface of the phosphor became stained and the efficiency fell rapidly, while any area subjected to a high beam current temporarily ceased to emit. This latter phenomenon, which is reversible, is termed 'blacking-out'.

Since the manufacturers of the phosphors were confident that the phosphors themselves could withstand the working conditions imposed by the banana tube, it was assumed that all the faults resulted from the processing, i.e. that the stains and loss of efficiency resulted from insufficient cleaning of the substrate, contamination from impurities in the substrate, or chemicals remaining inside the phosphor layers after the screen processing, and that 'blacking-out' was the result of poor thermal contact between the phosphor and the substrate.

In screen processing the following properties are required of the phosphor-coated metal strips:

- The metal should have a minimum effect on phosphor emission characteristics.
- Good electrical, physical and thermal contact should exist between metal and phosphor.
- The phosphor layer should have the texture and thickness for optimum efficiency.
- The phosphor screen should have uniform emission.
- These properties should remain good throughout life.

The phosphor can be deposited by a number of different techniques, such as settling, spraying, monolayer deposition,

photoprinting deposition, cataphoretic coating, electrostatic deposition, rolling, or pressure impregnation.

The last four methods seem particularly attractive from the point of view of uniformity and good adhesion. The effort was, however, concentrated on the first four, mainly because of the store of experience and equipment available for an immediate start.

With the numerous variables involved in both substrate materials and phosphor processing, it was necessary to assess results by carrying out short tests under high loading conditions rather than longer tests under average working conditions. All screens were mounted in standard banana tubes and processed in a similar manner.

The main properties to be determined were:

- Resistance to 'blacking-out'.
- Relative initial efficiency of the phosphors.
- Rate of loss of efficiency.

The first point was checked, at both the start and the finish of a standard 4-hour test, in which the electron beam was made to scan one colour stripe only with a constant current of 1 mA for 1 min. Points (b) and (c) were checked by measuring the light output at intervals during the course of 4 hours while the phosphor was bombarded by a constant current of 500  $\mu$ A. The results of the tests showed the most successful combination of screen processing and substrate material to be the photoprinting process using an aluminium substrate.

In the photoprinting process the phosphor is dispersed in a polyvinyl-alcohol solution sensitized with potassium dichromate. The mixture is sprayed on the substrate, which is shielded in such a way that the phosphor will cover only its allocated area on the aluminium surface. The process is repeated for all the phosphors. The finished triplet is exposed to ultra-violet light, washed and finally baked at 450°C.

### (4) THE GLASS ENVELOPE

Owing to the mechanically strong shape of the tube it can be evacuated safely when the wall thickness is only 1½ mm. It is desirable from considerations of both weight and price to work with the thinnest wall practicable. In the case of the banana tube, the limiting factor is the production of X-rays. Prototype tubes made from hard glass produce X-rays at the rate of about 1 röntgen per hour, at 1 ft from the tube, when the tube is operated at 25 kV with a current of 500  $\mu$ A. However, by using a lead-containing glass, L146, the X-ray level has been lowered to not more than 0.15 milliröntgen per hour, which is within the limits set by B.S. 415: 1957, provided that the minimum wall thickness is at least 2 mm. To ensure a good safety margin against implosion, all experimental tubes have been subjected to a total pressure of 2½ atm.

The dimensions of the envelope with tolerances are shown in Fig. 10. Moulded cylinders only have been used so far, and with the majority of them it has been difficult to select a satis-

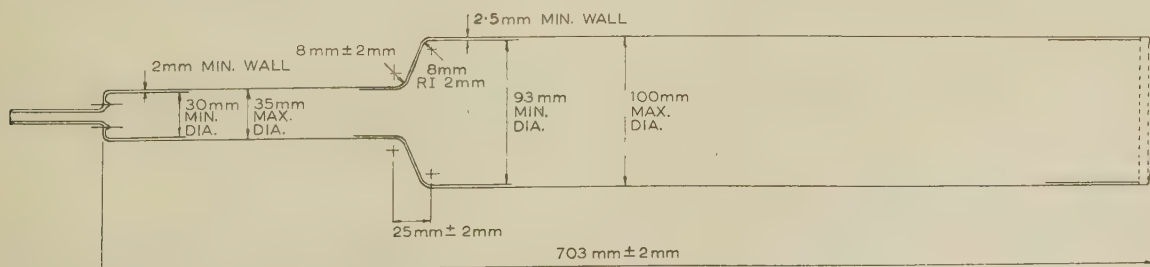


Fig. 10.—Major tolerance specifications of the glass envelope of the banana tube.



factory window area. No special measures to improve the optical quality have been requested from the manufacturers, since it is certain that a moulding process would not be considered for quantity production. The cylinders would be made by the continuous Vello process, the speed of which is such that the cost of the tubing is little greater than that of the basic materials. The quality obtained by this process meets the specification, and the physical tolerances should be about an order of magnitude better than required.

Since the screen carrier fits closely inside the glass cylinder, an unobstructed entry is necessary for correct positioning. This is possible at the end of the cylinder remote from the gun, simply by sealing the end with a 6 mm thick glass plate of 100 mm diameter as a final operation prior to pumping.

In order to obtain a field-free space within the confines of the cylinder, the inner surface of the glass can be made conductive and maintained at the final anode potential. Since most of the glass surface which can affect the electron beam consists of the window area of the tube, it is essential that the conductive coating also should be transparent and colourless. A surface resistivity of about  $1 \text{ M}\Omega$  per square is adequate to dispose of any stray charges which might land on the window area. It is advantageous to aim at the highest resistivity permissible in order to allow the percentage of light transmitted through the conductive layer to be as high as possible. The most successful coating used so far is tin oxide. This gives a hard-wearing stable surface of over 85% transmittance. It increases the reflectivity of the glass from about 4% to 11%.

Owing to the presence of a layer of tin oxide on the glass walls, the end plate cannot be sealed on to the cylinder by the normal heating process. This would cause local discolorations of the conductive layer or even evaporation. It can be avoided by sealing the parts with the aid of a low-melting-point glaze. Corning 186 glaze is found to be completely successful in forming a vacuum-tight seal between these parts. The highest temperature reached during the joining process is  $450^\circ \text{C}$ .

## (5) PRELIMINARY LIFE TESTS

### (5.1) Phosphor Life

It was realized from the outset that a fundamental objection to the system could be raised if it were established that the phosphor efficiencies decrease too rapidly during life. This effect could be investigated, however, only after a satisfactory technique had been developed for the deposition of the phosphor on a metal substrate. With the present technique of screen manufacture it has been possible to carry out only a few preliminary life tests.

To make the optimum use of the life-test equipment, the phosphor stripes should be bombarded as in normal operation. However, it was considered undesirable to attempt this, as the circuit stability which must be maintained over the test period is too critical. It was decided that, for the purpose of life tests, special tubes would be used in which the phosphors were deposited in sequence along the metal strip (Fig. 11), instead



Fig. 11.—Sequence of phosphors used for life-test purposes.

of across its width. With this arrangement the beam traverses the length of the tube, covering the three phosphors sequentially, through the action of the line time-base only.

In order to obtain the most useful results from these tests, the operating conditions must be strictly controlled. These include the e.h.t. and cathode current, and the stability of the

photometer used to measure the light output. Possibly less obvious, and certainly more difficult to control or measure, are slight variations in focus setting, slight movement of the tubes or associated parts when removing accumulated dust from the window area, and a possible shift of spectral response of the phosphors during life, which could affect the reading of the photometer. The most serious error is almost certainly caused by variations which can occur in the cathode quality. If this falls during life a greater drive voltage is needed to maintain the constant beam current required for the test. This causes the spot size to enlarge, which in turn lowers the current density falling on the phosphor. Not only does the phosphor become less saturated by this action but also new phosphor is bombarded, giving the apparent result that phosphor properties improve with life.

To diminish the errors caused in this manner, each phosphor section is scanned over half its length, and every 100 hours the normally unscanned portions are bombarded for a short period while light-output measurements are taken from them. In this way a comparison is afforded throughout life with their apparent initial efficiency.

During the test the phosphors are bombarded with a beam current of  $500 \mu\text{A}$ . Measurements are taken after 3, 6, 12 and 24 hours, and subsequently after every 100 hours.

All three phosphors have shown very similar changes of efficiency during life (see Fig. 12), but since not all the variables

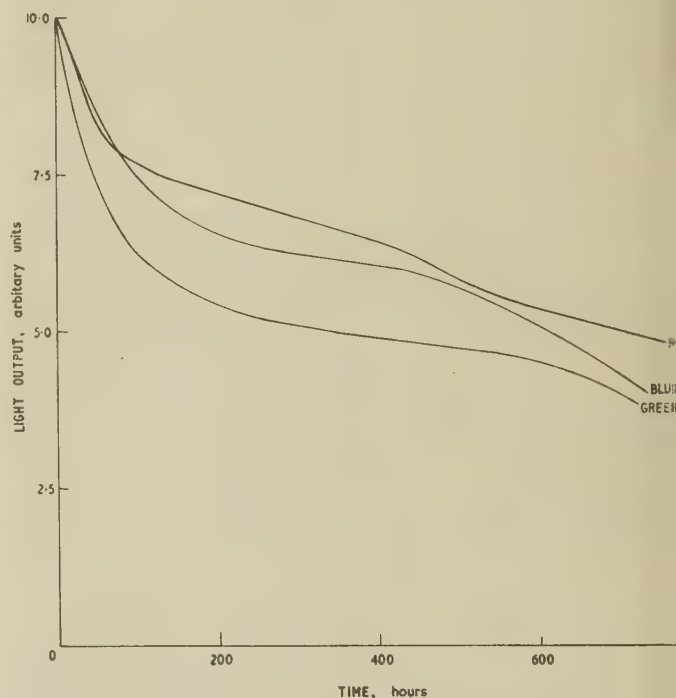


Fig. 12.—Change of efficiency of the banana-tube phosphors during a life test.

mentioned above have been satisfactorily controlled the validity of the results is limited. No areas of phosphor ceased to emit or became detached, but a slight brown stain appeared on the bombarded areas of the phosphors.

### (5.2) Cathode Life

So far the only tubes tested have failed to reach 1000 hours because of serious deterioration in cathode quality. Separate tests on cathode quality, under the loading conditions of the



banana tube, carried out in standard 17in cathode-ray tubes, indicate that the cathode is able to withstand 2000-hour life tests successfully with very little loss of emission. This problem has not yet been investigated. It is likely that the deterioration of the cathodes within banana tubes is caused by poor gas pressure brought about by inadequate stoving or cleaning schedules of one or more of its components.

### (5.3) Tin-Oxide Life

During the test the window area became brown and its transmission was reduced by approximately 5%. After cutting open the bulb it was established that the change in spectral transmissions was confined solely to the layer of tin oxide. This is assumed to have been caused by X-ray bombardment.

An essential routine operation during the test was to clean the window area every few days. Dust collected very rapidly owing to the charge maintained on the glass walls by the tin-oxide coating. A possible way to overcome this problem is to coat the outside of the glass as well as the inside. The outside wall could then be maintained at earth potential. The objections to this are first that the reject rate of the bulbs from tin-oxide faults would increase, and secondly the light transmitted by the window would fall and the reflections increase.

If the inner wall of the tube could be left non-conductive the collection of dust would be drastically reduced. A short experiment with some stainless-steel stocking mesh, 12 × 22 stitches to the inch, retained over the window area showed it to be substantially invisible during normal picture viewing. If mesh of this type can be mounted on the heat-dissipation shield in a regular manner, so that it is sufficiently far from the axis of the tube to allow the electron beam to be retained within the confines of the mesh and shield, conducting glass will be unnecessary.

### (6) CONCLUSIONS

The initial object of the project was to produce the best picture the display system is capable of giving. The banana tube in its present form substantially accomplishes this, provided that the display unit is correctly set up.

When considering the possibility of applying it to a domestic receiver, the present solution has several shortcomings, such as an expensive electromagnetic-focus lens with its associated circuitry, the need for stabilized spot-wobble modulation, h.t. and e.h.t., and a fairly difficult setting-up procedure which is influenced by the orientation of the receiver or by stray magnetic fields.

In order to make the receiver a sound domestic possibility, the electron optics must be modified, not only to ease circuitry

problems, but also to reduce the effects of stray magnetic fields on the electron beam. One approach to the improvements required is an all-electrostatic electron-optical system which will positively locate the beam on its correct phosphor. If this principle could be successfully applied, the setting-up procedure should be little more difficult than that for an electrostatic-focus cathode-ray tube used in present black-and-white television receivers, and stray magnetic fields should be no more significant.

### (7) ACKNOWLEDGMENTS

The authors wish to acknowledge the team effort so essential in successfully manufacturing a new vacuum device. Thanks are due in particular to Mr. D. Cox and Mr. A. Maycock, whose enthusiastic support over several years has ensured a flow of processed tubes.

The development of suitable phosphors with a short afterglow has been carried out by Dr. S. Rothschild and Mr. R. Gill, of the Mullard Research Laboratories, working in conjunction with Dr. H. A. Klasens, of the Philips Research Laboratories, and the phosphor production group in Eindhoven.

From the outset of the project the wholehearted collaboration of Mr. F. G. Blackler and Mr. D. Maskell, of the Cathode-Ray Tube Development Department, Mullard Radio Valve Co., Mitcham, has been indispensable. They have been responsible for the supply of processed screens, and in the later stages for the manufacture of the complete tubes.

The authors gratefully acknowledge contributions made by Mr. R. Lake and Dr. G. Davis, of the Materials Research Laboratory at Mitcham, who have assisted in determining suitable substrates for the phosphors.

The matt-black enamel powder, used for coating the screen carrier, was developed by Blythe Colour Works Ltd.

The authors also wish to thank the Director of the Mullard Research Laboratories and the Directors of Mullard Ltd. for permission to publish this paper.

### (8) REFERENCES

- (1) SCHAGEN, P.: 'The Banana-Tube Display System: a New Approach to the Display of Colour-Television Pictures' (see page 577).
- (2) FREEMAN, K. G.: 'Circuits for the Banana-Tube Colour-Television Display System' (see page 604).
- (3) JACKSON, R. N.: 'Colorimetry of the Banana-Tube Colour-Television Display System' (see page 613).
- (4) KLASENS, H. A.: 'The Temperature-Dependence of the Fluorescence of Photoconductors', *Physics and Chemistry of Solids*, 1959, **9**, p. 185.

[The discussion on the above paper will be found on page 630.]



# MECHANICAL AND MANUFACTURING ASPECTS OF THE BANANA-TUBE COLOUR-TELEVISION DISPLAY SYSTEM

By H. HOWDEN, A.M.I.Mech.E.

(The paper was first received 17th November, 1960, and in revised form 10th February, 1961. It was published in May, 1961, and was read before the ELECTRONICS AND COMMUNICATIONS SECTION 15th May, 1961.)

## SUMMARY

The major mechanical components of the banana-tube colour-television display system are described, together with the materials and manufacturing techniques used to achieve results consistent with the requirements of the system. Development has proceeded to a stage where a fully engineered version more suitable for quantity production can be considered.

## (1) INTRODUCTION

The unusual feature of the banana-tube system is the method of obtaining field scan by the movement of optical elements. The elements, in the form of three cylindrical lenses retained in critical dimensional relationship, are rotated coaxially with the electron tube at 1 000 r.p.m., which is a convenient sub-multiple of the field scan frequency.

During early assessments it was considered that the realization of the original concepts of a mechanical scanning system would present major problems, the solutions to which might well be outside the limitations imposed by the requirements of a domestic television receiver. The permissible variations between lenses in the rotating system, particularly with regard to surface finish and positioning, the noise generated by mechanical movement and the resulting wear were each considered to present problems of magnitude. The partial solution to these problems during the construction of laboratory prototypes is dealt with, as well as subsequent developments to improve performance and reliability, and to reduce costs.

## (2) ROTATING LENS DRUM

### (2.1) General Considerations

The configuration and dimensions of the rotating-lens system are governed by electron-tube and optical requirements. For a picture with a 20 in diagonal and using the present optical system, three lenses each 0.500 in in diameter and about 19 in long are spaced circumferentially at 120° intervals in a cylindrical drum as shown in Fig. 1. The lens pitch-circle diameter is

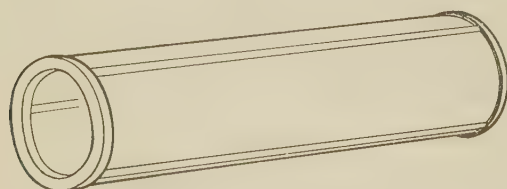


Fig. 1.—Rotating-lens drum.

5.50 in, giving overall drum dimensions approximately 6 in diameter by 22 in long.

Inaccuracies in lens positioning will result in line jitter in the scanned raster. Maximum permissible line displacement, to

eliminate completely noticeable line movement in the view image, has been taken as 0.10 line. In a 3-lens system this is equivalent to an angular lens misalignment of 0.03°, giving a linear tolerance, measured as a chord across any two adjacent lenses, of  $1.5 \times 10^{-3}$  in.

No allowance has been made for line displacement due to radial errors in lens positioning or to the effects of incorrect centring of the rotating system, and it is evident, therefore, that displacements within the limit 0.10 line cannot be consistently achieved in manufacture.

Table 1 shows measured variations in lens position in some experimental drums giving interlace errors of up to about 0.4 line.

Table 1

COMPARISON OF LENS POSITIONAL VARIATIONS IN SOME EXPERIMENTAL DRUMS

Drum		1	2	3	4
Lenses 1 to 2	Left	in 5.262	in 5.262	in 5.274	in 5.278
	Centre	5.260	5.255	5.275	5.281
	Right	5.261	5.259	5.275	5.281
Lenses 2 to 3	Left	5.262	5.263	5.279	5.278
	Centre	5.256	5.260	5.281	5.282
	Right	5.260	5.259	5.280	5.280
Lenses 3 to 1	Left	5.262	5.262	5.273	5.277
	Centre	5.260	5.261	5.277	5.283
	Right	5.262	5.260	5.273	5.283

### (2.2) Acrylic Lens Drums

In order to avoid possible random variations in lens position due to the effects of differential expansion and contraction with varying temperatures, early lens drums were made entirely of clear unplasticized polymethyl methacrylate. This material, whilst providing suitable optical properties, has been found to possess a number of undesirable characteristics which make it unsuitable for use for lenses in a final receiver. The requirement of a high-quality surface finish is difficult to achieve even after careful and repeated lapping and polishing, and electrostatic charges rapidly acquired in use cause dust to adhere to lens surfaces. Cleaning results in surface scratches, giving light scatter and consequent deterioration in lens resolution. The application of anti-static polishes reduces the tendency to build up an electrostatic charge, but is found to be effective only for short periods of time.

Subsequent work has been aimed at producing lens drums from other materials, e.g. metal and thermosetting plastics with glass lenses. The methods used for acrylic drums are, however, considered generally applicable to drums made in other materials and will therefore be described.



Referring to Fig. 2, polished lenses and preformed drum segments are clamped radially to a cylindrical metal mandrel, the lenses in machined V-grooves and the segments to the surface of the cylinder. The small gap between the V-groove and lens

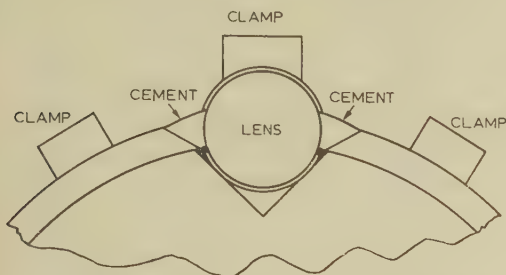


Fig. 2.—Method of cementing lenses to lens supporting segments.

surface is filled with an extruded ribbon of silicone elastomer, and cement, a pre-mixture of acrylic monomer with catalyst, is injected into the joints by a pressurized syringe. By virtue of its seeping properties the cement fills the variable gap between the necessarily accurately positioned lenses and the drum segments. A locating spigot is subsequently machined on each end of the assembly and end caps are finally cemented in position (see Fig. 3).

Ultimate joint strengths in excess of 1000 lb/in<sup>2</sup> have been recorded on experimental joints made by the above process.

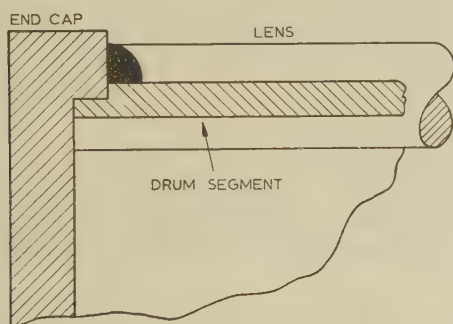


Fig. 3.—Method of attaching end caps to lens drum barrel.

### (2.3) Drums with Glass Lenses

The inherent problems associated with acrylic lenses have led to a consideration of glass as an alternative lens material. Initial difficulties of obtaining solid glass rod, manufactured to the required tolerances and free from internal flaws and surface defects, have largely been overcome by the use of thin-wall (1 mm) glass tubing.

The tubes, filled with liquid of high refractive index (1.40–1.43) or glycerol and water mixtures or petroleum oils, compared with about 1.5 for glass, will provide a relatively hard scratch-proof surface and are likely to show some improvement in resolution due to the higher quality of surface finish. Volumetric expansion coefficients of up to  $0.9 \times 10^{-3}$  for these liquids, compared with about  $0.36 \times 10^{-4}$  for glass, will render the use of an expansion/contraction device necessary. A suitable arrangement is shown in Fig. 4. The maximum volumetric differential within an extreme temperature range  $-10^\circ\text{C}$  to  $+50^\circ\text{C}$  is calculated to be  $\pm 0.45 \text{ in}^3$  for an 80/20% glycerol-water mixture.

The use of metal or plastic segments in drums containing glass lenses required careful consideration of the bonding medium. A

technique is known for bonding acrylic materials to glass, involving the pre-treatment of the glass with vinyltrichlorosilane, and giving joint strengths in excess of the ultimate strength of the glass itself. The inherent flexibility of the bonding medium accommodates variations in linear dimensions with reasonable temperature changes over joint lengths of up to about 20 in.

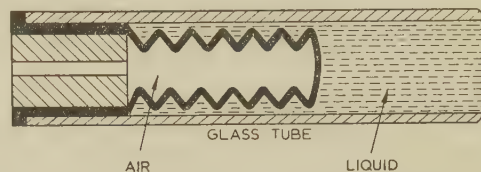


Fig. 4.—Rubber expansion/contraction bellows for liquid-filled glass-tube lenses.

The limiting rotational speed of such a lens drum is therefore the limit of the peripheral velocity of the glass, and this may be determined from the expression for the limiting centrifugal stress

$$f = \frac{Wv^2}{g}$$

where  $f$  = Limiting stress  $\approx 750 \text{ lb/in}^2$  for glass

$W$  = Weight, lb/in<sup>3</sup>

$v$  = Peripheral velocity.

$$\text{Therefore } v = \sqrt{\frac{fg}{W}} = \sqrt{\frac{750 \times 32.2 \times 12}{0.095}} = 1750 \text{ in/s.}$$

For a 6-in-diameter drum the maximum permissible rotational speed will be  $1750/6\pi \times 60 = 5500 \text{ r.p.m.}$

Bonds of comparable strength, of the type shown in Fig. 2, have also been made between glass tubing and thin sheet metal using epoxy-resin adhesives.

### (2.4) Anti-Reflective Coating

An important feature of the banana-tube system is the improvement in image contrast ratio in conditions of high ambient illumination. The picture is presented against a non-reflective background provided by a black coating on the drum segments between lenses. The quality of this coating, therefore, its surface texture and reflectivity will have an important effect on picture quality.

Chemical and paint coatings have been found to be inefficient as non-reflective finishes, particularly after handling. Finger marks and abrasions show as an irritating flicker in the picture at a frequency of  $16\frac{2}{3} \text{ c/s.}$

Table 2 shows the reflectivity of some coatings measured by photometer under 60 W tungsten-filament illumination, the most satisfactory results being obtained with dyed woven fabric materials glued to the drum surface.

Table 2  
REFLECTED LIGHT READINGS OF SOME DRUM COATINGS  
UNDER 60 W ILLUMINATION

Material	Light reading
	ft-lamberts
Matt black cellulose paint ..	0.32
Matt black water paint ..	0.18
Black woven cloth ..	0.13



### (3) DRUM SUPPORT BEARINGS

#### (3.1) Requirements of the Bearing System

The necessity for providing ready withdrawal facilities for the electron tube has eliminated the possibility of supporting the rotating drum about a simple 2-bearing arrangement coincident with the drum axis. It is more convenient to provide an aperture in one end of the drum, through which the tube may be removed for servicing or replacement, and to support this open end on an external system of bearings contained in free-running rollers.

The requirements of the supporting bearings to operate quietly and for long periods without attention have involved an extensive investigation into the performance characteristics, in terms of the ultimate life, of available bearing materials and bearing types.

The required life expectancy, based on a maximum likely viewing time over five years, has been assessed as 10 000 hours.

The arrangement of rubber-tyred rollers shown in Fig. 5 has been adopted after experimental investigations into the load-carrying capacity, more particularly of suitable rubbers for the tyres, and the stability requirements of the system.

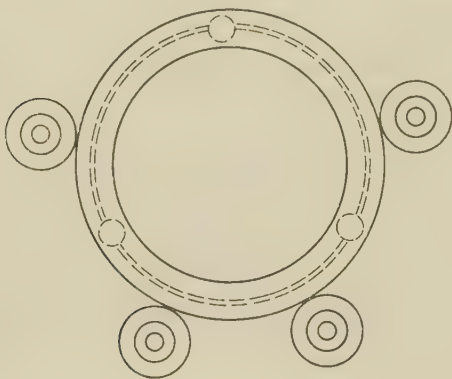


Fig. 5.—Arrangement of supporting rollers for open end of lens drum.

Tests have been carried out on three distinct types of bearing:

- Ball bearings.
- Lubricated metal sleeve bearings.
- Dry plastic sleeve bearings.

From space considerations 1.5 in has been chosen as a suitable roller diameter. The rotational speed of the roller is then 4000 r.p.m. for a drum speed of 1000 r.p.m., and the applied radial load on the bearing is approximately 1 lb for a drum weight of 4 lb.

#### (3.2) Ball Bearings

Ball bearings of the rigid radial journal type mounted singly as shown in Fig. 6(a) have proved to be unsuitable owing to high noise level. An ultimate bearing life of 320 hours has been recorded for a commercial bearing, 3 200 hours for a selected bearing, and over 10 000 hours for a selectively-assembled precision bearing.

Track and ball imperfections and relative movement between track raceways are believed to be the major source of noise, and this is substantiated by the improvement obtained with precision bearings, particularly when such bearings are mounted in pairs and preloaded axially as shown in Fig. 6(b). Such an arrangement, however, is expensive, and it had been established that other methods, showing considerable improvements both in quiet running and cost, are possible.

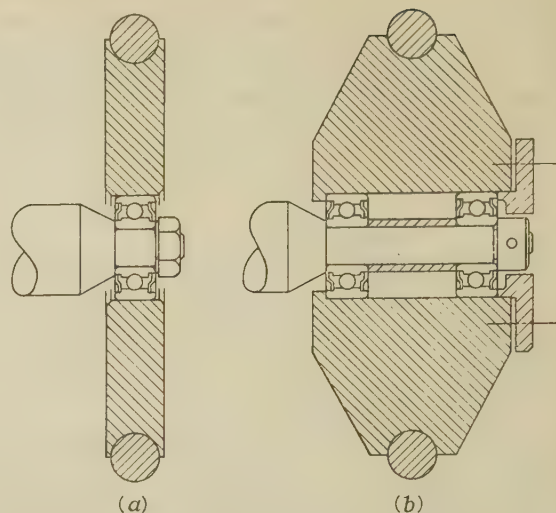


Fig. 6.—Method of mounting ball races in bearing test.

- (a) Single bearing.
- (b) Twin axially preloaded bearing.

#### (3.3) Sleeve Bearings

A sleeve bearing presents a possible alternative solution. Large numbers of this type of bearing are in everyday use, usually in metal for other than low-speed applications, and oil lubricated. The method of supplying the oil varies from occasional and often haphazard external applications for intermittently operating mechanisms, to pressure feeds, where the cost of such devices can be justified in heavily loaded and continuously running bearings.

##### (3.3.1) Coated Sleeve Bearing.

The main problem in the design of a small long-life low-cost metal sleeve bearing is to provide a film of lubricant between the load-carrying surfaces. In the simplest arrangement shown in Fig. 7(a) using a solid metal sleeve rotating about a fixed shaft

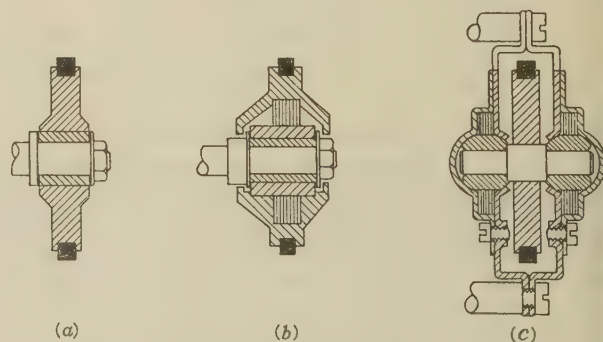


Fig. 7.—Types of bearing used in sleeve bearing tests.

- (a) Single rotating bush.
- (b) Single rotating bush with oil circulating system.
- (c) Twin self-aligning rotating shaft.

metal contact will occur on initial starting from rest, owing to the absence of sufficient hydrodynamic pressure to support the load, and also through loss of lubricant due to leakage from bearing ends. If metal pick-up can be prevented during these periods by the prior application of an anti-friction coating, an increase in bearing life can be expected. The required time between periodic external applications of lubricant will also be increased, and if the degree of scuff resistance of the coating



sufficiently high it may be possible to run such a bearing in a dry state, i.e. without any additional lubrication.

The results of a series of tests intended to substantiate this statement are given in Table 3, and for purposes of comparison Table 4 is included showing the results obtained with uncoated bearings both with and without oil lubrication.

Table 3

LIFE TEST ON COATED SLEEVE BEARINGS

Shaft coating	Bush coating	Lubricant	Duration of test	Remarks
A	Nil	Nil	hours 3½	Seized
A	Nil	Molybdenized grease	20	Shaft worn 0.002 Bush worn 0.025
A	Nil	Mineral oil	59	Shaft worn 0.002 Bush worn 0.030
B	B	Molybdenized grease	6	Seized
C	C	Nil	8	Shaft worn 0.012 Bush worn 0.002
C	C	Mineral oil	16	Seized

Table 4

COMPARATIVE TEST ON UNCOATED BEARINGS

Lubricant	Duration of test	Remarks
	hours	
Molybdenized mineral oil ..	2	Seized
Mineral oil .. ..	32	Seized
Nil .. ..	5	Seized

In the test, the bearing material was bronze alloy, the shaft material was mild steel and the bearing diametral clearance was 0.0005–0.0015 in for a bearing diameter 0.250 in and length 0.375 in.

The surface velocity is therefore 196 ft/min for a convenient speed of rotation for comparative test purposes of 3000 r.p.m. The radial bearing load was 1.25 lb, and the bearing pressure is therefore 13.3 lb/in<sup>2</sup>. The pressure-velocity rating is 1610 lb/in<sup>2</sup>-ft/min.

The maximum attained life of 59 hours falls far short of the required 10 000 hours, and it is evident that, although some of the anti-friction coatings prevent complete bearing seizure, the presence of an oil lubricant is significant in promoting bearing life.

The quantity of lubricant provided by an initial application in this simple system, and allowing for centrifugal losses, is very

small. As all bearings were dry on completion of the test, loss of lubricant can be regarded as a major factor contributing towards bearing failure, and improved results are therefore to be expected if the initial supply of lubricant is increased.

### (3.3.2) Sintered Metal Bearings.

Table 5 shows results with an increased oil content obtained by the use of sintered porous metal bushes containing about 25% by volume of lubricating oil, again in the configuration of Fig. 7(a). It is interesting to note the improvement obtained by using sintered iron bushes, compared with the more usual sintered bronze. In each case bearing failure was again due to failure of the lubricant. A further series of tests was therefore undertaken on a bearing of new design, incorporating an oil-circulating system and using a number of different lubricants.

### (3.3.3) Sleeve Bearing with Oil Circulation.

In the new bearing shown in Fig. 7(b) a further increased volumetric oil content is provided by a reservoir in the form of a felt pad in close contact with the outer surface of a sintered bronze bush. Ducts are incorporated in the rotating housing for returning the lubricant fed along the bearing surface under hydrodynamic pressure and centrifuged off the bearing ends. The felt pad also provides filtration to eliminate any contaminating solid particles which may find their way into the system. The return feed is by capillary attraction through the felt and porous bearing material.

Table 6 shows results obtained with the new bearing using a variety of commercially available lubricants. An improvement of four times the total bearing life is noticed compared with the results obtained using the same lubricant (type A) in the simple rotating bush bearing, and a further improvement is obtained by using a molybdenized mineral oil.

### (3.3.4) Two-Bearing Arrangements.

A subsequent test intended as a performance comparison between sintered bronze bearings using rotating bushes on a fixed shaft, and fixed bushes with rotating shafts [Fig. 7(c)] and using lubricant A, showed a total life before lubricant failure of 9600 hours. The bearing bore in this case was 0.187 in, giving a surface velocity of 147 ft/min and a pressure-velocity rating for the two 0.312 in long bushes of 1570 lb/in<sup>2</sup>-ft/min.

In view of the considerably improved performance obtained using the two-bearing configuration of Fig. 7(c) compared with either of the two rotating bush bearings of Figs. 7(a) and (b), no further work has been undertaken on the latter type. The reason for failure in every case, namely gumming due to oxidation of the lubricant, clearly indicated that the ultimate life of a hydro-dynamically lubricated bearing, containing a relatively small amount of lubricant, is limited to the life of the lubricant.

Table 5

LIFE TEST ON SINTERED METAL BEARINGS

Bearing material	Lubricant	Duration of test	Remarks
		hours	
Sintered bronze ..	Mineral oil (A)	288	Lubricant partially solidified
Sintered bronze ..	Mineral oil plus extreme pressure additive	360	Lubricant partially solidified
Sintered iron ..	Mineral oil (A)	1690	Lubricant partially solidified

Bearing dimensions: bore, 0.250 in; length, 0.375 in.  
Speed of rotation, 3000 r.p.m.



Table 6

LIFE TEST ON THE NEW BEARING USING DIFFERENT LUBRICANTS

Lubricant	Duration of test	Remarks
	hours	
Mineral oil A .. ..	1 200	Lubricant solidified
Mineral oil B .. ..	1 340	Lubricant solidified
Mineral oil C .. ..	360	Lubricant solidified
Molybdenized mineral oil	4 700	Bush worn and vibrating
Silicone oil .. ..	165	Bush badly worn
Molybdenized silicone oil	670	Lubricant partially solidified

The difference in performance between the two types can possibly be explained by increased turbulence in the rotating bush assisting oxidation by churning and cavitation and resulting in premature lubricant breakdown.

The test results shown in Table 5 further indicate that the bush material has some effect on lubricant life. Sintered iron is shown to advantage compared with the more usual and readily available sintered bronze. Much work remains to be done to substantiate this, especially in view of the difficulty of obtaining small quantities of die-formed parts of suitable shape in sintered materials other than bronze.

#### (3.4) Dry Bearings

The problems associated with small lightly-loaded hydro-dynamically-lubricated metal sleeve bearings have led to an investigation of the performance of dry plastic bearings and bearing materials.

Plastic bearings, usually in reinforced laminated thermosetting materials with water lubrication, have been in use for many years, and more recently thermoplastic grease-lubricated bearings have been used for low-speed heavy-load applications. Plastic and composite bearings materials, intended for use without additional lubrication, are of comparatively recent introduction,

and information is not readily available on their performance continuously operating conditions in the medium-to-high speed ranges.

Early tests with nylon have shown dimensional instability with rising bearing temperature, sufficient to cause complete seizure after a few hours' running even with diametral clearances as high as about 0.003 in for a 0.250 in-diameter bearing.

Polytetrafluorethylene, whilst exhibiting less dimensional instability and providing further improvements when used as a coating on metal surfaces and as an impregnant for porous metal bushes, shows little resistance to abrasive wear, the material exuding from the bearing ends as a finely divided powder.

Table 7 shows test results obtained with the simple single rotating bush and fixed shaft arrangement of Fig. 7(a), using various plastics, specially compounded thermoplastic mixtures, proprietary bushes and dry bearing materials.

With one exception all bearings failed at less than 1 000 hours continuous operation. The exception (Type G1) is, however, sufficiently interesting to merit further comment. It is the only bearing tested, other than ball bearings, to have achieved the stated objective of 10 000 hours' operation without attention. As such, it can be regarded as the only bearing shown by experimental test to be suitable for use on the drum supporting rollers of the banana tube device.

The bearing dimensions tested were 0.375 in bore, 0.375 in bearing length and 8.9 lb/in<sup>2</sup> specific radial bearing pressure. The speed of rotation was 3 000 r.p.m. giving a pressure-velocity rating of 2 620 lb/in<sup>2</sup> ft/min.

An initial diametral clearance of 0.001 in increased progressively after bedding-in wear of a further 0.0006 in to a measured final clearance of 0.006 in. The large initial clearance would appear to limit the usefulness of the material to applications calling for a low-cost reliable bearing, not requiring close running fits. Some reduction in clearance may be possible by reducing bearing wall thickness and thus improving the efficiency of the heat-conducting path.

Table 7

LIFE TEST ON SMALL DRY BEARINGS AND DRY BEARING MATERIALS

Material	Duration of test	Initial clearance	Final clearance	Remarks
	hours	in $\times 10^{-3}$	in $\times 10^{-3}$	
Nylon .. ..	0.25	0.8	Nil	Seized
Nylon .. ..	13	2.5	Nil	Seized
Hard Nylon .. ..	0.5	0.4	Nil	Seized
Hard nylon .. ..	24	2.7	Nil	Seized
Molybdenized nylon	24	1.7	2.7	Heavy vibration
Polytetrafluorethylene (P.T.F.E.)	24	2.7	38	Excessive clearance
Polytrifluoroethylethylene (P.T.C.F.E.)	120	0.5	20	Excessive clearance
P.T.F.E. plus molybdenum powder	48	0.1	20	Excessive clearance
P.T.F.E. plus tin powder	96	0.3	6	Large clearance
P.T.F.E. plus bronze powder	130	0.4	9	Large clearance
P.T.F.E. plus stainless-steel powder	17	0.3	5	Vibration and scuffing
P.T.F.E. plus glass-fibre	180	0.3	7	Vibration and scuffing
Proprietary bearings				
A .. ..	72	2	6	Rapid wear and pick-up
B .. ..	6	0.5	6	Heavy vibration
C .. ..	72	0.1	20	Excessive clearance
D .. ..	810	0.5	11	Excessive clearance
E .. ..	668	0.5	23	Vibration and scuffing
F .. ..	384	0.7	Nil	Partially seized
G1 .. ..	10 056	1.0	6	Still running satisfactorily
G2 .. ..	339	0.1	Nil	Seized

Bearing diameter: 0.250-0.375 in.  
Speed of rotation: 3 000 r.p.m.  
Radial bearing pressure: 1.250 lb.



#### (4) DRIVE AND BRAKING SYSTEM

##### (4.1) System Description

With a field scan frequency of 50 c/s (or single-frame period of 0.02 sec) and using a 3-element optical system, a synchronized lens-drum rotational speed of  $60/(0.02 \times 3) = 1000$  r.p.m. is required.

Owing to the cost and complexity of alternative systems, and the necessity for smooth and quiet operation, a squirrel-cage induction motor, in combination with a magnetic brake for speed control, has been adopted as a suitable method of providing the drum drive.

Two possibilities exist for interconnecting driving motor and driven drum, direct or indirect drive. Using the indirect method shown in Fig. 8, a smooth-face pulley on the motor shaft drives the machined rim of the drum end-plate through a rubber-tyred idler wheel free running about a spring-loaded countershaft. The motor-pulley diameter can then be chosen to give the required drum speed for any convenient motor-shaft speed.

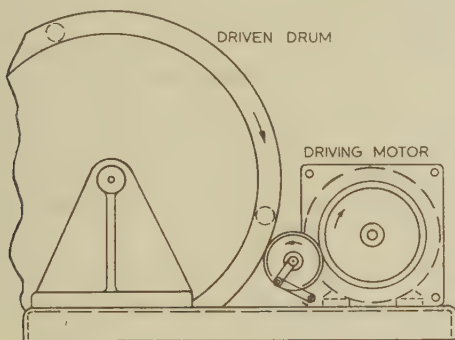


Fig. 8.—Rim drive for rotating lens drum.

The method has the disadvantage that the number of bearings required on the motor, countershaft and drum spindle are all potential sources of wear and noise. It is also found that a rubber rim drive of sufficient stiffness to transmit the driving torque is a further source of objectional noise.

A direct motor drive, using the minimum number of moving parts, and with motor shaft and drum axis coincident, has therefore been chosen. A coupling with some angular flexibility is fitted between the motor shaft and drum. The motor is then required to run at a speed fractionally in excess of the drum synchronous speed and is locked into synchronism by an electromagnetic brake actuated from an amplified reference signal taken from the rotating drum.

##### (4.2) Drive Motor

The speed of rotation of an induction motor is determined by the number of wound stator poles and the supply frequency. A 4-pole motor operated from a 50 c/s supply will have a pole speed of 1500 r.p.m. If the supply frequency drops below exactly 50 c/s the required synchronous speed will never be attained, and the motor speed will be further reduced by the inherent rotor slip. A 4-pole motor with a pole speed of 1500 r.p.m. must therefore be used and must be designed to operate at one-third slip.

The slip at which maximum torque occurs is dependent on motor resistance. If this is chosen to give maximum torque at an operating speed of 1000 r.p.m. the speed will be independent of torque variations at 1000 r.p.m., i.e. the gradient of the speed/torque curve at this point will be zero, and the motor will not respond to control braking.

The motor in use has speed/torque characteristics of the form shown in Fig. 9. The necessary increase in rotor resistance to

achieve this has the disadvantage of increasing rotor losses with consequent heating and less efficient operation.

The torque required to drive the drum at a steady speed of 1000 r.p.m. against frictional resistance has been found by measurement to be about 10 oz-in. For reasons of economy the mean braking torque has also been made 10 oz-in. The minimum torque output from the motor should therefore be 20 oz-in. The motor in use produces a drive torque of about 25 oz-in, and is inherently capable of locking the drum into synchronism from rest in approximately 20 sec with an applied voltage of 200 V.

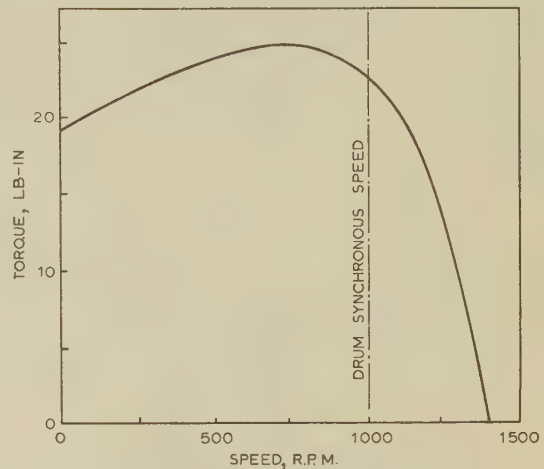


Fig. 9.—Speed/torque characteristics of drum drive motor.

##### (4.3) Magnetic Brake

Two methods of providing the necessary braking torque have been used in experimental machines. Initially an eddy-current disc brake was used, whereas in later machines an integral brake is incorporated within the motor housing consisting of a d.c. winding on the motor stator.

In the first method, shown in Fig. 10(a), an annular copper disc rigidly attached to the driving end of the drum rotates

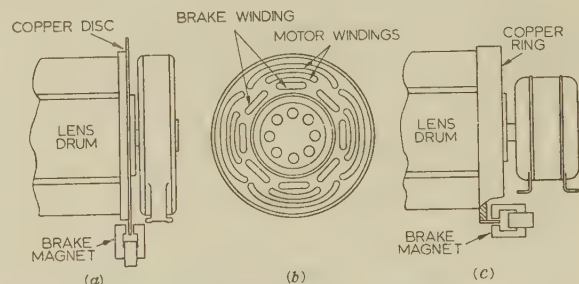


Fig. 10.—Speed-control brake.

- (a) Separate brake with axial air-gap.
- (b) Motor with integral brake.
- (c) Separate brake with radial air-gap.

between the poles of an electromagnet. The braking torque produced is then proportional to the velocity of the disc and the square of the magnetic field. The strength of the magnetic field, for any given magnet configuration and power input, is inversely proportional to the square of the linear air-gap between the magnet poles.

The difficulty of maintaining extreme axial stability in the rotating drum with sleeve-type bearings on the motor shaft



necessitates the use of a large air-gap, thus reducing the braking efficiency and increasing the power requirements of the braking system.

The integral brake method also has disadvantages in that the additional winding causes a further undesirable temperature rise of the motor assembly and has proved to be complicated and expensive in manufacture.

It is considered that an external separately mounted brake with a radial air-gap between magnet poles and using possibly an eddy-current ring as shown in Fig. 10(c) would be a more suitable arrangement.

The effects of stray magnetic fields from the motor and magnetic brake on the picture have been minimized. Some electron-beam deflection giving incorrect colour rendering on the viewed image can occur, particularly when using external brakes in close proximity to the electron tube. Efficient magnetic screening of motor and brake, and the suitable disposition of the components is therefore necessary. A possible final arrangement is shown in Fig. 11.

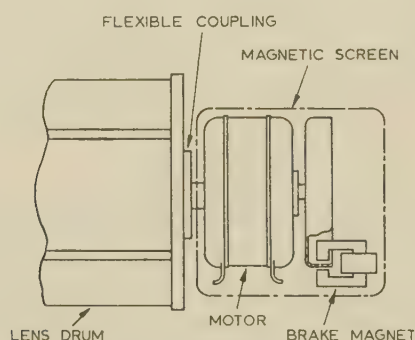


Fig. 11.—Arrangement for motor and brake.

## (5) NOISE

### (5.1) Source of Noise

High-quality sound reproduction has become an accepted feature of domestic television. The maintenance of this feature is therefore a prime requirement of any new receiver.

In a system such as the banana-type display using mechanically moving parts, the sound associated with this movement must be inaudible at viewing distance, or at least sufficiently subdued to be indistinguishable above normal speaker background noises.

The major sources of noise emanating from the rotating field scan mechanism of early experimental banana-tube receivers were found to be the following in order of magnitude:

- Bearings.
- Vibration due to out-of-balance and out-of-roundness effects.
- Wind noise.
- Motor magnetic hum due to 50 c/s excitation.

A very considerable reduction in noise level was found to be necessary at this stage, and subsequent modifications have, in fact, given marked improvements in this respect.

In later machines, the main sources of noise were end float of the driving-motor shaft, and out of roundness of the drum support rollers. These are dealt with in Sections 5.2 and 5.3.

### (5.2) Motor Noises

Axial movement of the motor rotor assembly, due to the accumulation of dimensional tolerances of motor casing and shaft, has been reduced, and intermittent bumping of the motor shaft eliminated, by the use of felt packing washers positioned between motor-shaft shoulders and bearing ends. Vacuum

varnish impregnation of the wound stator core has effected substantial reduction of lamination vibration and consequent motor magnetic hum.

### (5.3) Vibration

The effects of out of roundness of the rubber-tyred rollers, and to a lesser extent the drum rim, are found to be more significant and more difficult to eliminate. The significance of the noise emanating from the rubber rollers and the importance of subduing this has been demonstrated by sliding the drum round at its synchronous speed on water-lubricated fixed rubber pads. The reduction in noise under these conditions is marked, the noise from the mechanism being reduced to an almost inaudible level at a distance of a few feet. The method, however, is not considered applicable to a domestic television receiver.

Using rubber rollers, permanent deformation of the material under load in the at-rest state, owing to the inherent compressive set characteristics of rubber and rubber-like materials, inducing radial movements of the drum about its axis, and hence vibration of the rotating system.

The minimum frequency of disturbing vibrations at a drum speed of 1000 r.p.m. will be 1000 cycles/min and the maximum several thousand cycles per minute, depending upon the number of flats which may have developed on the supporting rollers.

In order that drum resonance shall not occur, and the harmonic components of the periodic disturbance may be ignored, the resonant frequency of the supported drum should be less than 1000 cycles/min. A safe margin would be provided by a drum resonant frequency of 750 cycles/min.

The necessary deflection to give this resonant frequency may be determined from the following relationship for simple harmonic vibrations:

$$T = 2\pi\sqrt{\frac{w}{eg}}$$

where  $T$  = Periodic time, sec.

$w$  = Supported weight, = 2 lb.

$e$  = Stiffness of supports, lb/in deflection.

and 
$$N = \frac{30}{\pi} \sqrt{\frac{eg}{w}}$$

where  $N$  = Frequency of vibrations, cycles/min

$$\text{Thus } e = \frac{w}{g} \left( \frac{\pi N}{30} \right)^2 = \frac{2}{32 \cdot 2 \times 12} \left( \frac{\pi \times 750}{30} \right)^2 = 32 \text{ lb/in.}$$

Therefore the required deflection is  $2/32 = 0.062$  in.

The provision of this large deflection without the added cost and complication of using separate high-deflection mounts has proved difficult. Soft rubbers with sufficiently low compressive set characteristics have not been found. Reasonable results have, however, been obtained using silicone rubbers of hardness 50° BS by suitably shaping the rubber to give deflections of about 0.04 in under load.

Under these circumstances drum resonance will occur during acceleration from rest to synchronous speed, but the acceleration will be sufficiently rapid to prevent vibrations of large amplitude from being attained.

### (5.4) Residual Noises

It is anticipated that residual noises such as that due to turbulence will be effectively subdued by enclosing the frame scan mechanism and drive system in a suitably shaped case lined with a sound-absorbing material.



## (6) VIEWING MIRROR

### (6.1) Requirements

In order to provide a reasonably adequate field of view the dimensions of the curved viewing mirror must be larger than the picture image. A mirror of 28 in width has been chosen giving a horizontal viewing angle of approximately  $50^\circ$  for a picture with 20 in diagonal.

The mirror is cylindrical in shape with a hyperbolic cross-section, the mirror axis lying parallel to the axis of the lens drum. Movement of the observer results in a movement of the image relative to the mirror. Under these circumstances unevenness and undulations in the mirror surface will produce image distortions with viewer movements.

### (6.2) Glass Mirrors

The few glass mirrors manufactured for experimental purposes have not been entirely satisfactory in this respect, random variations in surface shape and consequent image distortions being discernible. The mirror backings were made by the established technique of sagging a heated glass plate on to a shaped former, and the method clearly requires further development before mirrors of the required accuracy can be consistently produced.

### (6.3) Metal Mirrors

Electro-polished metal mirrors have been made experimentally with the required hyperbolic shape and distortion-free. The quality of surface finish, however, has been found inferior to glass, the crystal boundaries of the metal giving an orange-peel effect on the mirror surface.

### (6.4) Plastic Mirrors

Vacuum aluminized thermoplastics may provide a more suitable alternative. Such materials of sufficient thickness and adequately supported, possibly on a plastic moulded backing frame, would appear likely to compare favourably in cost with curved-plate glass mirrors and have the added advantage of reduced weight.

## (7) CABINET DESIGN

The original objectives of the banana-tube project and its possible future application to a fully-engineered domestic colour-television receiver have led to a consideration of possible cabinet designs.

Recent tendency in receiver cabinet design is towards reductions in cabinet depth by the use of wide-angle tubes. In the banana-tube device front-to-back cabinet depth is determined by the diameter of the field-scan drum and its position relative to the viewing mirror. This compares favourably with receiver cabinets using direct-viewing wide-angle tubes.

Experimental machines built for system analysis purposes have been based on an image size of 16 in  $\times$  12 in, giving a diagonal of 20 in. Using a 6 in-diameter drum this gives an overall cabinet depth of about 12 in. Other image sizes could be obtained by scaling the dimensions of tube and field-scan components up or down, but a decrease in image size would probably not give a corresponding decrease in cabinet width. Any increase in image size would benefit the image-width/overall-depth ratio, and the present dimensions can therefore be regarded as a reasonable minimum.

The volumetric requirements of circuit, tube, field-scan and drive mechanism has been assessed as 7.5 ft<sup>3</sup>, and the minimum cabinet width is 36 in for a picture of the present dimensions. Possible final cabinet designs based on these dimensions are shown in Figs. 12(a) and (b).

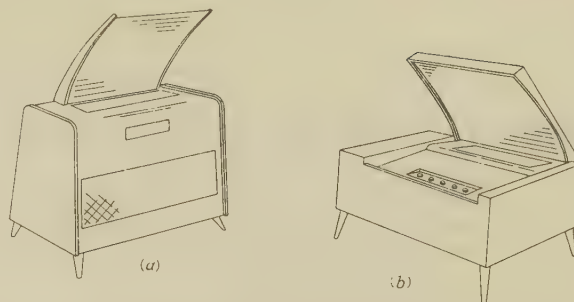


Fig. 12.—Possible cabinet designs.

A first prototype receiver has been built generally in accordance with Fig. 12(a) using an internal open-type metal framework on which flat panels forming the side, front and rear members of the cabinet are fastened by spring clips. Wood-frame cabinets are considered unsuitable owing to the necessity for providing a support for the rotating-field scan mechanism of sufficient dimensional stability, independent of external effects, e.g. variable atmospheric environment.

The construction used is found to be particularly convenient for a development prototype, the panels being quickly removable to give ready internal access. For simplicity of maintenance the method is also likely to provide a more acceptable basis for a final cabinet design than the conventional open-back screw-in chassis box construction.

## (8) CONCLUSIONS

The construction of the major mechanical components of the proposed new colour television receiver has been considered, and it has been shown that problems concerning the reliability of and noise from the rotating field scan mechanism need not be a basic objection to the system.

The unusual cabinet proportions, and the presence of a large and essentially visible rotating drum, can probably be made acceptable by careful attention to cabinet design.

## (9) ACKNOWLEDGMENTS

The author wishes to acknowledge the contributions made to initial concepts by Mr. G. Birkbeck, and to assistance given in detail design by Messrs. J. Thomas and P. Grealy of Mullard Research Laboratories. The author wishes to acknowledge contributions made by the following:

Messrs. P. H. Collins and J. Pentney of I.C.I. Plastics Laboratory, for their work on plastic lens drums.

Wills Pressure Filled Joint Ring, Ltd., and the Glacier Metal Co., Ltd., for the supply of dry bearing material samples for test purposes.

E.M.O. Instrumentation, Ltd., for their suggestions on precision ball-bearing types and methods of support.

Precision Rubbers, Ltd., for advice on synthetic rubbers for the drum support rollers.

Messrs. J. E. Nash and W. Hume of Small Electric Motors, Ltd., for their suggestions on electric-motor types.

Mr. D. C. Carter of Robinson King and Co., Ltd., for his work on curved-glass mirrors.

The electrical design of the integral motor is due to Mr. L. A. Voice of Mullard Research Laboratories.

The author also wishes to thank the Director of Mullard Research Laboratories and the Directors of Mullard, Ltd., for permission to publish the paper.

[The discussion on the above paper will be found on p. 630.]



## CIRCUITS FOR THE BANANA-TUBE COLOUR-TELEVISION DISPLAY SYSTEM

By K. G. FREEMAN, B.Sc., A.Inst.P.

*(The paper was first received 17th November, 1960, and in revised form 10th February, 1961. It was published in May, 1961, and was received before the ELECTRONICS AND COMMUNICATIONS SECTION 15th May, 1961.)*

## SUMMARY

The circuits necessary to operate the banana-tube colour display are described under the headings of tube supplies, drum synchronization and video-signal processing. Circuit techniques which are peculiar to this form of colour-picture display are described in some detail.

## (1) INTRODUCTION

In order to produce colour pictures on the banana-tube display a wide variety of circuits is necessary. For a complete receiver, of course, some of these circuits would be identical or very similar in form to those employed in present monochrome receiver practice, whilst others would perform functions which would be common to all colour receivers intended for use with a particular transmission system—for example, the well-known N.T.S.C. system. Circuits of these types will be discussed only briefly here where they differ from established practice.

The remaining circuits will be described as follows:

**Tube Supplies.**—This Section will deal with the circuits concerned with the production of a reasonably focused spot and a satisfactory time-sequential scanning of the tri-colour phosphor triplet—and possibly an additional white phosphor stripe. It will include such functions as focus, focus modulation, spot-wobble, spot-wobble modulation 'earth's-field' correction, field shift, etc., as well as any deviations from conventional practice of line-scan, e.h.t., etc.

**Drum Synchronization.**—As the field scan in the banana display is produced by means of a rotating lens drum, the problem of synchronization with acceptable interlace is very important and interesting and is discussed in some detail.

**Video-Signal Processing.**—This Section will deal with the various video-signal circuits necessary for producing a tri-colour picture on the single-gun tube. Although time-sequential gating of the primary red, green and blue signals may be employed and a possible circuit is briefly described, it is widely acknowledged that for single-gun tubes and composite video signals of the N.T.S.C. type the most logical and convenient method of operation is that known as self- or direct-decoding. A method of self-decoding for this display is described and the difficulties and some alternative methods are also considered.

As the various operating tolerances form the subject of another paper<sup>1</sup> they will be mentioned here only in so far as they affect the design of the various circuits.

## (2) TUBE SUPPLIES

## (2.1) Line Scan

The electron optics of the present display have already been described elsewhere in some detail.<sup>2</sup> The main feature is the permanent magnetic field produced by the bar-magnet assembly surrounding the tube, which for a number of reasons has a non-uniform field gradient along the length of the bulb. It

will be clear that with such a non-uniform field the current waveform in the deflector coils to produce a linear scan will not necessarily be linear. However, to improve further the resolution of the device, an experimental deflector-coil assembly was used, consisting of a pair of conventional 90° coils with a further pair of small 'corrector' coils mounted within them. The main coils are each 197 turns of No. 29 s.w.g. wire wound on a 2.3 in diameter mandrel. The corrector coils are each 180 turns of No. 34 s.w.g. wire wound on a 1.0 in mandrel. The yoke consists of two 8-slot cores. The four coils are connected in series, and the current waveform for linear scan at an e.h.t. of 25 kV is shown in Fig. 1. Some linearity correction was necessary and some care in transformer design appears to be needed to avoid ringing. The present design of line time-base which incorporates provision for adjustable line-scan centre employs two line-output pentodes type EL81 in parallel, with a type EY81 as booster diode. The design is by no means optimum one, but since it is envisaged that a final design would incorporate the e.h.t. supply from an overwind on the transformer—as is common practice—it was not felt desirable to expend much effort on this part of the circuit design, particularly as the initial concern was the appraisal of the display device itself.

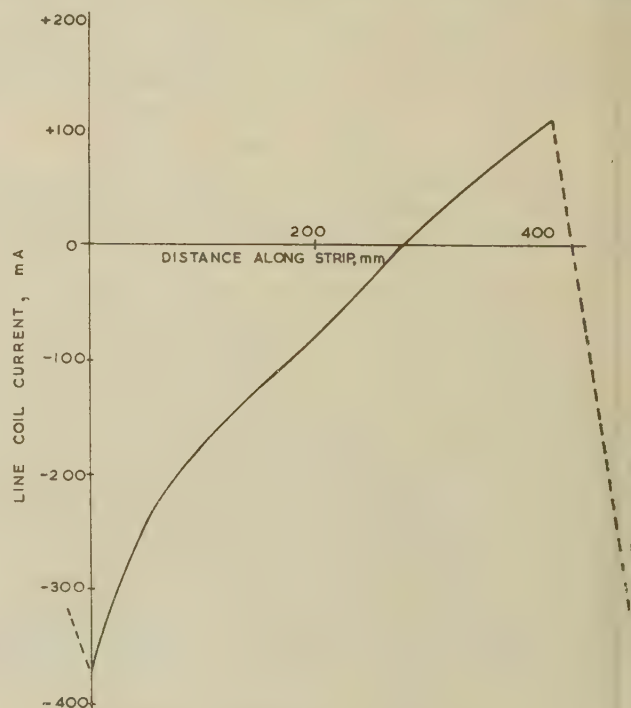


Fig. 1.—Line-scan current waveform.

## (2.2) E.H.T.

As mentioned above it is the usual practice to derive the required e.h.t. power from an overwind on the line transformer. The e.h.t. requirement for the banana tube is of the order

Mr. Freeman is at the Mullard Research Laboratories.



00  $\mu$ A at 25kV. In order to ensure stable operation of the display, the e.h.t. must be stabilized against the effects of mean beam current and mains voltage fluctuations. From considerations of the effect of changes in e.h.t. on spot-wobble amplitude on the phosphor triplet, etc., it appears necessary to stabilize the e.h.t. to within 2 or 3% or less. With an overwind e.h.t. supply a good shunt-stabilized, pulse-regulated or a similar type of circuit should just be capable of meeting this requirement, which is perhaps somewhat more stringent than for a shadow-mask-tube display. In the present experimental apparatus the e.h.t. is supplied by a separate stabilized power unit.

### (2.3) Focus

The spot-size requirements of this display and the high peak beam currents necessary ( $\sim 2.5$  mA), combined with the unconventional electron optics, place severe demands on the performance of the electron gun. So far, the best performance as regards spot size has been obtained with magnetically focused triode guns. At present, a high-quality electromagnetic focus coil is used, working at a current of 107 mA, which for best results must be maintained constant within less than 2%. Current stabilization is therefore necessary to eliminate the effects both of mains voltage fluctuations and of the change of coil resistance with warm-up due to the large thermal capacitance of the coil case.

In view of this complication, investigations are in hand to arrive at a satisfactory solution using a permanent focus magnet. Initial results show promise.

### (2.4) Focus Modulation

Focus modulation is necessary during line scan. A satisfactory arrangement has been reached by using a separate small coil (consisting of 240 turns of No. 34 s.w.g. wire) to provide only the change in focusing field. This coil is mounted on the neck of the tube inside the main focus coil, and a very useful first-order approximation to the required current variation is conveniently obtained by driving this coil in series with the line deflector coils. The effect on the performance of the latter is small.

### (2.5) Spot Wobble

As with all single-gun colour tubes, the tri-colour picture is obtained by time-sequential sharing of the beam current between the three phosphors. In the banana tube this is achieved by wobbling the spot across the phosphor triplet at a high video frequency in a manner analogous to that used in the well-known Lawrence tube. To minimize visibility of dot structure and loss of resolution, this frequency should be as high as possible in the video spectrum, but too high a frequency adds to the circuit difficulties and is unnecessary. From considerations of circuit simplicity and dot-interlace requirements it is most convenient to employ the colour subcarrier frequency (2.6578125 Mc/s for the British 405-line version of the N.T.S.C. system) which gives two important advantages. In the first instance, a complete receiver for N.T.S.C.-type signals will contain a subcarrier phase-locked circuit which provides a ready source of drive for the colour-selection circuits. Secondly, colour selection at the subcarrier frequency permits the use of self-decoding techniques which will be discussed later. Although with gated operation any higher multiple of the subcarrier frequency giving dot-interlace (e.g.  $\frac{7}{2}f_{sc}$ ) could be used, this arrangement is in fact too complex to be practicable.

For the banana system there appears at first sight to be a better choice of colour selection waveforms than in the Lawrence

tube, which, owing to the high capacitance of its switching grid ( $\sim 3000$  pF), is effectively limited to sine-wave switching. The banana tube, with its single-line phosphor triplet, is not so limited, and it would be desirable to use sawtooth spot wobble to obtain a continuous colour sequence RBGRBG . . . , which would be most suitable for self-decoding operation of the tube. However, the power required for spot wobble is not negligible and stable wobbling waveforms involving more than the second harmonic of the colour-selection frequency do not appear to be easily obtainable. For the most part, therefore, work has been confined to sine-wave spot wobble, which gives a reversing colour sequence, e.g. RGBGRGBG . . . , although some work has been carried out on the introduction of the second harmonic to obtain a first-order approximation to the continuous colour-sequence sawtooth waveform.

To date, in the interests of keeping the banana tube itself as simple as possible, electromagnetic spot wobble has been employed. The alternative possibility of electrostatic spot wobble has been considered only briefly and has not so far been investigated practically. Apart from the difficulties of supplying power to deflection plates inside the tube, which is at a potential of 25kV, it would appear that deflection voltages significantly in excess of 1 kV (p-p) are necessary. For electromagnetic spot wobble, a pair of small coils are mounted on the neck of the tube before the line deflector coils. With sine-wave spot wobble, the most convenient arrangement, of course, is to tune the coils to resonance at the colour-selection frequency and to drive the circuit with a class C output stage. In the worst case (because of the need to modulate the spot-wobble amplitude for reasons discussed in the next Section) the coils need to generate an m.m.f. of the order of 80 AT (p-p) in order to deflect the spot to the outer edges of the outer stripes (a peak-to-peak deflection of 8 mm).

For a given h.t. line voltage, output-valve peak current and coil dimensions, it can be shown that maximum m.m.f.s are obtained when the coil inductance is reduced to the point where the full available peak current of the valve is required to maintain class C operation. The choice of coil dimensions is of necessity a compromise, since the coils must be screened to prevent undesirable radiation. Since the size of the screening box is limited by the available neck space, large coils in a small box would have their effective Q-factor appreciably reduced, whereas small coils would inevitably result in reduced deflection sensitivity. The present arrangement, which, though satisfactory, is not claimed to be an optimum design, consists of two coils,  $1\frac{1}{2}$  in  $\times$   $\frac{3}{4}$  in, each of 4 turns of No. 18 s.w.g. wire, arranged with the larger dimension round the circumference of the neck in a brass box measuring 3 in  $\times$  4 in  $\times$  2 in. The coils connected in series give a total inductance of  $2.5 \mu$ H and are tuned with a variable capacitor of about 1200 pF which is capable of withstanding the r.f. circulating current of several amperes. The effective coil Q-factor *in situ* in the box is about 60, and satisfactory performance is obtained using a type EL81 pentode operated in class C from a 300 V h.t. line.

It is shown elsewhere<sup>1</sup> that, for stable colour rendering, the spot-wobble amplitude and therefore the h.t. supply to the spot-wobble output stage must be stabilized to within 2 or 3%. At present, of course, all power supplies are stabilized. For a domestic receiver with an unstabilized power supply it would be necessary to provide a stabilized h.t. line to this stage.

It has been mentioned that some work has been done on the introduction of the second harmonic to the spot-wobble waveform. In fact, with appropriately phased 40% second harmonic a useful first approximation to a sawtooth waveform is obtained, which gives a desirably longer dwell time on the centre phosphor stripe. This has been achieved by modifying the spot-wobble



tuned circuit to have a reduced response to the fundamental and an increased response to the second harmonic by the addition of extra components (Fig. 2). The resulting efficiency of this circuit is not high, and it was found necessary to use two type

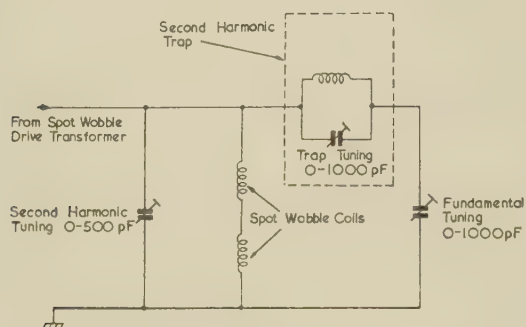


Fig. 2.—Second-harmonic spot-wobble output circuit.

EL81 pentodes in parallel and a 2:1 step-up transformer of 17 primary and 34 secondary turns. In addition to low efficiency the tuning of this circuit was found to be very critical and subject to unaccountable (probably temperature-dependent) drifts. Thus, although this type of spot-wobble waveform is very desirable, it does not appear easy to obtain in practice.

### (2.6) Spot-Wobble Modulation

For satisfactory colour selection in the banana tube it will be clear that a constant amplitude of spot wobble across the phosphor triplet is necessary along the length of the triplet. In the absence of any constraining fields, the required selection-frequency current amplitude in the coils is inversely proportional to the distance of the spot from the deflection centre. However, the presence of the magnetic 'tram-line' field, which rises to a maximum strength at the far end of the tube, appreciably modifies this requirement. Fig. 3 shows the required variation of spot-wobble-coil current amplitude as the spot scans the length of the triplet with the magnetic field configuration used in the present display. In order to meet the rather close spot-wobble amplitude tolerance (which arises as a result of the requirement of a uniform white across the raster), this modulation waveform must be reproduced with its amplitude within 2 or 3% of the

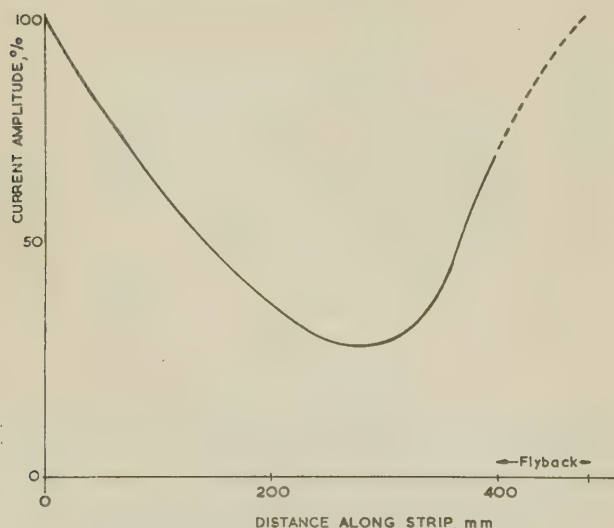


Fig. 3.—Spot-wobble modulation waveform.

required value at each point along the scan. For much of the experimental work a convenient technique based on the passive convergence circuit used in current shadow-mask-tube receivers has been used. Fig. 4 shows the circuit used at present. A fairly pure sine-wave of appropriate phase is derived from a pulse obtained from the line transformer by means of an inductively low-side-coupled double-tuned circuit. This is then integrated, clipped and partially detected, and with the addition of a further portion of line-flyback pulse, something near to the required asymmetric waveform is obtained, and this is used to grid modulate the spot-wobble output valve. As the fairly high Q-factor of the spot-wobble circuit tends to smooth out the effect of rapid transitions in the modulating waveform this must be taken into account. This type of circuit does not give entirely satisfactory performance, and indications are that an accurately correct modulating waveform can be obtained only by means of a fairly elaborate active circuit.

Modulation of the spot-wobble output valve in this way leads to an additional difficulty owing to feedback through the output. This is not insignificant at 2.66 Mc/s and leads to phase modulation of the spot wobble by as much as 30°, which is quite unacceptable. The necessary neutralization is, however, readily achieved by earthing the centre tap of the coils, which enables an appropriate amount of anti-phase sine wave to be coupled back to the grid via a small adjustable capacitor.

As an alternative to modulation of the spot-wobble current, investigations have been carried out into the possibility of using two much smaller coils mounted after and even on the line deflection yoke and driven with a current of constant amplitude. The displacement with line scan of the beam path in the vertical non-uniform field produced by these coils can then be made to yield a suitable variation of spot-wobble deflection sensitivity. Unfortunately, in addition to being much less sensitive, this arrangement leads to a variable tilt of the spot wobble with respect to the stripe triplet and a consequent misregistration of verticals in some parts of the raster. This effect is almost certainly due to the effect of field non-uniformities, and adjustments of modulation are difficult with this arrangement; it has not been pursued.

### (2.7) Field Shift

Although it is essential that the excitation of the phosphor triplet should yield a satisfactorily uniform white, an interesting possibility with the banana tube is to use a separate wide white phosphor stripe parallel to the tri-colour triplet to produce optimum black-and-white pictures on monochrome transmissions. Deflection on to this adjacent white strip could easily be arranged to take place, for example in the absence of a reference colour burst from the transmitted signal, by passing direct current through a pair of field coils on the line-deflection yoke. With two series field coils each of 1000 turns of No. 28 s.w.g. wire, a current of only 8 mA is required to deflect the scan on to a white phosphor stripe 1 mm from the tri-colour triplet. In general, partly owing to the constraining effect of the magnetic tram-line field, the resultant scan will not be a straight line, but provided that the spot remains on the stripe and the curvature of scan is not so large as to produce noticeable curvature of the scanning lines in the final demagnified image this is not important.

### (2.8) Earth's Field Correction

As with most known colour displays the banana tube exhibits susceptibility to the earth's magnetic field, but for this tube the effects are very pronounced, as accurate colour selection depends on accurate tracking of the spot along and across the stripe triplet.



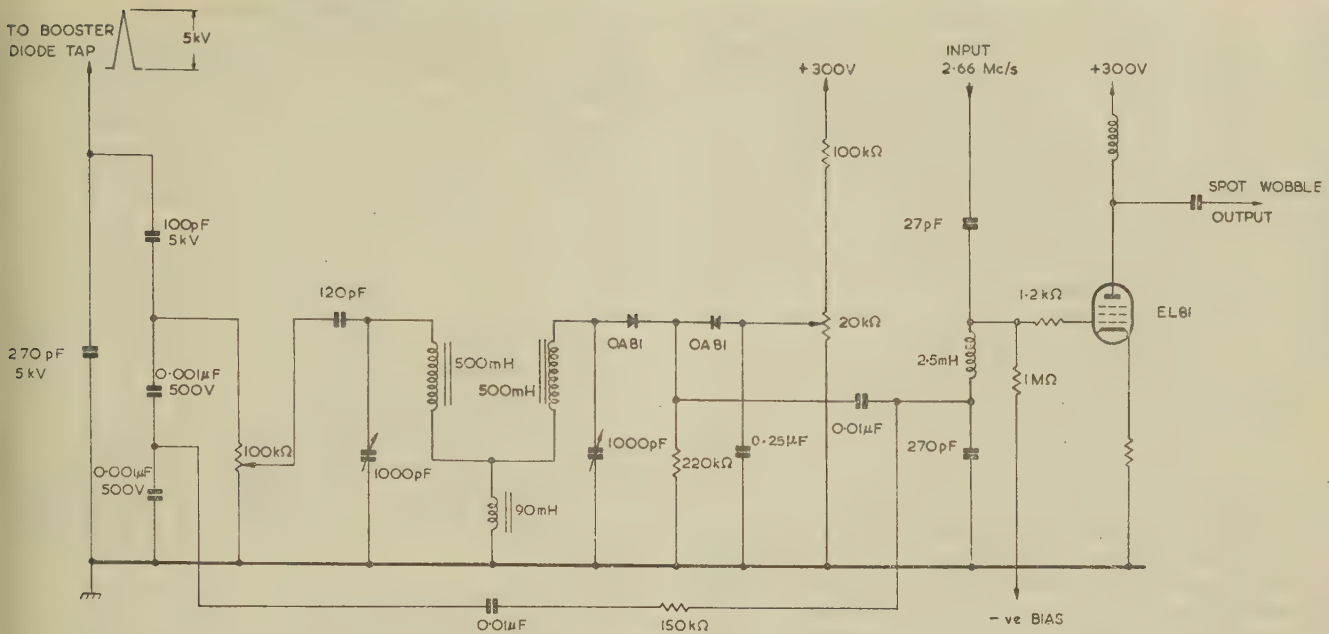


**Fig. 4.**—Spot-wobble modulation circuit.

which is controlled from the neighbourhood of the gun by what might be termed a 'dead-reckoning' process. The various effects have been investigated<sup>3</sup> and the salient conclusions are given elsewhere.<sup>1</sup> The most important effect is a transverse displacement of scan, which increases to a maximum near the end of the scan and consists of a fixed displacement with a maximum value of about 8 mm, caused by the vertical component of the earth's field, and a variable displacement with a maximum peak-to-peak value of 3 mm, which is caused by the horizontal component of the field, and which, of course, varies with the orientation of the display. As the effect of the field is cumulative throughout the length of the beam, it is apparent that correction for these effects is not possible by judicious adjustment of the focus or line coils and the field-shift current alone. In the present display, correction for both effects, at least to first order, is achieved by supplying an adjustable current to a large coil surrounding the tube and parallel to the triplet plane. This current needs to be stabilized to a few per cent, but for a coil of 650 turns of No. 42 s.w.g. wire a current of the order of only 10 mA is necessary and this could be easily derived from the stabilized h.t. line by applying the spot-wobble output stage, assuming that thermal effects do not cause a significant change in the resistance of the coil.

### (3) DRUM SYNCHRONIZATION<sup>4</sup>

### (3.1) Introduction

In the banana-tube display the field scan is obtained by the motion of three cylindrical lenses fixed symmetrically around the periphery of a cylindrical drum. To obtain proper field scan the drum must be rotated at the appropriate submultiple of the field frequency, and the phase of the rotation must be accurately fixed with respect to the field synchronizing pulse to yield a stationary and satisfactorily interlaced raster. As the mechanical and electrical tolerances are discussed in detail elsewhere<sup>1</sup> they will be mentioned here only in so far as they apply to the circuit functions. Systematic errors due to deviations of the optical elements from their correct locations are a problem for the mechanical designer and only the elimina-

tion of the random errors due to non-uniform rotation of the drum are considered.

High-speed variations in drum velocity, i.e. at greater than 1 c/s, are chiefly mechanical in origin, and may, for example, be due to changes in friction and in motor torque. These speed variations will in turn lead to phase variations, which will be evident as lack of interlace, accompanied by line crawl and weaving or jitter. Owing to the flywheel type of synchronization inherent with this device, the line pulses can have only a negligible effect on the field scan and loss of interlace of the ordinary kind cannot occur.

Intermediate-frequency variations in drum velocity, i.e. over periods of the order of a few seconds, will be visible as an oscillation, or jitter, of the raster as a whole. Variations in this frequency band will be determined principally by the response of the controlling servo mechanism to transient changes of torque.

Finally, very-low-frequency variations may be visible. They may be caused by slow changes in driving and control torque due to changes in the motor, h.t. and heater supply voltages, etc., largely as the result of mains-voltage fluctuations.

### (3.2) Control System

### (3.2.1) General Considerations.

The mechanical arrangement for producing the field scan and its associated control equipment can be considered as a time-base system analogous to that used in a line-scan circuit employing

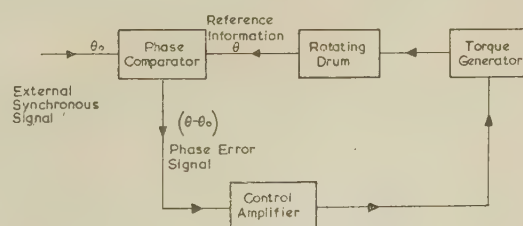


Fig. 5.—Elementary servo system.



automatic frequency control. However, whereas the control system and oscillator of the latter may be substantially free of noise and fluctuations, the mechanical system may suffer large and random variations of torque, which must be rendered ineffective by the control system. On the other hand, owing to the low bandwidth requirement, the noise associated with the field synchronizing pulse is much lower than that associated with the line synchronizing pulse. The design requirements are thus fundamentally different. Fig. 5 shows the basis of an elementary servo system for drum synchronization, which consists of the following components:

A source of information as to the instantaneous position of the drum.

A comparator where this information is compared with an external synchronization signal and an error signal derived.

A control amplifier deriving an output from the error signal suitable for actuating the control-torque generator.

A source of control torque.

The source of reference signals must give an accurate and unambiguous indication of the instantaneous position of the rotating drum, and their phase accuracy must be comparable with the required accuracy of positioning of the optical elements.

Disturbances of torque should be as small as possible, which is necessarily a problem for the mechanical designer. On the other hand, it can be shown that the mechanical damping on the drum should be as high as possible, i.e. the smooth friction torque should be large.

### (3.2.2) Mechanical Control System.

The most convenient of the possible methods is to drive the drum from an induction motor and to control by means of an eddy-current brake. The induction motor provides a cheap and smooth form of drive, and smooth control is possible with the eddy-current brake, which also provides useful smooth damping on the mechanical system. The design of the integral motor and brake at present in use and its characteristics are fully described elsewhere.<sup>5</sup>

### (3.2.3) Phase Reference Generator.

Of the various possible methods of obtaining accurate positional information from the rotating drum, the best appears to be one using a photo-electric device that responds to the interruption of a beam of light by the rotating drum. The present system uses a small lamp on the outside of the drum opposite a photo-transistor mounted on the inside. The light falling on the photo-transistor is modulated by the passage of the lens rods and a clean reference pulse of some ten volts amplitude is obtained each time. The advantage of taking the reference information from the lens rods themselves will be obvious.

## (3.3) Design of the Control Circuit

### (3.3.1) Mechanical Characteristics and Smoothing Effect of Inertia.

In the present system the torque required for driving the drum at 1000 r.p.m. is about 10 oz-in ( $7 \times 10^5$  dyn-cm). Ideally the mean braking torque should be as high as possible, but for economy it has been made equal to the torque required to drive the drum alone, so that the total torque required from the motor is 20 oz-in.

It is evident that the mechanical inertia of the system will tend to maintain the velocity of the drum constant in the presence of variations of friction torque and drive torque. From an approximate analysis of the system it appears that the inertial smoothing will be effective for periods up to a maximum of about 0.01 sec. Ideally the servo mechanism should compensate for all changes of torque period longer than this and so should have a bandwidth of about 15 c/s.

### (3.3.2) Limitations due to Sampled Operation.

The information fed into the phase detector is not continuous but consists of a signal sampled at 50 c/s, and this constitutes a limitation on the servo system. The bandwidth is, in fact, further limited, since it can be shown<sup>6</sup> that a sampled system cannot convey unambiguous information at frequencies greater than half the sampling rate,  $\omega_s$ .

The output from a sampled system should be smoothed to remove high-frequency components from the signal. Unfortunately, an ideal low-pass filter introduces excessive phase shift which affects the circuit stability. A very useful filter for sampled operation is the holding circuit which maintains the output constant at the last sampled value until the next sampling interval when the output changes instantaneously to the new sampling value. An approximate method of obtaining the frequency and phase characteristics of this circuit has been described<sup>7</sup> which is useful at frequencies below  $\frac{1}{2}\omega_s$ . The amplitude is substantially constant up to  $\frac{1}{4}\omega_s$ , but the phase shift is quite large even at this frequency, so that it is the latter characteristic of the holding circuit that has most influence on the servo mechanism.

### (3.3.3) Phase Comparator.

The phase comparator compares the reference signal from the drum with the field synchronizing pulse and yields an error signal dependent on their relative phase. The sensitivity of the phase detector will be determined by the slope of its characteristic measured in volts per radian. To obtain high sensitivity without overloading, a characteristic of the form shown in Fig. 6

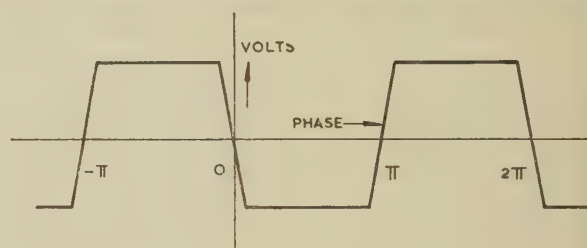


Fig. 6.—Phase-comparator characteristic.

used. Since operation on only one of the sloping edges of the characteristic gives stable operation, the slope of the unsaturated portion need not be closely controlled. If a waveform of triangular shape is sampled by a short pulse, the output will depend upon the relative pulse phases. The most suitable type of sampling gate consists of a switch in series with the signal, as shown in Fig. 7. If there is no charge leakage from the capacitor and the switch has a low impedance the circuit will behave as an ideal holding circuit.

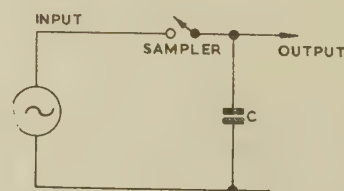


Fig. 7.—Basic sampling gate.

### (3.3.4) Complete Servo Mechanism.

As it is not possible to give here the full analysis of the servo system only the important conclusions will be given.

For a well-damped transient characteristic it is desirable that the resonance peak of the closed-loop system should not exceed



3 dB. For a circuit without phase correction this restricts the permissible loop gain and also restricts the bandwidth to 0.06 c/s. This is very low compared with the required bandwidth of 15 c/s. Further increase in bandwidth must be accompanied by some phase correction. Fig. 8 shows a suitable type of phase lead

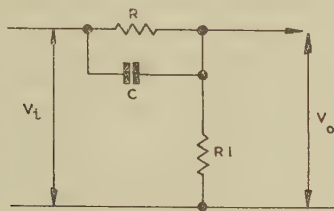


Fig. 8.—Phase lead network.

network, which has made it possible to increase the loop gain by 33 times and the bandwidth to 2 c/s without losing the required transient characteristic.

### 3.5) Steady-State Characteristics.

Analysis of the steady-state characteristics of the loop shows that for a static vertical tolerance of  $\pm 2\frac{1}{2}\%$  for the raster position (which is for an assumed 5% overscan) the maximum allowable change in drive torque is 6%. This is not sufficient to enable the servo mechanism to cope with possible variations in the mains supply voltage to the motor and it would be desirable to raise the circuit gain by about five times. If this were obtained by increasing the system bandwidth, further compensation and an increase in amplifier gain of about 25 times would be necessary, although this would result in a bandwidth closer to the target figure of 15 c/s. An alternative solution would be to incorporate an open-loop correction to offset the effects of mains-voltage variations.

### 3.6) Design of Experimental Drum Control Circuit.

Fig. 9 shows the complete experimental control circuit used at present, which is built in accordance with the principles outlined above. The operation is as follows:

The positive-going reference pulses produced by the photo-transistor are amplified and differentiated to yield a trigger pulse for the flip-flop  $V_2$ , which is adjusted to give a 50 c/s square wave with a unity mark/space ratio. This is partially integrated

and clipped by  $V_{3a}$  to give the desired reference waveform with sloping edges for operation of the phase comparator. This reference waveform is sampled in the phase detector, which consists of a 4-diode ring driven into conduction by push-pull field synchronizing pulses produced by  $V_{3b}$ . The output is stored in the  $0.1 \mu\text{F}$  capacitor in the grid circuit of  $V_6$ , which functions as a d.c. amplifier. It is coupled to the output pentode  $V_7$  by means of a voltage divider, which is shunted by a  $0.25 \mu\text{F}$  capacitor to function as a phase lead network. Additional phase correction is provided in the screen and cathode circuits of  $V_6$ . The magnetic brake windings form the anode load of the output pentode, the average brake current being adjusted by altering the negative grid bias to the valve. Although basically as designed, the performance is slightly more complex owing to the presence of additional time-constants. There is a time-constant due to the brake winding inductance in series with the driving impedance. The brake winding has a large number of turns to yield a high sensitivity and in consequence may have an inductance as high as 50 H. It is therefore necessary to shunt the windings by a resistance to limit the voltage across them if the current is suddenly turned off, as may happen during pull-in. A  $25 \text{ k}\Omega$  damping resistor limits the voltage change to less than 1350 V for a current change of 50 mA, but this is still undesirably high. The type EL84 pentode has an anode impedance of  $38 \text{ k}\Omega$  which is approximately doubled by cathode feedback. The parallel output resistance is thus about  $20 \text{ k}\Omega$ , giving a time-constant of  $2.5 \times 10^{-3}$  sec and a phase shift of  $45^\circ$  at 65 c/s.

Additional phase shift occurs owing to the finite charging impedance of the phase detector. The diode impedance can be kept low by driving the diodes well into conduction, but owing to its low gating duty cycle ( $\sim 1/50$ ) the effective source impedance of the reference waveform, which is the charging impedance of the  $0.1 \mu\text{F}$  capacitor, is about  $50 \times 1.5 \text{ k}\Omega$ , i.e.  $75 \text{ k}\Omega$ . This gives a time-constant of  $7.5 \times 10^{-3}$  sec. To avoid introduction of a further phase delay of  $180^\circ$  at 50 c/s it is desirable that the output be taken from the flip-flop with such a polarity that the control is derived from the leading, or triggered, edge of the pulse.

The position of the photo-transistor is adjustable over a limited range and serves as a fine vertical shift control.

### (3.3.7) Performance of the Experimental Circuit.

The experimental unit appears to behave substantially as predicted. The transient oscillation frequency is of the order

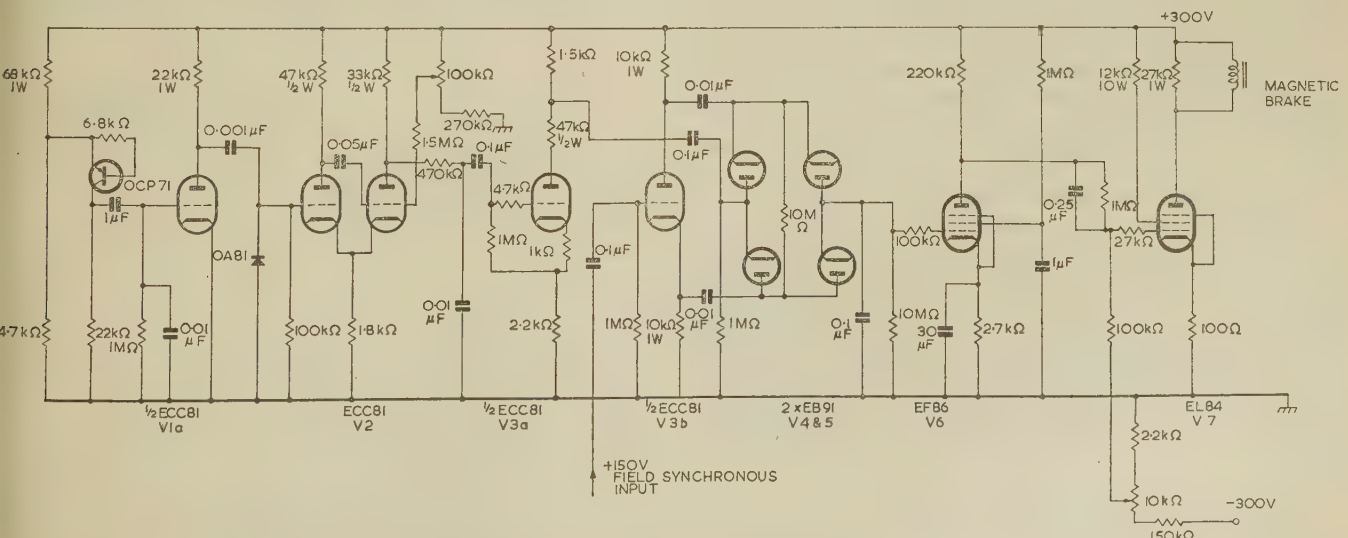


Fig. 9.—Complete experimental drum control circuit.



of one or two cycles per second, and despite the limited bandwidth the synchronizing performance seems to be fairly adequate, although some jitter is apparent to the critical observer.

Although no attempt has been made to analyse the pull-in performance, two points are apparent. One is that, owing to the relatively low frequency of operation, pull-in times may be quite large. The other is that the catching range cannot be more than the servo-system bandwidth, and will be less than  $\pm 2$  c/s for a bandwidth of 2 c/s. The uncontrolled drum speed must therefore be within 4% of the correct drum speed for pull-in to be at all possible.

The pull-in characteristics of the present integral-motor unit are unsatisfactory. In an alternative, and economically preferable, design employing a separate synchronous motor driving the drum through an idler wheel, the motor has been arranged to run nearer to its synchronous speed when driving the drum at 1000 r.p.m. This tends to make the drum run near to this speed under a wider range of conditions and pull-in is more satisfactory. For the integral motor system the pull-in range might be extended by means of a 2-mode control system, a velocity control loop being employed to bring the drum speed within the catching range of the phase control loop.

#### (4) VIDEO-SIGNAL PROCESSING

##### (4.1) Gating Circuits

In the banana tube the time-sequential sharing of the beam current between the primary phosphors is obtained by means of the spot wobble. The problem is then to provide the gun of the tube with an appropriate sequential signal so that the required tri-colour picture is reproduced.

An obvious method of producing the required video signal is to simulate 3-gun tube operation by gating or sampling the primary red, green and blue signals in synchronism with the passage of the spot over the phosphor stripes. The difficulties involved in obtaining satisfactory colour pictures by this method have already been considered by the author,<sup>8</sup> and it has been shown that quite complex circuits are necessary for adequate performance. The circuit at present in use employs low-level gating of the red, green and blue signals followed by a 30 Mc/s wideband video amplifier, which, in order to provide the required drive, employs a 40 W anode-dissipation transmitting valve for the output stage.

The main difficulty with this technique is that it is necessary accurately to match the overall transfer characteristics of the three channels in order to obtain satisfactory grey-scale rendering.<sup>9</sup> One solution is to use the low-level gating circuit for colour-difference-signal gating only, the luminance signal being separately supplied to another electrode, e.g. the grid, of the cathode-ray-tube gun. This, of course, makes it necessary that the efficiencies of the phosphors be balanced to give an acceptable white.

Both these methods have enabled colour pictures to be obtained on the banana tube which are limited in performance only by the limitations of the display device itself, but these methods of tube operation, though of great value in the laboratory, are too uneconomic for a domestic receiver. The stringent requirements of a gating circuit make simpler yet satisfactory circuits extremely unlikely, and the need to decode the received signal completely or almost completely cannot be ignored. Quite apart from this it seems a basically unsound approach deliberately to turn a single-gun tube into a simulated 3-gun display.

##### (4.2) Self-Decoding Circuits

With N.T.S.C.-type colour signals, fortunately, an alternative method of operation is possible, which is more in keeping with

the single-gun nature of the tube. In such signals the colour difference information is carried on a high video-frequency subcarrier, which is modulated in quadrature, and by performing the colour selection at this subcarrier frequency and applying the composite signal directly to the tube it is possible (assuming primary phosphors of the correct colour point) to obtain an approximation to the required colour picture according to the nature of the signal and the processing, if any, which it undergoes in the receiver. (It is, of course, necessary to balance the phosphor efficiencies so that an acceptable black-and-white picture is obtained in the absence of colour information.) Operation of the tube in this way is known as direct- or self-decoding and is widely dealt with in the literature, so that familiarity with its principles will be assumed. Reference 10 gives a useful introduction to the subject, whilst a recent survey by Jackson<sup>11</sup> draws attention to the more important points.

With sine-wave spot wobble the colour selection occurs in reversing colour sequence (r.c.s.), whilst N.T.S.C.-type signals are more suited to continuous-colour-sequence (c.c.s.) operation. Direct application of the presently used N.T.S.C. signal thus leads to very great errors in brightness, hue and saturation. Methods of tube operation and signal processing are known which appreciably reduce these errors, but a number of these are not practicable for the banana tube. Systems using blue as the central stripe colour, for example, are undesirable as they lead to increased visibility of colour fringing owing to the low luminance contribution of blue.

##### (4.3) Tripler and Modulated-Tripler Decoding

With the well-established N.T.S.C. system of transmission the most feasible simple decoding system for the banana tube appears to be the so-called 'trippler', which has been described by Loughlin.<sup>12</sup> With sine-wave spot wobble, c.c.s. operation is obtained by sampling or gating the composite video signal of the tube. This is achieved by pulsing the tube on by applying the third harmonic of the reference subcarrier frequency of appropriate amplitude and phase to a suitable electrode of the gun such as the grid (or the first anode if available). Fig. 10 shows the basic principle.

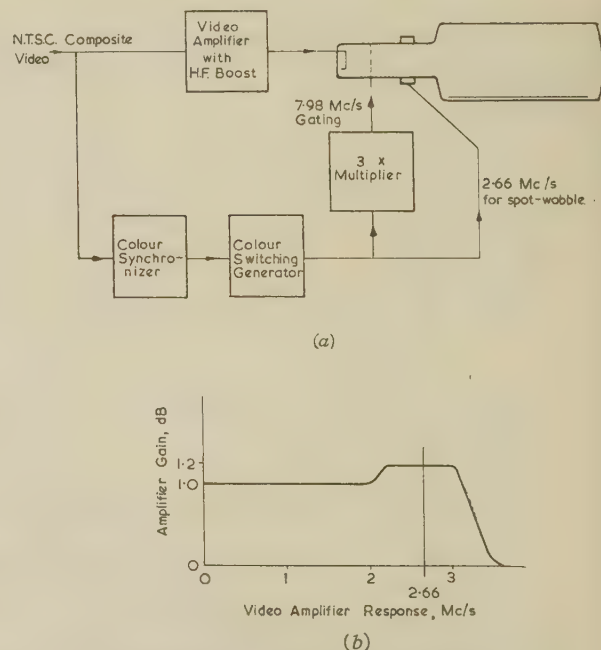


Fig. 10.—Basic tripler decoder.



With this arrangement using green as the central stripe, acceptable reproduction is obtained along the orange-cyan axis, but elsewhere noticeable errors in chromaticity and luminance occur.<sup>12</sup> However, an equally important defect of this method of operation is that the third-harmonic sampling occurs on all signals. Although the narrow sampling angle is of value in improving the purity of saturated colours, its use on white or near-white signals results in a reduction of the possible beam-current duty cycle by a factor of nearly 3. As the usable peak current is limited by the fact that spot-size increase and therefore loss of resolution occurs at high beam currents, this means in practice a similar reduction in permissible peak beam current and therefore of picture highlight brightness.

A simple method of overcoming this undesirable brightness limitation, which may be called the 'modulated tripler', has been described by Dressler and Neuwirth,<sup>13</sup> in which the amplitude of the third-harmonic sampling sine wave is made to depend upon the amplitude of the chrominance signal. In this way the maximum possible highlight brightness, which almost always occurs on very desaturated colours, can be obtained without sacrificing the purity of saturated colours. The loss of brightness due to the lower effective duty cycle in the latter case is offset by boosting the amplitude of the chrominance signal. The luminance and colour errors which still occur may be similar in nature to those with simple tripler operation, but there is a further complication. On low-brightness saturated signals only a low amplitude of modulating signal is obtained from the chroma envelope detector, which means that there is insufficient tripler sampling available to obtain the requisite saturation in the display, i.e. low-brightness signals are essentially ungated and substantially orange-cyan colour rendering occurs. This deficiency may be overcome to some extent by adjusting the tripler output-stage bias to ensure that a measure of gating still occurs on such signals.

#### (4.4) Signal Processing

With the methods of operation described above the colour selection occurs at 120° intervals at the subcarrier frequency. The N.T.S.C. signal in its normal form is not entirely suited to this as the subcarrier signal phases corresponding to the primary colours are not 120° apart. In addition, the luminance signal is not appropriate to single-gun operation of this kind. Loughlin has shown<sup>12</sup> that for c.c.s. operation with infinitesimally narrow sampling it is necessary to correct the luminance signal from the form

$$E_Y = 0.3E_R + 0.59E_G + 0.11E_B$$

to the form  $E_M = 0.33E_R + 0.33E_G + 0.33E_B$

and to convert the chrominance subcarrier to a symmetrical form, by means of two circuit configurations known respectively as the Y-to-M convertor and the elliptical-gain amplifier.

The M-Y signal for effecting the Y-to-M conversion is readily derived by appropriate synchronous detection of the chrominance signal. The narrow bandwidth of this correction signal is no limitation as the Y and M signals are in any case identical in the absence of colour.

Conversion of the N.T.S.C. chrominance signal to the symmetrical form can be achieved by applying it to an amplifier whose gain is arranged to be an elliptical function of the subcarrier phase. A suitable dual-control valve with the chrominance signal applied to one control electrode and appropriately phased second harmonic of the reference subcarrier applied to the other is all that is required.

These two modifications to the N.T.S.C. signal result in a c.c.s. signal which is still only correct for very narrow sampling angles. Owing to the effects of spot size and sampling by means of a sine wave of appreciable gating angle ( $\sim 40^\circ$ ), some errors of reproduction will remain, particularly of saturation. These errors of saturation may, however, be further reduced by means of the so-called 'diode correction' circuit,<sup>15</sup> in which the amplitude of the chrominance signal is detected and a proportion of this signal subtracted from the luminance signal to reduce the latter and hence decrease the conduction angle on saturated colours.

#### (4.5) Correction for Effects of Desaturated Green Phosphor

It has been shown elsewhere<sup>2, 14</sup> that the banana-tube primary green phosphor is considerably less saturated than specified for the N.T.S.C. system. Jackson has dealt with the colorimetric implications of this,<sup>14</sup> and some thought has been given to the problem of suitable correcting circuits.

It is shown<sup>14</sup> that considerable correction is possible by slight adjustment of the M-Y synchronous-detection phase angle towards the green-magenta axis (giving a new monochrome signal which has been termed the  $E'_W$  signal) combined with a modification of the amplitude of the diode correction signal. No additional circuit functions are therefore necessary.

#### (4.6) Practical Experimental Circuit

Fig. 11 shows a block diagram of an experimental circuit embodying the features described above, but which is far from being intended as a final design. The positive-going composite video signal from the video detector is amplified in V<sub>1a</sub>, the chrominance signal is removed by the band-stop filter, and the resulting luminance signal is delayed and further amplified by

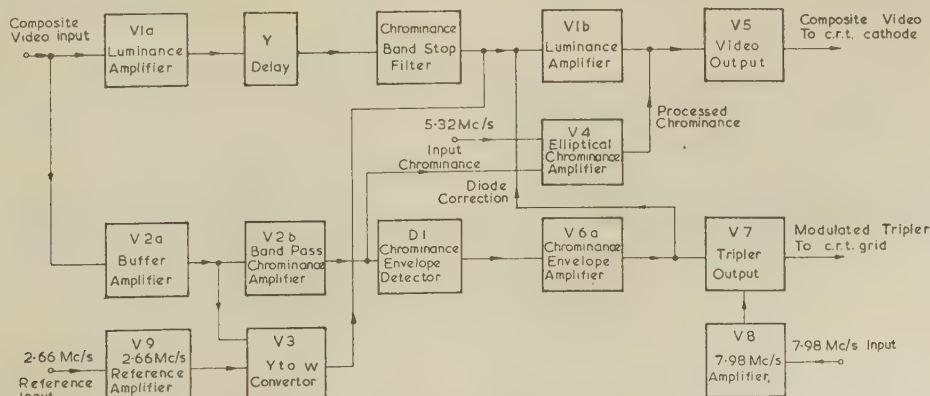


Fig. 11.—Complete experimental decoder circuit.



$V_{1b}$ . The composite video signal is also supplied to the amplifier  $V_{2a}$ , which acts as a buffer stage to the Y-to-W convertor,  $V_3$ , and to the second chrominance amplifier,  $V_{2b}$ , with its band-pass filter. The signal derived from  $V_3$  is added to the  $-Y$  signal at the grid of  $V_{1b}$  to give the required W-type luminance signal. The chrominance signal from  $V_{2b}$ , on the other hand, is fed to one control grid of the dual control valve  $V_4$ , which has its anode connected to that of  $V_{1b}$  for readdition of the chrominance and luminance signals. Application of the second harmonic of the subcarrier reference frequency to the other control grid of  $V_4$  provides the desired elliptical amplification. The resulting composite video signal is then amplified by  $V_5$  for application to the tube-gun cathode. The chrominance signal from  $V_{2b}$  is also envelope detected by  $D_1$ . This, after amplification by  $V_{6a}$ , provides the required diode correction signal, which is fed to the grid of  $V_{1b}$ , and also the required modulation signal for the tripler output stage  $V_7$ , which follows the design of Dressler and Neuwirth. The modulated output is then applied to the tube control grid, with appropriate arrangements for adjusting the tube bias.

The circuit in its present form is not as simple as is desirable, but some simplifications may prove to be possible. For example, it is open to question whether the benefits of elliptical amplification correction warrant the extra cost involved. In addition, the use of a tube gun with an additional modulating electrode would eliminate the need to recombine the modified luminance and chrominance signals as at present.

#### (4.7) Signal Recoding

Owing to the restrictions imposed for various reasons, it seems that other methods of operating the banana tube as a c.c.s. display are likely to be a difficult proposition. The alternative, which is more suited to sine-wave spot wobble, is to operate the tube as an r.c.s. display. This would dispense with the modulated-tripler sampling circuit, but it would be necessary to recode the N.T.S.C. signal in the receiver into a form more suitable for r.c.s. operation. An obvious, but complicated, way is completely to decode and recode the composite video signal, but Loughlin<sup>12</sup> has described a simplification using axis selectors, which are elliptical amplifiers with very large eccentricities. As two of these are required together with a second-harmonic modulator and the usual Y-to-M conversion, it is unlikely that the complete self-decoding circuit will be significantly less complex than the modulated tripler at present in use. Moreover, as with the c.c.s. system, this signal processing is correct only for very narrow sampling angles—as might perhaps be obtained with sixth-harmonic sampling. It remains to be seen whether ungated operation with a recoded r.c.s. signal can give acceptable colour rendering.

#### (5) CONCLUSIONS

The circuit requirements for operation of the banana-tube colour display have been described, and it has been shown that the special requirements of this system can, in principle, be satisfied, although in some aspects the circuits are perhaps more complex than is desirable for a domestic receiver. The implications of this are considered elsewhere.<sup>1</sup>

#### (6) ACKNOWLEDGMENTS

The development of the wide variety of circuits involved in this display device of this kind must of necessity be the task of more than one person, and the author gratefully acknowledges the many important contributions and suggestions of his numerous colleagues, including Messrs. T. Jacobs and P. L. Mothersole. Particular acknowledgment is due to Mr. N. D. Richards, who was almost solely responsible for the development of the drum synchronization circuit and from whose report the description given here is derived.

The author also wishes to thank the Director of Mullard Research Laboratories and the Directors of Mullard Ltd., for permission to publish the paper.

#### (7) REFERENCES

- (1) FREEMAN, K. G., and OVERTON, B. R.: 'Appraisal of the Banana-Tube Colour-Television Display System' (see page 624).
- (2) EASTWELL, B. A., and SCHAGEN, P.: 'Development of the Banana Tube' (see page 587).
- (3) FREEMAN, K. G.: 'The Effect of the Earth's Magnetic Field on the Banana Tube Colour Television Display', Mullard Research Laboratories Technical Note, No. 340, April 1959.
- (4) RICHARDS, N. D.: 'The Design of a Mechanical Frame Time-Base for a Television Display System', Mullard Research Laboratories Report No. 2231, June, 1959.
- (5) HOWDEN, H.: 'Mechanical and Manufacturing Aspects of the Banana-Tube Colour-Television Display System' (see page 596).
- (6) TRUXAL, J. G.: 'Automatic Feedback Control System Synthesis' (McGraw-Hill, 1955), p. 500.
- (7) BROWN, R. G., and MURPHY, G. J.: 'An Approximate Transfer Function for the Analysis and Design of Pulse Servos', *Transactions of the American I.E.E.*, 1953, 70, Pt. II, p. 453.
- (8) FREEMAN, K. G.: 'A Gating Circuit for Single-Gun Colour Television Tubes', *Journal of the British Institution of Radio Engineers*, 1959, 19, p. 667.
- (9) JACKSON, R. N., and JACOBS, T.: 'An Investigation into the Subjective Effects of Some Differences between the Red, Green and Blue Transfer Characteristics of a Colour Television System', *Acta Electronica*, July, 1957, 2, p. 9.
- (10) Hazeltine Laboratories Staff: 'Principles of Colour Television' (Wiley and Son, 1956), Chapter 16.
- (11) JACKSON, R. N.: 'Single Gun v. Three Gun Tubes—The Influence on Colour Receiver Design', *Journal of the Television Society*, 1960, 9, p. 207.
- (12) LOUGHLIN, B. D.: 'Processing of the N.T.S.C. Colour Signal for One-Gun Sequential Colour Displays', *Proceedings of the Institute of Radio Engineers*, 1954, 42, p. 299.
- (13) DRESSLER, R., and NEUWIRTH, P.: 'Brightness Enhancement Techniques for the Single-Gun Chromatron', *Conventional Record of the Institute of Radio Engineers*, 1957, pp. 3 and 220.
- (14) JACKSON, R. N.: 'Colorimetry of the Banana-Tube Colour Television Display System' (see next page).
- (15) CLAPP, R. G.: 'The Colorimetry of Sequential Displays', *Acta Electronica*, July, 1957, 2, p. 181.

[The discussion on the above paper will be found on page 630.]



# COLORIMETRY OF THE BANANA-TUBE COLOUR-TELEVISION DISPLAY SYSTEM

By R. N. JACKSON, Graduate.

The paper was first received 17th November, and in revised form 10th February, 1961. It was published in May, 1961, and was read before the ELECTRONICS AND COMMUNICATIONS SECTION 15th May, 1961.)

## SUMMARY

The principal sources of errors in colour reproduction of the banana tube are the colour phosphors employed, the finite spot size of the tube and the self-decoding colour circuits. The errors due to these causes are analysed, particular attention being given to the use of an incorrect green primary phosphor and to methods of evaluating the importance of random errors in the chromaticity and luminance of the phosphors. Methods of alleviating errors due to the incorrect green primary by special correction circuits are discussed.

## LIST OF SYMBOLS

- $P_1, P_2$  and  $P_3$  = Set of hypothetical primary colours.  
 $C_1, C_2$  and  $C_3$  = Hypothetical complementaries corresponding to  $P_1, P_2, P_3$ .  
 $P'_1$  = Incorrect receiver primary.  
 $C'_1, C'_2, C'_3$  = Error complementaries.  
 $W$  = Reference white for which  $P_1, P_2, P_3$  are balanced.  
 $R, G, B$  = N.T.S.C. primary colours.  
 $c, m, y_w$  = Complementaries corresponding to  $R, G, B$ .  
 $C$  = C.I.E. illuminant C.  
 $C_W$  = White colour close to illuminant C.  
 $E'_y$  = N.T.S.C. luminance signal.  
 $E_M$  = Monochrome signal for continuous colour sequence display.  
 $E'_R, E'_G, E'_B$  = Gamma-corrected red, green and blue primary-colour signals, respectively.  
 $x, y$  = C.I.E. chromaticity diagram co-ordinates.  
 $u, v$  = Uniform chromaticity-scale co-ordinates.  
 $S_R, S_G, S_B$  = Red, green and blue colour signals.  
 $E'_W$  = Monochrome signal for c.c.s. display with sulphide-green primary.  
 $E'_s$  = Colour sub-carrier signal for c.c.s. display with sulphide-green primary.

## (1) INTRODUCTION

The accuracy of colour reproduction in the banana-tube system is governed by three main factors in the design of the device. These are as follows:

- The primary colour reproducing phosphors.
- The physical dimensions of the cathode-ray tube (screen structure and spot size).
- The type of picture drive circuits employed.

Of these three, the first factor has assumed a high importance in the present device since the need to use phosphors which have a short decay time has narrowed the choice of materials compounds in the sulphide group. Among these compounds suitable red- and blue-emitting phosphors can be found, but the green-emitting phosphors provide colours considerably less saturated than those specified for colour television, as, for instance, in the N.T.S.C. system, a version of which has been adopted experimentally in this country.

Other departures from the correct or desired phosphor colours are likely to arise during manufacture of any colour tube. For instance, stray particles of one colour phosphor may get deposited in the area of another or a phosphor may change its emissive quality during some stage of processing of the tube. If a satisfactory picture is to be achieved, a close watch must be kept on this type of error. For the banana tube, an experimental system of defining limits for the colour and efficiency of emission of the phosphors has been drawn up.

The second factor, that of tube dimensions, arises because the cathode-ray tube has a finite spot size. With the time-sequential type of colour selection employed there is thus the possibility of colour impurity occurring as a result of the transition of the spot from one luminescent stripe to the adjacent one. The degree of such impurity will be dependent upon the relative dimensions of the spot, the luminescent stripe itself and the non-luminescent 'guard bands' between adjacent stripes. The situation is further complicated by the fact that the spot size is variable with beam current and deflection.

The third factor is largely related to the economics of the receiver design. Within the limitations of the colour phosphors employed a picture of high colorimetric fidelity can be obtained, provided that sufficiently elaborate circuits are used to drive the tube. However, when considering the design of a domestic receiver, a saving in circuit complexity, and therefore in cost, can be achieved at the expense of some degradation of colour fidelity.

In practice, the three factors listed above are found to be highly interdependent. Thus the design of the cathode-ray tube and the colour circuits can no longer be separated, but each unit must be carefully 'tailored' to suit the other so as to provide optimum colour performance. Possibilities may then exist for adjusting the performance of one part of the receiver in order to compensate for errors occurring in another.

## (2) COLOUR-PHOSPHOR ERRORS

### (2.1) Desaturated Green Phosphor

The colours of the N.T.S.C. transmission primaries and those of the banana-tube colour-phosphor targets are plotted on the C.I.E. chromaticity diagram in Fig. 1. The N.T.S.C. primaries are  $R, G$  and  $B$  in the diagram. The red and blue phosphor targets for the banana tube are the same as the respective N.T.S.C. red and blue primaries, but the green-phosphor colour is given as  $G_s$ .

At first sight the colour of the green phosphor may appear to be so desaturated as to provide an extremely serious drawback to the system. The situation is, however, not so unfavourable as this diagram implies. There are two reasons for this. First, it must be borne in mind that colour changes expressed in terms of  $x$  and  $y$  coefficients on the C.I.E. chromaticity diagram are not equally perceptible to the eye over all parts of the diagram.

Much information is available as to the relative perceptibility of the colours represented,<sup>1, 2, 3</sup> and Fig. 2 indicates the relevance of this as applied to the N.T.S.C. primary and complementary



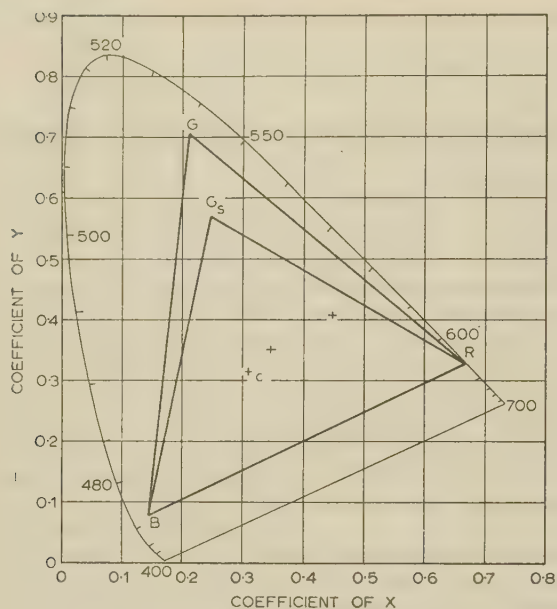


Fig. 1.—N.T.S.C. transmission primaries ( $R, G, B$ ) and banana-tube phosphor colour targets ( $R_s, G_s, B_s$ ).

colours and white. This diagram is based on data according to Judd. The smallest perceptible change in chromaticity under moderately good conditions of observation has been determined experimentally, and this unit has been termed the just noticeable difference (j.n.d.) of chromaticity. In Fig. 2 each full-line

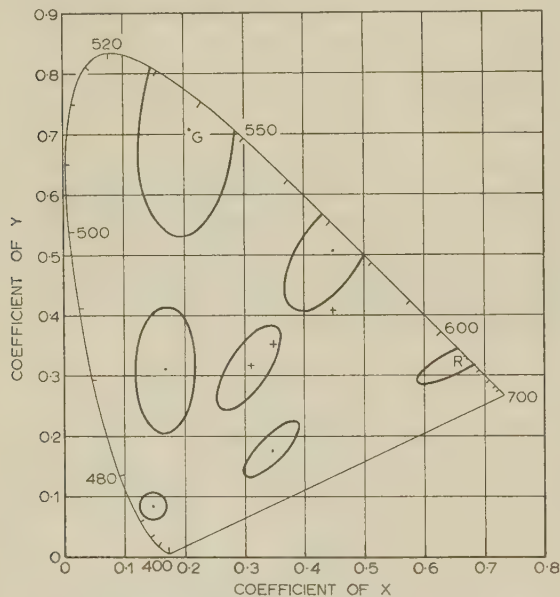


Fig. 2.—Approximate perceptibility of chromaticity changes in the region of N.T.S.C. primary and complementary colours.

ellipse is the locus of points whose chromaticity is 100 times the j.n.d. from the colour at the centre of the ellipse. It can be seen that the eye is much less sensitive to chromaticity changes in the region of green than to changes in any other part of the colour gamut.

In the second case, an examination of the distribution of colours commonly occurring in natural scenes shows that the gamut of colours available in the banana tube does not, in itself, seriously limit the fidelity of reproduction.

Fig. 3 shows the banana-tube colour gamut compared with Wintringham's data,<sup>4</sup> showing the total range of industrial paints, dyes and textile pigments, and with MacAdam's data with regard to the colours of some natural objects. It can be seen that the banana tube is, in fact, capable of reproducing a very high proportion of these colours. A complete system in which the transmission primaries were based upon the colour

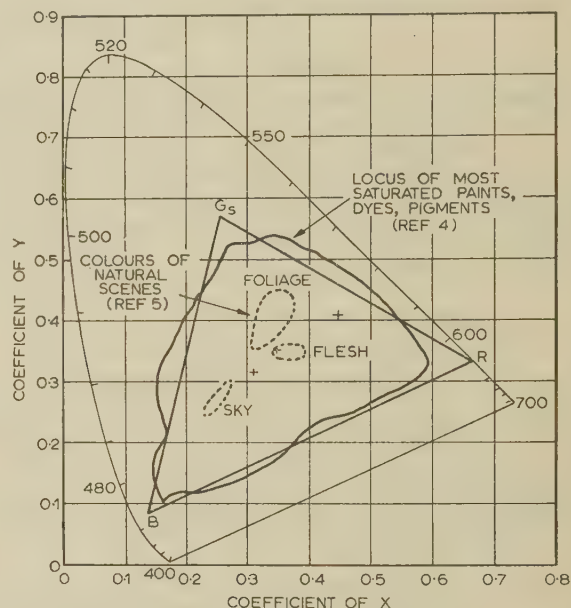


Fig. 3.—Comparison of banana-tube colour gamut with data of Wintringham and MacAdam (References 4 and 5).

chosen for the banana tube would provide an adequate reproduction of almost all normal scenes, although it would obviously be less satisfactory than a system based on the N.T.S.C. primaries.

The present difficulty therefore arises from the fact that the banana phosphor colours differ from the normal transmission primaries. Thus colours which are within the actual gamut of the banana tube will not be reproduced correctly since the transmitted signal does not suit the requirements of the tube.

Now it is not reasonable to expect that the specification for the transmission system should be changed in order to suit a particular display device. Particularly is this so when the change required implies a degradation in performance. However, the fact that all the colours within the available banana-tube gamut are present in the transmitted signal leads us to suppose that some form of signal translation should be possible in order to extract the required information. In practice it has been found that, by means of suitable circuit techniques, such a signal translation can be effected. For a domestic receiver a simple low-cost translation circuit is required. One possibility for providing a 'first-order' correction has been investigated and is described in Section 4.2.5.

## (2.2) Visual Effects of Reproduction with Incorrect Primaries

As stated in Section 1, other undesirable deviations from the specified primary colours may arise as a result of the processes to which the phosphors are subjected during the manufacture of the tube. These clearly result in errors in reproduction of nature similar to those caused by the incorrect green primary. However, since they are not predictable deviations they cannot



allowed for in the receiver circuits, and they must therefore be kept to a sufficiently small order so as not to impair the performance of the device.

Before proceeding to the derivation of a system of tolerances for the phosphor-emission colour and efficiency, it is desirable to consider the type of errors caused by an incorrect receiver primary and some of their visual effects.

Fig. 4 shows an elementary colour triangle representing an

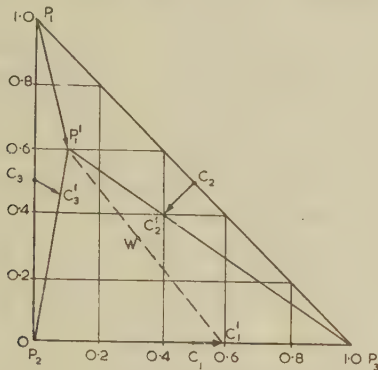


Fig. 4.—Elementary colour triangle.

additive tricolour system having a set of three hypothetical primaries  $P_1$ ,  $P_2$  and  $P_3$  and reference white  $W$ . The unit equation for this system is thus

$$0.33P_1 + 0.33P_2 + 0.33P_3 = 1.0W \quad (1)$$

Let us suppose that a receiving device which is required to synthesize pictures which have been analysed according to this system has a set of primaries  $P'_1$ ,  $P'_2$  and  $P'_3$ , where  $P'_1$  is an incorrect primary (Fig. 4). A number of significant points may now be deduced. The gamut of the receiver picture is less than that of the system, and hence there will be a compression of the colours of the system to within the triangle  $P'_1$ ,  $P'_2$ ,  $P'_3$ . The primary  $P_1$  will be reproduced as  $P'_1$ , and all colours along the lines  $P_1$ - $P_2$  and  $P_1$ - $P_3$  will be reproduced as along  $P'_1$ - $P'_2$  and  $P'_1$ - $P'_3$ , and hence in error. For instance, complementaries  $C_2$  and  $C_3$  will become desaturated to  $C'_2$  and  $C'_3$ , respectively. Formally the efficiencies of the phosphors  $P'_1$ ,  $P'_2$ ,  $P'_3$  in the receiver will be adjusted so that equal excitation will again reproduce the correct reference white,  $W$ . If this is so, the complementary  $C_1$  will be moved to  $C'_1$  and all colours between  $P_2$  and  $P_3$  will then be reproduced in varying degrees of error.

The receiver primaries may be regarded as a new trichromatic system having the same reference white as the system of Fig. 4, and it is evident that the relative quantities of light from  $P_1$ ,  $P_2$  and  $P_3$  required to match  $W$  will not be the same as the quantities required from  $P'_1$ ,  $P'_2$  and  $P'_3$ . For instance, referring to the system of Fig. 4, the ratio of primary  $P_1$  to primary  $P_3$  required for a white mix is

$$\frac{P_1}{P_3} = \frac{0.33}{0.33} = 1.0$$

The required ratio of  $P'_1$  to  $P_3$ , in the same units, is given by

$$\frac{P'_1}{P_3} = \frac{C'_2 P_3}{C_2 P'_1} = \frac{0.72}{0.36} = 2.0$$

Thus the relative luminance values in the displayed picture will be considerably disturbed.

The visual effects of these errors on colour pictures are not ways as might be anticipated at first sight. In order to investigate these phenomena a simulator unit has been constructed which enables the effective primary colours of a colour

display unit to be varied over a wide range of chromaticities at will. This is achieved by matrixing the red, green and blue colour signals of a colour-television system, which are then viewed on a display having the correct phosphors. For instance, in order to simulate a desaturated green phosphor, a constant fraction of the green signal may be fed into the red and blue channels of the system. The matrix unit is so arranged as to be continuously variable and 'self-balancing', i.e. the contributions of the three new primary colours are automatically adjusted to preserve the white point.

Tests with this apparatus and with a number of actual banana tubes have shown that, almost invariably, the first noticeable effect of desaturating a given primary is the alteration in the relative luminance values. In the case of desaturation of a green primary the drop in apparent red luminance is most noticeable. In fact, since red is the least efficient phosphor, the actual red brightness is not decreased in a practical case. The green brightness is usually increased, with a consequent increase in overall picture brightness. However, the eye appears to adapt itself rapidly to this increased overall brightness, and the net effect is that red objects still appear to be darker than normal. For the banana tube the relative contributions to total luminance are given by

$$1.0C = 0.25R + 0.65G + 0.10B \quad (2)$$

whereas, for the N.T.S.C. primaries, the contributions are

$$1.0C = 0.30R + 0.59G + 0.11B \quad (3)$$

The ratio of reproduced to intended luminance for red in the banana tube is thus  $0.25/0.30 = 0.83$ .

The next most noticeable effect depends very much upon the primary which is being moved. Referring to Fig. 4 once more, we may note that, although the error  $P_1 - P'_1$  is geometrically much larger than  $C_1 - C'_1$ , the actual visibility of the error will depend on the relative magnitudes of the j.n.d.'s in the regions concerned. If  $P_1$  were a green primary it is probable that  $C_1 - C'_1$  might be the greater visual error since the j.n.d. at magenta is much smaller than that at green. This has been borne out in practice with the simulator. In many pictures the first noticeable chromaticity change, on moving the green primary, is the change in magenta.

It should also be noted that, where a choice in the position of  $P'_1$  exists, it is desirable that this should lie on the line from  $P_1$  to  $W$ . This serves to eliminate the error  $C_1 - C'_1$  completely. Since the sulphide group of phosphors do allow some latitude in the choice of green this principle has, in fact, been adopted for the banana tube.

A further phosphor defect which needs to be considered in conjunction with the above is that of incorrect luminance efficiency. Since it is not readily possible to adjust the relative duty cycles or drive conditions of the three phosphors in a self-decoding display, it is very necessary that the phosphor efficiencies should be such as to provide the correct white. If these efficiencies are not correct, or if they alter with life, there will be a twofold effect. First, the white will be changed and an unacceptable colour cast may be imparted to the display. Secondly the relative luminance values will again be disturbed, with possible detrimental effects upon the picture.

### (2.3) Colour-Tolerance Limits

Bearing in mind the above effects, an experimental colour-tolerance diagram has been constructed showing the limits within which the colour primaries and the white balance of the display tube should lie in order to maintain acceptable colour pictures. The diagram (Fig. 5) is constructed in the following manner:

First, the primary-colour target chromaticities are marked on

the diagram, and the colour triangle is drawn. In Fig. 5 these are the N.T.S.C. specified primaries ( $R$ ,  $G$ ,  $B$ ). The accuracy of reproduction for these colours alone is then specified in terms of the permissible departure from the target colour in j.n.d.'s. For instance, the limit shown in Fig. 5 is 100 times

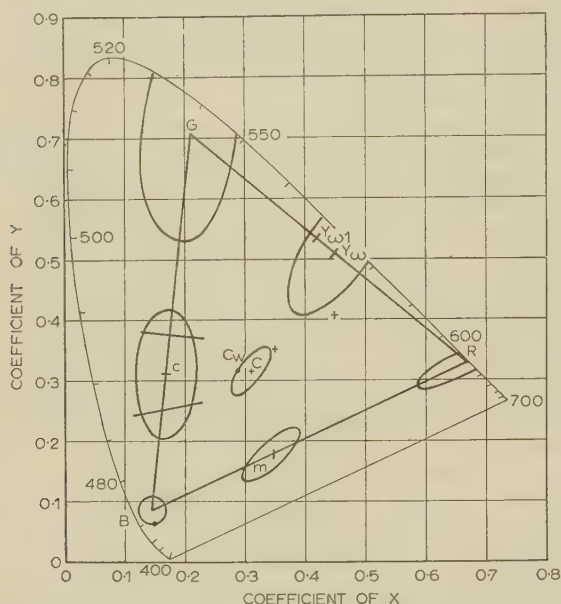


Fig. 5.—Basic tolerance diagram.

The limits are 100 times the j.n.d. for primaries and complementaries and 50 times the j.n.d. for white.

the j.n.d. This gives a limit line drawn around each point which is an ellipse centred on the target colour. The white balance target  $C$  is then marked, together with the complementary colour points  $c$ ,  $m$  and  $y_w$ . Similar elliptical limits of suitable dimensions are then prescribed around these points. The limits shown are 100 times the j.n.d. for the complementaries and 50 times the j.n.d. for white.

The diagram is then inspected for incompatibilities. Clearly, if all colours are to be reproduced within the limits prescribed, certain combinations of primary-colour target and balance conditions are not permissible. For instance, if a red primary is chosen which is within the 100 times the j.n.d. limit for red, it is not permissible for the cyan complementary to approach near to the 100 times the j.n.d. cyan limit if white balance is to be maintained.

By constructing lines from the extreme limits of the primary colours and tangential to the limits for the respective complementaries or white, it is possible to reduce the boundaries in various regions further so as to avoid these anomalies, as shown.

Allowance must also be made, on the diagram, for the errors of luminance reproduction which may occur. With N.T.S.C. primaries the relative luminance contributions which result in correct white balance are as given in eqn. (3). However, if the efficiency of, for instance, the green phosphor were too high, the white balance might be disturbed in such a way that a white  $C_w$  and a yellow complementary  $y_{w1}$  would result (Fig. 5). The relative luminance contributions are then found to be given by

$$1.0C_w = 0.25R + 0.66G + 0.09B$$

Thus the ratio of reproduced to intended luminance for red colours is reduced to  $0.25/0.30 = 0.83$  and that for green colours is increased to  $0.66/0.59 = 1.12$ . Similar calculations may be performed for the extreme limits of balance for all other colours.

Variations in the ratio of reproduced to intended luminance of this order appear to be tolerable in practice, although noticeable, and it may not be necessary to make any further changes in the diagram as applied to N.T.S.C. phosphor colour. However, where one or more of the primaries lie near the colour limit of 100 times the j.n.d., the relative luminances may already be adversely affected, as has been shown above [eqn. (2)] for the banana-tube green phosphor. In this case it may be necessary to impose further limits restricting the colour-balance conditions to ensure that excessive luminance errors do not occur.

It can be seen from the above that the colour tolerances drawn around the complementary colours and white constitute, in effect, restrictions on the relative luminous efficiencies which the phosphors may have if a satisfactory colour balance is to be obtained. From the diagram a table may be drawn up showing the limits of relative luminous efficiency for the phosphors, and this may also take into account other relevant factors such as the relative beam-current duty cycles for the phosphors, and normal operating conditions. Such a Table thus enables the efficiency tolerances to be presented in a more concise and manageable form.

It must be noted, however, that the tolerances laid down in this type of diagram are not simultaneous. As soon as a given primary has been established at a given point on the diagram a restriction is automatically placed upon other areas of the diagram, and alterations must be made accordingly.

When considering the relative luminances of the colours the diagram represents a serious drawback, since, as we have seen, alteration of the chromaticity of any one primary results in alteration of the relative luminances of all three primaries. This, in turn, means that any luminance limits imposed to take account of changes in the relative efficiencies of the phosphors must be recalculated. It would appear that some form of chart showing the relationship between relative luminance of the three primaries and certain changes in chromaticity would be a valuable aid in this type of work, and some study is being made of this possibility.

#### (2.4) Uniform Chromaticity Scale

It has been found that there are some advantages to be gained by plotting the tolerances on a uniform chromaticity scale diagram such as that described by MacAdam<sup>6</sup> or that of Bencze, Enridge and Schaub.<sup>7</sup>

Uniform chromaticity scale diagrams are transformations of the C.I.E. diagram. They derive their name from the fact that the length of a straight line connecting any two points on such a diagram is approximately proportional to the perceptibility of the chromaticity difference between the two colours represented by these points. This feature enables the significance of a given colour error to be more readily assessed when plotted on such a diagram. Furthermore, specification of the colour limits becomes easier since the ellipses of Fig. 5 assume an approximately circular form when plotted on a uniform chromaticity scale. The limits may thus be specified in terms of circles of radius equal to a given number of scale units.

Fig. 6 shows the limits of Fig. 5 plotted on the  $u-v$  diagram of MacAdam, in which the co-ordinates  $u$  and  $v$  are related to the  $x$  and  $y$  co-ordinates of the C.I.E. system by the following equations:

$$u = \frac{2x}{6y - x + 1.5}$$

$$v = \frac{3y}{6y - x + 1.5}$$

Because of the difficulty of translation between uniform chromaticity scales and the internationally accepted C.I.E.



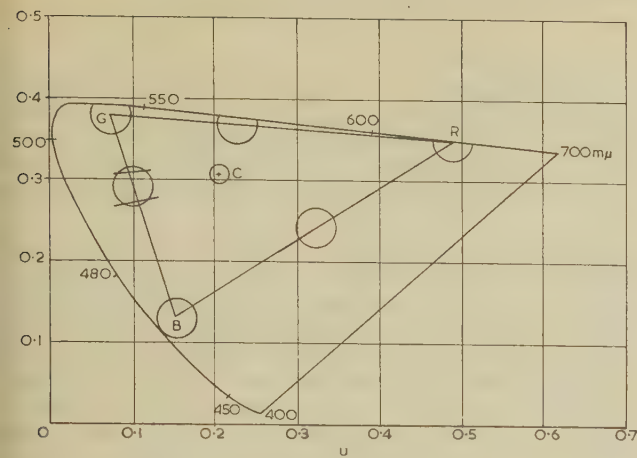


Fig. 6.—Colour tolerances on uniform chromaticity scale.

chromaticity diagram, these scales do not commend themselves for wide use outside the laboratory.

### (2.5) Use of the Tolerance Diagram

In practice the colour tolerance diagram has proved very useful in prescribing limits for colour reproduction and in assessing the effects of various phosphor colour and efficiency deviations within and beyond these limits. The actual values of the limits were initially chosen by a large amount of guesswork and little knowledge, but these have been found, in practice, to be quite reasonable figures to aim at. At first a limit of 100 times the j.n.d. was also used for white, but it was found to be too large. On the basis of experience this has now been reduced to 50 times the j.n.d. On later diagrams also, the centre of the white ellipse has been moved from illuminant C to a point close to equal-energy white, since excessively blue whites appear not to be tolerable in practice.

As applied to the banana tube the diagram is modified since the most saturated sulphide green phosphor available falls just within the limit of 100 times the j.n.d. for green. Fig. 7 shows the diagram at present in use. The various shaded areas represent the limits within which the red and blue primaries and the three

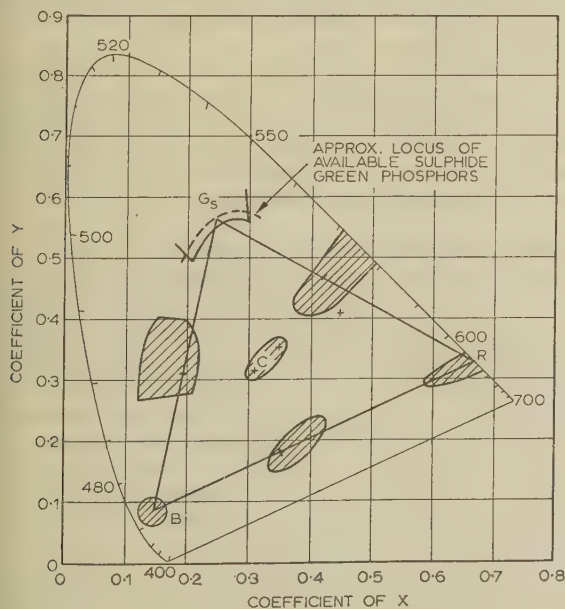


Fig. 7.—Banana-tube tolerance diagram.

complementary colours and white should lie. These are based on the ellipses of the original diagram but are modified so as to give effect to various restrictions on the relative luminance contributions of the primaries and to avoid anomalies as described above.

The locus of available green phosphors is shown by the dotted line. Limits for the variation of the green primary along this locus are marked, and some latitude for the saturation of the green is also allowed for reasons of practical expediency. The final tolerance limit for the green phosphor is thus indicated by the heavy line around  $G_s$ .

### (3) EFFECTS OF SPOT SIZE AND STRIPE STRUCTURE

The degree of colour impurity arising as a result of the finite size of the cathode-ray-tube spot will be decided by the relative sizes of the spot and the colour stripes, the size of the non-luminescent guard-bands, the current distribution in the spot and the type of colour drive signal employed.

The stripe structure at present chosen for the banana tube consists of 2mm-wide luminescent stripes separated by 1mm guard-bands, and colour selection is normally carried out by the application of a lateral sine-wave 'spot wobble' which causes the beam to traverse the stripes in the reversing colour sequence  $RGBGRGBG \dots$ , as shown in Fig. 8. Ideally the drive wave-

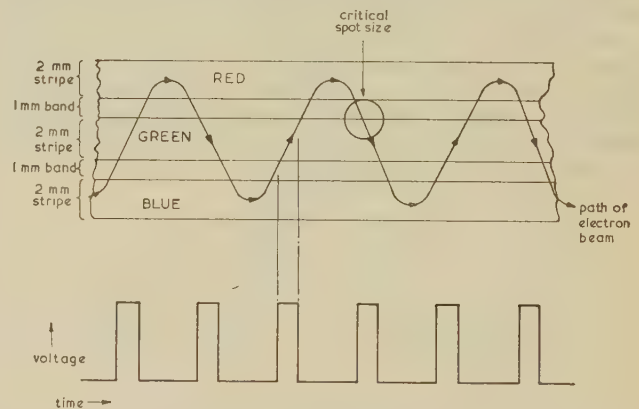


Fig. 8.—Colour stripe structure (above) and ideal grid drive voltage waveform for green field (below).

form would consist of rectangular pulses timed to correspond to the traversal of the spot over the colour stripes. For instance, the drive waveform for a green display is indicated in the diagram. It can be seen that, with this type of colour drive, a pure saturated green is obtained, provided that the spot size is less than 2 mm in the direction transverse to the stripes.

When the spot exceeds this size it will commence to overlap the adjacent colour stripes. This will result in an error in the reproduced chromaticity. For the green stripe, as shown in the diagram, the error will be one of saturation, both blue and red contamination being added to the green light output. Where the spot is traversing an outer stripe, however, a hue error will occur, the red or blue colour fields being contaminated with green light.

Further colour errors can occur as a result of the increase in spot size with beam current. While the spot remains small compared with a colour stripe, an increase in beam current results in an approximately linear increase in light output. However, as the spot enlarges, an increasing amount of the beam current falls into the guard-band area and hence fails to produce light output. The slope of the light-output/beam-current characteristic is thus reduced. As a result of this effect,

local variations in the reproduced colour can occur in high-brightness areas of the picture.

Calculation of the expected errors due to these effects proves to be extremely difficult. The spot varies along the length of the scanning line, both in dimensions and shape, which means that the effects are liable to vary over different parts of the raster. Spot size is also variable with beam current. Furthermore the distribution of current in the spot is not according to any simple function which could be readily manipulated in calculations. Similarly the drive waveform does not consist of rectangular pulses. For these reasons, no full analysis of these errors has at present been made. However, some indication as to the actual performance under practical conditions may be gained from colour measurements which have been made.

For these measurements the display was set up to give good reproduction of an electronic colour-bar pattern giving bars of all primary and complementary colours at 100% saturation. The colour drive used was a constant tripler self-decoding system<sup>8,9</sup> with full colour-signal correction circuits. In this type of receiver the tube is pulsed into conduction by sinusoidal pulses for a time equivalent to 40° of the sine-wave spot-wobble frequency. (This corresponds to the time taken for the beam to traverse a green stripe.) When satisfactory reproduction had been achieved the red and blue signals were removed from the bar pattern leaving only the vertical green bar, which extended from the left-hand edge of the raster to the centre. A photo-electric tri-colorimeter was then used to measure the colour at the centre of this bar at various levels of peak drive voltage. From a previous experiment the peak currents corresponding to various levels of drive were known, and hence the results are plotted as percentage saturation of the green colour bar versus peak beam current (Fig. 9).

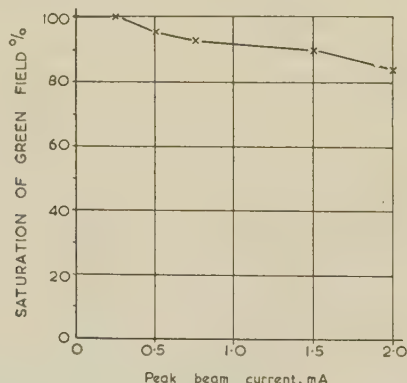


Fig. 9.—Change in saturation with beam current.

Although no great accuracy can be attached to these measurements, which probably also include effects due to electron scatter, the indication is that the order of this type of error is reasonably low in the present system.

#### (4) ERRORS DUE TO DECODING CIRCUITS

##### (4.1) Gated Operation

If the tube is driven by the high-quality colour gate described by Freeman,<sup>10</sup> the colour errors contributed by the circuit itself will be virtually negligible. The only sources of colour errors will then be due to phosphors and to spot size as above. However, this is not an economical circuit and is unlikely to be used in a domestic receiver.

##### (4.2) Self-Decoding Operation

###### (4.2.1) Tripler Operation.

A more practical way of using the banana tube employs a method known as self-decoding. In this type of operation N.T.S.C. composite video signal is applied either directly or after modification to the electron gun. Decoding of the signal to red, green and blue light intensity values takes place within the tube itself.

A convenient method of operation is the tripler circuit described by Loughlin.<sup>8</sup> Details of the circuit configuration involved may be found in the accompanying paper by Freeman. With this type of decoder the spot is deflected across the colour stripes by a sine-wave spot wobble as shown in Fig. 8, instead of being driven with the gating waveform shown in Fig. 8 the tube is pulsed into conduction for short periods at a rate equal to three times the frequency of the spot wobble. During these conducting periods, which occur at the points indicated in Fig. 10 and give rise to a continuous colour (self-

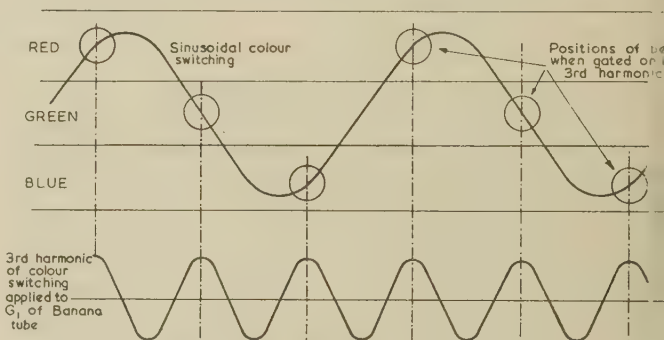


Fig. 10.—Action of tripler circuit.

tion) sequence (c.c.s.)—*RGB—RGB...*, etc., the tube samples the colour drive signal and thus performs the demodulation action.

The fidelity of reproduction achieved depends upon the degree to which the N.T.S.C. signal is modified to suit the requirements of the tube, and it is interesting to study the effects of some possible signal modifications so as to obtain some idea as to the order of complexity which may be required to ensure satisfactory performance.

The following analysis is based on calculations by Rudolph. These calculations all relate to the tripler receiver and assume the banana tube gamma to be 2.0 (except as in Section 4.2.2) and the spot size to be infinitesimally small. The spot-size effects mentioned in Section 2 are therefore additional to the errors indicated in Figs. 11, 12, 14, 15 and 16.

###### (4.2.2) Direct Application of N.T.S.C. Composite Signal.

In the first case the composite N.T.S.C. signal at the video detector of the receiver may simply be amplified and applied direct to the cathode of the tube. This represents the minimum of circuit complexity. The resultant errors are shown in Fig. 11, which assumes the display to have the same N.T.S.C. primaries. In this diagram the dots represent the desired colours and the arrow tips lie on the colours actually reproduced. The figures represent the ratio of reproduced luminance to intended luminance. This diagram is similar to that given by Loughlin<sup>8</sup> for a c.c.s. receiver.

This method of drive results, as can be seen, in large errors of both chromaticity and luminance. Errors of up to 200 times the j.n.d. are apparent, notably in green, yellow and magenta. Although the eye is relatively insensitive to errors in green



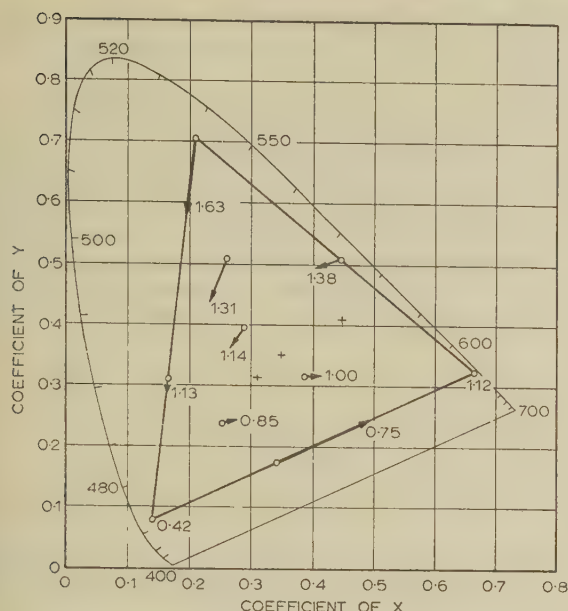


Fig. 11.—Colour and luminance errors due to direct application of N.T.S.C. signal.

yellow saturation, these errors add to those caused by a short-decay green phosphor, and for this reason this type of operation cannot be recommended for the banana tube.

#### (4.2.3) Monochrome Correction.

It has been shown<sup>8</sup> that the N.T.S.C. signal can be converted to the correct form for the continuous colour-sequence display of the tripler type by means of the two circuit configurations known, respectively, as monochrome correction and sub-carrier modification.

The luminance component of the N.T.S.C. colour signal is defined<sup>12</sup> as

$$E_Y' = 0.3E_R' + 0.59E_G' + 0.11E_B'$$

where  $E_Y'$  = Luminance signal.

$E_R'E_G'E_B'$  = Gamma-corrected primary red, green and blue signals, respectively.

The monochrome signal  $E_M'$  required by a c.c.s. display is given<sup>8</sup> as

$$E_M' = 0.33E_R' + 0.33E_G' + 0.33E_B'$$

The function of the monochrome corrector is to convert the N.T.S.C. luminance signal to the required form. A correction signal  $E_M' - E_Y'$  may be obtained by synchronous detection of the colour sub-carrier at a phase of  $19^\circ$  to the reference and with a gain of 0.58. When this correction signal is added to the  $E_Y'$  signal the required monochrome signal  $E_M'$  is obtained.

With this correction a considerable improvement results in the performance of the display. Fig. 12 shows some of the errors remaining. It can be seen that the undesirable green and yellow desaturation has been almost completely eliminated. The remaining large errors are the shift of magenta towards red and the very low blue luminance.

#### (4.2.4) Complete Signal Translation.

The N.T.S.C. colour sub-carrier signal may be represented vectorially as shown in Fig. 13(a). The colour sub-carrier signal required for a c.c.s. single-gun display, however, is as shown in Fig. 13(b). Circuits can be devised to convert the N.T.S.C. sub-carrier from the form of Fig. 13(a) to that of

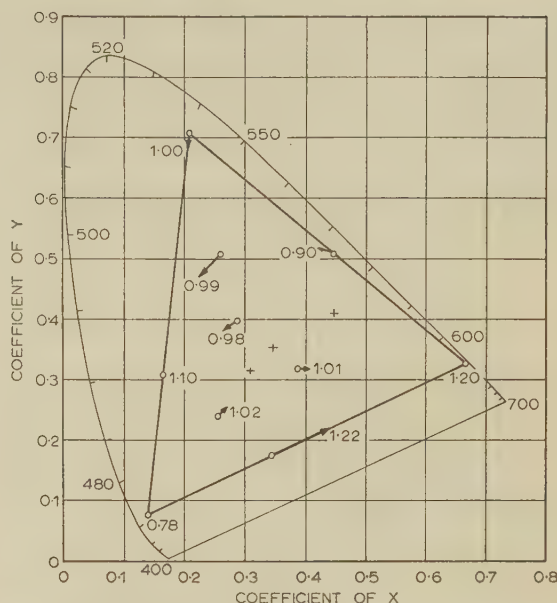


Fig. 12.—Errors due to use of N.T.S.C. signal with monochrome correction only.

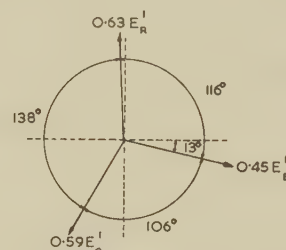


Fig. 13A.—Vector representation of N.T.S.C. sub-carrier.

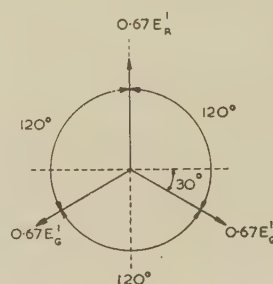


Fig. 13B.—Vector representation of c.c.s. sub-carrier.

Fig. 13(b). This type of circuit is known as a sub-carrier modifier or equi-angle corrector since the angles between the vectors of Fig. 13(b) are equal. When this form of correction is used in conjunction with monochrome correction, substantially correct pictures are possible except for colour-phosphor and spot-size errors.

#### (4.2.5) Circuit Correction for Incorrect Green Phosphor.

So far the decoding errors have been considered assuming the display device to have true N.T.S.C. primary colour phosphors. However, when the same circuits are used in conjunction with a sulphide-green phosphor, additional errors arise as mentioned in Section 2.1.

The errors arising purely as a result of the incorrect green





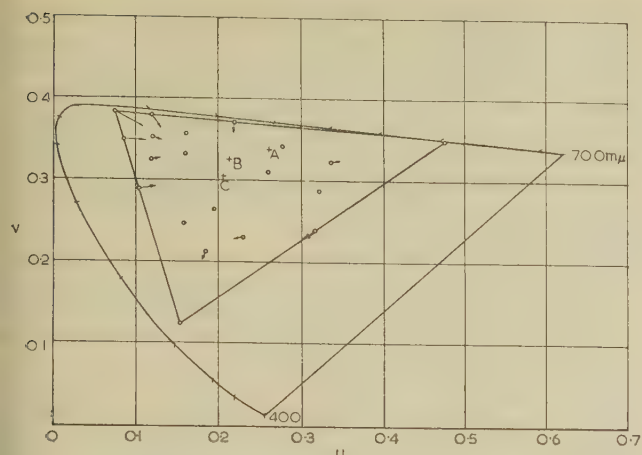


Fig. 16.—Errors shown in Fig. 15 plotted on uniform chromaticity scale diagram.

chromaticity scale of MacAdam. Good colour fidelity is indicated in all important areas of the colour gamut.

#### (4.3) Application of the Analysis to the Banana Tube

##### 4.3.1) Factors to be Considered.

The foregoing analysis has shown that good colour fidelity may be achieved with a horizontal-stripe colour tube employing a colour decoder of the tripler type and having a sulphide-green primary-colour phosphor. However, when applying the results of this analysis to the banana tube in its present form there are a number of additional factors to be considered in order to gain a better indication of the performance of the tube.

The finite spot size has already been considered. Other factors are the gamma of the display tube, the effect of some inevitable variations in the primary-colour duty cycles of the tripler receiver, and the performance of the receiver when an alternative circuit known as the modulated tripler is used.

##### 4.3.2) Effect of the Gamma of the Cathode-Ray Tube.

The N.T.S.C. signal is gamma-corrected according to normal television practice to allow for the non-linear beam-current/picture-drive characteristics of the display tube. The system assumes a power law for the display tube with a gamma of 2.2. The diagrams so far presented are based on calculations which assume a power law with a gamma of 2 for ease of calculation. However, the banana-tube gamma varies with picture drive. At low drive levels, i.e. beam currents less than  $500\mu\text{A}$ , it approximates to a gamma of 2. At high beam currents, however ( $>1\text{mA}$ ), it has a much higher gamma, and 3 would be a nearer approximation. The effects of an increase in the gamma of a display can be seen in Fig. 17, where the tips of the arrows lie on the colours which would be reproduced by a display device having a gamma of 3, compared with one having a gamma of 2 (dots). It is seen that the effect is to cause a general increase in the saturation of colours within the triangle and a shift of those colours between the primaries and complementaries, towards the nearest primary. This increase in saturation at high beam currents tends to oppose the desaturation due to the increase in spot size at these currents.

##### 4.3.3) Variations in Duty Cycle.

The calculations of Section 4.2 were made assuming that the beam-current duty cycles remained constant for all conditions of colour drive signal. This is the condition which would obtain if a 'multiplicative' form of gating were used. For

instance, if the composite video signal were applied between grid and cathode of the display tube and if a sine wave of frequency equal to three times the spot-wobble frequency were applied to the first anode of the tube, the tube would be pulsed into conduction on positive half-cycles of the third harmonic

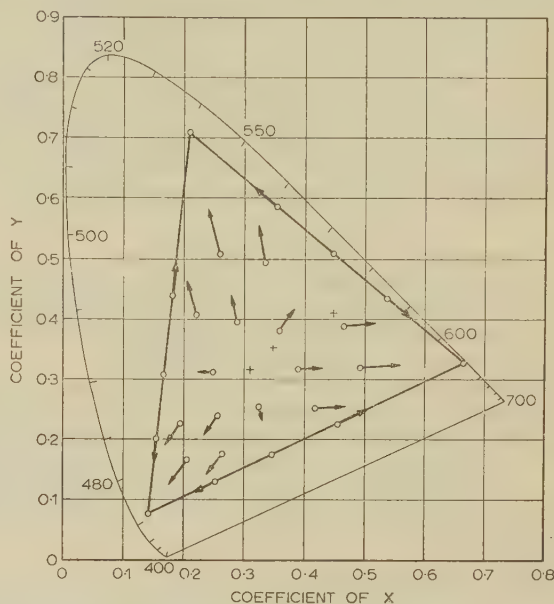


Fig. 17.—Behaviour of a display with a gamma of 3.

signal. The sampling time of the tube would then be substantially independent of the colour drive signal.

The present banana tube, however, has a triode gun. It is therefore necessary to apply the video signal to the cathode of the tube and the third-harmonic signal to the grid, as described by Freeman.<sup>9</sup> The two signals will thus add and the sampling time or duty cycle will vary with changes in video signal. Provided that the amplitude of the third-harmonic sampling signal is sufficiently large, the duty cycle can always be kept small and the effects of this variation minimized. The error diagrams plotted relate to infinitely narrow sampling. However, the additional errors caused by sampling duty cycles of up to  $40^\circ$  of one cycle of the spot-wobble sine wave are very small. This is probably the longest sampling period which would occur with this form of circuit.

It can be seen that an infinite number of error diagrams is necessary to portray the colour performance at all the possible levels of video drive.

##### (4.3.4) Modulated Tripler.

An alternative method of operation of the banana tube which results in an increased picture brightness is possible. This is the so-called 'modulated tripler'<sup>14</sup> in which the duty cycles are varied as a function of the chrominance signal amplitude. The operation of this type of decoder is more complex, and a full analysis of its colorimetric performance when used in conjunction with the banana tube has not yet been made. Calculations by Dressler and Neuwirth<sup>14</sup> on the operation of this decoder with the single-gun chromatron indicates that the order of error involved when direct application of the N.T.S.C. composite video signal is employed is similar both for the direct and modulated tripler receivers. Some variation from their results may be expected for a banana receiver, however, owing to differences in the colour-stripe structure.

It is worth noting that direct application of the N.T.S.C.



composite video signal to the banana tube without any third-harmonic pulsing whatsoever, i.e. with no signal processing of any sort, results in a displayed picture whose colour gamut is confined to the orange-cyan axis. Since the beam-current duty cycle in a modulated tripler receiver is made inversely proportional to the amplitude of the chrominance sub-carrier signal, it follows that at low chrominance signal amplitudes, when the duty cycle is very large, the receiver will tend to operate as an orange-cyan display. This will tend to occur for low-brightness colours as well as for low-saturation colours. For complete colour fidelity, therefore, it would be necessary to derive a true saturation signal which was wholly independent of picture brightness and use this to modulate the colour duty cycle.

### (5) CONCLUSIONS

The principal factors governing the fidelity of colour reproduction with the banana-tube colour-television display have been analysed, and an attempt has been made to indicate the quantitative effects of some of the errors involved.

The final performance of a receiver of this type must inevitably be closely tied with the economics of the design. It has been shown that circuits can be devised which result in a performance close to complete fidelity with the phosphors chosen and that the effects of the finite spot size—which detract from the performance achieved by the final receiver of Section 4.2.5—are of a reasonably small order.

Consideration of the error diagrams of Figs. 11 and 17 suggests that it is not likely that direct application of the N.T.S.C. composite video signal, together with a third-harmonic pulsing waveform, will result in satisfactory picture reproduction. This is because the errors involved in such a process add to those errors which are inherent as a result of the necessity to use an incorrect green primary. The addition of a monochrome corrector stage, at least, may be considered a necessity for this display. Sub-carrier modification is also desirable, although whether the improvement afforded by this circuit would ultimately warrant the additional expense is a matter for some conjecture.

Once these signal corrections are available, however, the additional correction required in order to achieve almost complete fidelity can be obtained at very small extra cost. The  $E'_w$  signal is available by slight adjustment of the detection phase and gain of the normal monochrome corrector circuit, and only a slight increase in chrominance gain is required. The additional requirement is for a diode corrector circuit. It is likely that this correction would in any case be considered desirable for a single-gun display of this type in order to offset the effects of finite spot size, as described by Clapp.<sup>13</sup> Its inclusion does not, in any case, involve undue expense or complication.

When considering the performance of a given receiver as a whole it will be apparent, as already mentioned, that there is a great deal of interdependence between the various error-producing factors and that the final design must make due allowance for this. For instance, to take one typical example, improved colour purity at high beam currents can be achieved in a number of ways. Either the width of the guard bands may be increased or the beam-current duty cycle may be reduced by means of diode correction. Alternatively alteration to the electron-gun design may be made. Thus the same defect is seen to be simultaneously dependent upon the screen-stripe structure, the circuit configuration and the electron optics of the system.

In a similar way the chromaticity and luminance errors in the picture are a function both of the colour of the primary reproducing phosphors and of the type of colour decoder circuit used. It is therefore reasonable to consider deliberate adjustment of the colour primaries as an alternative to adjustment of the circuit-elements. It has already been shown that, with careful

choice of the position of the green primary, it is possible to eliminate errors which might occur in the region of magenta colours. Further investigation along these lines shows that it is possible to choose a set of red and blue primaries for use in conjunction with the sulphide-green primary, such that the relative luminance contributions of these three primaries in white mixture are in the correct relationship [eqn. (3)]. Errors in the reproduced luminances due to the use of this green primary are thus eliminated.

The elimination of the luminance errors in this way carries with it the disadvantage of a further restriction of the picture colour gamut, and a circuit correction may therefore be preferred; nevertheless, the illustration does serve to indicate some of the possibilities open to the designer.

Finally, although the particular requirements of the banana-tube display have made it necessary to adopt the desaturated sulphide-green phosphor, it should be noted that this phosphor is also an attractive proposition for other display tubes. The willemite type of green phosphor at present used in conventional colour tubes exhibits an afterglow which is longer than that of the red and blue phosphors used, and results in the annoying phenomenon of 'colour trailing'. A short-decay green phosphor could therefore be used to replace the conventional type with good effect.

It is shown that a colour tube employing a sulphide-green phosphor is capable of competing satisfactorily with other display tubes on grounds of colour fidelity. Ultimately the design of a domestic receiver based on such a tube would involve a compromise between the conflicting demands of circuit simplicity and economy on the one hand and fidelity of reproduction on the other.

### (6) ACKNOWLEDGMENTS

The author is very conscious of the debt he owes to Mr. D. A. Rudd, who has performed all the calculations relevant to Section 4, and to Mr. N. D. Richards, whose co-operation in the colour tolerance work and the construction of the colour matrix has been highly valued.

Thanks are also due to the Director of the Mullard Research Laboratories, Mr. P. E. Trier, and to the Directors of Mullard Ltd., for permission to publish the information contained in this paper.

### (7) REFERENCES

- (1) JUDD, D. B.: 'Estimate of Chromaticity Differences and Nearest Colour Temperature on the Standard 1931 I.C. Colorimetric Co-ordinate System', *Journal of the Optical Society of America*, 1936, **26**, p. 421.
- (2) MACADAM, D. L.: 'Visual Sensitivities to Colour Differences in Daylight', *ibid.*, 1942, **32**, p. 247.
- (3) STILES, W. S.: 'A Modified Helmholtz Line Element of Brightness-Colour Space', *Proceedings of the Physical Society (London)*, 1946, **58**, p. 41.
- (4) WINTRINGHAM, W. T.: 'Colour Television and Colorimetry', *Proceedings of the Institute of Radio Engineers*, 1951, **39**, p. 1135.
- (5) MACADAM, D. L.: 'Reproduction of Colours in Outdoor Scenes', *ibid.*, 1954, **42**, p. 166.
- (6) MACADAM, D. L.: 'Projective Transformations of I.C. Colour Specifications', *Journal of the Optical Society of America*, 1937, **27**, p. 294.
- (7) BEKENRIDGE, F. C., and SCHAUB, W. R.: 'Rectangular Uniform-Chromaticity-Scale Co-ordinates', *ibid.*, 1939, **29**, p. 370.
- (8) LOUGHLIN, B.: 'Processing the N.T.S.C. Colour Signal in One Gun Sequential Displays', *Proceedings of the Institute of Radio Engineers*, 1954, **42**, p. 299.



- (9) FREEMAN, K. G.: 'Circuits for the Banana-Tube Colour-Television Display Systems' (see page 604).
- (10) FREEMAN, K. G.: 'A Gating Circuit for Single-Gun Colour Television Tubes', *Journal of the British Institution of Radio Engineers*, 1959, **19**, p. 667.
- (11) RUDD, D. A.: 'Some Decoding Errors in Single-Gun Colour Television Displays', Mullard Research Laboratories Technical Note No. 443, 1960.
- (12) Federal Communications Commission of Washington D.C. (U.S.A.). Public Notice 53-1163, 1953, Section 3.681.
- (13) CLAPP, R. G.: 'The Colorimetry of Sequential Displays', *Acta Electronica*, 1958, **2**, p. 182.
- (14) DRESSLER, R., and NEUWIRTH, P.: 'Brightness Enhancement Techniques for the Single-Gun Chromatron', *Institute of Radio Engineers Convention Record*, 1957, **5**, p. 220.

[The discussion on the above paper will be found on page 630.]

---

## APPRAISAL OF THE BANANA-TUBE COLOUR-TELEVISION DISPLAY SYSTEM

By K. G. FREEMAN, B.Sc., A.Inst.P., and B. R. OVERTON, B.Sc., Member.

*(The paper was first received 17th November, 1960, and in revised form 10th February, 1961. It was published in May, 1961, and was received by the ELECTRONICS AND COMMUNICATIONS SECTION 15th May, 1961.)*

## SUMMARY

The many factors which determine the potentialities and limitations of the banana tube as a possible solution to the colour-display problem are considered in some detail. Limitations imposed by tolerances set by the requirements of the system are stated and an appraisal of the picture quality is made. Some indication of possible cost compared with other displays and an overall appraisal and indication of future possibilities are given.

## (1) INTRODUCTION

A new and interesting colour-display device has been proposed. No investigation of such a new device would be complete without a study of its potentialities and limitations. This paper gives the result of such a study of the banana-tube system in its present state of development, and it should be read in conjunction with the papers describing other aspects of the investigation.<sup>2,3,6,7,8</sup> A critical approach has been adopted to indicate where any further development should be concentrated.

There are three main aspects to consider. First the various electrical and mechanical tolerances affecting picture quality must be evaluated. These will determine the reliability of the device, its ease of adjustment, and the degree of circuit complexity necessary to reduce variations in performance to an acceptable level. For example, if normal fluctuations in the mains supply voltage lead to intolerable colour errors, additional circuits are required to stabilize the appropriate power supplies.

Second, it is important to determine the limitations of the display device itself, for if these are severe the probability of the resulting receiver being a success will be small. However, it is difficult to consider the device completely apart from the circuits used to drive it, so the study must, to some extent, take the latter into consideration.

Third, an attempt must be made to obtain some estimate of the possible cost of a domestic receiver.

## (2) TOLERANCES

The acceptable deviations from their design values of the various mechanical and electrical parameters affecting the picture quality can be determined accurately only by a thorough subjective investigation. It is possible, however, on the basis of existing knowledge of allowable picture errors, to make some fairly reliable estimates of the order of tolerances involved. These estimates will indicate the factors of importance in designing a receiver with stable performance. The classification of the tolerances which follows is to some extent a rather arbitrary one, and it will be appreciated that there is some overlap.

## (2.1) Mechanical, Optical and Related Tolerances

In order that a correctly operated tube shall produce an acceptable final picture a number of mechanical, optical and related tolerances must be satisfied. Quantitative limits cannot be easily set to the mounting of the mechanical components,

which must be sufficiently rigid to ensure that any mechanical movement is small enough to have a negligible effect on the picture.

## (2.1.1) Position of Lens Rods on Drum Periphery.

Assuming that the drum is perfectly synchronized, it is evident that the lens rods must be sufficiently accurately located on its periphery to ensure absence of noticeable line jitter in the final picture. Richards suggested in the early stages<sup>1</sup> that ideally the scanning lines in the final picture should not be displaced by more than one-tenth of the line interval (i.e.  $1/4000$  of the picture height) from their correct position. He therefore put radial and tangential tolerances on the position of the lens rods on the drum.

For a three-element lens drum one-tenth of the line interval is equivalent to  $1.8'$  of arc, and with the present lens-drum radius of  $6.8$  cm the tangential tolerance,  $t$ , is thus  $3.6 \times 10^{-3}$  cm. The effect of radial displacements is more complex, being a function of position in the raster. However, Richards has shown that in the worst case the equivalent tangential displacement,  $t'$ , for a radial displacement,  $r$ , is given by  $t' = 0.73r$ .

He thus proposed an overall drum construction tolerance given by

$$|0.73r + t| < 3.6 \times 10^{-3} \text{ cm}$$

This calculation, of course, takes no account of the additional errors due to incorrect centring of the drum, such errors being possible since one end of the banana lens drum is open and without a centre bearing. Howden has shown<sup>2</sup> that with the experimental models a tolerance of  $0.4$  of a line was achieved. Such a tolerance may be acceptable for domestic viewing.

## (2.1.2) Rotation of the Drum.

The effect of deviations of the drum from its correct speed and phase are conveniently discussed here, although they are closely bound up with the electrical requirements in the servo mechanism. As indicated elsewhere<sup>3</sup> these deviations are of three types, namely low-frequency deviations giving picture drift, intermediate-frequency deviations giving apparent picture jitter and high-frequency deviations giving line jitter.

On the basis of a simple subjective experiment, Richards<sup>1</sup> has tentatively proposed the tolerances shown in Table 1, which must be met mainly by the efforts of the servo loop.

Table 1

TOLERANCES FOR DRUM ROTATION

Deviation frequency	Proposed tolerance
c/s	(peak deviation in lines)
20	0.21
2	0.12
0.2	0.3
0.05	2.4
0	9.5



The tolerance for zero frequency is based on a limitation of the aperture of the system to give the effect of 5% overscan. A drift of  $\pm 2\frac{1}{2}\% = \pm 9.5$  lines is then permissible before the edge of the picture comes into view.

#### 2.1.3) Lens-Rod Diameter.

It is obvious that considerable differences and variations in lens-rod diameter would lead to positional variations in the slit image, and noticeable variations in the demagnification and brightness of the lines (giving rise to flicker). In practice it appears that the only reason for setting any diameter tolerance is in order that the lens-rod positional tolerances set in Section 2.1.1 may be easily and conveniently met. In practice a diameter tolerance of  $\pm 0.0005$  in has been set.

#### 2.1.4) Mirror Shape.

The mirror must be made sufficiently accurately so that no image distortion is apparent under normal viewing conditions—including the movement of the viewer's head up and down or from side to side over a restricted angle. No quantitative specification has yet been made.

#### 2.1.5) Flicker.

Relative differences in the optical transmission of the three lens rods will give rise to a flicker component at  $16\frac{2}{3}$  c/s, which will have a high visibility compared with 50 c/s flicker. This variation in the relative transmission may be due to differences in the optical properties of the lens materials themselves, or, more probably, the differential accumulation of dust on the surfaces of the lenses.

A preliminary experiment shows that for a plain field of 5 ft-L brightness this  $16\frac{2}{3}$  c/s flicker becomes objectionable when the difference in effective lens transmission exceeds a value somewhere between 2% and 10%. More refined experiments would be necessary to determine the tolerance more accurately.

#### 2.1.6) Drive Torque.

In Section 2.1.2 it was stated that a  $\pm 2\frac{1}{2}\%$  static variation in the vertical position of the picture is allowable. When the drum is phase-locked, such shifts will occur as a result of the servo mechanism counteracting the effect of changes in drive torque. For this  $2\frac{1}{2}\%$  tolerance it has been found that the maximum allowable percentage change in the drive torque is  $\pm 6\%$  for the present experimental model. Since the torque is proportional to the square of the applied voltage this means a mains supply-voltage tolerance of  $\pm 3\%$ , and this is much smaller than the variations likely to be encountered in practice. Some means of improving this performance must be found.

#### 2.1.7) Pull In.

With the present experimental integral motor the pull-in range is only  $\pm 2$  c/s, corresponding to a  $\pm 4\%$  change in the uncontrolled speed of the drum. This must be improved if satisfactory performance under domestic conditions is to be achieved. If a separate motor is used the speed can be chosen to be close to synchronous speed and its characteristics designed to give a much greater pull-in range. Alternatively a two-mode synchronization system may be used.

### (2.2) Electrical Tolerances

Owing to the method of colour selection in the present banana system the colorimetric quality of the picture is very sensitive to changes in a large number of electrical parameters. The tolerances to variations in these parameters have been fairly extensively investigated,<sup>4</sup> but it is possible to give here only a

brief account of the results. The effects of the earth's magnetic field and the susceptibility to stray fields are considered in a separate Section.

#### (2.2.1) Fundamental Tolerances.

The most stringent requirement for the banana tube, as with any colour tube, is that it should produce a satisfactorily uniform and acceptable white, and this will also be a measure of its ability to produce satisfactory colour pictures. The important tolerances will therefore be determined for a white picture. Self-decoding operation of the tube will be assumed.

If the relative phosphor efficiencies are unchanged with life and have been balanced to give the correct white under ideal tube-operating conditions, errors will arise due to incorrect spot-wobble amplitude and inaccurate tracking of the unwobbled spot down the middle of the central phosphor stripe. These lead to two types of error in the white produced. Constant errors in tracking and spot-wobble amplitude will produce a uniform white of the incorrect chromaticity—i.e. they will affect the overall white. Local errors in tracking and spot-wobble amplitude will produce local white errors.

As a basis for calculation, relative duty-cycle tolerance limits, which seemed reasonable in the light of experience, were chosen to be  $\pm 15\%$  for the overall white and  $\pm 5\%$  for the local white errors. Recent practical investigations have indicated that the local white error tolerance at least may have been chosen to be too small by about a factor of two, but it does give a starting-point to enable some estimation of the electrical tolerances to be made.

From this postulate it is possible to deduce the spot-wobble amplitude and tracking tolerances for the two cases, and thence the tolerances for the various electrical (and mechanical) parameters. It is clear that the spot-wobble amplitude and tracking tolerances will depend upon the spot-wobble amplitude *vis-à-vis* the strip triplet structure, but typical operating conditions have been taken which in fact appear to give near maximum tolerances with the present structure. In addition, these tolerances may be expected to be modified by the effect of spot size (which on current peaks is comparable with the phosphor strip width). Since the spot shape is not circular and the current distribution in the spot cannot be represented by a simple function, a complete mathematical analysis would present a very formidable task. However, a simple analysis has been made for a uniform rectangular spot to obtain some estimate of the possible effect of spot size. From this it has been found that the assumption of an infinitesimally small spot is not likely to lead to very great errors in determining tolerances where the white balance is concerned.

The following Sections indicate how the tolerances arise. To simplify calculation and experimental observation in the first instance individual tolerances only are determined, based on the assumption that only the variable under investigation produces an error. Where relevant, the observed tolerances for just-noticeable colour errors are also given. The tolerances, where all the parameters vary simultaneously, will be considered later.

#### (2.2.2) Factors Affecting the Overall White.

Three variables which affect the overall spot-wobble amplitude (calculated tolerance  $\pm 9\%$ ) are:

(a) *Spot-wobble output-stage h.t. voltage.*—Since the spot-wobble output stage is operating in Class C the spot-wobble current amplitude is approximately proportional to the h.t. voltage, so that the latter will have the same calculated percentage tolerance as the spot-wobble amplitude, i.e. an individual tolerance of  $\pm 9\%$ . The observed tolerance was, in fact,



$\pm 5\%$ . H.T. stabilization is therefore necessary to accommodate mains fluctuations.

(b) *Spot-wobble output tuning*.—Detuning of the spot-wobble output stage will also affect the current amplitude. From the circuit specification it is a simple matter to deduce the tolerance on the resonant frequency of this circuit and hence the component tolerance (for thermal effects, etc.) for the tuning components, particularly the inductance. The calculated individual tolerance is about  $\pm 10$  kc/s. In practice, hue errors, due to phase change with detuning, will probably lead to a closer tolerance (e.g.  $\pm 2\frac{1}{2}$  kc/s for a  $5^\circ$  phase change) which may be difficult to meet in practice.

(c) *E.H.T. voltage*.—The spot-wobble sensitivity is inversely proportional to the square root of the e.h.t. voltage. Thus the percentage tolerance for the latter is approximately twice that for the spot-wobble amplitude ( $\pm 20\%$ ).

The calculated tolerance for constant transverse displacements is  $\pm 0.42$  mm. There are two variable factors which may affect the tracking:

(i) *Axial rotation of the tube*.—This is easily deduced from the equivalent transverse-displacement tolerance, and is calculated to be  $\pm 37'$  of arc. Rigid clamping is therefore necessary to avoid tube movement.

(ii) *'Field-deflection' coil current*.—It is evident that if such a coil is used a tolerance must be set for its current, but this will not be considered here.

### (2.2.3) Factors Producing Local White Errors.

The calculated tolerance for variations in the spot-wobble amplitude along the phosphor triplet is  $\pm 3\%$ . The factors which affect this amplitude locally include:

(a) *Spot-wobble modulation—waveform amplitude and phase*.—With the present system it is necessary to modulate the amplitude of the spot-wobble coil current in order to obtain constant visual spot-wobble amplitude, and deviation of the modulation waveform from its correct amplitude and phase will cause local white errors. Calculated tolerances for the waveform at present required are  $\pm 2\frac{1}{2}\%$  for the amplitude and  $\pm 0.6 \mu$ s for the phase. The observed amplitude tolerance was  $\pm 10\%$ . The modulation of spot wobble necessitates a very stable modulation-waveform generator.

(b) *Longitudinal scan displacements*.—Similarly, owing to the need to modulate the spot-wobble current, errors will occur due to longitudinal scan displacements, particularly at the far end where the modulation changes rapidly. The end-of-scan displacement has a calculated tolerance of  $\pm 6$  mm. The following tolerances have therefore been determined: line-scan centring  $\pm 4$  mm (observed tolerance  $\pm 8$  mm) line-scan current amplitude  $\pm 2\%$ , e.h.t. voltage  $\pm 8\%$  (observed tolerance  $\pm 3\%$ ). The longitudinal position of the stripe triplet and therefore of the tube will also be of some minor importance. As previously mentioned, the earth's magnetic field effects are discussed separately.

There are a number of factors, other than the earth's magnetic field, which produce local transverse displacements (tracking errors). (The calculated tolerance for these is  $\pm 0.14$  mm.)

The errors produced by these factors can be largely corrected in the setting-up procedure. The tolerance which is given refers to the mechanical stability which must be achieved once setting-up is completed. The factors are:

(i) *Line-coil orientation*.—The calculated tolerance of  $\pm 11'$  of arc is deduced from experimental knowledge of the spot path for known coil orientations.

(ii) *Focus-coil orientation*.—Experimental evidence indicates that the orientation of the focus coil on the tube neck is extremely

critical. Although no quantitative tolerances have been determined a very rigid focus mount is necessary.

(iii) *Gun centrality*.—In this case, also, no quantitative estimate of the tolerance has yet been made.

(iv) *Triplet coaxiality*.—Non-coaxiality of the stripe triplet with the (correct) tramline field can produce tracking errors.

To obtain either a correctly tracking unwobbled spot or correct duty cycles with spot wobble, it is necessary to mount the strip triplet straight to within the local tracking tolerance. However, as there are four stripe edges which will affect the duty cycle the tolerance for each of these has been taken as  $1/\sqrt{4}$  of the tracking tolerance, and calculated to be  $\pm 0.07$  mm. This constructional tolerance should be possible to meet.

Incorrect focusing of the spot can also lead to local errors in the white and in colour rendering. The experimentally determined tolerance for the focus-coil current is  $\pm 1.7\%$ .

### (2.2.4) Summary of Electrical Tolerances.

The calculated and observed individual tolerances given above were determined, as explained, on the assumption that only the variable under investigation produced any error. In practice several parameters are likely to vary simultaneously, so that a somewhat closer tolerance must be set to allow for this. Table 2 gives calculated r.m.s. tolerances which have been derived from the calculated individual tolerances on the assumption that each type of error is equally likely to occur. This may not be strictly true, but at least it gives an approximate idea of the requirements for a practical receiver.

Table 2

R.M.S. OPERATING TOLERANCES

Variable	R.M.S. Tolerance
Spot-wobble output-stage h.t. voltage .. ..	$\pm 4\%$
Spot-wobble output tuning .. ..	$\pm 5$ kc/s
E.H.T. voltage .. ..	$\pm 2\%$
Axial rotation of tube .. ..	$\pm 16'$ of arc
Spot-wobble modulation:	
(i) Waveform amplitude .. ..	$\pm 1\%$
(ii) Waveform phase .. ..	$\pm 0.2 \mu$ s
Line-scan centring .. ..	$\pm 1.3$ mm
Line-scan current amplitude .. ..	$\pm 0.6\%$

For overall white and local white the relative duty-cycle tolerances are 15% and 10% respectively.

The tolerances for the factors affecting the overall white (namely the spot-wobble output-stage tuning and h.t. voltage and the axial rotation of the tube) are, of course, still based on the assumption that perfect phosphor balance is achieved and that no relative change in phosphor efficiencies occurs with tube life. If, as must be, any provision is made for such errors, the electrical operating tolerances will be tightened still further. However, it must be emphasized that these tolerances cannot be regarded only as indicating the order of magnitude.

### (2.3) Magnetic-Field Susceptibility

Although the tramline magnetic field has a constraining influence, particularly at the end of scan, the present method of colour selection is essentially a 'dead-reckoning' one and is easily disturbed by extraneous magnetic fields in the neighbourhood of the device. These are of two types, namely the components of the earth's magnetic field (which, although constant, will vary in their effect according to the orientation of the display) and stray fields from transformers, etc.

The effects of the earth's field on the present display have been fairly thoroughly investigated.<sup>5</sup> As the phosphor-str-



plane is at about  $70^\circ$  to the vertical, both the horizontal and vertical components of the earth's field may in turn be resolved into components normal and transverse to the strip plane, and both of these resultant components will therefore vary with the orientation of the display in the horizontal plane.

The effects produced have been deduced, taking the vertical,  $H_V$ , and horizontal,  $H_H$ , components of the earth's magnetic field as approximately 0.45 and 0.18 oersted respectively and a operating e.h.t. of 25 kV. The calculations ignore the confining effect of the tramline field, which to some extent will mitigate the effects of the earth's field.

The components of the earth's field normal to the stripe plane will produce a transverse displacement of the scan. The resolved component of  $H_V$  will produce a constant end-of-scan displacement of about 8 mm, and for satisfactory tube operation it is necessary to correct for this.

The resolved component of  $H_H$  will produce an end-of-scan displacement which is a function of orientation and which will have a peak value of 1.3 mm. Since the permissible displacement is only 0.14 mm it is clear that in the absence of an adjustable compensating field the permissible rotation of the displacement will be severely limited. Calculation shows that, in the most favourable case with the tube axis E-W, the rotational tolerance is  $\pm 27^\circ$ . In the worst case, with the tube axis N-S, the tolerance is only  $\pm 6^\circ$ . Practical investigation has confirmed the order of magnitude of these two tolerances.

The components of the earth's field transverse to the stripes in the stripe plane) will have a twofold effect. In the first place the landing distance of the beam from the gun will be affected, i.e. the scan linearity will be modified. With the present modulated spot-wobble this will in turn result in an incorrect duty cycle.

The resolved component of  $H_V$  will produce a constant linearity (and therefore spot-wobble amplitude) error. The magnitude of its effect will not be determined as in practice it will be compensated for automatically during initial setting-up.

The resolved component of  $H_H$  will produce a variable orientation-dependent end-of-scan displacement of about  $\pm 5$  mm, which corresponds to a linearity variation of  $\pm 1.2\%$ . As a linearity error this is not significant. The effect on the spot-wobble amplitude, however, is such as to produce a rather greater than tolerable error in duty cycles in the extreme case, since the longitudinal end-of-scan positional tolerance is  $\pm 4$  mm. Compared with the tolerance for transverse displacements the restriction on orientation from this point of view is not important.

It is evident that the banana tube is very susceptible to the effects of stray fields, whether constant or slowly varying. It is difficult without subjective investigation to determine a tolerance for varying fields, but from the earth's field study it is possible to set a tolerance for non-varying fields. The resolved component of the earth's horizontal field normal to the stripe plane is  $0.18 \cos 60^\circ = 0.09$  oersted. This field, which exists throughout the electron path, produces an observed peak end-of-scan transverse displacement of about 1.3 mm. Since the transverse-displacement tolerance is  $\pm 0.14$  mm the individual tolerance for uniform stray fields is about  $\pm 0.01$  oersted. In practice the stray fields will probably be fairly localized and a larger maximum value would be permissible. However, since the practical r.m.s. tolerance is of the order of  $\pm 0.003$  oersted, it seems safe to stipulate that the maximum value of stray fields in the neighbourhood of the tube bulb must not exceed 0.01 oersted.

#### (2.4) Limitations and Requirements Set by Tolerances

It is clear that some of the operating tolerances for the present banana display are small. This is particularly so from the

point of view of obtaining a uniform white in the reproduced picture, even if the tentative  $\pm 5\%$  tolerance for local relative duty-cycle variations is considered two or three times too pessimistic. From the tolerance figures available it is possible to draw a number of conclusions:

(a) The need to modulate the spot-wobble amplitude leads to a considerable number of close tolerances, in particular for the line-current amplitude, spot-wobble modulation, e.h.t. and, above all, the normal h.t. line voltages. All of these should therefore be well stabilized. An electron-optical configuration which dispenses with the need to modulate the spot-wobble would eliminate most of them, including the e.h.t. and much of the h.t. voltage stabilization. (In practice, of course, the e.h.t. is normally stabilized for other reasons.)

(b) Even with this important simplification, however, stabilization of the spot-wobble h.t. voltage is necessary to as little as about  $\pm 2\%$  to allow some margin for phosphor efficiency variations. This is not difficult but is an undesirable complication in a domestic receiver.

(c) The 'dead-reckoning' colour selection with the dimensions involved makes initial setting-up a difficult proposition, as the accuracy with which the tracking adjustments must be made precludes any method which relies entirely upon direct visual inspection of the scan along the stripes, or on setting-up with the tube and ancillary components removed from the drum. Experience suggests that the final setting-up can be done only by adjustment of the various controls for the most satisfactorily uniform white raster. With so many interdependent parameters involved (tube and line-coil orientation, focus-coil position, earth's field correction, spot-wobble amplitude, and—in the present display—spot-wobble modulation) this tends to be a rather laborious and skilled task.

(d) As already seen, a further consequence of the dead-reckoning colour selection is the great sensitivity of the display to the effects of magnetic fields, and the display cannot be rotated far without readjustment.

### (3) APPRAISAL OF PICTURE QUALITY

An attempt is made here to assess the quality of the pictures produced on the banana display with the electronic and mechanical operating conditions which have been achieved in the laboratory at this stage in the investigation.

#### (3.1) Brightness

Although virtually all the gun current in the banana tube (unlike the shadowmask tube) falls on the phosphors, there are a number of factors limiting the brightness of the banana pictures. In the first place there is a demagnification of the triplet image in the frame direction by about 5 : 1 so that the phosphor stripes must be wider by this factor than the required width in the final image. This involves a corresponding increase in beam current to obtain a given brightness. Other limiting factors are, of course, the peak current available from the gun, the acceptable loss of resolution on high-lights due to spot-size increase, the current saturation, if any, of the phosphors and the mean current available from the e.h.t. generator.

Measurements on the present tubes show that, at an e.h.t. of 25 kV, highlight brightnesses of 25–30 ft-L are obtainable. This requires a mean beam current of the order of 400  $\mu$ A on average picture material, a figure which compares favourably with that for current shadowmask tubes.

#### (3.2) Contrast and Resistance to Effects of Ambient Light

The potential inherent contrast range is extremely high. In practice it is difficult to ensure perfect 'blacks' owing to several effects. The tin-oxide coating and the internal blackened metal



shield may reflect some of the intense light produced by areas of the phosphor stripes subjected to high instantaneous beam currents. Reflection also occurs from the lens surfaces inside the drum, and the inevitable accumulation of dust on the tube and lens rods causes appreciable scatter which in the final image manifests itself as a form of horizontal streaking in the neighbourhood of high-lights. In practice the resultant contrast ratio is still very good, being of the order of 40 : 1 under typical conditions.

Another importance feature of a display device that must be considered is its performance in the presence of high levels of ambient light. This is particularly important for colour-picture display as dilution of the picture by ambient light produces not only a loss of brightness contrast but also a more disturbing desaturation of the colours.

In this aspect the banana system has a distinct advantage over direct-view displays. The picture is viewed as a virtual image which is seen against a black background determined by the low-reflectivity exterior of the lens drum. The amount of ambient light returned to the viewer's eye is thus small, and the display therefore retains its good contrast and colour saturation under very high levels of ambient light.

Table 3 gives a typical comparison of the behaviour of the banana and shadowmask tubes under ambient light.

Table 3

COMPARISON OF BANANA AND SHADOWMASK TUBE CONTRAST RATIOS

Ambient light	Banana tube	Shadowmask tube
Nil	40 : 1	25 : 1
4 ft-L (100 W lamp at 6 ft from display)	32 : 1	7 : 1
16 ft-L (100 W lamp at 3 ft from display)	19 : 1	4 : 1

Contrast range measured on black and peak-white squares of test card C gamma wedge for an initial high-light brightness of 25 ft-L.

Ambient light measured as brightness of a vertical white card at front of display unit.

### (3.3) Resolution

The acceptability, or otherwise, of the resolution in a colour picture is very much a subjective matter, and there is in any case little available information to enable accurate determination of the relationship between spot size and subjective resolution. However, it is possible to make some general comments on this aspect of the banana display.

It can be shown that if the stripe triplet can be made wider than the value determined from the final desired raster and the demagnification, the tracking tolerance and therefore the colour purity are improved. In addition, some overlap of the stripes in the field of view helps to reduce line visibility in picture areas of pure saturated primary colours. For these reasons a 50% overlap of successive triplets in the image has been chosen. This will inevitably result in some loss of vertical resolution, but this does not appear to be significantly large.

The horizontal resolution will be limited by the spot size and effects associated with the rate of sequential colour selection adopted. The requirements of high brightness, simple electron optics and small spot size are necessarily conflicting. The spot size must therefore be the result of a compromise.

The convenient choice of the 2.66 Mc/s sub-carrier frequency for spot wobble also limits the resolution. A 2.66 Mc/s interlaced dot structure will be visible everywhere in the picture and higher-frequency information will be attenuated. Furthermore,

luminance information having a frequency near that of the sub-carrier will lead to unpleasant low-frequency coloured patterns which will tend to obscure any remaining high-frequency resolution.

The resolution at present obtained is probably inadequate for domestic use with the 405-line standard.

### (3.4) Colour Fidelity and White-Field Uniformity

The factors determining colour fidelity have been discussed by Jackson.<sup>6</sup> It has been shown that the effect of spot size may not be serious. Errors arising as a result of self-decoding and the use of an incorrect green phosphor can be appreciably reduced at the cost of circuit complexity. The errors likely in a domestic receiver will therefore depend upon the circuits finally chosen, which will involve a compromise between circuit simplicity and fidelity of colour reproduction.

Associated with these effects, the ability of the device to produce a satisfactory and uniform white must be considered. The precision of tube operation necessary to achieve this has been discussed (Section 2.2.1), and it will be clear that this is likely to be a difficult requirement to satisfy in a domestic receiver.

### (3.5) Image Registration

Owing to the side-by-side arrangement of the three phosphor stripes in the tube the image of the wobbled triplet in the final picture will be seen as three adjacent horizontal coloured lines for each scanning line. The visibility of these lines as separate images is, of course, appreciably reduced by the optical demagnification of the system, and also by the 50% overlap mentioned earlier. However, single horizontal white lines in the picture still have apparent coloured edges. The visibility of this 'fringing' is dependent upon the phosphor stripe configuration. For example, if blue is chosen as the centre stripe, only 11% of the luminance is emitted by this stripe; most of the luminance will be emitted by the outer stripes and horizontal white lines will have distinct red and green edges. This fringing effect is a minimum for a central green stripe, and this configuration has been adopted for the experimental tubes although it limits somewhat the choice of self-decoding techniques.

The third alternative of a red central stripe does not appear to offer much scope with self-decoding, unless complete signal recoding is employed.

For verticals, registration is dependent primarily upon the nature of the spot wobble. If the video signal consists of a pattern of very small white spots (of duration less than one cycle of spot wobble), the reproduced spots will be coloured according to the spot-wobble phase at the time of the video-signal pulse. The result will be a reproduced pattern of spots of different colours. This colouring effect is still evident on lower-definition signals, so that vertical edges have coloured fringes, the colour depending upon the position in the raster. This fringing of verticals can be appreciably exaggerated if the spot-wobble is 'tilted' with respect to the triplet.

There is a further cause of colour fringing of verticals which occurs for off-axis viewing and which is a fundamental feature of the optical system. As the drum rotates the optical path lengths from the screen in the tube to the observer vary in a slightly different way for the three phosphor stripes. Each stripe will generate a flat picture plane which is substantially coincident with those of the two other stripes. The largest deviation (approximately 2 mm) occurs at the top and bottom of the picture where the screen is viewed at an oblique angle. An observer looking at the picture from a central position will not notice this effect, but some parallax will be discernible with off-axis viewing.



### (3.6) Miscellaneous Features

#### (3.6.1) Afterglow.

The phosphor-afterglow requirements have already been explained,<sup>8</sup> and of the colour phosphors at present available the afterglow of the green is still not satisfactory.

#### (3.6.2) Scratch Flicker.

Surface scratches on the lens rods produce very unpleasant flickering shapes in a plane in front of the picture. Special care is necessary to obtain lenses of sufficiently high quality.

#### (3.6.3) Mechanical Noise.

The use of a mechanical field-scan system for a domestic receiver inevitably raises the problem of noise. Work by Lowden has done much to reduce the noise level of the present experimental display, particularly from bearings, and most of the residual noise is probably due to air disturbance by the lens rods. However, although a surprisingly low noise level is now possible, further investigation is needed for a domestic receiver.

#### (3.6.4) Dust.

It has already been pointed out that the accumulation of dust on the lens rods results in a loss of contrast. Moreover, the accumulation of dust, particularly where moving parts are involved, is very undesirable. Experience with projection receivers indicates that, at the e.h.t. voltage involved, steps must be taken to minimize the accumulation of dust.

### (3.7) Presentation

Whereas direct-view displays have very wide angles of view (an excess of 100° in the vertical and horizontal planes), the angle of view of the banana display is limited in comparison. This is due to the fact that the picture is viewed as a virtual image which appears to be situated some distance behind the mirror. In the horizontal plane the viewing angle is thus limited by the side edges of the mirror (or any surrounding box, which will cause a further restriction). In the vertical plane the viewing angle is limited by the top and bottom edges of the mirror. The present maximum total horizontal angle of view at large distances without any loss of any part of the picture is about 44°, and similarly the total vertical angle of view is about 5°. These figures correspond to an area 1 ft 2 in high by 7 ft 9 in wide at a viewing distance of 8 ft from the bottom of the mirror.

For this viewing angle to be achieved the picture size must be less than the viewing aperture. For example, for the present display the viewing angle figures given above are for a picture 2 in high by 16 in wide which is viewed in a mirror with a projected size of 15 × 27½ in. This in turn is mounted on top of a cabinet measuring approximately 30 × 34 in. The picture is thus small in comparison with the overall dimensions of the display, and this effect must be exaggerated slightly by the fact that the picture is a virtual image located about 12 in behind the bottom edge of the mirror. The extent to which this effect is acceptable is a matter for individual taste.

The banana display has a distinct advantage as regards depth from front to back (an aspect that is now important in monochrome practice) as it has a front-to-back dimension in the region of the drum of only about 12 in, which is less than half of that possible for a shadowmask receiver and is comparable with present monochrome practice.

The picture presented by the banana-tube display is inherently square-cornered and the aspect ratio can readily be chosen to be correct. It is likely, therefore, that the picture shape of a banana-tube receiver would conform to the transmission standards.

In the experimental models a 30 × 40 cm raster has been chosen. This renders picture detail at the same size as the popular 17 in picture tube. The picture area is, of course, considerably greater than for a 17 in tube.

### (3.8) Stability

If the banana-tube display is to have any chance of success it must exhibit adequate stability of operation over periods of at least several hundred hours, for a wide range of mains supply voltages and ambient temperatures, and while subject to repeated switching on and off. The present experimental models have not been satisfactory in this respect. The general use of fully stabilized power supplies (excluding valve heaters and motor supply) and reasonably refined circuit techniques in the experimental equipment has failed to give adequate stability.

The stability of the phosphor colour and efficiency also needs to be considered. It is certain that phosphor efficiency will change with temperature and during life. At present there is inadequate experience to indicate how serious the effects will be, but the phosphor operating conditions are very much more rigorous than in a direct-view tube. Furthermore, any local variation in phosphor performance will appear as a vertical feature of the picture, and this again sets a limit on the variations which can be tolerated.

### (4) COST

The cost of production is a key factor in the assessment of any display device for use in a domestic colour-television receiver. As mentioned by Schagen,<sup>7</sup> the banana concept initially offered a reasonable chance of providing a receiver competitive in price with a receiver incorporating a shadowmask tube. The investigation of the system has permitted increasingly accurate estimates of the cost to be made and they have confirmed this initial impression. However, the two television receivers being compared are complex, hardly any of the major components are common and neither is sufficiently developed in Europe to have established production techniques. In these circumstances the accuracy of the best cost comparison is not high, say ±15–20% for each figure.

With this reservation the latest cost comparison can be given as follows:

Table model, 21 in, monochrome—current techniques	100 units
Banana consolette—techniques which can be visualized for use in the immediate future	272 units
Banana consolette—techniques visualized as possible optimum	224 units
Shadowmask consolette—current techniques	307 units

No attempt has been made here to visualize the optimum techniques of the future for building a shadowmask receiver and the effect they would have on the cost price.

Perhaps the most important fact which arises from this study of costs is the following. The cost of the shadowmask-tube receiver or the banana-tube receiver is likely to be over twice that of the corresponding black-and-white receiver, even taking into account anticipated development of the colour receivers.

### (5) CONCLUSIONS

It is appropriate to enumerate and assess the most significant features of the banana-tube system in order to judge it in relation to other known devices and as a solution to the problem of colour television.

The banana-tube receiver fulfils two of the essential requirements of modern television viewing to an extent that cannot be



matched by a receiver based on any other known display device.

First, the picture may be viewed in a room having normal lighting; with other devices almost complete darkness is necessary to achieve good contrast and colour saturation.

Second, the cabinet may be very shallow and therefore meet the demand which has dominated the post-war development of the television receiver.

Furthermore, the banana system could meet, in principle, the stringent reverse-compatibility requirements of producing a good black-and-white picture by using a separate white-phosphor stripe as described elsewhere.<sup>3</sup>

The light, small and simple colour tube is one of the most attractive features of the banana concept.<sup>8</sup> As well as its effect on the cost of a receiver it has a number of subsidiary advantages over the more cumbersome direct-view tubes, including ease of handling and storage.

A comparison has been made which showed the estimated cost of a banana-tube receiver to be somewhat less than that for a shadowmask receiver. If this were to be substantiated it would be a fact of the greatest importance.

While the initial cost is of prime importance, the cost of maintenance must also be considered. Tube replacement and the subsequent adjustment of the receiver will be a major factor. It is well known that the adjustment associated with a shadowmask tube is much more complex than that associated with a black-and-white tube. At present the adjustment following the insertion of a new banana tube requires a similar degree of skill and experience and occupies a similar length of time. However, the banana tube itself should be much cheaper than a shadowmask tube and will be very much easier to handle.

Against this must be offset the probable need for regular attention to the mechanical and optical parts of the receiver. Furthermore, in certain respects, the operating conditions of the banana tube are likely to be more stringent than the corresponding conditions in the shadowmask tube, and more frequent replacement may be necessary. It would seem unwise to assume that the banana-tube receiver would be significantly cheaper to maintain.

Any discussion on the acceptability of the unconventional features of the banana system, particularly the cabinet styling, must inevitably introduce personal opinion and be indecisive. The following important factors must be considered.

The limited number of observers who have seen laboratory demonstrations certainly did not object to the virtual image, while the flatness and squareness of the picture were considered to be clear advantages. On the other hand, the limited viewing angle will undoubtedly be a disadvantage in domestic viewing conditions.

The special problems of the mechanical and optical parts of the system, namely noise, jitter, flicker, dust accumulation and duration of reliable performance, would appear to be soluble

in the laboratory. The investigation has not proceeded far enough to establish whether or not these problems can be solved for a mass-produced domestic receiver.

Some limitations of the picture quality have been discussed. Despite these limitations, pictures giving an overall satisfactory impression and comparable with those of a shadowmask tube are produced. Further development to improve both the resolution and the brightness is desirable in order to give a margin which would allow for the spread of performance inherent in mass-production and domestic use.

The stability of performance of a colour-display device is of fundamental importance. In this respect there are three features of the banana-tube system in its present form which are unsatisfactory. They are the stringent tolerances which arise from the method of colour selection, the susceptibility to magnetic fields and the phosphor performance. Any further development of the system must be concerned with these features.

#### (6) ACKNOWLEDGMENTS

The authors are indebted to Mr. H. A. Lambert for preparing the cost estimates.

Acknowledgment is due to those colleagues concerned with the investigation, including Mr. T. Jacobs and Mr. N. I. Richards, who made important contributions in the early stages.

The authors also wish to thank the Director of Mullard Research Laboratories and the Directors of Mullard Ltd. for permission to publish the paper.

#### (7) REFERENCES

- (1) RICHARDS, N. D.: 'The Design of a Mechanical Frame Timing Base for a Television Display System', (Mullard Research Laboratories Report No. 2231; June 1959).
- (2) HOWDEN, H.: 'Mechanical and Manufacturing Aspects of the Banana-Tube Colour-Television Display System' (see page 596).
- (3) FREEMAN, K. G.: 'Circuits for the Banana-Tube Colour-Television Display System' (see page 604).
- (4) FREEMAN, K. G.: 'Operating Tolerances for the Banana-Tube Colour-Television Display System' (Mullard Research Laboratories Report No. 2230; June 1959).
- (5) FREEMAN, K. G.: 'The Effect of the Earth's Magnetic Field on the Banana Colour-Television Display System' (Mullard Research Laboratories Technical Note No. 340; April 1959).
- (6) JACKSON, R. N.: 'Colorimetry of the Banana-Tube Colour-Television Display System' (see page 613).
- (7) SCHAGEN, P.: 'The Banana-Tube Display System: a New Approach to the Display of Colour-Television Pictures' (see page 577).
- (8) EASTWELL, B. A., and SCHAGEN, P.: 'Development of the Banana Tube' (see page 587).

### DISCUSSION ON THE ABOVE SIX PAPERS BEFORE THE ELECTRONICS AND COMMUNICATIONS SECTION, 15TH MAY, 1961

**Mr. A. V. Lord:** Dr. Schagen has compared the relative brightness obtained from shadow-mask and banana-tube displays. Presumably, his figures for the shadow-mask display refer to an older form of tube; the latest version is reported to give a brightness of 40 ft-L for a total beam current of 1.6 mA. Will he compare the relative merits of the latest shadow-mask and banana displays with regard to brightness and beam current?

Dr. Schagen and Mr. Eastwell describe the sulphide phosphors used in the banana tube. These have chromaticities similar to those used in the latest shadow-mask tube; they also have short afterglow. It is perhaps unfortunate that, owing to the

50 fields/sec scanning standard, such colour displays will tend to show flicker at brightness levels above 20–25 ft-L. Perhaps their high-brightness potentialities may be only exploited fully on a 60 fields/sec standard where the flicker threshold is in the neighbourhood of 70 ft-L. The lower peak brightness and the relatively long afterglow of the phosphors used in the older type shadow-mask tube gave 50 fields/sec pictures remarkably free from flicker and interline effects.

Mr. Freeman discusses signal processing for the banana display in terms of the N.T.S.C. form of colour signal. Does he agree that the S.E.C.A.M. form of signal would demand greater



circuit complexity? One feature of the S.E.C.A.M. system, claimed by its proponents, is that the complete composite signal may be applied to the tube; there is no need to 'notch out' the chrominance by means of a band-stop filter. One-gun displays, such as the banana system, are likely to suffer from difficulties due to beats between the colour-switching wave and high-frequency signal and noise components. Such beats would be more pronounced if variable-frequency chrominance signals of the S.E.C.A.M. type were applied to the tube.

Mr. Jackson does not favour changing the specification of the transmitted signal in order to suit the synthesis primaries of a particular display device. If, however, the vast majority of colour displays were to employ the all-sulphide phosphor trio, should a change in the transmission parameters then be considered?

Acoustic noise from the mechanical field-scan system is analysed in Mr. Howden's paper. How does the noise level due to the drum compare with that experienced from conventional television receivers where loudspeaker hum and the vibrations of transformer laminations are often audible?

Messrs. Freeman and Overton's appraisal of the banana system shows a critical and realistic attitude. Have developments made since the submission of their paper resulted in any improvements which might modify their conclusions significantly?

**Mr. L. C. Jesty:** The tube is potentially so cheap that its cost would be a fraction of that of a shadow-mask tube. Therefore it might be worth making it a little more complicated and expensive if by this means considerable savings could be achieved in other directions, the object being to make the complete receiver cheap. With this in mind, would it help if the neck, instead of being coaxial with the banana part, was tipped up to one corner? It would still come conveniently outside the lens drum. One would have to put in an ion trap, but it might simplify the present rather complicated beam bending and scanning. Then there is the question of guiding the spot along the phosphor triad. One might use index stripes in the structure of the screen. This could help with the difficult beam-guidance problem.

Have the authors considered the feasibility of this development for a very cheap colour receiver? A colour-television receiver must give good colour, but it might be possible with this system to sacrifice certain features such as picture size, brightness, viewing angle, etc., if this led to a worthwhile reduction in cost. By this means one could provide a colour receiver which is not in the luxury market, and this would help materially in launching a colour-television service.

**Mr. W. Buchanan:** In the advantages which are claimed for the tube and the philosophy of design, it appears that we are to make as cheap a tube as possible so that the circuits—or, in this case, mechanical equipments—which are permanent or can be repaired, will take the major part of the cost. Will the authors comment on whether the same amount of ingenuity should be applied to making a vacuum device with complications in it, designed so as to permit cheap reconditioning? The complications would be permanent in the tube and not part of the cathode, for instance, which will wear out. It is a very difficult question to answer but one which has to be given thought in proposing a philosophy of design for new systems.

I do not think too much emphasis should be placed on the attraction to the viewer of shallow cabinets. The present trend in this way, in monochrome, is largely a matter of circuit versus chassis and cabinet costs.

**Mr. C. A. Marshall:** What we have seen tonight is an excellent laboratory prototype, but the ultimate aim and object must be a television receiver. Can we, for a moment, imagine that a

few years have gone by and that the system is being considered for domestic television?

I cannot visualize mechanical scanning ever being accepted, in view of the great success of all-electronic scanning systems. With regard to the limit in angle of view (which I think is connected with the mirror), the public would be quite convinced that this was not really acceptable. They see their ordinary black-and-white picture on a nearly flat tube and over a very wide angle, so they are sure to make comparisons.

On the question of stability of operation, in Messrs. Freeman and Overton's paper there is a rather alarming paragraph which says, 'The general use of fully stabilized power supplies . . . and reasonably refined circuit techniques in the experimental equipment has failed to give adequate stability'. If this is the case, it is a serious limitation.

Mechanical noise, jitter, flicker and dust are still serious problems and all these factors tend to prejudice the system for use in domestic receivers unless some very significant changes occur. Although these problems could be solved, perhaps, in the laboratory prototype, one is tempted to ask how the system would then perform after a year's use in a dusty room.

Finally, bearing in mind that the scanning for the whole picture in any one colour occurs on one stripe of phosphor, what is the expected life of the phosphor?

**Mr. I. J. P. James:** Mr. Freeman has rather written down the colour-difference gating method of colour selection, which I should think would involve a gating frequency lower than that necessary with the full bandwidth gating. In addition, with gray-scale pictures the luminance signal would be the only one applied to the cathode-ray tube, since the colour-difference signals disappear. This will eliminate chopping of the gray-scale signals and improve the signal/noise ratio. Will the author comment?

On the question of single-gun versus 3-gun tubes, there is the matter of servicing the sets in the home. Does one need a complete television colour-bar waveform in order to set up the various controls? I do not think one needs this with an ordinary 3-gun shadow-mask tube receiver.

**Mr. A. Isaacs:** It would appear from the geometry of the tube that the line scan is basically non-linear. Is this non-linearity corrected by the built-in magnetic field or by the circuit design? If the tube is non-linear, will the proposed new type of tube improve its non-linearity?

Any colour receiver which is produced in the foreseeable future must be capable of displaying monochrome pictures which use existing studio techniques. These include synchronizing the field frequency to that of the mains, and also locking the field component of the mixed synchronizing waveform to that of an external mixed video signal, i.e. master-slaving (commonly called 'Sync-Lock' or 'Gen-Lock'). In the case of master-slaving there is a step change in field frequency of 0.25 c/s which may last for 8 sec on 405-line standard. Unless the field-lock system controls in less than a line period, the above change in frequency will produce a noticeable phase error in the field of the received picture.

**Dr. G. J. Phillips:** It would appear that a larger-diameter cylindrical lens would improve the picture brightness. If vertical registration of the three coloured images is the limitation, have the authors considered using a prism to improve the vertical registration?

**Mr. K. A. Russell (communicated):** It would seem possible for the banana tube to be used to advantage with a S.E.C.A.M.-type colour signal if the phosphors are scanned green/red, green/blue on successive lines with a duty cycle of 120°/240° respectively (the red and blue phosphor stripes would have to be wider than



the green stripe, of course). A delay line should not be necessary if the red and blue phosphors produced sufficient light for two lines each time they were scanned.

It is appreciated that such a method might make it impossible to use a truly constant luminance signal, but will the authors comment on it and say if such a scheme has been considered by them?

Details of the spot-wobble deflection system were not given, but it may be deduced that a single deflection coil is employed in the display systems demonstrated and described.

Have the authors considered using a double-deflection system consisting of a magnetic yoke with its ends at either end of the main line-deflection coil, so that the magnetic fields crossing the neck of the tube are in opposite directions? This should cause the electron beam to be deflected when it passes the first limb of the yoke and to be deflected back on to a parallel track on passing the second limb of the yoke. This system might simplify the tracking of the electron beams down the phosphor stripes and get over some of the problems concerned with modulating the spot-wobble amplitude.

## THE AUTHORS' REPLIES TO THE ABOVE DISCUSSION

**Dr. P. Schagen** (*in reply*): *To Mr. Lord.*—The comparison of relative brightness obtained with shadow-mask and banana-tube displays was indeed based on the published data for an earlier shadow-mask tube and measurements with one of the early banana tubes. The latest version of the shadow-mask tube is reported to give a brightness of 40 ft-L for a total beam current of 1.6 mA. Measurements of a recent banana tube yield approximately the same figure.

I agree that the American 60 fields/sec standard allows these higher brightness potentialities to be more fully exploited. With the European standard of 50 fields/sec the older phosphors with their longer afterglow were more advantageous in this respect. On the other hand, the high efficiencies of the sulphide phosphors do provide the opportunity to improve the resistance of the shadow-mask tube to ambient illumination by employing a more strongly absorbing grey filter in front of the tube.

*To Mr. Jesty.*—Mr. Jesty suggested that it might be worth while making the banana tube a little more complicated in order to ease the beam bending and guiding problems. This is, in fact, the approach which we had in mind when we referred to the principle of 'positive guidance'. Recent laboratory experiments have indicated that it is possible to achieve a much better tracking of the beam along the phosphor stripes with the aid of electrostatic fields inside the tube. This makes, in addition, the permanent magnetic deflecting field superfluous and provides good focusing. The spot wobble is in this case generated by an h.f. alternating potential on deflection plates along the length of the screen, which no longer requires amplitude modulation at line frequency.

Placing the neck of the tube at an angle to the main envelope would not materially ease the electron optical problems.

*To Dr. Phillips.*—Dr. Phillips's suggestion, to bring the virtual images of the three colour lines closer together with the aid of a prism in order to enable the use of lens rods with larger diameter, is not easily applicable to the banana tube since the screen is viewed from the scanned side. With the mallet tube, on the other hand, it has been suggested to superimpose the images of the three lines completely by the use of narrow dichroic mirrors.

**Mr. B. Eastwell** (*in reply*): *To Mr. Buchanan.*—Already considerable ingenuity has gone into making colour-display vacuum devices. Apart from the banana tube, all these devices involve considerable technological complications which account for the high cost of the more conventional display tubes. Further complications to enable complete reconditioning to be an easy possibility would increase cost still further, not only because of the basic cost of the additional features, but also owing to the higher reject rates which would result during tube processing.

*To Mr. Marshall.*—At present the life of the banana-tube phosphors is considerably shorter than that of the phosphors in the shadow-mask tube, where it is no problem. However, it

has already been established that the type of screen processing employed when depositing the phosphors on an aluminium substrate plays a vital role in their life properties. In addition it is known that the vacuum in the banana tube is between one and two orders less than could be achieved with improved pumping schedules. Thus, at present the phosphors are subjected to considerable ion bombardment. Both these aspects are to be investigated more fully. In addition, work is to be carried out on the basic properties of the phosphors. Their target life is 2 000 h.

**Mr. B. R. Overton** (*in reply*): *To Mr. Jesty.*—We have not to any great extent considered the feasibility of the banana system for a very cheap colour receiver. It is probable that, to make any appreciable reduction in the cost, it would be necessary to make such large sacrifices in the quality and presentation of the pictures that the end-result would not be acceptable.

*To Mr. Buchanan.*—The fact that recent developments in tube manufacture and circuits have permitted the production of shallow cabinets does not alter the fact that shallow cabinets have considerable attraction for the viewer, particularly now there is such a premium on living space. However, at the moment any possible colour receiver will have a total volume of the order of 8 ft<sup>3</sup> and what the banana system gains in shallowness it must lose in width. There are thus a number of pros and cons regarding cabinet size and shape, which we have enumerated in the appraisal paper, but which, in the last resort must be a matter of individual taste.

*To Mr. Marshall.*—At the start of this project the objections Mr. Marshall states were well appreciated. It was felt that, if the problem of colour-television reception (a cheap, reliable receiver giving a good-quality picture) could be completely solved in this novel manner, prejudice against mechanical or optical systems would not matter. We are now describing the work carried out, explaining both what we have achieved and the difficulties encountered. It is in the light of this information that the system should be assessed for further development.

**Mr. H. Howden** (*in reply*): *To Mr. Marshall.*—The main purpose of this investigation to date has been to construct a machine which will assist in the development of the banana-tube system and enable it to be demonstrated. No attempts have been made at this stage to eliminate the dust problem, other than to substitute glass lenses for the earlier plastic lenses. It will be necessary in any final receiver to provide some protection for the high-potential tube envelope and the rotating-lens drum, e.g. by enclosing them within a reasonably dust-tight envelope containing a glass window. Accumulated dust on the exposed viewing surfaces could then be removed by normal domestic methods, and the device would then, in this respect, be similar to a conventional receiver.

*To Mr. Lord.*—On the subject of acoustic noise from the field scan mechanism, measurements taken on the prototype in an



ambient laboratory background of 43 dB with the meter 6 ft from the receiver are:

<i>Black and white 17 in receiver</i>	<i>Banana-tube receiver</i>
45 dB	Drum alone, 46 dB
	Drum plus time-base, 47 dB

**Mr. K. G. Freeman (in reply):** In reply to Messrs. Lord's and Russell's points about the possible use of the S.E.C.A.M. or a similar system with the banana tube, we have not given much consideration to this: unlike the N.T.S.C. system it does not appear to lend itself at all readily to self-decoding techniques with single-gun tubes. I therefore agree that the S.E.C.A.M. form of signal would demand greater circuit complexity, and also that the noise and beating effects would be worse, particularly in the variant of the system where frequency modulation of the chrominance sub-carrier occurs.

Mr. Russell's proposals are interesting, but I cannot see how they would work. The use of red, green and blue primary phosphors means that only light of these colours can be stored by the afterglow, whereas for the S.E.C.A.M. system it is required to store colour-difference signals. The general conclusion is that the S.E.C.A.M. type of system is not suitable for a good-quality domestic single-gun display.

Taking Mr. Lord's last point, in so far as the conclusion of the appraisal paper is that the banana system in its present form is not a feasible basis for a domestic receiver, any developments since the papers were written cannot affect that conclusion. In fact, of course, proposed improvements, such as the introduction of positive guidance into the tube, would go a long way towards eliminating the stringent electrical tolerances which make the present system untenable, but then the system would differ appreciably from that described.

However, many of the other features which give cause for concern, namely mechanical reliability, phosphor life, dust accumulation, flicker etc., would still have to be dealt with. Furthermore, attention would still have to be paid to designing tuned amplifiers of adequate stability for the self-decoding circuits, as these are at least in part responsible for the lack of stability under laboratory conditions, a feature to which Mr. Marshall drew attention.

There is some ambiguity in Mr. James's question about the use of colour-difference gating, as the gating frequency is of necessity determined by the rate of colour selection. I assume that he meant that with colour-difference gating it would be possible to reduce the bandwidth of the gating circuit (i.e. to increase the rise time) since errors in the colour-difference gating will only affect colour rendition, and with this I agree. In practice, some degradation of bandwidth may be permissible and the grey-scale rendering could be better than with  $R, G, B$  gating. As I have shown in Reference 8 of the circuit paper, however,  $R - Y, G - Y, B - Y$  colour-difference gating necessitates a signal-handling capacity of  $1.87 Y$  in the  $B - Y$  channel. The use of an  $M$ -luminance signal reduces this requirement to  $1.33 M$ , but there is then the complication of deriving the  $M$  signal.

With regard to the signal/noise ratio, I again agree that colour-difference gating will result in an improvement (particularly in desaturated areas of the picture) and this should also apply to the beating effects mentioned by Mr. Lord. There is little doubt that these effects are the result of intermodulation between the beam-current gating and the noise and luminance information in the region of the gating frequency. A reduction in the amount of gating will therefore reduce these effects, as would the use of a higher gating frequency. However, important as all these points are, I am sure Mr. James will share my opinion that signal gating is neither an economically nor philosophically

appropriate way to use a single-gun colour tube in a domestic receiver.

As regards the servicing requirements in the home, we must therefore endeavour to compare a self-decoding banana receiver with a 3-gun shadow-mask receiver. I do not agree that for the latter a composite video colour-bar signal is entirely unnecessary, as it is possible to think of faults in the automatic phase-control circuit or the synchronous detectors which would be very difficult to put right without one. For a self-decoding banana receiver there would also be several channels requiring critical adjustment of relative phases (e.g. in the present modulated tripler there are three such channels), which could not be easily done on ordinary colour-picture material. It is therefore reasonable to assume that the test signal would be even more necessary.

In reply to Mr. Isaacs, the non-linearity of line scan which arises as a result of the geometry of the tube is partly corrected by the magnetic field of the 'tram-lines' and partly by the circuits (and design of the deflector coil). However, as will be seen from the circuit paper, the line-scan current waveform finally required is not unduly non-linear. The proposed tube using positive guidance is not likely to make much difference to the line-scan current requirements.

On the question of the effect of step changes in field frequency, as encountered in master-slaving etc., I am now inclined to agree that this will be a difficult problem with a mechanical field-scan system. I have performed the experiment of switching suddenly from mains lock (49.8 c/s at the time) to sub-carrier lock (50 c/s), and on the present display this produces a transient displacement of the raster by about 50 lines lasting about 1 sec. Although it is known that the holding and catching performance of the present drum synchronization is not the best we have achieved, the magnitude of the effect observed is sufficient to indicate that it might be very difficult indeed to reduce it to an insignificant level.

With regard to the query from Mr. Russell about the method of spot-wobble, there is a fairly detailed description in Section 2.5 of the circuit paper, and it will be seen that in the demonstration apparatus one pair of coils was used.

The suggestion of using a double deflection for spot-wobble (with coils before and after the line coils) is interesting and was at one time considered. However, very elaborate screening was necessary to avoid pick-up in the line coils as this causes the spot to perform most peculiar gyrations on its way along the stripes. Even with the present system, with one pair of coils before the line coils, some slight aberrations occur, no doubt because the electron beam does not pass through the centre of the line coils at every instant. As the positive-guidance type of tube offers a more attractive way of overcoming the tracking and spot-wobble modulation difficulties connected with the present dead-reckoning method of colour selection, the spot-wobble problem of the latter has not been pursued.

**Mr. R. N. Jackson (in reply):** To Mr. Lord.—I do not, in general, consider that the specification of the transmitted signal should be changed to suit new developments in the display device unless these developments offer some really significant advantage which may be used. Whereas it may be desirable to change the standard if the result is to provide a signal which, when fully exploited, would be capable of giving better pictures, it is certainly not desirable to lower the potential system performance in order to satisfy a current technological situation which may in any case be only of a transitory nature. Applying this dictum to the present case of the sulphide colour phosphors, I would say that the restriction of colour gamut represents a degradation of the potential system performance and that it would be unwise to alter the system to suit.

## DISCUSSION ON 'TELEVISION BAND COMPRESSION BY CONTOUR INTERPOLATION'\*

**Prof. M. P. Beddoes** (*Canada: communicated*): Some points were made in Section 2 which are in error.

It is stated that a limitation to the Cherry-Gouriet<sup>D</sup> slope-feedback coding method is instability in the feedback loop, which limits the maximum scanning velocity ratio to 3 : 1. Instability can be encountered as the velocity ratio is increased; but in our experiments with a variable-velocity magnetic scanner<sup>E</sup> in the feedback loop, scanning velocity ratios as high as 20 : 1 were obtained. Higher ratios were not attempted because wastage in the circuit, produced by heavy damping, became excessive.

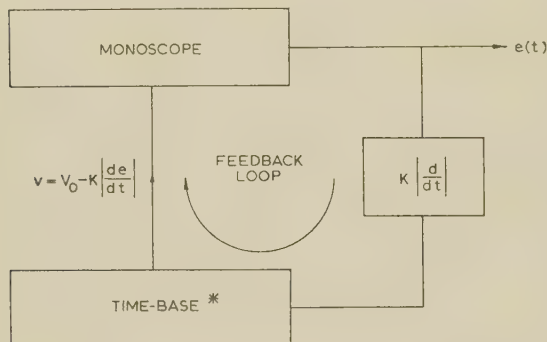


Fig. A.—Block diagram of slope-feedback coder.

\* A variable-velocity magnetic scanner was used in the experiments.

Arising from the previous point, we might well ask, What is the main limitation to the Cherry-Gouriet coder? The answer has been given in a recent paper,<sup>F</sup> where it is shown that the main limitation is that the coder does not remove all the high frequency components. Consequently, on passing the coded signal through a channel with reduced bandwidth such components are suppressed. Amplitude distortion of the received signal results, and this leads to spatial errors. The errors have been shown to be extremely noticeable and they cannot be compensated for.

The work of Schroter<sup>G,H</sup> and that of Cherry-Gouriet were grouped together. This is misleading because Schroter's method exploits picture-to-picture correlation, whereas the Cherry-Gouriet method exploits point-to-point correlation along a scanning line. The two methods are only similar in that they are both examples of linear prediction.<sup>I</sup>

The main theme of the Gabor-Hill paper—the use of interpolation to reduce the bandwidth so that existing methods for compressing along a line can be used too—seems to be very

good: the principal disadvantage will be that a considerable amount of apparatus is required at the receiver.

It is reported that Gouriet 'proposed to measure the "picture detail" by the square of the rate of amplitude change'. This should read, '... the modulus of the rate of amplitude change'.

**Prof. D. Gabor and Dr. P. C. J. Hill** (*in reply*): Prof. Beddoes' own work, to which he refers, was carried out in this department under the supervision of Prof. E. C. Cherry, and we are in a position to correct his statements on the basis of information kindly supplied by Prof. Cherry.

Prof. Beddoes may be unaware that Prof. Cherry and his colleagues have continued research work into television compression, operating at the full scanning rate and picture quality according to the British standards. Prof. Cherry confirms that a velocity ratio of 3 : 1 is about the practical limit; ratios greater than this lead to instability. The ratio of 20 : 1, to which Prof. Beddoes refers, may relate to his own earlier work; his paper<sup>F</sup> deals with his own low-speed system (100 lines, 20 frames/sec). The conditions pertaining to a full-speed system are much more stringent.

Again, Prof. Beddoes states that a spatial distortion of the picture is inherent in the Cherry-Gouriet system. It is not; it appears only if the receiver-spot-position control signal is derived from the spot-velocity signal by integration, but it does not appear if a separate 'position signal' is transmitted.

Prof. Beddoes states that the main limitation to the Cherry-Gouriet system is that it does not remove all the high-frequency components. In more recent work (yet unpublished) Prof. Cherry and his colleagues use systems of detail detection which discriminate against noise and enable the high-frequency components of the signal to be included in the coding process.

The work of Schroter and that of Cherry-Gouriet are indeed related, inasmuch as both use non-uniform scanning velocities.

### REFERENCES

- (D) CHERRY, E. C., and GOURIET, G. G.: 'Some Possibilities in the Compression of Television Signals by Recoding', *Proceedings I.E.E.*, Paper No. 1401 R, January, 1957 (100, Part III, p. 9).
- (E) BEDDOES, M. P.: 'A Variable-Velocity Scanner for Magnetic Deflection of a Scanning Spot', *ibid.*, Monograph No. 241 R, June, 1957 (104 C, p. 481).
- (F) BEDDOES, M. P.: 'Experiments with a Slope-Feedback Coder for Television Compression', *I.R.E. Transactions on Broadcasting*, March, 1961, BC-7, p. 12.
- (G) SCHROTER, F.: 'Speicherempfang und Differenzbild Fernsehen', *Archiv der Elektrischen Übertragung*, 1953, 7, p. 1.
- (H) SCHROTER, F.: 'Fernsehen und Moderne Informations-Theorie', *ibid.*, 1955, 9, p. 1.
- (I) HARRISON, C. W.: 'Experiments with Linear Prediction in Television', *Bell System Technical Journal*, 1952, 31, p. 7.

\* GABOR, D., and HILL, P. C. J.: Paper No. 3507 E, May, 1961 (see 108 B, pp. 303 and 360).



# THE PREDICTION OF AERIAL RADIATION PATTERNS FROM NEAR-FIELD MEASUREMENTS

By JOHN BROWN, D.Sc.(Eng.), Associate Member, and E. V. JULL, B.Sc., Ph.D.

(The paper was first received 8th March, and in revised form 1st May, 1961.)

## SUMMARY

A new method is described of predicting an aerial radiation pattern from near-field measurements. The essence of this method is the expansion of the radiated field in terms of a series of radially expanding modes. The amplitude and phase of each mode are calculated by a Fourier analysis of the measured near field, and the radiation pattern obtained as a Fourier series containing these measured amplitudes and phases. The theory is described in detail for a cylindrical (2-dimensional) aerial, and experimental results are presented to confirm the validity of this theory. The way in which the method may be extended to 3-dimensional aerials is explained. The method has the advantage that it can be applied anywhere in the near field.

## LIST OF SYMBOLS

- $\lambda$  = Free-space wavelength.  
 $\beta$  = Free-space phase-change coefficient ( $=2\pi/\lambda$ ).  
 $a$  = Radius of cylinder containing aerial = half the length of the aerial aperture.  
 $b$  = Radius of cylinder on which measurements are made.  
 $r, \theta, z$  = Cylindrical co-ordinates.  
 $H_n^{(2)}(x)$  = Hankel function of order  $n$  and argument  $x$ .  
 $a_n$  = Complex amplitude of  $n$ th radial mode.  
 $c_n(b)$  = Response constants (see Section 3.2).  
 $b_n = 2a_n c_n(b)$ .  
 $s = \sin \phi$ .  
 $F_r(\phi)$  or  $F_r(\phi)$  = Radiation pattern of receiving aerial.  
 $P(\theta)$  = Measured pattern using a receiving aerial moving round the cylinder of radius  $b$ .  
 $E_z$  =  $z$ -component of electric field.  
 $\rho$  = Radius of cylinder, used in the analysis of Section 8.  
 $x', y', \xi, \eta$  = Co-ordinates used in Section 8 and defined by Fig. 8.  
 $B_r$  = Half-power beam width of the receiving aerial.

## (1) INTRODUCTION

Accurate measurements of the radiation pattern of an aerial can be obtained only at distances of the order of the Rayleigh range or greater.<sup>1</sup> For an aerial with an aperture of maximum dimension  $2a$  the Rayleigh range can be taken as  $4a^2/\lambda$ , where  $\lambda$  is the operating wavelength, and for large antennae it becomes so large that the provision of a suitable test site is a major problem. Attempts have been made to overcome this problem by developing computational techniques by which patterns measured in the near field, i.e. at distances less than the Rayleigh range, may be corrected to give the far-field pattern. These methods have so far relied on the use of asymptotic expansions of the radiated field: the first term of the expansion is the far-field pattern, and the remaining terms give the difference between the far-field and near-field patterns.<sup>2,3</sup> These difference terms involve derivatives of the field patterns, and this leads to difficulties

in achieving sufficient accuracy in measuring the near-field pattern. An alternative procedure is to measure the field distribution in the aperture of the aerial and to use the Fourier transform relation between the aperture distribution and the radiation pattern. This method also has limitations, which become more pronounced if the antenna is designed for low side-lobe levels; these limitations are discussed in Section 5.

The proposals discussed in the present paper are based on an alternative approach in which the radiated field is expressed as a sum of modes. The discussion is restricted to 2-dimensional problems, but the method can be extended to three dimensions as explained in Section 5. The modes used are the radially expanding fields which would arise in a radial transmission line, and the essential feature of the method is that the amplitudes and phases of these modes are deduced from measurements at any convenient distance from the antenna. These amplitudes and phases specify the radiated field completely and can therefore be used to calculate the far-field radiation pattern. In principle, there is no restriction on the distance at which the measurements can be made, and a feature of the method is that there is no distinction between what are usually regarded as near-field measurements and the measurement of the aperture distribution. Previous methods for correcting near-field patterns to give true radiation patterns have been restricted, by the approximations used, to the use of measurements made at appreciable distances from the aerial.

## (2) EXPANSION OF THE RADIATED FIELD IN TERMS OF MODES

We suppose that the aerial and its associated feed lie entirely within a cylinder of radius  $a$ , and that the polarization is such that it gives  $E_z$  as the only component of electric field. Cylindrical polar co-ordinates  $r, \theta, z$  are used. Outside  $r = a$  there are no sources of radiation, and a general solution of Maxwell's equations satisfying the radiation condition at infinity is

$$E_z(r, \theta) = \sum_{n=-\infty}^{\infty} a_n H_n^{(2)}(\beta r) \exp(jn\theta) \quad (1)$$

Since we are concerned with a two-dimensional problem, there is no dependence on the co-ordinate  $z$ . The time-dependent factor  $\exp(j\omega t)$  is suppressed.

The origin of the co-ordinate system is obviously the centre of the cylinder  $r = a$  and lies within the region occupied by the aerial. The only restriction on this cylinder is that it should contain the aerial, and so the position of the origin with respect to the aerial is not specified precisely. The effect of this on the results is considered below.

The radiation pattern of the aerial is the variation of the magnitude of  $E_z$  with direction  $\theta$  in the limit as  $r$  tends to infinity. The leading term of the asymptotic expansion of the Hankel function is

$$H_n(\beta r) \simeq \left(\frac{2}{\pi\beta r}\right)^{1/2} \exp\left\{-j\left[\beta r - \frac{(2n+1)\pi}{4}\right]\right\} \quad (3)$$

Written contributions on papers published without being read at meetings are invited for consideration with a view to publication.  
 Dr. Brown and Dr. Jull are in the Department of Electrical Engineering, University College, London.

so that, for very large values of  $r$ ,

$$E_z(r, \theta) \simeq \left(\frac{2}{\pi\beta r}\right)^{1/2} \exp\left[-j\left(\beta r - \frac{\pi}{4}\right)\right] \sum_{n=-\infty}^{\infty} a_n \exp\left(jn\theta + \frac{jn\pi}{2}\right) \quad (4)$$

The radiation pattern can thus be expressed as

$$F(\theta) = \sum_{n=-\infty}^{\infty} a_n \exp\left[jn\left(\theta + \frac{\pi}{2}\right)\right] \quad (5)$$

The function  $F(\theta)$  is complex and gives phase as well as amplitude information. In practice, the radiation pattern is usually only quoted in amplitude, so that  $|F(\theta)|$  will suffice.

The effect of the choice of the origin of co-ordinates can be determined very simply in the limiting case of large values of  $r$ . Suppose that a change is made from  $O$  to  $O'$  as in Fig. 1, and

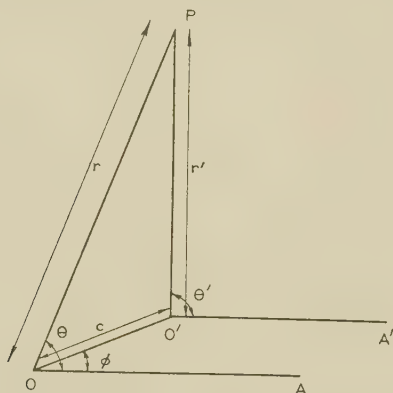


Fig. 1.—Effect of a change in the origin of the cylindrical co-ordinate system.

that the co-ordinates measured from  $O'$  are  $r', \theta'$ . The new origin,  $O'$ , will be in the region occupied by the aerial, so that the separation,  $OO'$ , cannot exceed  $a$ . From the geometry of the diagram we have

$$r' = [r^2 + c^2 - 2rc \cos(\theta - \phi)]^{1/2} \quad (6)$$

where  $c$  is the distance  $OO'$ , and

$$\frac{\sin \theta}{r} = \frac{\sin \theta'}{r'} + \frac{c \sin \phi}{rr'} \quad (7)$$

if the axes  $OA$  and  $O'A'$  are assumed parallel.

As we are concerned with the limit as  $r$  tends to infinity, we have

$$r' \simeq r - c \cos(\theta - \phi) + O(1/r) \quad (8)$$

$$\theta' \simeq \theta + O(1/r) \quad (9)$$

Inserting these results in eqn. (4), and neglecting terms which are of the order of  $1/r$ , we have

$$E_z(r', \theta') = \left(\frac{2}{\pi\beta r'}\right)^{1/2} \exp\left[-j\left(\beta r' + \beta c \cos(\theta' - \phi) - \frac{\pi}{4}\right)\right] \sum_{n=-\infty}^{\infty} a_n \exp\left(jn\theta' + \frac{jn\pi}{2}\right) \quad (10)$$

so that the radiation pattern in the new co-ordinate system is

$$F'(\theta) = \exp[-j\beta c \cos(\theta - \phi)] \sum_{n=-\infty}^{\infty} a_n \exp\left(jn\theta + \frac{jn\pi}{2}\right) \quad (11)$$

$\theta$  and  $\theta'$  being equal to the order considered. Hence,

$$F'(\theta) = \exp[-j\beta c \cos(\theta - \phi)] F(\theta) \quad (12)$$

and the radiation patterns differ only in phase. In practice, phase is not considered, the patterns are identical, and this confirms that the choice of the centre of the bounding cylinder  $r = a$ , is unimportant.

### (3) DETERMINATION OF THE MODE AMPLITUDES

#### (3.1) Field Measurements

Suppose that the electric field is measured in amplitude and phase for points lying on the cylinder  $r = b$ . Then

$$E_z(b, \theta) = \sum_{n=-\infty}^{\infty} a_n H_n^{(2)}(\beta b) \exp(jn\theta) \quad (13)$$

where  $E_z(b, \theta)$  gives the amplitude and phase as deduced from the measurements. Eqn. (13) can be regarded as a Fourier series and the unknown amplitudes,  $a_n$ , are therefore given by

$$a_n H_n^{(2)}(\beta b) = \frac{1}{2\pi} \int_0^{2\pi} E_z(b, \theta) \exp(-jn\theta) d\theta \quad (14)$$

The Hankel function on the left-hand side of eqn. (14) can be obtained from tables or calculated, and so each amplitude can be obtained in terms of known or measured quantities. The calculated amplitudes can be inserted in eqn. (5) to give the far-field radiation pattern.

Measurements of the electric field can be made, using a suitable probe.

#### (3.2) Measurements using a Receiving Aerial

In practical antenna measurements a probe is seldom used as it gives inadequate sensitivity; instead, a suitable antenna is employed, aligned with its direction of maximum reception towards the antenna under test. It has been predicted previously<sup>4</sup> that the results so obtained are dependent on the size of this receiving aerial if measurements are made in the near field, and experiments have confirmed these predictions.<sup>5</sup> The present method is well suited for making allowances for these effects. The response of the receiving aerial to each of the radial modes depends on its radiation pattern and on the distance from the origin at which the measurements are made. If the aerial is allowed to move round the circle of radius  $b$  which is illuminated by the  $n$ th mode,

$$E_n(r, \theta) = H_n^{(2)}(\beta r) \exp(jn\theta) \quad (15)$$

the output from the aerial is

$$g_n(\theta) = c_n(b) \exp(jn\theta) \quad (16)$$

The most significant feature of this result is that the angular variation,  $\exp(jn\theta)$ , is identical with that of the incident field given by eqn. (15). This result, which materially simplifies the later analysis, can be predicted from the facts that, on the circle  $r = b$ , the only variation of the incident field is in phase, and this phase variation is linear with the angle. The response constant,  $c_n(b)$ , can be calculated by a modification to an analysis previously used to verify the reciprocity theorem,<sup>6</sup> and details of the calculation are given in Section 8. This calculation confirms the form of eqn. (16) and gives the following expression for  $c_n(b)$ :

$$c_n(b) = j^n \int_{-\infty}^{\infty} F_r(s) \exp(-j\beta b \cos \phi + jn\phi) \frac{ds}{\sqrt{(1-s^2)}} \quad (17)$$



here  $\phi = \sin^{-1}(s)$  and  $F_r(s)$  is a function defined by the radiation pattern of the receiving aerial.

If the incident field has the form of the expansion given in (13), then an application of the superposition theorem shows that the output of the receiving aerial will be

$$P(\theta) = \sum_{n=-\infty}^{\infty} a_n c_n(b) \exp(jn\theta) \quad . \quad . \quad (18)$$

We therefore have

$$a_n c_n(b) = \frac{1}{2\pi} \int_0^{2\pi} P(\theta) \exp(-jn\theta) d\theta \quad . \quad . \quad (19)$$

giving the amplitudes,  $a_n$ , in terms of the measured pattern,  $P(\theta)$ , and the response constants,  $c_n(b)$ .

A convenient method of calculating the constants  $c_n(b)$  is discussed in Sections 8.2 and 8.3, where it is shown that a suitable approximation to the pattern  $F_r(s)$  leads to an expression for  $c_n(b)$  in terms of a Hankel function. An asymptotic series is used to obtain numerical values of the Hankel function.

### (3.3) The Application of the Method

The measurements required for an application of the method described in the previous Sections can be obtained by straightforward techniques. The only difference from a conventional pattern measurement is that the phase must be measured as well as the amplitude. It should be noted that this is essential in any procedure designed to give far-field patterns from near-field measurements. Numerical methods for evaluating Fourier series from the experimental observations are well-established in other fields<sup>7</sup> and can be applied directly. The number of terms required in the Fourier expansion can be estimated from the dimensions of the aerial. Chu<sup>8</sup> has considered in detail the types of pattern that can be obtained from an aerial of given size and has shown that, unless the modes in the expansion are limited to values of  $n$  less than or equal to  $\beta a$ , the aerial will show the disadvantages of supergain. The dimension  $a$  is the radius of the smallest cylinder which completely surrounds the aerial.

Supergain aerials are subject to serious ohmic losses in the aerial structure, and their radiation properties are very sensitive to frequency. In practice, therefore, supergain aerials are seldom used, and we may safely conclude that the expansion of the radiated field for any practical aerial will not contain significant terms in the Fourier expansion for  $n$  greater than  $\beta a$ . A similar result, specifically proved for aperture aerials, has been given by Woodward and Lawson.<sup>9</sup> We therefore seek an expansion involving the  $(2\beta a + 1)$  terms running from  $-\beta a$  to  $+\beta a$ , and as the amplitude of each term is complex,  $2(2\beta a + 1)$  real numbers are required. At each observation point two quantities, amplitude and phase, are measured, and so the minimum number of observation points is  $(2\beta a + 1)$ . These should be distributed at equal intervals in the angular range  $0-2\pi$ . The radiation from a directive aerial is usually restricted to a finite range of angles so that in practice the number of observations may be much less than  $(2\beta a + 1)$ .

A better indication of the number required is given by considering the probable beam width of the aerial. For a constant-amplitude constant-phase distribution, the angular separation between the first two zeros is  $2 \sin^{-1}(\lambda/l)$ , where  $l$  is the length of the aperture. If  $l$  is much larger than  $\lambda$ , this separation is  $\lambda/l$  rad. Such an aerial could be contained within a radius of  $l$ , so that  $(\beta l + 1)$  observation points uniformly spaced should suffice. This gives an angular interval between points of approximately  $2\pi/\beta l$ , i.e.  $\lambda/l$ . We thus have the rather surprising result that the radiation pattern of the average aerial

can in principle be specified completely by making measurements at angular intervals approximately equal to the half-power beam width. This result is a corollary to that of Woodward and Lawson, who showed that an aerial of aperture length  $l$  can be used to give specified amplitude of radiation at points separated by the order of  $\lambda/l$  in angle.

The calculations require a knowledge of Hankel functions of various orders and argument  $\beta b$ . These functions are only tabulated for the first few orders, and in the numerical work involved in the present investigation an approximation given in Section 8.2 was used. This is sufficiently accurate for the purpose provided that the argument  $\beta b$  is appreciably larger than the order. We have seen above that the largest order we need consider is  $\beta a$ , and so the approximation can be used provided that the distance  $b$  at which the measurements are made is appreciably greater than  $a$ . The only situation in which the use of the asymptotic series would present difficulties is that in which the measurements are made in close proximity to the aerial.

## (4) EXPERIMENTAL RESULTS

The experimental work described here was undertaken to confirm as far as possible the validity of the method described in the previous Section. The conditions under which the measurements were made did not allow accurate measurements of the far-field radiation patterns, and the procedure used was to compare the predictions of the far-field patterns obtained from two sets of measurements using receiving aerials of different sizes. The agreement obtained between these predicted results is considered to be within the limits of experimental error.

### (4.1) Apparatus

The measurements were made with a parallel-plate spectrometer which has been fully described previously.<sup>10</sup> It consists of two parallel circular plates separated by absorbing wedges round the circumference to maintain a spacing of  $\frac{3}{8}$  in. The general arrangement used is shown in Fig. 2. The aerial whose pattern is to be measured is placed at the centre of the spectrometer and the receiving aerial is free to move round the circumference. A reference signal is taken from the oscillator and combined with the output from the receiving aerial to enable measurements of amplitude and phase to be taken. The important parameters of the system are

Free-space wavelength ( $\lambda$ )	: 1.085 cm
Aperture of aerial under test ( $2a$ )	: 12.7 cm = 11.7 $\lambda$
Distance of receiving aerial ( $b$ )	: 54.1 cm = 49.9 $\lambda$
Aperture of receiving aerial:	
(i)	: 1.06 cm = 0.98 $\lambda$
(ii)	: 4.23 cm = 3.9 $\lambda$
(iii)	: 12.7 cm = 11.7 $\lambda$

We can see from these figures that the Rayleigh distance,  $4a^2/\lambda$ , is 149 cm, and that the measurements are being made at approximately one-third of this distance.

### (4.2) Results

The power patterns, as measured by the three receiving aerials, are shown in Fig. 3. These clearly demonstrate the effect on the side-lobe levels of changes in the size of the receiving aerial, and confirm that this size must be taken into account in any method of correction to obtain far-field patterns. Phase measurements were made with the 0.98  $\lambda$  and 11.7  $\lambda$  receiving aerials and show even more pronounced differences (Fig. 4). These measurements are used to express the measured patterns in the form (Section 3)

$$P(\theta) = \sum_n a_n c_n(b) \exp(jn\theta) \quad . \quad . \quad . \quad (20)$$

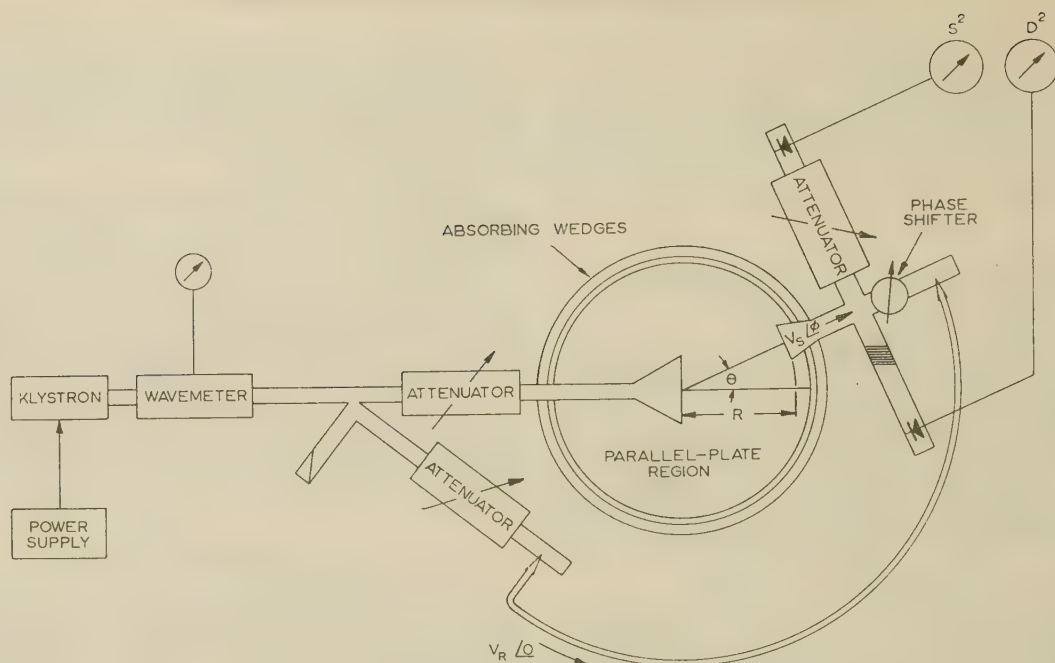


Fig. 2.—General arrangement for pattern measurements.

$$S^2 = V_S^2 + V_R^2 + 2V_S V_R \cos \phi$$

$$D^2 = V_S^2 + V_R^2 - 2V_S V_R \cos \phi$$

$V_S$  and  $V_R$  are the signal and reference levels shown.

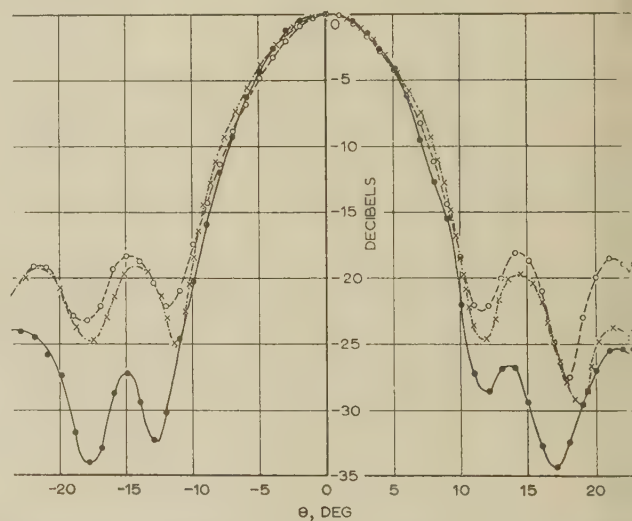
The patterns were considered sufficiently symmetrical with respect to  $\theta = 0$  for the series to be expressed in terms of cosine terms; this is equivalent to the assumption that  $a_n = a_{-n}$ . The result,  $c_n(b) = c_{-n}(b)$ , is evident from eqn. (17), provided that the receiving aerial is symmetrical about its axis. Hence, we write

$$P(\theta) = a_0 c_0(b) + 2 \sum_n a_n c_n(b) \cos(n\theta) \\ = \frac{1}{2} b_0 + \sum_n b_n \cos(n\theta) \quad \dots \quad (21)$$

The amplitude and phase measurements give the real and imaginary parts of  $P(\theta)$ , and a numerical Fourier analysis is carried out on each part to obtain each constant  $b_n$  in the form  $|b_n| \angle \phi_n$ . The values of these constants are shown in Table 1. From the discussion in Section 3.3, we expect the number of significant amplitudes to be  $\beta a$ , i.e.  $\pi \times 11.7$  or 37. This is in good agreement with the results given in the Table, where the amplitudes of the various coefficients drop quite markedly as  $n$  reaches values around 40.

The amplitudes,  $a_n$ , of the mode expansion can be extracted from the measured results provided that the response constants,  $c_n(b)$ , are known. These have been calculated from a suitable approximation to the integral in eqn. (18), which is derived in Section 8.2. Numerical values, normalized with respect to  $c_0(b)$  as only relative results are required, are also tabulated in Table 1. The values of  $a_n$  are also shown, and a graphical comparison of the results obtained from the two sets of measurements is given by Fig. 5. The theory of the method predicts that these two sets should be identical. Reasonable agreement is obtained for the amplitude terms, but the phases diverge for  $n > 30$ .

The consistency of the two sets is limited by the accuracy of the measurements, and with the apparatus used this was not very high, particularly in regard to the phase values. Further, the properties of the receiving aerials used in predicting the response constants were estimated from the aperture sizes, and further errors may have been introduced here. The measured patterns

Fig. 3.—Power patterns as measured at a radius of  $49.9\lambda$  using different receiving aerials.

Aperture of transmitting aerial:  $11.7\lambda$   
Aperture of receiving aerials:

○ — ○ — ○ :  $0.98\lambda$   
× — × — × :  $3.9\lambda$   
● — ● — ● :  $11.7\lambda$

were taken to be zero for angles outside the range  $-30^\circ$  to  $+30^\circ$  as the levels were too small to measure. In view of the uncertainties, the agreement between the two sets of results is regarded as confirming the theoretical analysis and as showing that the method is a useful technique for the correction of near-field measurements.

One interesting feature emerges from Fig. 5(b): the  $a_n$  values are approximately constant up to  $n = 30$ , where a divergence in the two sets of values shows that the accuracy has deteriorated. If the centre about which the measurements



Table 1  
COMPARISON OF RESULTS OBTAINED USING TWO RECEIVING AERIALS

n	Results using receiving aerial of $11.7\lambda$ aperture						Results using receiving aerial of $0.98\lambda$ aperture					
	$ b_n $	$\angle \phi_n$	$\left  \frac{c_n(b)}{c_0(b)} \right $	$\angle \theta_n$	$2 a_n $	$\angle \psi_n$	$ b_n $	$\angle \phi_n$	$\left  \frac{c_n(b)}{c_0(b)} \right $	$\angle \theta_n$	$2 a_n $	$\angle \psi_n$
0	0.545	20.5	1.000	0	0.545	20.5	0.625	21.5	1.000	0	0.625	21.5
1	0.525	18	0.999	0	0.525	18	0.610	21	1.000	-0.1	0.610	21
2	0.550	23	0.997	-0.2	0.550	23	0.605	24	1.000	-0.4	0.615	24.5
3	0.565	25	0.992	-0.5	0.570	25.5	0.605	26.5	1.000	-0.8	0.605	27.5
4	0.535	18.5	0.988	-0.9	0.540	19.5	0.555	24.5	1.000	-1.5	0.555	26
5	0.550	19	0.981	-1.4	0.560	20.5	0.565	23	1.000	-2.3	0.565	25.5
6	0.530	16.5	0.972	-2.0	0.545	18.5	0.555	20.5	1.000	-3.6	0.555	24
7	0.530	16.5	0.962	-2.7	0.550	19	0.555	21.5	1.000	-4.5	0.555	26
8	0.500	15.5	0.951	-3.5	0.525	19	0.555	19	0.999	-5.8	0.555	25
9	0.480	13.5	0.939	-4.5	0.510	18	0.515	17.5	0.999	-7.4	0.515	25
10	0.450	12	0.925	-5.5	0.485	17.5	0.490	16.5	0.999	-9.1	0.490	25.5
11	0.410	11	0.909	-6.7	0.450	17.5	0.475	14	0.999	-10.5	0.475	24.5
12	0.385	10.5	0.893	-7.9	0.430	18.5	0.450	11.5	0.999	-13.2	0.450	24.5
13	0.340	5	0.876	-9.3	0.390	14.5	0.395	9.5	0.999	-15.4	0.395	25
14	0.320	3.5	0.858	-10.8	0.370	14.5	0.370	7	0.998	-17.9	0.370	25
15	0.280	0	0.839	-12.4	0.335	12.5	0.340	2	0.998	-20.5	0.340	22.5
16	0.260	0	0.819	-14.2	0.320	14	0.305	-1	0.998	-23.3	0.305	22.5
17	0.240	-3.5	0.798	-16.0	0.290	12.5	0.285	-6	0.998	-26.4	0.285	20.5
18	0.230	-7	0.777	-17.9	0.295	11	0.285	-8	0.997	-29.5	0.285	21.5
19	0.225	-10.5	0.754	-20.0	0.3000	9.5	0.295	-10	0.997	-32.9	0.295	23
20	0.220	-16	0.731	-22.1	0.300	6	0.295	-15	0.997	-36.5	0.295	21.5
21	0.220	-21.5	0.709	-24.3	0.310	3	0.275	-24	0.996	-40.7	0.275	17
22	0.220	-24	0.685	-26.7	0.320	2.5	0.270	-26.5	0.996	-44.1	0.270	17.5
23	0.220	-26	0.661	-29.2	0.330	3	0.280	-28	0.995	-48.3	0.280	20.5
24	0.215	-28	0.638	-31.8	0.335	4	0.280	-32	0.995	-52.6	0.280	20.5
25	0.205	-31	0.614	-34.5	0.330	3.5	0.290	-36	0.995	-57.0	0.290	21
26	0.190	-33	0.590	-37.4	0.320	4.5	0.270	-43.5	0.994	-61.7	0.270	18
27	0.175	-34.5	0.566	-40.3	0.310	6	0.260	-50.5	0.994	-66.5	0.260	16
28	0.165	-39	0.542	-43.3	0.305	4.5	0.235	-56.5	0.993	-71.5	0.235	15
29	0.150	-43.5	0.519	-46.5	0.290	3	0.215	-65	0.993	-76.7	0.215	12
30	0.140	-45	0.496	-49.6	0.280	4.5	0.195	-75	0.992	-82.1	0.195	7
31	0.115	-52	0.472	-53.0	0.245	1	0.175	-90	0.992	-87.5	0.175	-2.5
32	0.105	-55	0.449	-56.5	0.235	1.5	0.165	-102.5	0.991	-93.2	0.165	-9.5
33	0.085	-59	0.427	-60.2	0.190	1	0.150	-117.5	0.991	-99.5	0.150	-18
34	0.075	-67	0.405	-63.9	0.185	-3	0.140	-129.5	0.990	-105.5	0.140	-24
35	0.070	-69	0.384	-67.7	0.180	-1	0.140	-142	0.990	-111.6	0.140	-30.5
36	0.065	-71.5	0.357	-71.6	0.180	0	0.125	-156.5	0.989	-118.0	0.125	-38
37	0.055	-68	0.343	-75.5	0.160	7.5	0.110	-166.5	0.988	-124.8	0.110	-41.5
38	0.045	-63.5	0.323	-79.6	0.140	16	0.090	-176.5	0.988	-131.7	0.090	-45
39	0.035	-56.5	0.304	-84.0	0.115	27.5	0.070	-184	0.987	-138.6	0.070	-45.5
40	0.030	-51.5	0.287	-88.3	0.105	37	0.050	-191	0.986	-146.0	0.050	-45
41	0.030	-45					0.025					
42	0.020	-45					0.025					
43	0.015	-45					0.020					

$$2a_n = b_n \frac{c_0(b)}{c_n(b)}$$

$$b_n = |b_n| \angle \phi_n; \frac{c_n(b)}{c_0(b)} = \left| \frac{c_n(b)}{c_0(b)} \right| \angle \theta_n; a_n = |a_n| \angle \psi_n$$

All angles are expressed in degrees.

made corresponds to the phase centre of the aerial, then the radiation pattern will be a real function and all the constants, will be real. This is consistent with a constant phase for each term, as this constant phase can be absorbed in a factor multiplying the whole expression. The consistency of the phases  $a_n$ , therefore, is an additional argument supporting the validity of the method.

## (5) DISCUSSION

The method described in this paper is similar in many respects to the plane-wave-spectrum approach introduced by Booker and Clemmow.<sup>11</sup> In each case, the complete radiation field is deduced from the values of either the tangential electric field or the tangential magnetic field on a single surface. The Booker-Clemmow method uses a plane surface and leads to

expressions for the total field in the form of Fourier integrals, whereas in this paper the surface is a cylinder and the total field is found as a Fourier series. The Booker-Clemmow method is invaluable for theoretical work and is used in Section 8 to derive certain of the results required for the present method, but it is less suited to the interpretation of experimental results. There are two reasons for this: first, the surface required is a plane of infinite extent, and it is impossible to measure the fields everywhere on this plane. Practical investigations must be restricted to a finite region of the selected plane, and this leads to uncertainties as to the effect of the remainder of the plane over which measurements are not made. The cylinder is a closed surface, so this difficulty does not arise if the present approach is used (the fields are assumed to be independent of the co-ordinate in the axial direction). Second, the application

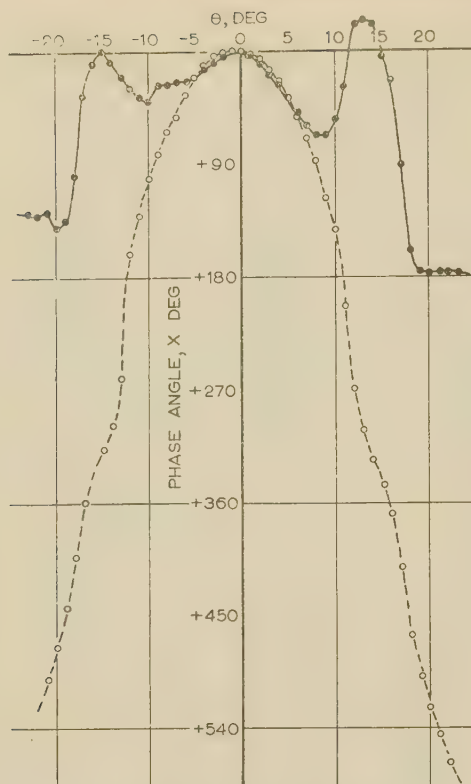


Fig. 4.—Measured phase patterns.

---○---○---○ :  $0.98\lambda$  receiving aerial.  
 —●—●—●—● :  $11.7\lambda$  receiving aerial.

of the Fourier integral to fields measured on a plane surface can provide the radiation pattern in only one hemisphere. The present method gives the complete radiation pattern, and this may be required, for example, if the aerial is designed specifically to have low values of radiation in the backward directions. Also, there is no difficulty involved in using the present method with aeriels giving coverage in all directions, whereas the Booker-Clemmow method is not suitable in such cases.

The theory developed in this paper makes no assumptions regarding the nature of the aerial other than that regarding the 2-dimensional nature of the radiation pattern. The extension to the more important practical case of 3-dimensional aeriels is discussed below. Although the experimental work was carried out on a microwave aerial, this is not intended to imply that the method is restricted to this part of the frequency spectrum. There is no obvious reason why the method should not be equally applicable to any type of aerial. The choice of aerial for the experimental work was made to enable the measurements to be carried out in a laboratory rather than out of doors and because suitable apparatus was available.

The major obstacle in using the technique described here is the computational effort required. This could be materially reduced if a standard site were used and measurements were made at a fixed distance with one receiving aerial. The response constants,  $c_n(b)$ , would then be fixed and need be calculated only once. Alternatively, they could be deduced from measurements on aeriels with known patterns. The Fourier analysis could be carried out on a digital computer. The calculations involved in the present work were made using a desk calculator, but this would not be feasible if large numbers of terms were required in the Fourier series.

It was pointed out in Section 1 that there is no distinction,

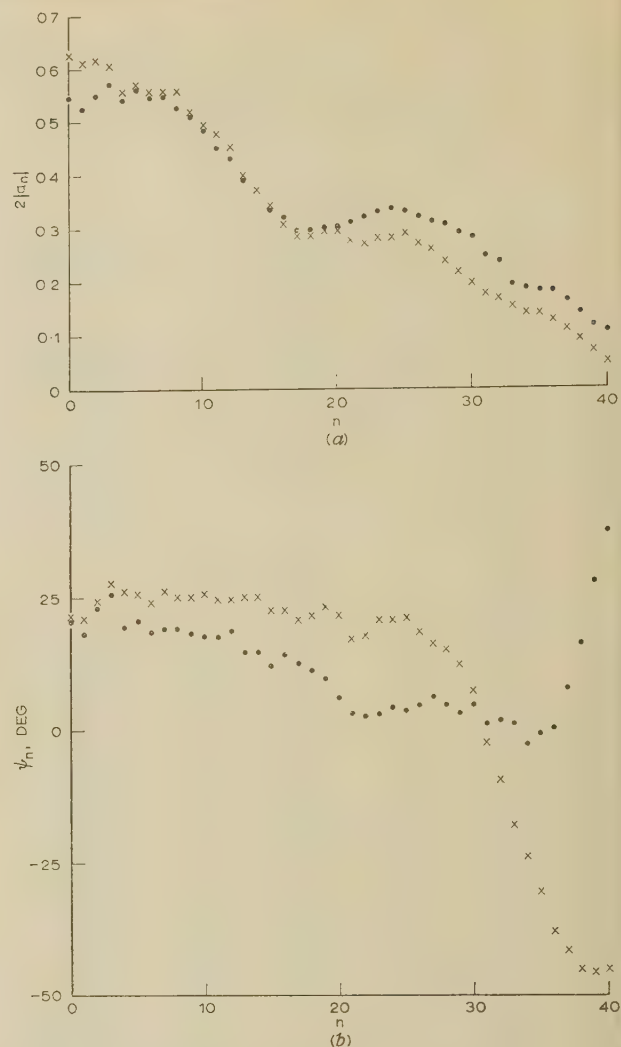


Fig. 5.—Fourier coefficients of the radiation patterns.

(a) Amplitudes,  $2|a_n|$ .  
 (b) Phases,  $\psi_n$ .

● Derived from measurements on the aerial with  $11.7\lambda$  aperture.  
 × Derived from measurements on the aerial with  $0.98\lambda$  aperture.

as far as the present method is concerned, between near-field measurements and measurements of the aperture field distribution. This is true in principle, but a practical difference arises as it is not possible to evaluate the Hankel functions required if measurements are made close to the cylinder  $r = a$  from the approximations used here. This difficulty could be overcome by tabulating these functions from the convergent series or from the recurrence relations.

The calculations given here apply only to cylindrical problems involving fields with an axial component of electric field. It is obvious that identical results would apply if the magnetic field were in the axial direction. An extension to 3-dimensional problems is possible in principle; the mode expansion would be in terms of spherical harmonics, and measurements made on the surface of a sphere would be used to give a double Fourier expansion. The amplitudes of this expansion could be corrected by the same type of argument as used in the present paper. In practice many large aeriels have a narrow horizontal and a much wider vertical pattern. An alternative procedure would then be to make measurements at a distance such that the vertical pattern was fully developed and to treat the horizontal pattern by the method described in this paper.



## (6) ACKNOWLEDGMENTS

The authors are indebted to Professor H. E. M. Barlow for facilities for carrying out this work. One of the authors (E. V. J.) is indebted to the Athlone Fellowship Committee and to the National Research Council of Canada for financial support during the period of the work.

## (7) REFERENCES

- CUTLER, C. C., KING, A. P., and KOCK, W. E.: 'Microwave Antenna Measurements', *Proceedings of the Institute of Radio Engineers*, 1947, **35**, p. 1462.
- BATES, R. H. T., and ELLIOTT, J.: 'The Determination of the True Side-Lobe Level of Long Broadside Arrays from Radiation Pattern Measurements Made in the Fresnel Region', *Proceedings I.E.E.*, Monograph No. 169 R, March, 1956 (**103 C**, p. 307).
- BICKMORE, R. W.: 'Fraunhofer Pattern Measurements in the Fresnel Region', *Canadian Journal of Physics*, 1957, **35**, p. 1290.
- BROWN, J.: 'A Theoretical Analysis of Some Errors in Aerial Measurements', *Proceedings I.E.E.*, Monograph No. 285 R, February, 1958 (**105 C**, p. 343).
- JULL, E. V.: 'The Prediction of Radiation Patterns from Near-Field Measurements', London University Ph.D. Thesis, July, 1960.
- BROWN, J.: 'A Generalized Form of the Aerial Reciprocity Theorem', *Proceedings I.E.E.*, Monograph No. 301 R, April, 1958 (**105 C**, p. 472).
- MANLEY, R. G.: 'Waveform Analysis' (Chapman and Hall, 1945).
- CHU, L. J.: 'Physical Limitations of Omni-Directional Aerials', *Journal of Applied Physics*, 1948, **19**, p. 1163.
- WOODWARD, P. M., and LAWSON, J. D.: 'The Theoretical Precision with which an Arbitrary Radiation-Pattern may be obtained from a Source of Finite Size', *Journal I.E.E.*, 1948, Part III, p. 363.
- SOLLOM, P. H., and BROWN, J.: 'A Centimetre-Wave Parallel-Plate Spectrometer', *ibid.*, Paper No. 2008 R, May, 1956 (**103 B**, p. 419).
- BOOKER, H. G., and CLEMMOW, P. C.: 'The Concept of an Angular Spectrum of Plane Waves, and its relation to that of Polar Diagram and Aperture Distribution', *ibid.*, Paper No. 922 R, January, 1950 (**97**, Part III, p. 11).

## (8) APPENDICES

## (8.1) Calculation of the Response Constants

We wish to determine the output from a receiving aerial which is illuminated by an incident field

$$E_z(r, \theta) = H_n^{(2)}(\beta r) \exp(jn\theta) \quad (22)$$

The receiving aerial is moved round the circle  $r = b$ , and the output is to be expressed as a function of position on this circle. At all positions, the aerial is oriented so that its direction of maximum reception is directed towards the origin, a typical position, shown in Fig. 6, being specified by the angle  $\theta_0$ . The properties of the aerial are completely specified by its radiation pattern, which can be used to determine the fields outside the aerial if it is supplied with power from a matched generator. The Lorentz reciprocity theorem is applied to the two sets of fields:

(a) Those existing when the aerial is illuminated by the field defined by eqn. (22).

(b) Those existing when the aerial is used as a transmitter, and is coupled by the feeder shown in Fig. 6 to a matched generator.

VOL. 108, PART B.

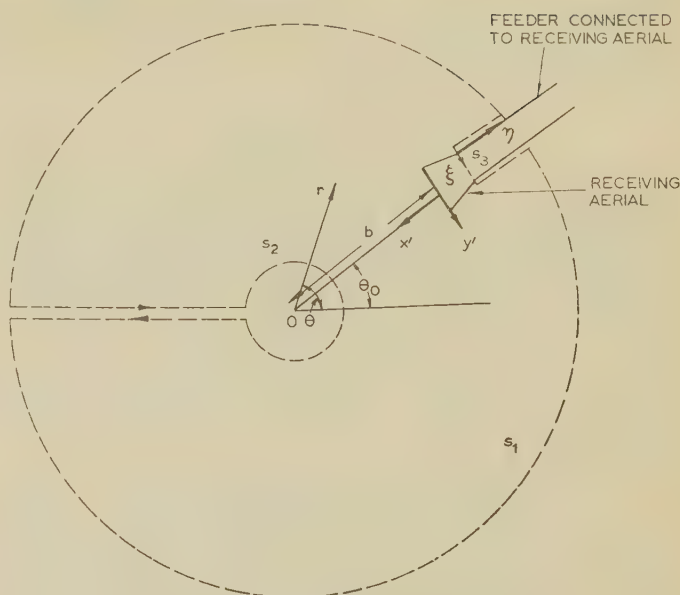


Fig. 6.—Geometry of the situation discussed in Section 8.1.

Since we are concerned with a 2-dimensional problem in which  $E_z$  is the only non-vanishing electric field component, we can write all fields in the form

$$\mathbf{E} = E_z \mathbf{i}_z \quad (23)$$

$$j\omega\mu\mathbf{H} = \mathbf{i}_z \times (\text{grad } E_z) \quad (24)$$

where  $E_z$  is a scalar function of the variables  $r, \theta$  (or any equivalent co-ordinates we may find convenient), and  $\mathbf{i}_z$  is a unit vector in the  $z$ -direction.

We will now detail the fields in the two conditions mentioned above:

(a) *Incident Radial Mode.*—We have in this case

(i) The incident field:  $E_{zi} = H_n^{(2)}(\beta r) \exp(jn\theta)$ . We note that  $E_{zi} = 0(r^{-1/2})$  as  $r \rightarrow \infty$ .

(ii) A field reradiated by the receiving aerial. This will be denoted  $E_{zir}$ , and the only property which we require is that  $E_{zir} = 0(r^{-1/2})$  as  $r \rightarrow \infty$ .

(iii) A wave in the feeder consisting of a single mode travelling from the aerial towards the termination which is assumed to be matched. Positions in the feeder will be denoted by the co-ordinates  $\xi, \eta$  shown in Fig. 6, and it follows from the behaviour of waveguide and transmission-line modes that this field must be of the form

$$E_{z \text{ rec}} = A\rho(\xi) \exp(-j\beta_m \eta) \quad (25)$$

where  $A$  is a complex amplitude constant,  $\rho(\xi)$  is a real function giving the transverse field distribution of the mode and is related to the power flow in the guide, and  $\beta_m$  is the phase constant of the mode.

This completes the specification of the field (a) as far as it is needed for the present problem.

(b) *Aerial used as a Transmitter.*—We have

(i) A single mode travelling from the generator to the aerial. For this mode

$$E_{zt} = \rho(\xi) \exp(j\beta_m \eta) \quad (26)$$

(ii) A radiated field,  $E_{zr}$ . This is most easily defined in terms of a plane-wave spectrum referred to the co-ordinates  $x', y'$  shown in Fig. 6, i.e.

$$E_{zr} = \int_{-\infty}^{\infty} F_r(s) \exp\{-j\beta[x'\sqrt{(1-s^2)} + y's]\} \frac{ds}{\sqrt{(1-s^2)}} \quad (27)$$

The function  $F_r(s)$  can be interpreted as the radiation pattern of the aerial when  $s$  is equal to  $\sin \phi$ ,  $\phi$  being measured from the  $x'$  axis.

Further, if  $b$  is finite,  $E_{zr} \rightarrow 0$  as  $r \rightarrow \infty$ . More precisely, we have  $E_{zr} = O(r^{-1/2})$  as  $r \rightarrow \infty$ .

The Lorentz theorem states that

$$\int_S (\mathbf{E}_a \times \mathbf{H}_b - \mathbf{E}_b \times \mathbf{H}_a) \cdot \mathbf{n} dS = 0 \quad (28)$$

where  $(\mathbf{E}_a, \mathbf{H}_a)$  and  $(\mathbf{E}_b, \mathbf{H}_b)$  are two solutions of Maxwell's equations satisfying all the boundary conditions.  $S$  is a closed surface and  $\mathbf{n}$  is a unit normal directed outwards from  $S$ . These two solutions will be taken as those discussed under (a) and (b) above. The fields can be written in the form given by eqns. (23) and (24), so that eqn. (28) becomes

$$\int_S [E_{az} \mathbf{i}_z \times (\mathbf{i}_z \times \text{grad } E_{bz}) - E_{bz} \mathbf{i}_z \times (\mathbf{i}_z \times \text{grad } E_{az})] \cdot \mathbf{n} dS = 0 \quad (29)$$

and this simplifies to

$$\int_S (E_{az} \text{grad } E_{bz} - E_{bz} \text{grad } E_{az}) \cdot \mathbf{n} dS = 0 \quad (30)$$

as each of the gradient terms is a vector which is perpendicular to  $\mathbf{i}_z$ .

The surface  $S$  will be chosen to be a cylinder with its axis parallel to the  $z$ -axis so that  $\mathbf{n}$  is also perpendicular to  $\mathbf{i}_z$ . We thus have

$$\int_S \left( E_{az} \frac{\partial E_{bz}}{\partial n} - E_{bz} \frac{\partial E_{az}}{\partial n} \right) dS = 0 \quad (31)$$

where  $\partial E_z / \partial n$  is the derivative of  $E_z$  with respect to the outward normal to  $S$ .

$S$  is now specified as shown in Fig. 6, and simple physical arguments show that the only possible contributions to the integral arise from

- $S_1$  : A cylinder of radius  $R$  centred on 0.
- $S_2$  : A cylinder of radius  $\rho$  centred on 0.
- $S_3$  : The cross-section,  $\eta = 0$ , in the feeder.

Further, as both  $E_{az}$  and  $E_{bz}$  tend to  $O(r^{-1/2})$  as  $r \rightarrow \infty$  and as differentiation with respect to  $n$  is equal to differentiation with respect to  $r$  on  $S_1$ , we see that the contribution from  $S_1$  also vanishes.

The integration over  $S_2$  is included to remove the singularity in  $E_z$  which exists as  $r \rightarrow 0$ . Inserting the appropriate expressions for  $E_{az}$  and  $E_{bz}$ , we have for this contribution

$$T_2 = - \int_{-\pi}^{\pi} \left[ (E_{zi} + E_{zir}) \left( -\frac{\partial E_{zr}}{\partial r} \right) - E_{zr} \left( -\frac{\partial E_{zi}}{\partial r} - \frac{\partial E_{zir}}{\partial r} \right) \right]_{r=\rho} \rho d\theta \quad (32)$$

In this integral, both  $E_{zir}$  and  $E_{zr}$  remain finite as  $r \rightarrow 0$ , and a non-vanishing contribution can therefore arise only from those terms involving  $E_{zi}$ . Hence

$$T_2 = \int_{-\pi}^{\pi} \left( E_{zi} \frac{\partial E_{zr}}{\partial r} - E_{zr} \frac{\partial E_{zi}}{\partial r} \right)_{r=\rho} \rho d\theta \quad (33)$$

In order to evaluate this integral we must express  $E_{zr}$  as a function of  $r, \theta$ . From the geometry of Fig. 6, we have

$$x' = b - r \cos(\theta - \theta_0) \quad (34)$$

$$y' = -r \sin(\theta - \theta_0) \quad (35)$$

Hence, substitution in eqn. (26) gives

$$E_{zr} = \int_{-\infty}^{\infty} F_r(s) \exp \left\{ -j\beta b \sqrt{1-s^2} + j\beta r [\sqrt{1-s^2} \cos(\theta - \theta_0) + s \sin(\theta - \theta_0)] \right\} \frac{ds}{\sqrt{1-s^2}} \quad (36)$$

Now  $s = \sin \phi$ , and  $\sqrt{1-s^2} = \cos \phi$ . Therefore

$$E_{zr} = \int_{-\infty}^{\infty} F_r(s) \exp \left[ -j\beta b \sqrt{1-s^2} + j\beta r \cos(\theta - \theta_0 - \phi) \right] \frac{ds}{\sqrt{1-s^2}} \quad (37)$$

and

$$\frac{\partial E_{zr}}{\partial r} = j\beta \int_{-\infty}^{\infty} F_r(s) \cos(\theta - \theta_0 - \phi) \exp \left[ -j\beta b \sqrt{1-s^2} + j\beta r \cos(\theta - \theta_0 - \phi) \right] \frac{ds}{\sqrt{1-s^2}} \quad (38)$$

Substitute these expressions in eqn. (33).

$$T_2 = \int_{-\pi}^{\pi} \left\{ j\beta H_n^{(2)}(\beta r) \int_{-\infty}^{\infty} \cos(\theta - \theta_0 - \phi) F_r(s) \exp \left[ -j\beta b \sqrt{1-s^2} + j\beta r \cos(\theta - \theta_0 - \phi) \right] \frac{ds}{\sqrt{1-s^2}} - \beta H_n^{(2)}(\beta r) \int_{-\infty}^{\infty} F_r(s) \exp \left[ -j\beta b \sqrt{1-s^2} + j\beta r \cos(\theta - \theta_0 - \phi) \right] \frac{ds}{\sqrt{1-s^2}} \right\}_{r=\rho} \exp(jn\theta) \rho d\theta \quad (39)$$

Reverse the order of the integrations.

$$T_2 = \beta \rho \int_{-\infty}^{\infty} \frac{F_r(s)}{\sqrt{1-s^2}} \exp(-j\beta b \sqrt{1-s^2}) \int_{-\pi}^{\pi} [jH_n^{(2)}(\beta \rho) \cos(\theta - \theta_0 - \phi) - H_n^{(2)'}(\beta \rho)] \exp[jn\theta + j\beta \rho \cos(\theta - \theta_0 - \phi)] d\theta ds \quad (40)$$

Now, by the integral definition of the Bessel function

$$\begin{aligned} & \int_{-\pi}^{\pi} \exp[jn\theta + j\beta \rho \cos(\theta - \theta_0 - \phi)] d\theta \\ &= \int_{-\pi}^{\pi} \exp[jn(\theta + \theta_0 + \phi) + j\beta \rho \cos \theta] d\theta \\ &= 2\pi(j)^n \exp[jn(\theta_0 + \phi)] J_n(\beta \rho) \end{aligned} \quad (41)$$

Also

$$\begin{aligned} & \int_{-\pi}^{\pi} \cos(\theta - \theta_0 - \phi) \exp[jn\theta + j\beta \rho \cos(\theta - \theta_0 - \phi)] d\theta \\ &= \int_{-\pi}^{\pi} \cos \theta \exp[jn(\theta + \theta_0 + \phi) + j\beta \rho \cos \theta] d\theta \\ &= -j \times 2\pi(j)^n \exp[jn(\theta_0 + \phi)] J_n'(\beta \rho) \end{aligned} \quad (42)$$

and hence

$$T_2 = 2\pi(j)^n \beta \rho \int_{-\infty}^{\infty} \frac{F_r(s)}{\sqrt{1-s^2}} \exp[-j\beta b \sqrt{1-s^2}] [H_n^{(2)}(\beta \rho) J_n'(\beta \rho) - H_n^{(2)'}(\beta \rho) J_n(\beta \rho)] \exp[jn(\theta_0 + \phi)] ds$$



$$H_n^{(2)}(\beta\rho)J_n'(\beta\rho) - H_n^{(2)'}(\beta\rho)J_n(\beta\rho) = \frac{2j}{\pi k\rho} \quad (44)$$

that

$$T_2 = 4(j)^{n+1} \int_{-\infty}^{\infty} \frac{F_r(s)}{\sqrt{(1-s^2)}} \exp[-j\beta b \sqrt{(1-s^2)} + jn\phi] ds \exp(jn\theta_0) \quad (45)$$

ally, we consider the integration over  $S_3$

$$\begin{aligned} &= - \int_0^{a'} \left\{ A\rho(\xi) \exp(-j\beta_m \eta) \frac{\partial}{\partial \eta} [\rho(\xi) \exp(j\beta_m \eta)] \right. \\ &\quad \left. - \rho(\xi) \exp(j\beta_m \eta) \frac{\partial}{\partial \eta} [A\rho(\xi) \exp(-j\beta_m \eta)] \right\}_{\eta=0} d\xi \\ &= -A \int_0^{a'} [j\beta_m \rho^2(\xi) + j\beta_m \rho^2(\xi)] d\xi \\ &= -2j\beta_m A \int_0^{a'} \rho^2(\xi) d\xi \quad (46) \end{aligned}$$

ere  $a'$  is the width of the feeder.

$\int_0^{a'} \rho^2(\xi) d\xi$  is a constant determined by the power input

en the aerial transmits. Since we are not concerned with

ollecting the results of the integrations and substituting into

$$T_2 + T_3 = 0$$

$$= 4(j)^n \exp(jn\theta_0) \int_{-\infty}^{\infty} \frac{F_r(s) \exp(-j\beta b \cos \phi + jn\phi)}{\sqrt{(1-s^2)}} ds \quad (47)$$

This equation gives the complex amplitude,  $A$ , of the signal

$$A = c_n(b) \exp(jn\theta) \quad (48)$$

ce we need no longer preserve the suffix on the angles, further, we are interested only in the way in which  $c_n(b)$  depends on  $n$  for a given aerial, and we can drop any constant factor which is equivalent to a change in the power flow considered for field  $b$ ]. Hence

$$c_n(b) = j^n \int_{-\infty}^{\infty} \frac{F_r(s) \exp(-j\beta b \cos \phi + jn\phi)}{\sqrt{(1-s^2)}} ds \quad (49)$$

constant, 4, being dropped as we are interested only in relative values.

## (8.2) Some Special Cases of the Response Constants

### (8.2.1) Omnidirectional Receiving Aerial.

The general expression for  $c_n(b)$  in eqn. (49) is difficult to evaluate exactly, and we consider some special cases chosen to respond to those likely to arise in practice. We first examine an omnidirectional receiving aerial as this should give results identical with the field measurements discussed in Section 3.1. For such an aerial  $F_r(s)$  is a constant which may be taken as unity, and so

$$c_n(b) = j^n \int_{-\infty}^{\infty} \frac{\exp(-j\beta b \cos \phi + jn\phi)}{\sqrt{(1-s^2)}} ds \quad (50)$$

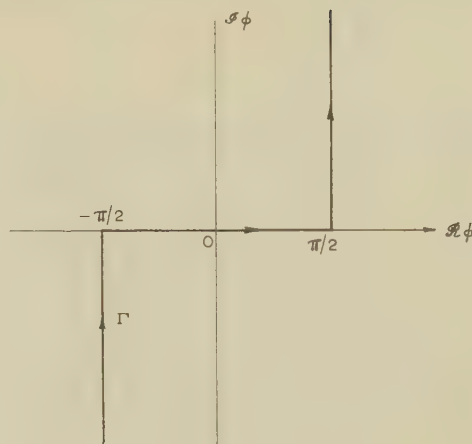


Fig. 7.—Integration contour used in Section 8.2.

The integration variable is changed to  $\phi$ , so that

$$c_n(b) = j^n \int_{\Gamma} \exp(-j\beta b \cos \phi + jn\phi) d\phi \quad (51)$$

$\Gamma$  being the contour shown in Fig. 7. The integral is the standard form for the Hankel function, i.e.

$$c_n(b) = \pi H_n^{(2)}(\beta b) \quad (52)$$

The output from an omnidirectional aerial moved round the circle  $r = b$  is thus

$$A = \pi H_n^{(2)}(\beta b) \exp(jn\theta) \quad (53)$$

and is therefore directly proportional to the incident field, as expected.

### (8.2.2) Approximate Result for Directive Receiving Aerial.

The response constant for a directive receiving aerial depends on the radiation pattern, as shown by eqn. (49). As we are concerned with relatively large values of  $\beta b$ , it is clear from the form of eqn. (49) that the only significant contributions to the integral will arise from values of  $\phi$  near zero, i.e. from plane waves which are incident from directions close to the maximum of the receiving pattern. It will therefore suffice to use for the pattern  $F_r(s)$  an approximation which is accurate for small values of  $s$ . The choice of a suitable approximation can be examined more conveniently if the integration variable in eqn. (49) is changed to  $\phi$  so that

$$c_n(b) = j^n \int_{\Gamma} F_r(\phi) \exp(-j\beta b \cos \phi + jn\phi) d\phi \quad (54)$$

where the integration contour,  $\Gamma$ , is shown in Fig. 7. We now approximate to the receiving pattern by the function

$$F_r(\phi) = \exp[-K(1 - \cos \phi)] \quad (55)$$

$K$  being a constant, expressed in terms of the half-power beam width,  $B_r$ , by the relation

$$K = \frac{\log_e 2}{2[1 - \cos(\frac{1}{2}B_r)]} \quad (56)$$

which ensures that

$$F_r(\pm \frac{1}{2}B_r) = 1/\sqrt{(2)}F_r(0)$$

The pattern defined by eqn. (55) has only one single lobe, but it does represent the shape of the major parts of the main lobes of practical patterns quite closely, as shown by Fig. 8.

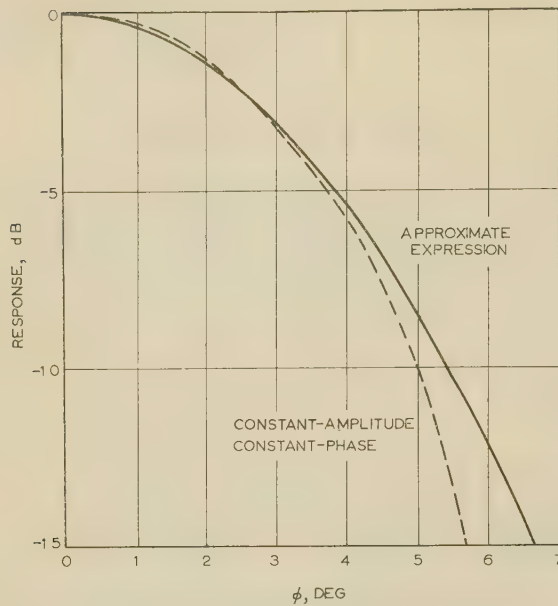


Fig. 8.—Comparison of the main lobes of radiation patterns.

— Approximate expression.  
 - - - Constant-amplitude constant-phase.

If the approximate pattern is used, we obtain

$$c_n(b) = j^n \int_{\Gamma} \exp [-K - j(\beta b + jK) \cos \phi + jn\phi] d\phi \quad (57)$$

and this can be expressed in terms of a Hankel function by using the integral representation given in eqn. (51). We thus have

$$c_n(b) = \pi \exp (-K) H_n^{(2)}(\beta b + jK) \quad (58)$$

It may be noted that this result reduces to that given in eqn. (51) when  $K$  is zero, i.e. when  $F_r(\phi)$  is independent of  $\phi$ .

In applications of this method we will usually be concerned with values of  $\beta b$  much larger than the highest value of  $n$  occurring in the mode expansion. Approximate expansions can then be used for the Hankel function. The one which is most convenient for the present purpose is

$$H_n^{(2)}(\rho) = \left(\frac{2}{\pi\rho}\right)^{1/2} \exp \left[ -j\left(\rho - \frac{n\pi}{2} - \frac{\pi}{4}\right) + \frac{n^2}{2\rho} + \frac{n^4}{24\rho^3} + \dots \right] \quad (59)$$

The terms which are omitted give negligible contributions in the numerical cases examined here. Since we are concerned with the relative magnitudes of the constants  $c_n(b)$ , it is convenient to evaluate the ratio  $c_n(b)/c_0(b)$ . Hence, from eqns. (58) and (59),

$$\begin{aligned} \frac{c_n(b)}{c_0(b)} &= \frac{H_n^{(2)}(\beta b + jK)}{H_0^{(2)}(\beta b + jK)} \\ &= \exp \left( \frac{jn\pi}{2} - \frac{jn^2}{2\rho} - \frac{jn^4}{24\rho^3} \dots \right) \end{aligned}$$

where  $\rho = \beta b + jK$ .

For the experimental results discussed in the paper we have

$$\begin{aligned} b &= 49.9; \beta b = 314 \\ \text{Aerial 1 : } B_r &= 5.95^\circ; K_1 = 258 \\ \text{Aerial 2 : } B_r &= 74.5^\circ; K_2 = 1.68 \end{aligned}$$

The effect of the term  $K_2$  is negligible except for a slight change in the amplitude of the terms with the highest values of  $n$ . The calculations for the first aerial require the term  $n^2/2\rho$  only, contributions from the term  $n^4/24\rho^3$  being negligible. The phase  $(n\pi/2)$  is dropped in the numerical work.



# A THEORY OF RECEIVING AERIALS APPLIED TO THE RERADIATION OF AN ELECTROMAGNETIC HORN

By D. MIDGLEY, B.Sc.(Eng.), Ph.D., Associate Member.

(The paper was first received 16th September, 1959, in revised form 6th March and in final form 31st May, 1961.)

## SUMMARY

Experimental and theoretical reradiation polar diagrams are compared for the  $H$ -plane of a rectangular pyramidal horn. A distinction is made between scattering, which is found to be due to the presence of higher modes, and reradiation, which is mainly responsible for the forward. The distinction applies to receiving aerials in general, and theory is presented in which every receiving aerial is regarded as a partial perfect absorber. The imperfection in normal operation is explained by the extent to which the incident field fails to correspond to the 'complementary' field that perfect absorption would require.

## LIST OF SYMBOLS

$E, E'$  = Electric field intensities, capable of co-existing.  
 $H, H'$  = Magnetic field intensities, capable of co-existing.  
 $\beta$  = Phase-change coefficient.  
 $\omega$  = Angular frequency.  
 $a, b$  = Aperture widths.  
 $u = \sin \theta/\lambda$ .  
 $\lambda$  = Wavelength.  
 $\theta$  = Azimuth angle from the outward normal to the aperture.  
 $\theta'$  = Azimuth angle from the inward normal to the aperture.  
 $D$  = Axial displacement.  
 $R$  = Radius of orbit (taken by measuring aerial).  
 $\mu, \epsilon$  = Permeability and permittivity of free space.  
 $P$  = Total power.  
 $f$  = A fraction.  
 $\mathbf{a}, \mathbf{c}, \mathbf{d}$  = Vectors.  
 $\eta$  = Intrinsic impedance of free space.

Prefixes	0 incident	$T$ transmitted
	$r$ reradiated	$R$ received by single path
	$s$ scattered	$R'$ received after return path
	$c$ complementary	

## (1) INTRODUCTION

Attention has been drawn to a lack of published information on the reradiation of receiving aerials.<sup>1,2</sup> A principal requirement is that some idea should be gained of the polar distribution of the reradiation. A few solutions of related diffraction problems exist for certain perfect shapes such as spheres, cylinders and semi-infinite planes. Among these the study of a plane wave incident upon a pair of semi-infinite planes is most closely related to the reradiation of an electromagnetic horn.<sup>3</sup> The class of diffraction problems for which such exact solutions exist does not yet appear to include shapes like a finite wedge, which could be substituted for an actual pyramidal horn. Approximate solutions are reported in Section 3 for the polar distribution of the reradiation from a particular horn. They are developed from a procedure suggested by Pippard, Burrell

and Cromie,<sup>1</sup> whereby the reradiation diagram is synthesized from contributions due to the higher modes, which exist only in the wider parts of the horn, when it is receiving.

Study of the horn problem induces more general thoughts on receiving aerials, which prompt the distinction of two parts in the reradiation. First there is the reradiation that would be inevitable even if the incident field were such as to give maximum absorption. This leads to conceptions of reversibility with electromagnetic radiation and of perfectly efficient complementary pairs of aerials. Then, there is the further reradiation or scattering occasioned by an arbitrary incident field, which excites the unwanted modes. This leads to a principle of field comparison for predicting the absorption of a receiving aerial, whatever the nature of the incident field. Attempts to support these ideas mathematically with the aid of the Lorentz reciprocity theorem are set forth in the Appendix. Brown<sup>4,5</sup> has given another development of that theorem for dealing with reception in a case where the incident field is not a uniform plane wave.

In Section 4, some aspects of the experimental problem of determining a reradiation diagram are discussed. A phase-reversal method is proposed for the forward area and a wave-interference method for the rear. Experimental and theoretical reradiation diagrams are compared, and experimental evidence of higher modes within the horn is given. The work is confined to the principal  $H$ -plane of the horn.

Although it is capable of extensions which could remove these restrictions, the theoretical discussion presupposes that operation is at a single frequency, that aerials are terminated on matched loads by single-mode feeders, and that no media other than free space and perfect conductors are involved.

## (2) THE REVERSIBILITY OF ELECTROMAGNETIC RADIATION AND COMPLEMENTARY PAIRS OF AERIALS

It is a consequence of the conjugate field theorem<sup>6</sup> that radiation may be regarded as a reversible process. If an ordinary aerial emits a certain outward travelling wave  $f(jkr - j\omega t)$ , it is at least possible to imagine a structure capable of returning a complementary wave  $f(jkr + j\omega t)$  of equal strength, in response to which the original aerial is a perfect absorber.

Therefore, let a complementary pair of aerials be defined as such that each absorbs all the radiation of the other. This implies that certain improbable and extensive structures are admitted to the class of aerials. For instance, one of many possible structures which are complementary to a dipole is a hollow conducting sphere with the dipole at its centre. The sphere requires an array of current elements with the correct strength and orientation in a layer approximately a quarter-wavelength from its inner surface.

Imagine the dipole to be replaced by a directional aerial and much of the outer sphere becomes redundant. But it is only at short ranges and optical frequencies that pairs of almost complementary radiators may be envisaged with both partners of identical or even similar shape.

Written contributions on papers published without being read at meetings are accepted for consideration with a view to publication.  
 D. Midgley is Reader in Electrical Engineering, Bradford Institute of Technology.

## (2.1) Absorption and Reradiation

A receiving aerial is the source of a reradiated field  $E_r$ ,  $H_r$ , which combines with the incident field  $E_0$ ,  $H_0$  to form the resultant  $E$ ,  $H$ :

$$E = E_0 + E_r \quad H = H_0 + H_r \quad \dots \quad (1)$$

This universally accepted definition of the reradiated field entails the paradoxical consequence that a perfect absorber must be considered to reradiate. Here, reradiation has the task of providing that destructive interference with the incident field without which there could be no absorption. The existence of the reradiated field, therefore, does not always necessitate the interpretation that power is lost from the system. In general, however, only part of the reradiated field is occupied in this way. The remainder is truly engaged in the process of scattering, often in a complex pattern arising from the excitation of higher modes of oscillation in the aerial.

Excitation of a receiving aerial by its complementary partner represents an ideal state in which the reradiation is, as it were, entirely concerned with absorption. The incident field is whatever remains when a receiving aerial is removed. Thus, in the example of the dipole and sphere, the unusual incident field left by removal of the dipole is a standing-wave system, such as occurs inside a resonant cavity. Reradiation from the dipole cancels the outward travelling components of the standing wave, leaving as resultant field only an inward travelling wave.

When there is arbitrary excitation, the performance of the receiving aerial deteriorates in that unwanted modes increase the reradiation, but so long as there is some absorption, a complementary component may be extracted from both incident and reradiated fields. Let this component of the reradiated field be designated  $E_{rc}$ ,  $H_{rc}$ , and that of the incident field,  $E_{0c}$ ,  $H_{0c}$ . The remaining components, designated  $E_{rs}$ ,  $H_{rs}$  and  $E_{0s}$ ,  $H_{0s}$ , may be regarded as scattering components.

$$E_r = E_{rc} + E_{rs} \quad H_r = H_{rc} + H_{rs} \quad \dots \quad (2)$$

$$E_0 = E_{0c} + E_{0s} \quad H_0 = H_{0c} + H_{0s} \quad \dots \quad (3)$$

Similar divisions of the reradiated field have been made. Brillouin<sup>7</sup> suggests a 'shadow field' and a 'scattered field', where only the latter contributes to the scattered power loss and the scattering cross-section. Aharoni<sup>8</sup> distinguishes a 'purely reflected field', which is the field of currents in a short-circuited aerial, and a 'reradiated field', which is the field of currents having the same distribution as occurs in transmission.

The components of  $E_r$ ,  $H_r$  proposed here are slightly different from both of these. A shadow field changes for different incident waves, whereas the complementary component of the reradiated field retains the same configuration and is easily predicted once for all. The currents responsible for the complementary component have the same distribution as occurs in emission, except that all travelling waves are reversed. It follows that their polar diagram is the reflection in the origin of the familiar emission polar diagram.

It should be mentioned that in resolving a given field into a complementary configuration and a remainder, there is an infinite choice of levels for the configuration. That level must be chosen which causes the complementary part to account for the power actually absorbed in the load of the receiving aerial.

Regarding a pair of aerials as a transmission system, there is a sense in which both partners contribute to the scattering, for the transmitter may be said to scatter energy in the wrong direction in the first place; hence the interpretation of  $E_{0s}$ ,  $H_{0s}$  as a scattering component of the incident field. In some instances, free from interference, the scattered power would be given unambiguously by integrating the scattering components of

the incident and reradiated fields, but it is preferable to compute powers in terms of the resultant field. Thus the scattered power might usefully be redefined as the actual power lost from the system, namely the integral of the resultant Poynting vector

$\int_S \mathbf{E} \times \mathbf{H} \cdot d\mathbf{S}$  taken over a surface enclosing both transmitter and receiver. This point of view avoids the notorious difficulties associated with the interpretation of scattered power.

$\int_S \mathbf{E}_r \times \mathbf{H}_r \cdot d\mathbf{S}$  taken over a surface enclosing only the receiving aerial. The latter leads too easily to the mistaken conclusion that a receiving aerial at best can reach only 50% efficiency, with much power being reradiated as is absorbed.

## (2.2) A Principle of Field Fitting

Taking the view that a complementary field is that which a receiving aerial most prefers, it follows that an approach to complete absorption and minimum scattering requires a good fit between the field actually appearing at the aerial and the complementary field. The comparison between the two fields need not be made throughout space. It is sufficient to make correlation over an aperture plane, or indeed any surface, which encloses the receiving aerial. If the surface is chosen to coincide with an equiphase surface of the complementary field, the latter is indistinguishable from the transmission field of the aerial on the surface.

Subject to this and other conditions given in the Appendix, it is possible to express the power transferred from one aerial

to another as  $\int_S \frac{\mathbf{E} \cdot \mathbf{E}'}{\eta} dS$ , where the integration is over a surface

enclosing only one of them.  $\mathbf{E}$  is the resultant electric field on the surface when one aerial transmits, and  $\mathbf{E}'$  is the field which would be there if the other aerial were to transmit.

This conception of absorption as being determined by the correlation between a field that a receiving aerial demands and the field that is actually present is valuable when the range is short and when the incident field is not a uniform plane wave. It augments the idea of an effective area for absorption, which would be difficult to apply in the absence of a uniform plane incident wave.

## (2.3) Reradiation of an Electromagnetic Horn

The rectangular horn is a good aerial for illustrating the existence of higher modes during reception and for distinguishing between complementary and scattered components in the reradiated field.

Let the taper of the horn be so slight that the field distributions may be assumed to be sinusoidal and the equiphase surface a plane, as in a rectangular waveguide. The horn is a continuation of such a waveguide operating in the dominant mode, so that the transmission and complementary fields over the aperture plane have the  $H_{01}$  mode configuration. In terms of co-ordinates taken from the centre of the aperture plane  $Oxy$  as in Fig. 11, the aperture distribution is specified by

$$E_x = E_m \cos(\pi y/a) \quad -\frac{1}{2}a < y < \frac{1}{2}a \quad \dots$$

In reception let a uniform plane wave  $E_0$ ,  $H_0$  be incident normally on the aperture. It may be resolved as follows on the basis of the rectangular distribution that it presents over the aperture:

$$E_{0c} = \begin{cases} E_0 \frac{4}{\pi} \cos(\pi y/a) & |y| < \frac{1}{2}a \\ 0 & |y| > \frac{1}{2}a \end{cases}$$



$$E_{0s} = \begin{cases} E_0 \frac{4}{\pi} \left[ \frac{\cos(3\pi y/a)}{3} + \frac{\cos(5\pi y/a)}{5} + \frac{\cos(7\pi y/a)}{7} + \dots \right] & |y| < \frac{1}{2}a \\ E_0 & |y| > \frac{1}{2}a \end{cases} \quad (6)$$

It is assumed that  $E_{0c}$  is zero outside the aperture, following practice for dealing with the horn in transmission. It is also assumed that  $E_{0s}$  outside the aperture does not lead to scattering

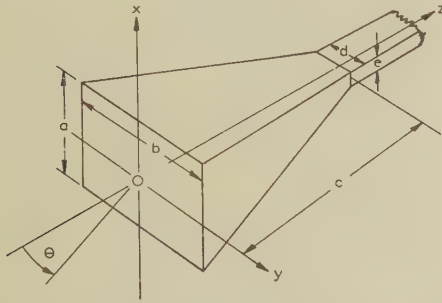


Fig. 1.—Rectangular horn and co-ordinate systems.

$$\begin{aligned} a = b = 20.3 \text{ cm} & \quad d = 7.7 \text{ cm} \\ c = 31.8 \text{ cm} & \quad e = 2.54 \text{ cm} \\ \lambda_a = 9.8 \text{ cm} & \end{aligned}$$

the exterior of the horn and its appendages. Experiments in which is observed the effect on the reradiation pattern due to movement of reflecting objects behind the horn help to verify this for a pyramidal horn, but not for a sectoral horn. These approximations are tolerable if the aperture dimensions exceed the wavelength by a factor of ten.

Fourier transforms of eqns. (5) and (6) lead to the reradiation diagram.

$$\text{The transform of } F(y) = \begin{cases} \cos(n\pi y/a) & y < \frac{1}{2}a \\ 0 & y > \frac{1}{2}a \end{cases} \quad (7)$$

where  $n$  is odd and  $u = \frac{-\sin \theta}{\lambda_a}$  is given by

$$G(u) = \int_{-\infty}^{\infty} F(y) e^{2\pi i u y} dy \quad (8)$$

$$= \frac{\frac{1}{2}n\pi \sin(\frac{1}{2}n\pi) \cos(\pi a u)}{(\frac{1}{2}n\pi)^2 - (\pi a u)^2} \quad (9)$$

$$= \frac{\frac{1}{2} \sin(\frac{1}{2}n\pi + \pi a u)}{(\frac{1}{2}n\pi + \pi a u)} + \frac{\frac{1}{2} \sin(\frac{1}{2}n\pi - \pi a u)}{(\frac{1}{2}n\pi - \pi a u)} \quad (10)$$

Curves for  $n = 3, 5, 7, 9$  are illustrated in Fig. 2. The interpretation is that the major contribution of a higher mode to the reradiation pattern is at an angle from the normal which increases with the mode number. It is noteworthy that where  $\pi a u = \frac{1}{2}n\pi$  a common zero occurs for all modes except  $n = 1$ .

The complementary component of the reradiated field has a radiation diagram which is the reflection in the origin of the transmission diagram, and in the  $xz$  plane is given by

$$E_{rc} \propto (m + \cos \theta') a \frac{\pi}{2} \frac{\cos(\pi a u')}{(\frac{1}{2}n\pi)^2 - (\pi a u')^2} \quad (11)$$

where  $m = \lambda_a/\lambda_g$  and  $\theta'$  and  $u'$  refer to angles measured from  $\pi$ . For the particular horn specified in Fig. 1,

$$E_{rc} \propto (1 + \cos \theta') \frac{\cos(6.5 \sin \theta')}{(2.47 - 42.3 \sin^2 \theta')} \quad (12)$$

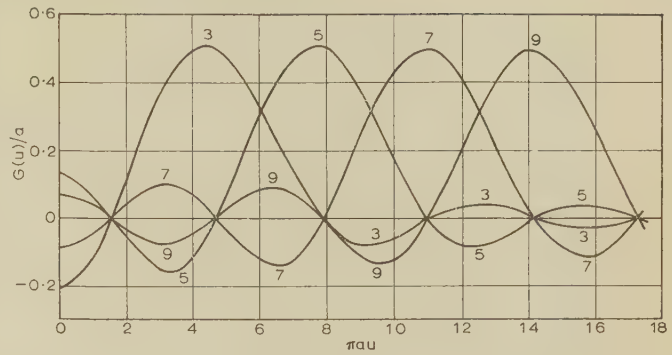


Fig. 2.—Fourier transforms of  $\cos(n\pi y/a)$   $-\frac{1}{2}a < y < \frac{1}{2}a$  for  $n = 3, 5, 7, 9$ .

The problem of finding the scattered component of the reradiated field is equivalent to that of a corner reflector excited by an aperture distribution of the form

$$F(y) = 1 - \frac{4}{\pi} \cos(\pi y/a) \quad (13)$$

A first approximation in the particular case is given by taking only the third-order mode, since higher modes than this exist in the evanescent form:

$$E_{rs} \propto (1 + \cos \theta) \frac{\cos(6.5 \sin \theta)}{22.1 - 42.3 \sin^2 \theta} \quad (14)$$

A second approximation may be made by a method of images,<sup>9</sup> in which an angular spectrum is synthesized from multiple images of the aperture distribution of eqn. (13). Contributions from the higher-order modes are then included, but the modification to the curve represented by eqn. (14) is small, mainly because the principal maxima in the Fourier transforms for modes other than the third lie outside the range of real angles, which ends at  $\pi a u = 6.5$  in this instance. These predictions of the reradiation pattern are compared with an experimental pattern in Figs. 3–6. Even an exact solution would be analysable into such a series of odd higher-order modes showing the same characteristic null at  $13.8^\circ$ . The null depends upon the absence

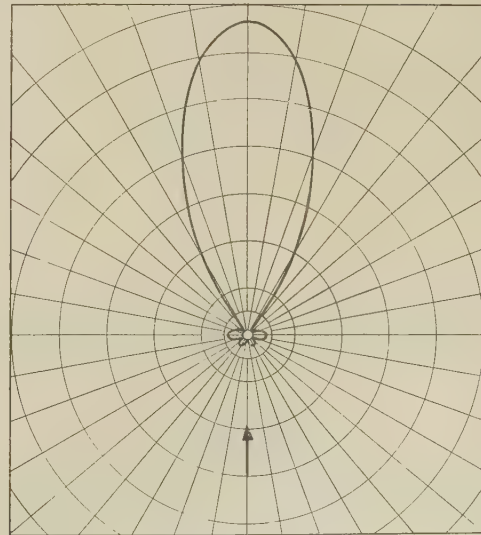


Fig. 3.—Polar diagram of the complementary component in the reradiation.

Arrow gives direction of incident wave.

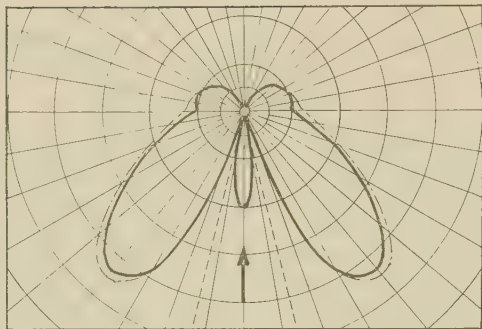


Fig. 4.—Polar diagram of the scattered component in the reradiation.

— Third mode only.  
 --- Fifth and seventh components included.

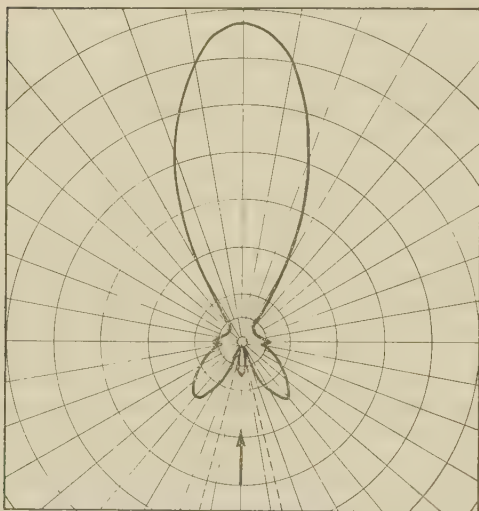


Fig. 5.—Complete theoretical reradiation polar diagram.

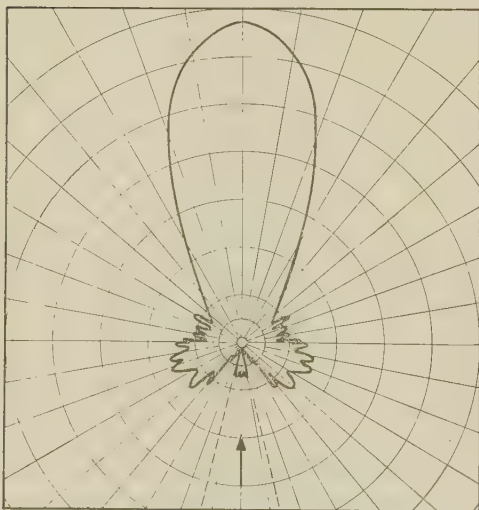


Fig. 6.—Experimental reradiation polar diagram.

of a reflection in the principal mode, and there can be no reflection if the matching arrangement at the throat remains adjusted for unity standing-wave ratio when the horn is transmitting.

### (3) EXPERIMENTAL METHODS

#### (3.1) Reradiation in Rear Sector

A simple method for recording the reradiation polar diagram is to allow a third directional aerial to perform an orbit around and directed toward the receiving aerial. This method must be replaced by others, however, for angles near  $0^\circ$  and  $180^\circ$ , where  $0^\circ$  represents the line joining receiver and transmitter.

In the shadow region as  $180^\circ$  is approached the limit of directivity of the measuring aerial ultimately fails to distinguish the reradiated from the incident field. If the orbit is continued a series of interference maxima and minima are recorded which are numerous for orbits taken at a large radius. Assuming they are too numerous to represent angular variations in the reradiation pattern itself, the maxima and minima are joined separately by smooth curves representing  $E_0 + E_r$  and  $E_0 - E_r$  from which the variation of  $E_r$  alone is deduced.

More points in the immediate vicinity of  $180^\circ$  are found by direct substitution of the receiving aerial. The measuring aerial maintains its position whilst the receiving aerial is removed and replaced. The vector difference in the measured field strength is the reradiated field, obtained directly from the definition in eqn. (1).

#### (3.2) Reradiation in Forward Sector

In the region around  $0^\circ$  a directional and therefore large measuring aerial is inadmissible, since the transmitter itself occupies that sector. One of the two aerials must obstruct the view of the other towards the receiver, depending upon which the greater range. Moreover reflections, for instance from the wall behind the receiving aerial, may no longer be distinguishable from the reradiation by directional means. A tolerably small reduction in the coupling between transmitter and receiver is possible if a short current-element performs the role of measuring aerial, in an orbit of relatively low radius. A phase-reversal method allows the reradiated field to be distinguished from other fields to which the weakly directional element remains sensitive. This consists in sliding the receiving aerial along the line joining it to the transmitting aerial over the short displacement which is necessary to reverse the phase of the reradiated field. The distance is  $\frac{1}{2}\lambda$  when the measuring aerial lies at  $\theta = 0^\circ$ , and this bearing does not change during the motion. But, in general, phase reversal requires a displacement  $D$  such that  $D(1 + \cos \theta) = \frac{1}{2}\lambda$  and there is a change in bearing

$$\delta\theta = \sin^{-1} \frac{\lambda \sin \theta}{2R(1 + \cos \theta)}, \text{ where } R \text{ is the radius of the orbit.}$$

The indeterminacy in  $\theta$  is tolerably small when  $\theta$  is small.

#### (3.3) Details of Experiments

Wavelength, 9.8 cm.

(a) Measuring aerial: conical horn, 40 cm diameter aperture.  
 Sector,  $38^\circ$ – $180^\circ$ .

Orbit radius, 130 cm.

(b) Measuring aerial: current-element, length 2.5 cm.  
 Sector,  $0^\circ$ – $42^\circ$ .

Orbit radius, 50 cm.

Reduction in received signal strength less than 1% to introduction of measuring aerial.

Maximum indeterminacy in bearing,  $\pm 1.1^\circ$ .

Transmitter range, 300 cm.



## (3.4) Measurement of Fields within the Horn

A thin rigid coaxial line may be introduced into the  $Oyz$  plane of the horn without greatly disturbing the existing field, since the line is everywhere perpendicular to the electric field. With the line opened to form a current-element probe of length 1.2 cm the variation in received signal strength is less than 2%.

Typical results of explorations of the electric field along lines parallel to the aperture plane are shown in Fig. 7. Near

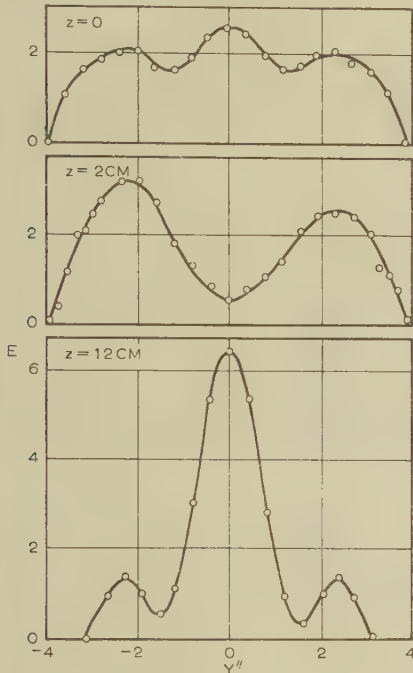


Fig. 7.—Variation of electric field intensity within the horn during reception.

the mouth of the horn the distribution alternates between the forms of the first two figures. Near the throat the third distribution predominates, with the subsidiary peaks diminishing, and the pure dominant mode remains in the waveguide.

In contrast, in Fig. 8 the field during transmission is entirely dominated by the dominant mode throughout the length of the horn.

## (4) CONCLUSIONS

For greatest absorption and least scattering with any receiving aerial, the incident field should correspond as closely as possible to an ideal which is complementary to the transmission field. This complementary field is like a motion picture of the transmission field played backwards; it is completely acceptable to the aerial and enjoys total absorption without causing scattered energy loss. Prediction of the absorption may be made in terms of a correlation between the given field and the complementary ideal, a procedure which has its greatest value in examples where the incident field is not a uniform plane wave.<sup>10</sup> For a directional aerial such as a horn is normally associated with radiation which is mainly confined to the forward direction at the mouth of the horn. Yet it has been predicted and confirmed that the essential reradiation is to the rear, where it amounts to a weakening of the resultant field in a shadow region and is a necessary accompaniment to the process of absorption. Whenever less essential reradiation or scattering occurs, generally

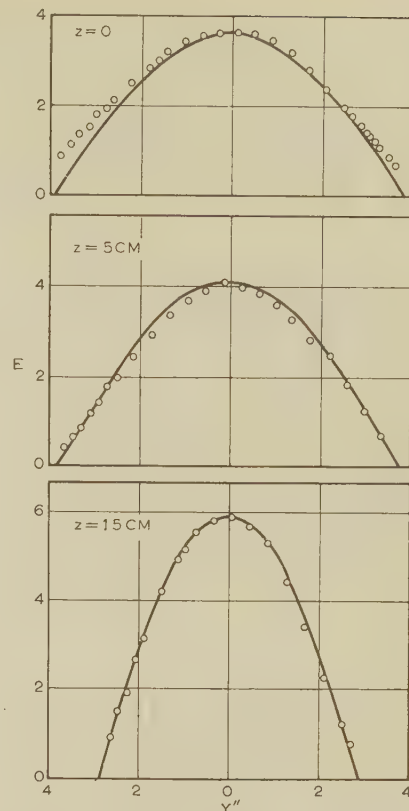


Fig. 8.—Variation of electric field intensity within the horn during transmission.

in all directions, and is due to the excitation of higher modes of oscillation in the aerial. For a rectangular horn subject to a normally incident plane wave, the scattering is not entirely chaotic. Each mode has a sector of greatest influence in the reradiation polar diagram, and there is one predictable null angle, common to all the higher modes.

Measurement of the local fields provides direct verification of the presence of higher modes during reception in a horn which transmits in the single dominant mode. The higher modes exist as standing waves up to the point where the horn is too narrow for further propagation, beyond which they are evanescent and diminish gradually. An exhaustive experimental study would lead to a surface-wave model of the electric field showing great intricacy and turbulence during reception in contrast with the smooth flow during transmission.

## (5) ACKNOWLEDGMENT

The author wishes to thank Mr. W. S. Stuart, formerly Senior Lecturer in the University of Leeds, for arousing his interest in receiving aerials and for many stimulating discussions of the subject.

## (6) REFERENCES

- (1) PIPPARD, A. B., BURRELL, O. J., and CROMIE, E.E.: 'The Influence of Re-radiation on Measurements of the Power Gain of an Aerial', *Journal I.E.E.*, 1946, **93**, Part IIIA, p. 720.
- (2) SILVER, S.: 'Microwave Antenna Theory and Design' (McGraw, 1949), p. 591

- (3) HEINS, A. E.: 'The Radiation and Transmission Properties of a Pair of Semi-infinite Parallel Planes', *Quarterly of Applied Mathematics*, 1948, **6**, p. 157.
- (4) BROWN, J.: 'A Theoretical Analysis of Some Errors in Aerial Measurements', *Proceedings I.E.E.* Monograph No. 285 R, February, 1958 (**105** C, p. 343).
- (5) BROWN, J.: 'A Generalized Form of the Aerial Reciprocity Theorem', *ibid.*, Monograph No. 301 R, April, 1958 (**105** C, p. 472).
- (6) BARLOW, H. M., and CULLEN, A. L.: 'Microwave Measurements' (Constable, 1950), Appendix V.
- (7) BRILLOUIN, L.: 'The Scattering Cross-section of Spheres for Electromagnetic Waves', *Journal of Applied Physics*, 1949, **20**, p. 1110.
- (8) AHARONI, J.: 'Antennae' (Clarendon Press, Oxford, 1946), p. 169.
- (9) MIDGLEY, D.: 'An Investigation into Microwave Radiation Problems'. Thesis. Department of Electrical Engineering, University of Leeds, June, 1953.
- (10) DONALDSON, A. R., FRENCH, I. P., and MIDGLEY, D.: 'Paraboloidal Reflectors with Axial Excitation', *Proceedings I.E.E.* Paper No. 3311 E, November, 1960 (**107** B, p. 547).

#### (7) APPENDIX

##### The Relation between Absorption and Scalar Products of the Aperture Fields

Let aeriels A and B be enclosed separately by aperture-forming surfaces, and let a large surface C enclose both.

Let the fields within C be  $E, H$ , when A transmits a given power  $P_T$  and B is terminated in a matched load which receives power  $P_R = fP_T$  a certain fraction of  $P_T$ . The remainder  $(1-f)P_T$  escapes across C and may be interpreted as the scattered power, following the proposal of Section 2.2.

It is a consequence of the Lorentz reciprocity theorem that, if B transmits  $P_T$  and A is terminated in a matched load,  $P_R$  is again received and the same fraction  $(1-f)P_T$  is lost. The new fields  $E', H'$  existing in C may be strikingly different from  $E, H$ , as, for instance, when A is a dipole and B is a strongly directional aerial.

Returning to the case where A transmits, let the load in B be replaced by an equivalent generator according to the compensation theorem. Let  $E', H'$  be the fields that would now be created by the equivalent generator acting alone and retrans-

mitting power  $fP_T$ . The power that would be returned to A is  $P_{R'} = f^2P_T$ :

$$P_R = fP_T \quad . \quad . \quad . \quad . \quad .$$

$$P_R = fP_R \quad . \quad . \quad . \quad . \quad .$$

$$P_R^2 = P_T P_{R'} = \left[ \int_S (E \times H) \cdot dS \right] \left[ \int_S (E' \times H') \cdot dS \right]$$

Eqn. (17) expresses the power  $P_R$  transferred from A to B in a way which involves integration over the surface surrounding only A, of the two quite different fields  $E, H$  and  $E', H'$ . Whereas  $E, H$ , has the form of A's transmission and complementary fields,  $E', H'$  is the field in which A would find itself if B were transmitting. The two integrals are not equivalent to one double integral, but vector manipulation converts a special case of the result into the form of a scalar product using the following identity:

$$(a \times b) \cdot (c \times d) = (c \cdot a)(d \cdot b) - (b \cdot c)(d \cdot a) \quad . \quad . \quad .$$

Consider the power  $\delta P_R$  crossing an element  $\delta S$  of A:

$$\begin{aligned} (\delta P_R)^2 &= [(E \times H) \cdot \delta S][E' \times H'] \cdot \delta S] \\ &= [(E' \times H') \cdot (E \times H)](\delta S \cdot \delta S) \\ &\quad - [(E \times H) \times \delta S] \cdot [(E' \times H') \times \delta S] \end{aligned}$$

The second term in eqn. (19) may be reduced to zero by choosing  $\delta S$  to be normal to either  $E \times H$  or  $E' \times H'$ . Applying identity (18) again to the first term of eqn. (19),

$$(\delta P_R)^2 = [(E \cdot E')(H \cdot H') - (E \cdot H')(E' \cdot H)]\delta S^2$$

The second term in eqn. (20) is zero if the  $E$ 's are, as in a horn H-plane, perpendicular to the  $H$ 's. Finally, if in magnitude  $E/H = E'/H' = \eta$ , one may write

$$(\delta P_R)^2 = \frac{(E \cdot E')^2 \delta S^2}{\eta^2} \quad . \quad . \quad . \quad . \quad .$$

$$P_R = \int_S \frac{(E \cdot E')}{\eta} \delta S \quad . \quad . \quad . \quad . \quad .$$

Thus the transfer of power in this particular case is determined by the scalar product of the two aperture distributions. Repeated evaluation for changing orientation leads to the conception of the result as a cross-correlation function, which predicts the polar diagram.



# THE DESIGN OF A NOISE GENERATOR FOR MEASUREMENTS IN THE FREQUENCY RANGE 30–1250 Mc/s

By I. A. HARRIS, Associate Member.

(The paper was first received 10th February, and in revised form 28th June, 1961.)

## SUMMARY

Departure of the source impedance of a noise generator from the nominal value gives rise to an uncertainty in the measurement of noise factor. A critical examination of the problem shows that, to obtain an uncertainty on this account of less than 2%, a source v.s.w.r. of about 0.98 is required. Because existing noise generators seldom meet this requirement and because there is a need for more consistent measurements of noise than those obtained hitherto at frequencies up to about 1200 Mc/s, a new noise generator has been developed. A description of the design, construction, calibration and use of the noise generator is given. It employs a precision source resistor of 2  $\Omega$  and a pair of specially developed thermionic diodes (E2790), using a form of diode mount designed to eliminate the effects of diode capacitance so that a v.s.w.r. better than 0.98 is obtained at all frequencies in the range. It is an absolute noise generator with an accuracy in noise level of  $\pm 2\%$  at frequencies up to about 300 Mc/s, and requires calibration at a single level for frequencies up to 1250 Mc/s. At present, this has been achieved with an estimated uncertainty of about  $\pm 5\%$  in noise level.

## (1) INTRODUCTION

The effect of spontaneous random fluctuations of electricity in an amplifier has long been described quantitatively by the noise factor, or noise figure, the factor by which the effective signal/noise power ratio at the source is degraded by the amplifier. Noise factor was originally defined in terms of available noise power and available gain in a manner that was designed to avoid the necessity of considering details of the effects of mismatches.<sup>1</sup> This method is useful in certain general circuit calculations, provided that the conditions attached to the meaning of 'available gain' are well understood.<sup>2</sup> The British Standard definition<sup>3</sup> of 'noise factor' is: the ratio of the total mean-square noise output e.m.f. to that part of it which is due to the thermal noise of the source. The source is taken to be a passive network at a temperature of 290° K; the noise is considered to be limited to the frequency range of the signal channel of the receiver; and the definition applies only to that part of the receiver in which no amplification or frequency conversion occurs. With wide-band amplifiers or receivers, a knowledge of their transfer characteristics as functions of frequency is required in order to measure noise factor with the help of a known noise source, unless the noise source has a non-reactive impedance that is independent of frequency over a sufficiently wide band. Given a noise generator with such a constant source impedance at all levels of the noise setting, the noise factor of a receiver with any reasonable bandwidth can be measured without ambiguity, using a detector that responds to mean-square voltage or current.

Comparisons between available noise generators, including simple saturated diodes, distributed coaxial saturated diodes and gas discharge tubes with their mounts and source resistors have often been found to show differences, particularly in the v.h.f. and lower part of the u.h.f. bands, where total inconsistencies of

2 dB or even 3 dB have sometimes been noticed. It is suspected that inadequate values of source v.s.w.r. relative to the nominal impedance are largely responsible for this. In order to obtain consistent results, there is need for a reappraisal of the conditions that must be satisfied by noise generators and need for a noise generator that conforms to the conditions reasonably accurately.

## (2) CRITERIA FOR A SATISFACTORY NOISE GENERATOR

The degree of consistency between measurements of noise factor depends broadly on the qualities of three pieces of apparatus. First, the amplifier under test must respond linearly to amplitudes up to several times the r.m.s. value of the greatest noise present during a measurement. Secondly, the special detector used must respond to voltages (or currents) as a true mean-square device up to a level several times the maximum r.m.s. noise applied. The detector should respond to the full bandwidth of the amplifier unless a narrow-band noise factor is required. Thirdly, the noise generator must satisfy the obvious requirements that the level of noise at the outlet must be established as a function of measured direct current or other readily determined property, that any frequency correction for this must be known, and that the source v.s.w.r. with the additional noise either 'on' or 'off' must be adequately close to unity. These requirements, except possibly the last, are widely appreciated. It remains to estimate the source v.s.w.r. that can be tolerated for a given inconsistency on this account and to choose the type of noise generator in which the condition is most likely to be realized.

### (2.1) Effect of Source Mismatch on Noise Factor Measurement

The effects of the various amplifier and source parameters on the value of noise factor and its measurement can readily be ascertained with the help of the general theory of linear active two-terminal-pair networks (four-poles) developed during the past seven years.<sup>4, 5</sup> In this, the noise properties of an amplifier are represented by a 'noise four-pole' at the inlet of the actual amplifier, which is then considered to be noise-free (Fig. 1).

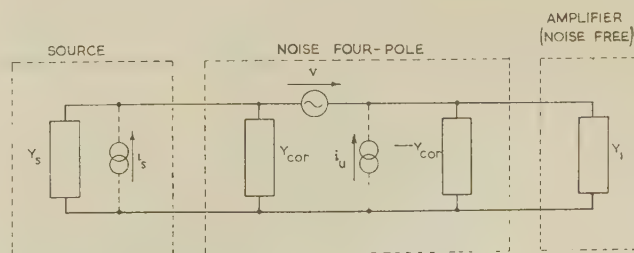


Fig. 1.—Input circuit for calculation of noise factor.

Four parameters specify the noise characteristics: a resistance,  $R_n$  (to define a series noise voltage  $v$ ); a conductance,  $G_n$  (to define a shunt noise current,  $i_n$ , uncorrelated with the noise voltage);

Written contributions on papers published without being read at meetings are invited for consideration with a view to publication.  
Mr. Harris is at the Laboratories of the Electrical Inspection Directorate, Ministry of Aviation.

and the two components of a correlation admittance,  $Y_{cor}$  (to define noise current correlated with the noise voltage). In Fig. 1, the second admittance,  $-Y_{cor}$ , is necessary to neutralize  $Y_{cor}$  for signals or noise from the source, so that it does not affect the input admittance,  $Y_1$ , of the amplifier. The following general expression for the noise factor,  $N$ , can be deduced from the equivalent network:

$$N = 1 + \frac{\int_0^\infty (G_n + R_n |Y_s + Y_{cor}|^2) (|A|^2 / |Y_s + Y_1|^2) df}{\int_0^\infty (G_s |A|^2 / |Y_s + Y_1|^2) df} \quad (1)$$

where  $Y_s$  is the source admittance, and  $A$  is the ratio of the voltage across the output load to the voltage across the input admittance,  $Y_1$ . Admittances are preferred to impedances because they simplify the analysis with diode noise sources. The ranges of integration are infinite so as to include all frequencies at which  $A$  may be non-zero. If  $A$  restricts the pass-band to a very small value, the narrow-band noise factor is obtained:

$$N = 1 + G_n/G_s + (R_n/G_s) |Y_s + Y_{cor}|^2 \quad (2)$$

The well-known fact that noise factor must be defined relative to a nominal source admittance is evident from eqns. (1) and (2), as is the fact that this is best chosen to be a pure conductance,  $G_s$ . Source mismatch is taken to mean the departure of the noise-generator admittance from this nominal conductance. The effect of source mismatch on the simple measurement of noise factor depends on the type of noise generator used.

With a noise generator employing a saturated diode the source admittance does not change appreciably when the diode is turned on or off. The method used to measure  $N$  is to increase the mean-square noise voltage at the output of the amplifier by the factor  $\alpha$  by adjusting the diode emission current,  $I$ . Then, for a standard source temperature of 290° K,

$$N = \frac{20IF}{(\alpha - 1)G_s} \quad (3)$$

where  $F$  is the frequency correction factor for the diode taken at the mid-band frequency of the amplifier.\*

If, in a measurement, the diode noise generator has a source admittance  $G'_s + jB'_s$  instead of the nominal  $G_s$ , the narrow-band noise factor is expressed

$$N' = 1 + G_n/G'_s + (R_n/G'_s)[(G'_s + G_{cor})^2 + (B'_s + B_{cor})^2] \quad (4)$$

In measuring the noise factor, however, it would normally be assumed that the source admittance had the nominal value, so that eqn. (3) would be used to obtain  $N_{meas}$  but the noise factor actually measured should be determined from the relation

$$N' = 20IF/[(\alpha - 1)G'_s]$$

The values of  $\alpha$  and  $F$  are given, and  $I$  is determined in the measurement, so that

$$N_{meas}/N' = G'_s/G_s \quad (5)$$

The true noise factor relative to  $G_s$  is given by eqn. (2), so that eqns. (2), (4) and (5) lead to the result

$$\frac{N_{meas}}{N_{true}} = \frac{G'_s + G_n + R_n[(G'_s + G_{cor})^2 + (B'_s + B_{cor})^2]}{G_s + G_n + R_n[(G_s + G_{cor})^2 + B_{cor}^2]} \quad (6)$$

It is not possible to give the maximum limits of error for a given mismatch expressed as a v.s.w.r. relative to  $G_s$ ; the best

\* This relation has usually been written in the form  $20IFR_n/(\alpha - 1)$ , which is correct only when the source is a pure resistance. Eqn. (3) is correct even when the source admittance is complex, provided that  $N$  is then understood to be relative to this source admittance.

that can be done is to take an example. Thus with  $G_n = R_n = 2/G_s$ ,  $G_{cor} = 0.7G_s$  and  $B_{cor} = 0$ , and with a source admittance  $(0.7 - j0.2)G_s$  giving a v.s.w.r. of about 0.67, the eqn. (6) gives  $N_{meas}/N_{true} = 0.74$  (i.e.  $-1.3$  dB). If, on the other hand, the source admittance is  $(1.4 + j0.2)G_s$ , which gives a v.s.w.r. of about 0.67, then  $N_{meas}/N_{true} = 1.44$  ( $+1.6$  dB). Thus two diode noise generators, each with a v.s.w.r. of 0.67 but with widely differing angles of admittance will give answers differing by the ratio 2.9 dB. Further examples show that, to obtain not more than  $\pm 2\%$  uncertainty on account of mismatch, a v.s.w.r. not worse than about 0.98 is required.

With a gas discharge tube, especially in a coaxial mount employing a line with a helical inner conductor surrounding the tube to obtain adequate coupling with the discharge at frequencies below 1000 Mc/s, the source mismatch depends on whether the discharge is on or off. The method used to measure  $N$  is to determine the ratio  $\alpha$  of the mean-square output voltages with the discharge on and off. Then, with the correct source admittance,

$$N = (T_g/T_0 - 1)/(\alpha - 1)$$

where  $T_g$  is the effective source temperature with the discharge on, and  $T_0$  is the source temperature with the discharge off. Usually,  $T_g/T_0$  is about 36. In this case the effect of source mismatch is complicated and depends on the input admittance of the amplifier. If, for example, the v.s.w.r. of the generator is 0.8 with the discharge on and 0.7 with the discharge off, and if the v.s.w.r. of the amplifier input is 0.5, then the uncertainty in  $N$  can be more than  $\pm 1$  dB. Improvement can be obtained by fixing  $\alpha$  and using a variable attenuator between the generator and the amplifier, but at present such an attenuator is not readily available with coaxial connectors.

## (2.2) Choice of Type of New Noise Generator

No way has yet been found of achieving the required v.s.w. with a coaxially mounted discharge tube for frequencies below 1250 Mc/s. With a suitably designed mount employing special diodes, on the other hand, techniques already developed with other measuring instruments enable such a v.s.w.r. to be obtained. The frequency-dependent correction for the noise level, necessary with any saturated diode, need be determined initially by basic methods only at a single level of noise, so that it is not a great disadvantage. Accordingly, it was decided to develop a noise generator using saturated thermionic diodes specially designed to suit the method of obtaining a v.s.w.r. not worse than 0.98 at all frequencies in the required band.

## (3) NOISE GENERATOR FOR THE FREQUENCY BAND 30-1250 Mc/s

### (3.1) General Description

This noise generator has been designed to conform strictly to the requirements set out in Section 2. An axial section of the diode mount and source-resistor assembly is shown in Fig. 2. The source resistor consists of a cylindrical film resistor surrounded by a coaxial copper outer conductor of tractorial axial section. With this form of resistor mount, which has been described before,<sup>6</sup> a v.s.w.r. relative to the nominal 50  $\Omega$  of 0.98 or better is attainable for all frequencies in the required band. The variable, determined source of noise is provided by a pair of small thermionic diodes, type E2790, specially developed for the noise generator. The reasons for using two diodes instead of one are connected with the necessity to neutralize the diode capacitance and to obtain adequate noise ratio.

Each diode has an effective capacitance of about 0.8 pF, and to neutralize this the inner conductor of the main coaxial line



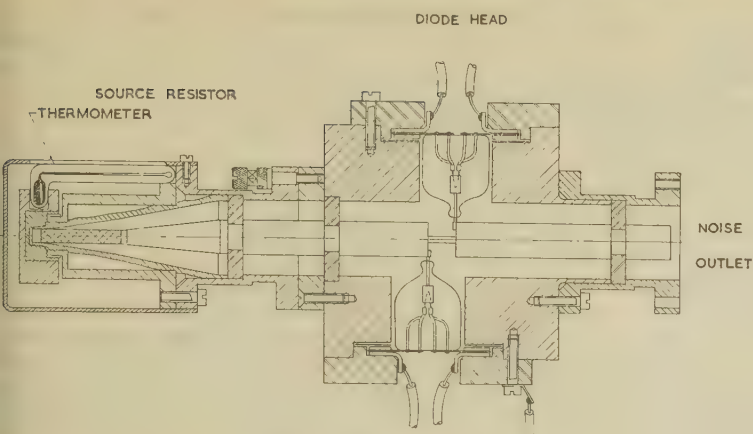


Fig. 2.—Axial section of diode noise generator.

undercut for the length between the two junctions with the diode anode connections, to form a low-pass  $\pi$ -section with the two diode capacitances.<sup>7</sup> The characteristic impedance of this  $\pi$ -section is made equal to  $50\Omega$ . Adjustable screwed plungers (not shown in Fig. 2) are located opposite each diode junction to enable the capacitance there to be set precisely to the correct value, which is ascertained by obtaining a measured v.s.w.r. for the whole diode head and source resistor close to unity at several frequencies. By these means, an effective source v.s.w.r. of nearly 0.99 has been obtained throughout the frequency range 0-1250 Mc/s. In order to keep the capacitance of each diode low enough to permit of its neutralization over the required frequency range, the electrodes have to be so small that the saturated emission current is limited to 10 mA per diode. Two diodes are therefore required for the measurement of noise factors up to 20 with a source resistance of  $50\Omega$ , using a 2:1 increase in mean-square output voltage or current.

In each diode, multiple connections from the two ends of the filament are brought out through seals to the two parts of a split disc. The r.f. circuit through each diode is completed at the split disc by a mica capacitor of about 200 pF, which effectively isolates the filament heating connections from the r.f. circuit, as illustrated in Figs. 2 and 3. If there is no d.c. short-circuit at the input of the amplifier under test, the anode currents of both diodes must pass through the source resistor to the positive h.t. connection, which is at earth potential. The resulting dissipation in the resistor, however, does not cause appreciable heating because at the maximum current of 20 mA the power in the resistor is only 20 mW, which after several minutes would cause a temperature rise of less than  $1^\circ\text{C}$ . Also, it has been verified experimentally that this direct current does not measurably increase the noise from the source resistor at frequencies higher than 30 Mc/s. The filament supplies are connected to the negative 100 V anode circuit, and the saturated diode current is adjusted in the usual way by varying the filament heating supplies.

### (3.2) Power Supply Unit and Indicating Instrument

So far as the generation of noise is concerned, it does not matter whether the emission currents of the two diodes are equal or not, but to ensure adequate filament life it is necessary to limit each diode emission to 10 mA at the maximum setting. Again, owing to the short lengths of the filaments, the emission current for a given filament-heating voltage may vary widely between diodes; consequently it is necessary to adjust each filament supply and to measure each emission current separately during the initial setting-up. When the noise generator is in use, the

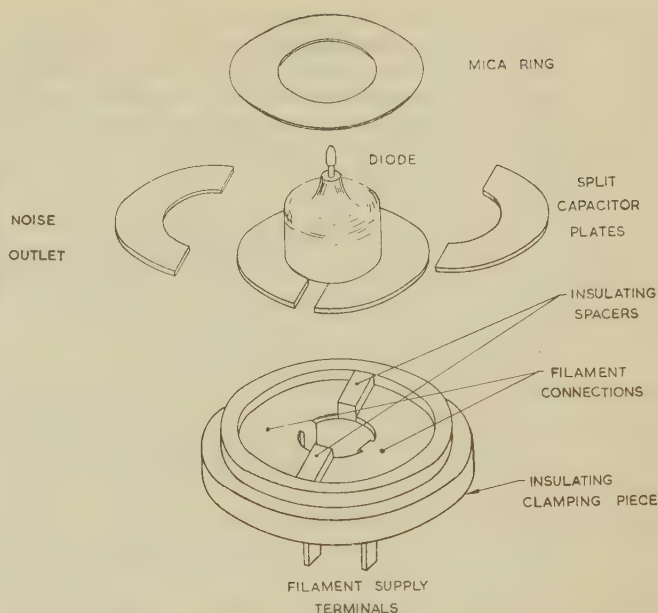


Fig. 3.—Exploded view of diode and blocking capacitor assembly.

sum of both emission currents must be indicated and must be adjustable by a single control. Finally, the extreme sensitivity of saturated emission current to small changes in filament heating requires an exceptionally fine control of the latter if the emission current is to be set with an acceptable precision. The power supply unit is designed to meet these requirements under normal variations in mains voltage and ambient temperature.

An attempt was first made to develop a power unit employing two separate d.c. filament supplies controlled by power transistors employing known transistor stabilization networks, but variation in the transistor characteristics with changes in ambient temperature resulted in unacceptably large variations in the emission current of the saturated diodes. The design of power unit adopted employs both thermionic valves and semiconductor devices, the diode filaments being heated with alternating current at a frequency of 20 kc/s. With this frequency, the peak-to-peak ripple on the diode emission is less than 0.2% of the steady component, which is low enough to cause no difficulty with modulation of the mean-square noise current. The output circuit of the filament supply unit is shown in Fig. 4, from which the method of measuring the emission current of each diode separately during the initial setting-up can be seen. The output pentode is fed from a 20 kc/s amplitude-stabilized oscillator, for which the stabilizing voltage is obtained from transformer  $T_3$  and rectifier W, together with a direct voltage that is varied to set the level of the diode filament heating to obtain the required emission current. The voltage developed across the resistor  $R_7$  by the combined emission currents is used for partial stabilization of the filament heating current.

The indicating instrument employs 4-terminal resistors  $R_3$ ,  $R_4$ ,  $R_5$  and  $R_6$  as shunts which are permanently in circuit. All meter switching is on the instrument side of the shunts, the resistance of the instrument being made high enough to avoid errors from small switch contact resistances.  $R_3$  and  $R_4$  are used to measure each diode current separately when these are equalized at 10 mA by varying the shunts  $R_1$  and  $R_2$  across the output transformers.  $R_5$  provides the current range 0-5 mA, and  $R_6$  provides the range 0-20 mA when the noise generator is in use. The two current meter ranges, the corresponding filament supply ranges and the standby facility in which the

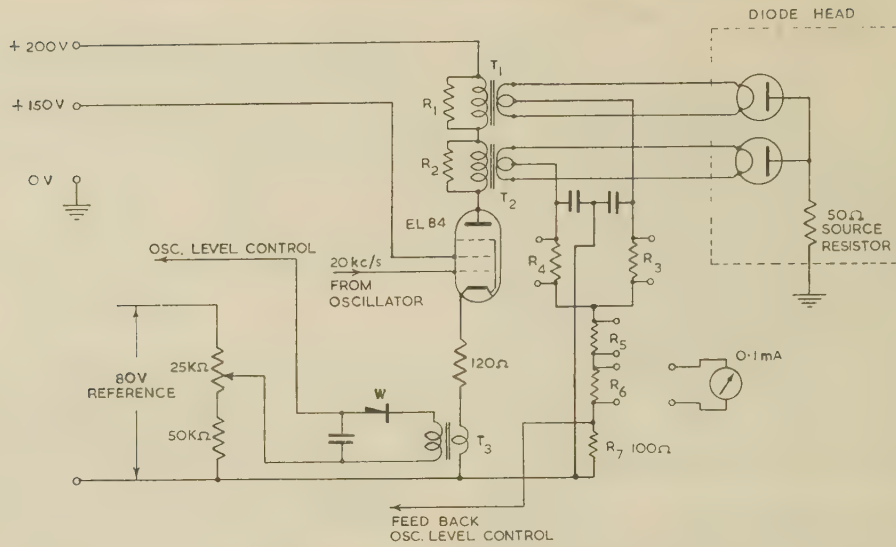


Fig. 4.—Diode filament supply circuit of power unit.

emission current can be reduced to 'zero' (less than  $1\mu\text{A}$ ) rapidly are all controlled by a single 5-position switch. This permits quick switching (5 sec) from 'diodes off' to 'diodes on' at any given level of emission current.

### (3.3) Design of the Undercut Section of Line

The equivalent circuit of the two diodes, the undercut section of the line and the source resistor is shown in Fig. 5. Each diode is represented by a capacitance  $C$ . The shunt conductance and the electronic contribution to the capacitance of each saturated diode, both functions of frequency, are negligible. The admittance seen looking to the left at  $AA'$  is  $G_s + j\omega C$ , where  $G_s$  is the conductance of the source resistor. At  $BB'$ , this admittance is transformed by the undercut section of line of length  $l$  and of real characteristic admittance  $Y_{01}$ . Thus at  $BB'$ , with the second capacitance taken into account, the admittance is

$$Y_B = \frac{G_s + j(\omega C + Y_{01} \tan \beta)}{1 + j[(G_s + j\omega C)/Y_{01}] \tan \beta} + j\omega C \quad (7)$$

where  $\beta = \omega l/v$  and  $v$  is the velocity of propagation. If  $\omega l/v \ll 1$  and  $\omega C \ll 1$ , eqn. (7) may be expanded as a power series, retaining terms as small as  $(\omega C)^2$  and  $\beta^2$ . There results

$$Y_B = G_s \left\{ 1 + \omega^2 \left[ \frac{2Cl}{Y_{01}v} - \left( \frac{G_s^2}{Y_{01}^2} - 1 \right) \frac{l^2}{v^2} \right] + j\omega [2C - Y_{01}(G_s^2/Y_{01}^2 - 1)l/v] \right\} \quad (8)$$

If

$$2C/Y_{01} = (G_s^2/Y_{01}^2 - 1)l/v \quad (9)$$

eqn. (8) becomes

$$Y_B = G_s \quad (10)$$

to the order of approximation of eqn. (8).

The values of  $l$  and  $Y_{01}$  determined by the undercut are chosen to satisfy eqn. (9); thus, if  $l$  is given,

$$Y_{01} = G_s \left\{ \sqrt{1 + (vC/lG_s)^2} - vC/lG_s \right\} \quad (11)$$

The value of  $l$  should be the minimum that results in a practicable thickness of the undercut section. In computing  $C$  the discontinuity capacitance of the step in the inner conductor must be included.

To estimate the change in diode capacitance at the upper frequencies, the equivalent distributed circuit of a mounted

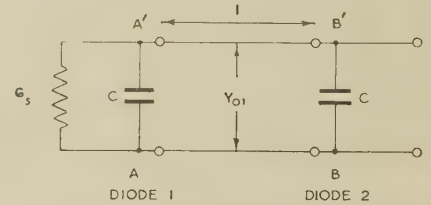


Fig. 5.—Equivalent r.f. circuit of noise generator.

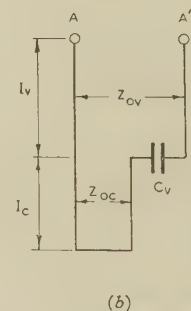
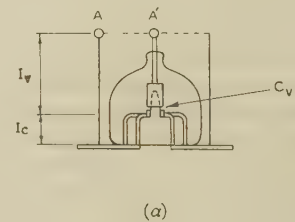


Fig. 6.

(a) Mounted diode.  
(b) Equivalent r.f. circuit.

diode, shown in Fig. 6, is used. The capacitance  $C_v$  of the actual electrodes is in series with a short-circuited line of length  $l_v$  and of characteristic impedance  $Z_{0c}$ . The whole is connected to the accessible terminals  $AA'$  through a length  $l_p$  of line of char-



istic impedance  $Z_{0v}$ . If  $\omega l_v/v$  and  $\omega l_c/v$  are small compared with unity, it can be shown that

$$C = C_v + Y_{0v} l_v/v + \omega^2 \left[ \frac{Y_{0v} (l_v)^3}{3} + C_v^2 \left( \frac{Z_{0v} l_v}{v} + \frac{Z_{0c} l_c}{v} \right) \right] \quad (12)$$

where  $Y_{0v} = 1/Z_{0v}$ . Eqns. (7) and (12) with  $Y_{01}$  given by eqn. (11) show that  $Y_B = G_s$  to within about 1% at all frequencies up to 1250 Mc/s when  $C_v = 0.5$  pF,  $l_v = 1.6$  cm,  $l_c = 0.8$  cm,  $Z_{0v} = 180 \Omega$  and  $Z_{0c} = 50 \Omega$ , typical for the diode E2790.

### (3.4) Frequency Corrections

#### (4.1) Current Transformation and Transit-Time Effect

The mean-square fluctuation of current in a short-circuit across the accessible diode terminals, associated with the frequency range  $f$  to  $f + df$ , is expressed

$$d\bar{i}^2 = 2eIF df \quad (13)$$

where  $I$  is the saturated emission current and  $e$  is the electronic charge.  $F$  is a frequency-dependent factor which is the product of  $\Psi$ , the correction factor for the transformation of mean-square current between the electrodes and the accessible connections, and  $\Phi$ , the correction factor depending on the electron transit time in the diode.  $F$  as a whole is best determined experimentally by comparison of the noise from the diode generator with the calculable noise from a hot source resistor at measured temperature. In the Appendix, means are given for calculating  $\Psi$  and  $\Phi$  from diode dimensions, so that a calculated curve for  $F$  versus frequency can be compared with the measured curve.

#### (4.2) Thermal Noise from the Filaments

Each diode filament is, in the radio-frequency circuit, equivalent to a small resistance  $R_c$  in series with the electrode capacitance  $C_v$ , which is equivalent to a shunt conductance across the accessible diode connections:

$$G_c = \omega^2 C_v^2 R_c \Psi \quad (14)$$

This equivalent conductance is at the filament temperature  $T_c$ , i.e. about 2500° K when the filament is emitting. The two limbs of the hairpin-shaped filament are effectively in parallel for the radio-frequency circuit, giving an effective resistance, apart from skin effect, of one-quarter of the series resistance of  $1.6 \Omega$  presented to the heating circuit. At the frequency 1250 Mc/s, skin effect about doubles the low-frequency resistance of hot tungsten wire of the diameter used. Again, the effective lumped resistance,  $R_c$ , in series with  $C_v$  is one-third of the distributed value along the wire, giving the value  $0.27 \Omega$  at 1250 Mc/s. Then with  $C_v = 0.5$  pF and  $\Psi = 2.7$ ,  $G_c = 11.3$  micromhos at 1250 Mc/s. It follows that the mean-square current fluctuation from two diode filaments is  $3.2 \times 10^{-24} \Delta f$  amperes<sup>2</sup> in a bandwidth  $\Delta f$ . The shot-effect mean-square current in a measurement of unity noise factor with  $\alpha = 2$  is  $3.2 \times 10^{-22} \Delta f$  amperes<sup>2</sup>. Therefore, under the worst possible condition in normal use of the noise generator, the thermal noise contribution of the filaments is only 1% of the total.

### (4) CALIBRATION AND USE

#### (4.1) Determination of Frequency Correction Factor

The method is to compare the noise from the generator with noise from another source that is readily calculable. A hot source resistor provides a standard which requires the least amount of measurement and calculation in making the comparison, but in order to ensure the correct value of source

conductance over a wide band, the temperature is limited to less than 200° C above room temperature. This results in a small increase in noise over that obtained from a similar source at room temperature, and unless a receiver with a very low noise factor is used to amplify the noise to a level at which it can be detected, the difference detected is too small for accurate assessment. Furthermore, unless the noise factor of the receiver is optimum for the nominal source conductance, the change in receiver noise with the small change in source admittance between the hot source and the noise generator will be of the same order as the noise difference being measured. Therefore the use of a hot source as a standard requires the use of head amplifiers with noise factors of not more than 2, adjusted for minimum noise when used with the nominal source conductance.

Such head amplifiers were not available when the noise generator described was calibrated, and a c.w. signal generator, specially calibrated, was used as the standard. The v.s.w.r. of about 0.97 relative to the nominal conductance was obtained by inserting a suitable attenuator in the outlet, and the calibration level at the outer end of this attenuator was established by measuring the power absorbed in a load of precisely the nominal conductance. The attenuator in the signal generator was checked also.

The effective noise bandwidth of the head amplifier for each frequency used was determined by graphical integration of the response curves obtained using a strictly square-law detector in the receiver. Then, if  $P$  is the power from the signal generator at the mid-band frequency of the receiver required to increase the detected output by the ratio  $\alpha$ , if  $I$  is the diode current required to give the same ratio and if the temperatures of the source conductances in the two sources do not differ by more than a few degrees,

$$F = 1.25 \times 10^{19} (P/\Delta f) (G_s/I) \quad (15)$$

where  $\Delta f$  is the noise bandwidth and  $G_s$  is the nominal source conductance. The experimental results are shown in Fig. 7.

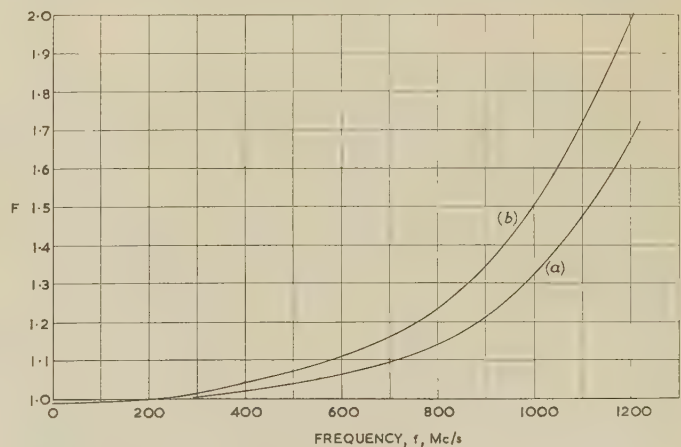


Fig. 7.—Observed and theoretical frequency correction curves.

(a) Observed. (b) Theoretical.

#### (4.2) Normal Use

If the source resistor in the noise generator is actually at the absolute temperature  $T_1$ , the noise factor at the standard temperature  $T_0$  ( $=290^\circ$  K) is expressed

$$N = 1 - \frac{T_1}{T_0} + \frac{20IF}{(\alpha - 1)G_s} \quad (16)$$

where  $I$  is the diode current (milliamperes) required to multiply

the mean-square noise output voltage of the amplifier by the factor  $\alpha$ , and  $G_s$  is expressed in millimhos.

#### (4.3) Measurement of the Four Noise Parameters of an Amplifier

The four noise parameters mentioned in Section 2.1 may be determined with the help of a noise generator of accurately known real source admittance. These parameters are functions of frequency and should be measured with a narrow pass-band filter preceding the square-law detector in the case of a wide-band amplifier. Five relative values of mean-square output voltage are determined:

- $n_1$  with source  $G_s$  and diode current zero.
- $n_2$  with source  $G_s$  and diode current  $I$ .
- $n_3$  with the coaxial inlet short-circuited.
- $n_4$  with a quarter-wavelength line, short-circuited at the outer end, at the inlet.
- $n_5$  with an eighth-wavelength line, short-circuited at the outer end, at the inlet.

The input conductance  $G_1$  and susceptance  $B_1$  of the amplifier must also be measured.

Then

$$R_n = \left( \frac{n_3}{n_2 - n_1} \right) \frac{20IF}{[(G_1 + G_s)^2 + B_1^2]} \quad (17)$$

$$G_{cor} = \frac{[(G_1 + G_s)^2 + B_1^2]n_1 - (G_1^2 + B_1^2)n_4}{2G_s n_3} - \frac{1}{2R_n} - \frac{G_s}{2} \quad (18)$$

$$B_{cor} = \frac{(G_1^2 + B_1^2)n_4 - [(G_s - B_1)^2 + G_1^2]n_5}{2G_s n_3} + \frac{G_s}{2} \quad (19)$$

$$G_n = R_n[(n_4/n_3)(G_1^2 + B_1^2) - (G_{cor}^2 + B_{cor}^2)] \quad (20)$$

These relations were calculated by an extension of a method used to determine analogous relations for an amplifier with a waveguide inlet.<sup>8</sup>

#### (5) CONCLUSIONS

Critical examination of the effect of mismatch of the noise generator relative to the nominal source impedance shows that a v.s.w.r. of at least 0.98 is necessary if an uncertainty less than  $\pm 2\%$  on account of mismatch is required. To meet this requirement in the v.h.f. and lower part of the u.h.f. bands, a diode noise generator has been designed and constructed using special techniques originally devised for other purposes, to give a v.s.w.r. not worse than 0.98 over the frequency range 30–1250 Mc/s. The frequency dependence of the noise level is determined by comparison with a known source having a similar v.s.w.r. The source resistance is  $50\Omega$ , and the accuracy in noise level varies from about  $\pm 2\%$  at frequencies up to 300 Mc/s, where the generator can be used as an 'absolute' instrument, to  $\pm 5\%$  for frequencies higher than about 400 Mc/s, where initial calibration against a known source is necessary. With improvements in the known source and the method of comparison, the accuracy at the higher frequencies may be improved.

#### (6) ACKNOWLEDGMENTS

The writer makes the following acknowledgments. First, for the co-operation of the staff of the M.O. Valve Co. Ltd., who made the diodes to a difficult specification, especially to Mr. R. E. Wyke and to Mr. D. Nash, whose ingenuity was largely responsible for the successful design and production of the diodes. Secondly, to Mr. W. Tatham and Mr. R. W. A. Siddle,

for the development and construction of the stabilized power units, and last to Mr. L. J. Graver of this laboratory for computations and some detail work in the design of the diode head.

#### (7) REFERENCES

- (1) FRIIS, H. T.: 'Noise Figures of Radio Receivers', *Proceedings of the Institute of Radio Engineers*, 1944, **32**, p. 419.
- (2) GOLDBERG, H.: 'Some Notes on Noise Figures', *ibid.*, 1944, **36**, p. 1205.
- (3) B.S. 2065: 1954, 'Glossary of Terms of Characteristics of Radio Receivers', Definition No. 202.
- (4) ROTHE, H., and DAHLKE, W.: 'Theory of Noisy Fourpoles', *Proceedings of the Institute of Radio Engineers*, 1956, **44**, p. 811.
- (5) BECKING, A. G. Th., GROENDIJK, H., and KNOL, K. S.: 'The Noise Factor of Four Terminal Networks', *Philips Research Reports*, 1955, **10**, p. 349.
- (6) HARRIS, I. A.: 'The Theory and Design of Coaxial Resistor Mounts for the Frequency Band 0–4000 Mc/s', *Proceedings I.E.E.*, Monograph No. 132 R, May, 1955 (103 C p. 1).
- (7) WOODS, D.: 'A Coaxial Millivoltmeter/Milliwattmeter for Frequencies up to 1 Gc/s' (to be published).
- (8) VLAARDINGERBROEK, M. T., KNOL, K. S., and HART, P. A. H.: 'Measurements on Noisy Fourpoles at Microwave Frequencies', *Philips Research Reports*, 1957, **12**, p. 324.
- (9) KOMPNER, R. *et al.*: 'The Transmission-Line Diode as a Noise Source at Centimetre Wavelengths', *Journal I.E.E.*, 1946, **93**, Part IIIA, p. 1436.
- (10) BENHAM, W. E., and HARRIS, I. A.: 'The Ultra High Frequency Performance of Receiving Valves' (Macdonald, 1957), Sections 6.1 and 10.4.
- (11) SMULLIN, L. D., and HAUS, H. A.: 'Noise in Electronic Devices' (Chapman and Hall, 1959), Chapter 4, p. 157.

#### (8) APPENDIX

##### (8.1) Transformation of Current in the Diodes

The transformation of current between the electrodes and the accessible diode connections cannot be compensated and must be determined. If the diode is considered equivalent to a capacitance  $C$  between the electrodes in series with a small inductance with a series resonant frequency  $f_0$ , the ratio of the mean-square noise current at the electrodes to that in a short-circuit across the accessible connections is expressed.

$$\Psi = [1 - (f/f_0)^2]^{-2}$$

for a narrow band of frequencies centred on  $f$ . If allowance is made for a series blocking capacitor of capacitance  $C_b$ , then

$$\Psi = [1 + C/C_b - (f/f_0)^2]^{-2} \quad (21)$$

A more accurate calculation based on the equivalent distributed-constant circuit of Fig. 6(b) leads to the result

$$\Psi = [C/C_b + (1 - a_c \phi_c \tan \phi_c) \cos \phi_v - a_v \phi_v \sin \phi_v]^{-2} \quad (22)$$

where  $\phi_v = \omega l_v/v$ ,  $\phi_c = \omega l_c/v$ ,  $a_v = C_v v/(Y_0 l_v)$  and  $a_c = C_v v/(Y_0 l_c)$ . The first series resonance occurs when  $1/\Psi = 0$ , i.e. when

$$(\cot \phi_v)/\phi_v = a_v/(1 - a_c \phi_c \tan \phi_c) \quad (23)$$

provided that  $l_c < l_v$ .

With a typical mounted diode, type E2790,  $l_v = 1.6$  cm,  $l_c = 0.8$  cm,  $C_v \approx 0.5$  pF,  $Z_{0c} \approx 50\Omega$ , and allowing for the open nature of the diode mount near the anode connection



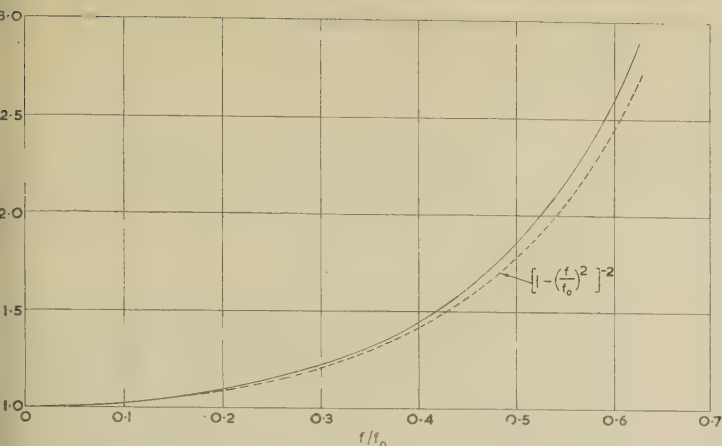


Fig. 8.—Correction factor for mean-square current transformation.

$l_v = 1.6 \text{ cm}$        $Z_{0v} = 180 \Omega$        $a_v = 1.68$   
 $l_c = 0.8 \text{ cm}$        $Z_{0c} = 50 \Omega$        $a_c = 0.94$

$v \approx 180 \Omega$ . Then  $a_v = 1.68$  and  $a_c = 0.94$ . In eqn. (23) it is found that  $\phi_v = 38.4^\circ$  for the first resonance and the corresponding frequency is  $f_0 = 2000 \text{ Mc/s}$ . The correction factor, plotted as a function of  $f/f_0$  with  $C_v$  infinite, is shown in Fig. 8. For comparison, the broken curve shows the correction factor based on the lumped circuit-element approximation. The first series-resonant frequency of the two diodes in the mount is determined with a standing-wave meter, varying the frequency of the supply until an impedance minimum was obtained at the mean position of the diodes. The value found was  $f_0 = 2040 \text{ Mc/s}$ . The value of  $C_b$  used was  $200 \text{ pF}$ , so that  $C_b = 0.005$  and  $(1 + C/C_b)^{-2} = 0.99$  gives the value of  $\Psi$  at the low-frequency end of the range.

### (8.2) Transit Angle Correction

When the transit time  $\tau$  of electrons in the saturated diode is not very small compared with the period of oscillation corresponding to the mid-band frequency, the noise from the diode is reduced. The factor  $\Phi$  that takes account of this, which is expressed as a function of the transit angle  $\theta = \omega\tau$ , has already been formulated theoretically and compared with experimental results.<sup>9</sup> The agreement found was satisfactory except for transit angles less than  $2 \text{ rad}$ , where the observed correction factor was appreciably less than the theoretical value. It is shown here that this departure can be explained by the effect of electrons scattered from the anode.

In the broadest meaning of the term, 'secondary emission' comprises elastically and inelastically reflected electrons as well as true secondary electrons. To a limited extent the three categories can be distinguished in an experimentally obtained graph of the energy distribution, although the division between inelastically reflected electrons and true secondary electrons is indefinite. For present purposes, the somewhat artificial division indicated in Fig. 9 is adopted, in which it is assumed that the inelastically reflected electrons have a roughly uniform distribution of kinetic energy from zero up to the energy of the primary electrons at the anode. When the anode voltage is not less than about  $100 \text{ V}$ , the contribution of the true secondary electrons to the induced fluctuations of current is not appreciable with small or moderate transit angles. Of the elastically reflected electrons, few actually reach the cathode because of their angular distribution about the direction normal to the electrodes.

Suppose the fraction  $s$  of the incident convection current at the anode is inelastically reflected or 'scattered' with a uniform

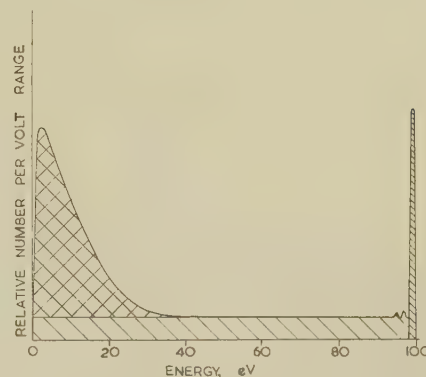


Fig. 9.—Energy distribution of secondary emission.

distribution of kinetic energy normal to the electrode surfaces from zero to  $eV$ , where  $V$  is the anode voltage. The fluctuations in the incident stream are present in proportion in the scattered stream, and it is clear that the latter fluctuations are correlated with those in the incident stream. From eqn. (6.15) of Reference 10, it can be shown that the excursions of the scattered electrons induce a current with a Fourier component related to the frequency range  $f$  to  $f + df$  by

$$\delta i = -\delta i_c (d_i/d)^{1/2} j\theta \gamma_4(\theta_s) e^{-j\theta_d}$$

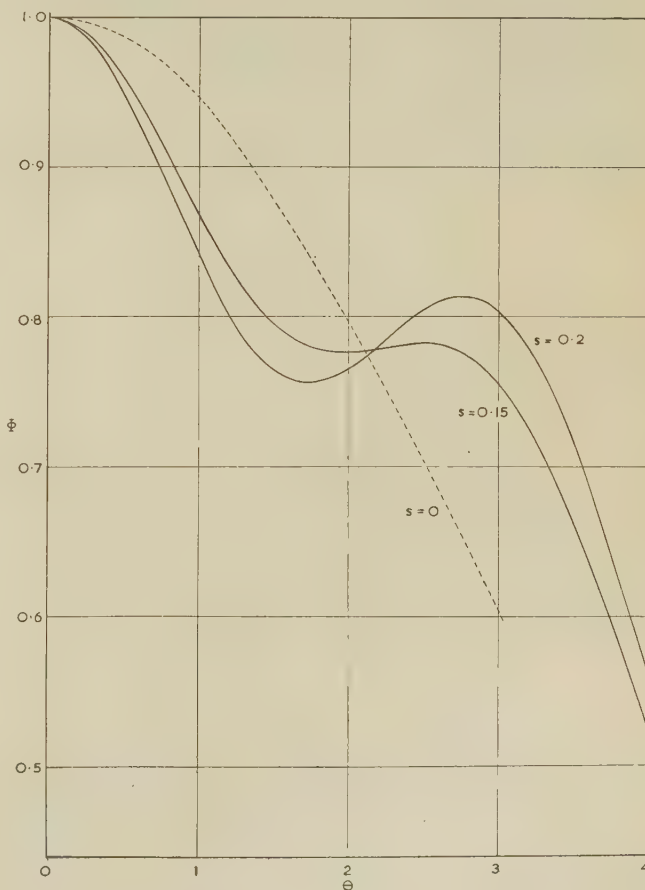


Fig. 10.—Transit-angle correction factor.

where  $\delta i_c$  is the convection current fluctuation at the cathode,  $d_t$  is the distance from the anode to the extremity of the excursion,  $d$  is the cathode-anode spacing and  $\theta_r$  is the transit angle of the excursion. The function  $\gamma_4$  is defined in Reference 10.

It is readily shown that  $d_t/d = \theta_t^2/\theta_d^2$ , where  $\theta_t$  is the transit angle to the extremity of the excursion, and  $\theta_r = 2\theta_t$ . For a given range of energy  $eU$  to  $e(U + dU)$  the proportion scattered is  $sdU/V$ , or  $2s\theta_t d\theta_t/\theta_d^2$ , where  $\theta_d$  is the transit angle for the whole distance  $d$ . Then, for all the scattered electrons,

$$\delta i = -\frac{4}{3}s \delta i_c e^{-j\theta_d} \int_0^{\theta_d} 2(\theta_t^3/\theta_d^4) j\theta_t \gamma_4(2\theta_t) d\theta_t$$

and with the correlated primary stream with the transit angle factor  $\gamma_3(\theta_d)$ ,

$$d\bar{i}^2 = 2eIdf \left| \gamma_3(\theta_d) - \frac{4}{3}s e^{-j\theta_d} \int_0^{\theta_d} 2(\theta_t^3/\theta_d^4) j\theta_t \gamma_4(2\theta_t) d\theta_t \right|^2 \quad (24)$$

The scattering of an electron is a random event which gives rise to additional fluctuations in the scattered stream. These fluctuations are of the nature of partition noise. Their contribution is

$$d\bar{i}^2 = 2eIdf \cdot s(1-s)^{\frac{8}{3}} \int_0^{\theta_d} (\theta_t^5/\theta_d^6) |2j\theta_t \gamma_4(2\theta_t)|^2 d\theta_t \quad (25)$$

The resultant mean-square fluctuation is the sum of eqns. (24) and (25). After substituting real notation for the functions  $\gamma_3$

and  $\gamma_4$  and carrying out the integration, the transit-angle correlation factor is found to be

$$\begin{aligned} \Phi = & \left\{ \frac{2}{\theta^2} (\cos \theta + \theta \sin \theta - 1) \right. \\ & - \frac{2s}{\theta^4} [(1 + \theta^2) \cos \theta - (1 - \theta^2) \cos 3\theta \\ & \quad \left. - \frac{2}{3}\theta^3 \sin \theta - 2\theta \sin 3\theta] \right\}^2 \\ & + \left\{ \frac{2}{\theta^2} (\sin \theta - \theta \cos \theta) \right. \\ & - \frac{2s}{\theta^4} [\frac{2}{3}\theta^3 \cos \theta + \theta^2 (\sin \theta + \sin 3\theta) \\ & \quad \left. + 2\theta \cos 3\theta + \sin \theta - \sin 3\theta] \right\}^2 \\ & + \frac{8s(1-s)}{\theta^6} \left( \frac{9}{4} + \theta^2 + \frac{\theta^4}{2} - \frac{9}{4} \cos 2\theta \right. \\ & \quad \left. - \frac{9}{2} \theta \sin 2\theta + \frac{7}{2} \theta^2 \cos 2\theta + \theta^3 \sin 2\theta \right) \quad (26) \end{aligned}$$

Curves have been plotted for the values 0, 0.15 and 0.2 of  $s$  and are shown in Fig. 10. The results are in broad agreement with the experimental results given by Kompfner and others and by Duval.<sup>11</sup>

In the diode type E2790, saturated with an anode voltage of 100 V, the transit time is estimated to be about  $2 \times 10^{-10}$  sec which with  $s = 0.15$ ,  $f_0 = 2000$  Mc/s and Fig. 8, leads to the theoretical curve shown in Fig. 7. The estimation of transit time in a diode with a V-shaped filament in a cylindrical anode is difficult, and it is probably inaccuracy in this estimate that explains the difference between the experimental and theoretical curves in Fig. 7.



## CRYSTAL DETECTORS TO COVER THE FREQUENCY BAND 26–40 Gc/s

By H. V. SHURMER, M.Sc., Ph.D., Associate Member.

*(The paper was first received 14th April, and in revised form 26th June, 1961.)*

## SUMMARY

After referring to unsuccessful attempts based on a wafer-type mount, a coaxial unit is described which operates over the frequency band 26–40 Gc/s, and is mechanically interchangeable with the American crystal 1N 53. The new crystal employs a silicon point contact of high sensitivity, and the mount was designed to give the best v.s.w.r. over the entire bandwidth.

The design technique is described in detail and experimental data are summarized. Notwithstanding some difficulty in manufacturing to the required sensitivity, a broad-band design has been achieved and the capabilities of Q-band detector crystals have been gauged.

## (1) INTRODUCTION

Hitherto the only British crystal valve available at Q-band has been the waveguide plug-in unit, now designated CV 2391/2, and intended primarily as a mixer and of limited bandwidth.<sup>1</sup> The present work arose from a proposal to use for a detector crystal a silicon point contact similar to that of the CV 2391/2 and to design the detector to give the best match over the whole of the Q-band (26–40 Gc/s).

It was at first thought that a waveguide plug-in arrangement might be the most suitable for the detector and, on account of the relatively low impedance of the point contact, it was proposed to form the crystal unit in ridge waveguide to facilitate broad-band matching. In addition to possessing lower impedance, ridge waveguide has a lower cut-off frequency and greater separation of higher modes than a plain rectangular waveguide of the same width and height.<sup>2</sup>

## (2) LOW-IMPEDANCE WAVEGUIDE WAFER MOUNTS

Some of the waveguide wafer-type mounts which were made in the early stages of this work are shown in Fig. 1. These units were designed to match, in characteristic impedance ( $72\Omega$ ) and cut-off frequency (3.14 cm), a double-ridge rectangular waveguide which was available.

The holes seen in each case at three of the corners fitted into locating spigots in the holder, and defined the orientation of the mount. A spring-loaded short-circuiting backing plate was brought into position after inserting the mount into the holder.

In one method of construction, the wafers were made in two halves so that the waveguide aperture could be formed by a filling operation. With the dumb-bell structures, jig drilling was as possible and the slots were milled from solid blanks.

In those units in which the aperture was partially or completely filled with glass, a hole was formed perpendicular to the axis of the aperture to accommodate the rectifying element, the radio output being taken coaxially from the base of the wafer.

In order to illustrate the principles involved, the r.f. design is discussed in Section 10.1 for a rectangular ridge wafer unit with the slotted section filled with glass. A 3-stage video output choke, made integral with the wafer, is discussed in Section 10.2.

Written contributions on papers published without being read at meetings are invited for consideration with a view to publication.  
Dr. Shurmer is with Associated Electrical Industries (Rugby), Ltd.

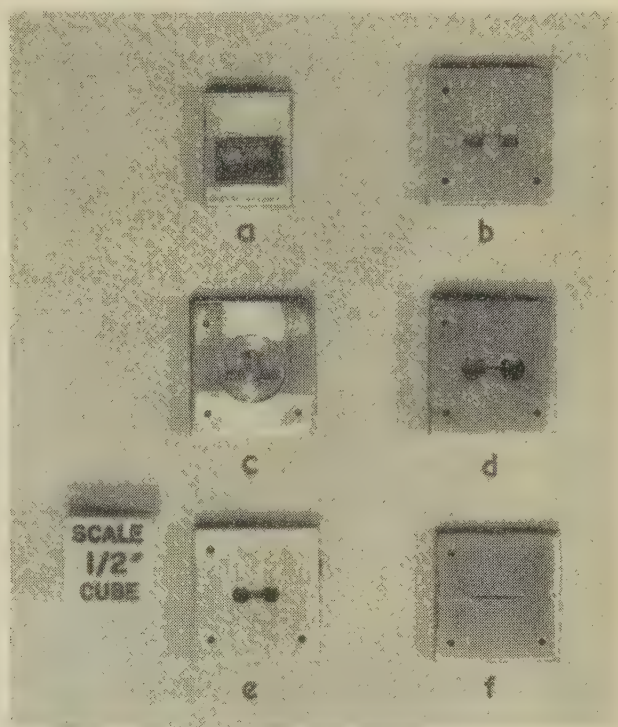


Fig. 1.—Waveguide plug-in mounts.

- (a) Existing mixer CV 2391.
- (b) Ridge structure, rectangular.
- (c) As for (b), but incorporating mica window.
- (d) Dumb-bell structure.
- (e) As for (d) but slot sealed in glass.
- (f) Low-impedance plain rectangular structure in glass.

Several units were adjusted using air-filled rectangular windows, but r.f. measurements on these gave results which could not be repeated consistently. This was attributed to difficulty in maintaining good electrical contact at the waveguide aperture. If it had proved possible to overcome this trouble, there would have remained the greater task of devising a satisfactory r.f. choking system for wafers formed in ridge waveguide and also sealed hermetically. These problems appeared intractable and led to the abandonment of the wafer form of construction in favour of a coaxial design, which had been started in parallel and to which more conventional techniques could be applied.

## (3) COAXIAL CRYSTAL MOUNT

Fig. 2 shows schematically the arrangement for the coaxial form of construction together with its equivalent circuit, the details quoted relating to the final design.

The body of the mount is machined in tellurium copper. A central pin of silver alloy is supported by a ceramic bead, the end of the pin external to the mount being shaped to plug into the inner of a coaxial line. On the internal side, the pin carries

a cat's whisker of molybdenum-tungsten alloy. This is crimped for resilience and electrochemically pointed to press against the prepared surface of a silicon cube, carried by a plunger inserted from the rear of the mount.

The unit is mechanically interchangeable with an American mixer crystal (IN 53).

### (3.1) R.F. Design

The microwave circuit within the crystal mount comprises several sections of transmission line, to which standard theory was applied, including the discontinuity capacitances discussed by Whinnery *et al.*<sup>3</sup> Possible errors due to proximity effects at the discontinuities were neglected.

The design procedure was to consider the normalized admittance over the specified bandwidth at successive planes of transition between sections, starting at the plane of contact of the cat's whisker and silicon cube.

The value used for the admittance of the point contact was that which had been derived for the original waveguide wave type crystal. This had first to be normalized to the characteristic admittance  $Y_{01}$  for the section of line of which the cat's whisker forms the inner conductor. The value of  $Y_{01}$  was obtained by fixing the cat's-whisker diameter on the basis of satisfactory experience with the earlier mixer and adopting a tentative figure for the diameter of the cylindrical cavity surrounding it.

The contact admittance thus normalized is shown for the

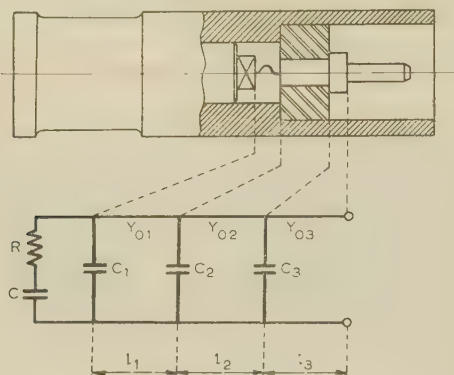


Fig. 2.—Coaxial mount. Schematic and equivalent circuit.

$R = 50\Omega$	$C = 0.05 \text{ pF}$	$Y_{01} = 1/222 \text{ mho}$
$l_1 = 0.064 \text{ cm}$	$C_1 = 0.017 \text{ pF}$	$Y_{02} = 1/35 \text{ mho}$
$l_2 = 0.373 \text{ cm}$	$C_2 = 0.044 \text{ pF}$	$Y_{03} = 1/61 \text{ mho}$
$l_3 = 0.051 \text{ cm}$	$C_3 = 0.021 \text{ pF}$	

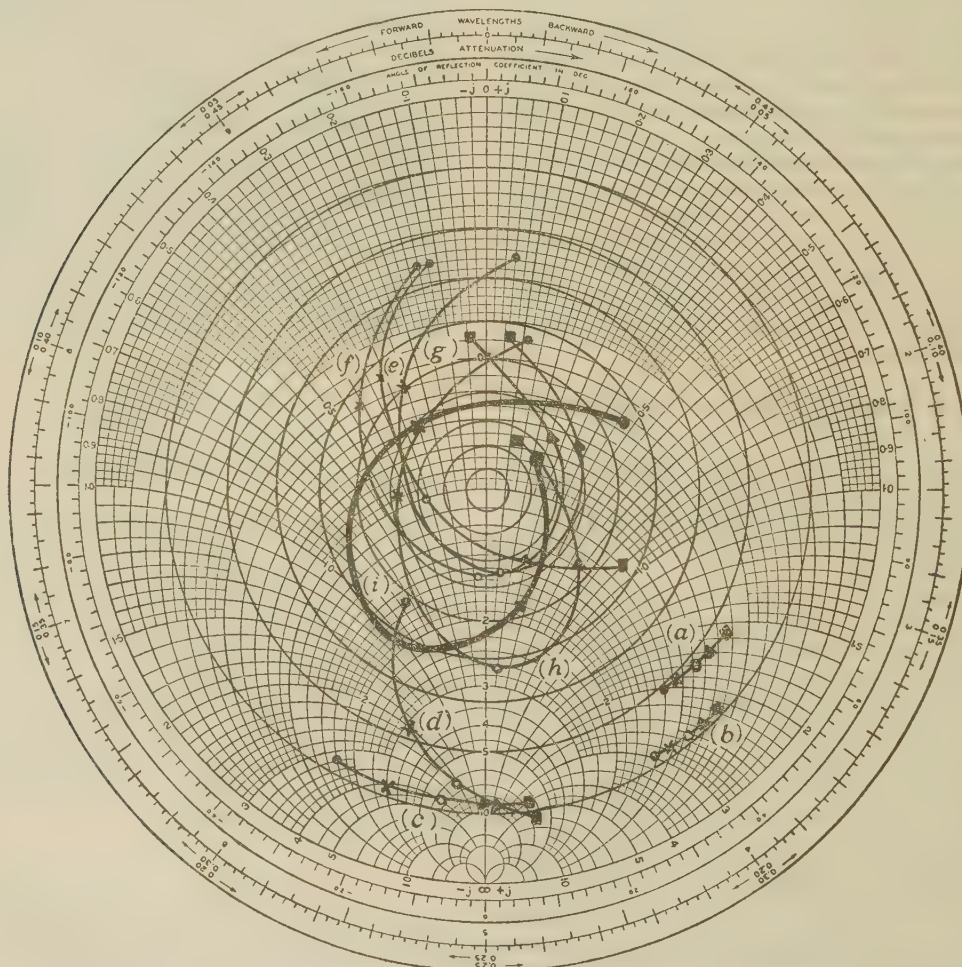


Fig. 3.—Normalized admittance plots at successive planes.

- 7.5 mm
- × 8.5 mm
- 9.5 mm
- ▲ 10.5 mm
- 11.5 mm



ave band 7.5-11.5 mm in Fig. 3, curve (a). In order to allow for the parallel-capacitance effects of discontinuities, it is convenient to use normalized admittance rather than impedance, and this is done throughout the design.

A discontinuity capacitance  $C_1$ , calculated for an inner line which terminates abruptly, was assumed to operate in parallel with the RC circuit representing the point contact. Correcting the normalized admittance of the contact for this capacitance gave curve (b).

The corresponding locus at the other end of the cat's whisker is given by curve (c). This is obtained by rotating points in curve (b) through angles corresponding to the electrical length of the cat's whisker at each wavelength.

The cat's-whisker length  $l_1$  was chosen so that curve (c) straddled the axis, which implied that at some point in the wave band, the associated inductance tuned out the capacitance of the contact. For this purpose it was found satisfactory to use the overall cat's-whisker length.

The next step in the design was to allow for the discontinuity capacitance at the plane of the internal face of the ceramic bead. The diameter of the inner conductor, which is the only disposable variable in fixing this capacitance, also determines the admittance transformations at both ceramic faces, as well as the discontinuity capacitances. Its choice was therefore a matter for some trial.

Having fixed this diameter, the discontinuity capacitance  $C_2$  at the internal face of the ceramic was obtained. By taking this into account, curve (d) was obtained from curve (c). Curve (e) was obtained by renormalizing to the characteristic admittance  $Y_{02}$  of the ceramic-filled section. The thickness of the ceramic bead was determined in the manner outlined below.

The transformation at the plane of the outer ceramic face results in an increase in all values of normalized admittance by the ratio of characteristic admittance of the ceramic-filled section to that immediately outside, which was fixed by the stipulated outline dimensions. The shape of curve to be aimed at after this transformation was one contained by the smallest circle about the centre of the diagram. This implied that, before transformation, the normalized admittance locus was to be of as compact a shape as possible and situated at the appropriate distance above the centre.

The ceramic thickness was chosen so as to give the desired final locus, derived in three stages. The first was to rotate points in curve (e) through angles appropriate to the electrical lengths of the ceramic thickness  $l_2$  at the various wavelengths, giving curve (f). The second stage was to allow for the discontinuity capacitance  $C_3$ , hence obtaining curve (g). Renormalizing points in this curve to the characteristic admittance  $Y_{03}$  of the section immediately outside the ceramic gave the desired locus [curve (h)].

In order to refer the admittance to a specified plane, which was at the step on the inner conductor external to the mount, one further rotation of points in curve (h) was necessary; this corresponds to electrical lengths associated with the distance  $l_3$  from the ceramic to the step. The locus thus obtained is curve (i).

By this design, it is seen that, over the bandwidth 7.5-11.5 mm, the minimum value which is to be expected for the v.s.w.r. in the input feeder is 0.37.

### (3.2) Experimental Confirmation of Admittance Locus

Measurements on batches of experimental crystals have shown satisfactory agreement with the admittance locus obtained by design. A typical plot referred to the reference plane of the shoulder on the pin is shown in Fig. 4, which also reproduces curve (i) of Fig. 3 for comparison.

### (3.3) Effect of Component Tolerances on R.F. Admittance

A summary of calculations which were made to determine the effect of component tolerances on the admittance loci is given below. The spread in calculated r.f. admittances was in all cases greatest at the highest frequency (corresponding to 7.5 mm), to which the quoted results apply.

*Cat's-whisker Length.*—A variation of 0.002 in corresponded to a change of about the radius of a 0.75 v.s.w.r. circle.

*Ceramic-Bead Thickness.*—For a variation of 0.002 in, a change again approximately equal to the radius of a 0.75 v.s.w.r. circle was calculated.

*Ceramic-Bead Permittivity.*—Variations of 2% in the permittivity were calculated to give changes equal to the radius of a 0.9 v.s.w.r. circle.

*Length of Pin Shoulder.*—It was calculated that an admittance change of slightly less than the radius of a 0.9 v.s.w.r. circle would result from a variation of 0.002 in in the length of the pin shoulder.

### (3.4) Crystal Holder

A waveguide to coaxial-line crystal holder, using a tapered ridge and transition of the type described by Cohn,<sup>4</sup> was constructed for test purposes and is illustrated in Fig. 5.

The broad-band properties of this holder were, however, not adequate for admittance measurements except by matching to the coaxial-line output of the crystal socket at each test frequency, and it is believed that for full utilization of the broad-band properties of the crystal a completely coaxial system may prove necessary.

The design of the radial section of the choke which provided d.c. isolation for the crystal is of interest and is described in Section 10.3.

### (4) EXPERIMENTAL DATA FOR NORMAL OPERATION

Measurements of figure of merit at 9.5 mm wavelength and of video resistance are given in the form of histograms in Figs. 6 and 7, respectively. They relate to 420 crystals as received for test, and the figure of merit represents the sensitivity measured in a holder matched to a 61  $\Omega$  line. The values are not corrected for the power loss due to mismatch of the crystal. The figure of merit is taken as the product of current sensitivity and the square root of the video resistance.

The figure of merit is seen to peak at about 20, but there is a large spread and sensitivities up to three times this figure have been observed. Video resistance peaks at about 7 k $\Omega$ , but for the majority of crystals it occurs above this value.

### (5) TESTS OF RUGGEDNESS

Tests of ruggedness were made on batches of approximately 50 crystals after first establishing the repeatability of measurements of the various parameters made on successive days. The tests were concerned with resistance to burn-out, vibrational stability, tensional stability, tropical exposure and temperature cycling.

#### (5.1) Resistance to Burn-Out

Tests made of resistance to r.f. overload at 8.6 mm with 0.25  $\mu$ s pulses, 1000 pulses/s, showed significant changes in r.f. admittance to have occurred after 1 h at a peak power of 10 mW, care having been taken to screen crystals from magnetron leakage power.

However, the sensitivity remained within specification in all cases. The changes in normalized admittance resulting from the exposure exceeded the radius of a 0.6 v.s.w.r. circle for only 4% of the crystals.

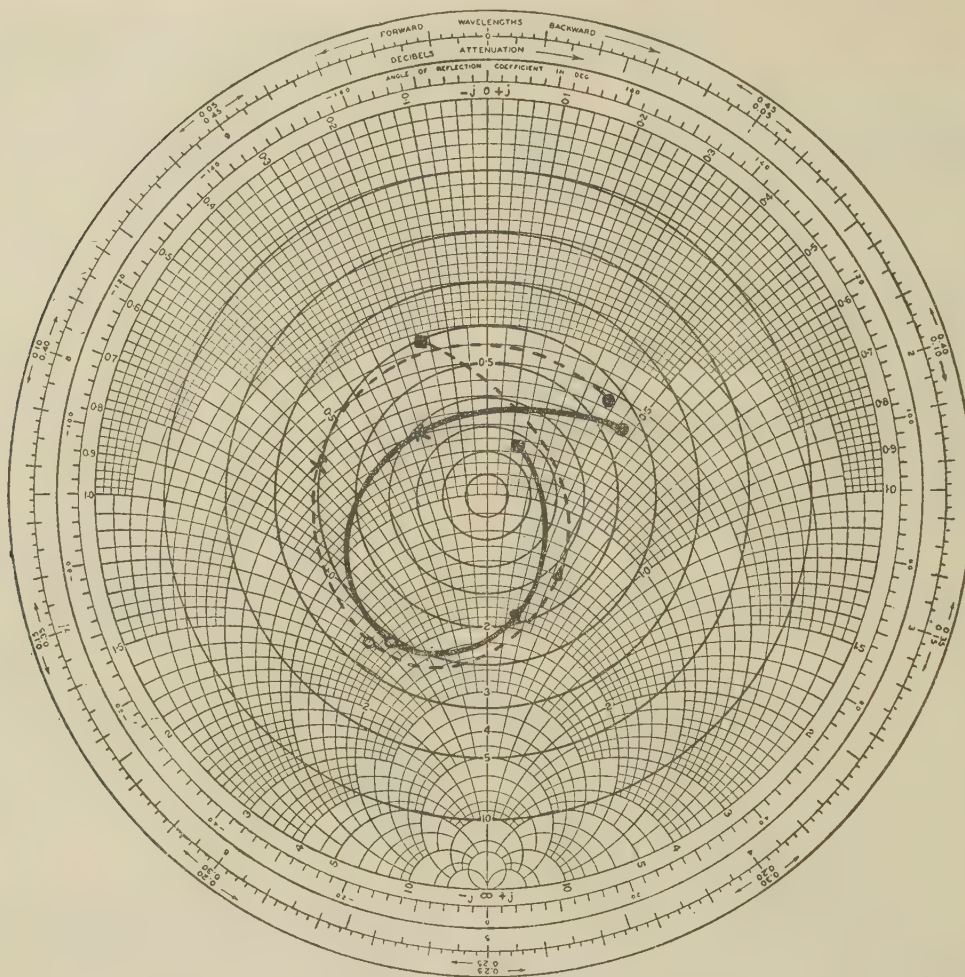


Fig. 4.—Comparison between measured and predicted admittance loci.

● 7.5 mm  
 × 8.5 mm  
 ○ 9.5 mm  
 ▲ 10.5 mm  
 ■ 11.5 mm

Measured ———  
 Predicted ———

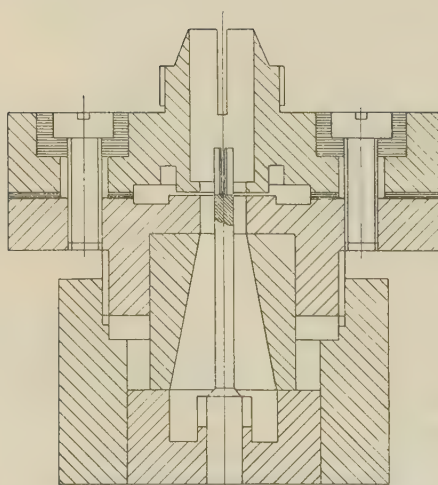


Fig. 5.—Coaxial crystal holder.

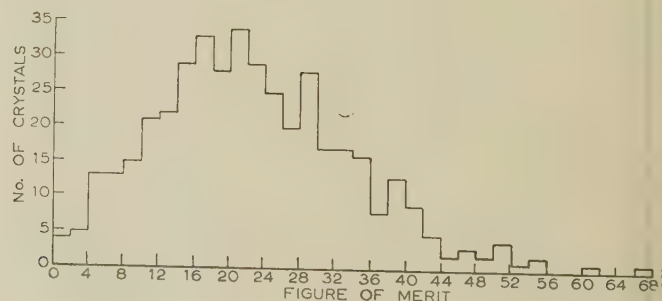


Fig. 6.—Figure of merit.

### (5.2) Vibrational Stability

Vibration at 50c/s with 12g peak amplitude was applied for 10min in each of two mutually perpendicular directions, one of these being along the axis. One unit only showed serious deterioration.

### (5.3) Tensional Stability

An axial tension on the centre pin was applied for 10sec at successively increasing levels, breakages occurring between 14 and 19 lbf. It is considered that crystals in service will not



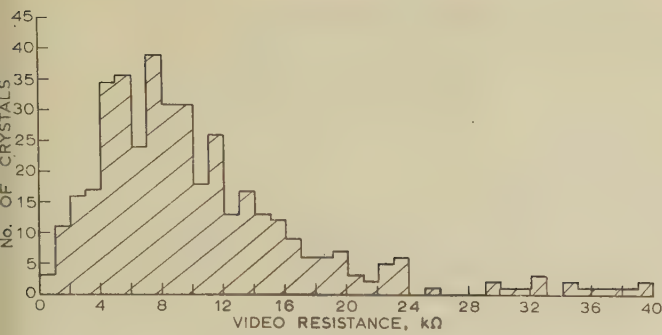


Fig. 7.—Video resistance.

be subjected to a tension of more than 2 lbf, and changes in electrical characteristics at this level were slight.

#### (5.4) Tropical Exposure

Climatic testing was done on the basis of the Tropical Exposure Test in Inter-Service Specification K114. It was found that units sealed by a soldering technique survived 7 cycles without appreciable deterioration, but that at the end of 84 cycles the average sensitivity was down by a factor of two.

#### (5.5) Temperature Cycling

Crystals subjected to six cycles of temperature over the range  $-40^{\circ}\text{C}$  to  $+70^{\circ}\text{C}$  showed changes in characteristics, but there were no catastrophic failures.

#### (6) NOTE ON MANUFACTURE

The point contact in VX 4150 is inherently more sensitive than hitherto used at X-band, with a figure of merit of about 40 (e.g. in CV 2355/6/7 crystals). A figure of merit of 15 at 9.5 mm would correspond to about 170 at 3.2 cm, since the degrading effect of the barrier capacitance increases approximately as the square of the operating frequency.

A figure of merit of 15 for the VX 4150 is therefore correspondingly more difficult to achieve, point-to-point variations in the silicon surface properties having much greater importance. Searching for points having the required properties is tedious, and the effort to adjust these crystals is, in fact, several times greater than for CV 2355/6/7.

#### (7) CONCLUSIONS

It is concluded that the coaxial form of construction gives satisfactory electrical performance over the bandwidth 26-40 Gc/s, using a design technique which is capable of scaling to higher or lower frequencies. The degree of ruggedness is shown to be adequate for normal applications.

Wafer-type crystals in ridge waveguide proved unsatisfactory because of r.f. choking difficulties.

Development of the semiconducting contact to give high sensitivity more consistently is desirable and the problem of a broad-band holder deserves further attention.

#### (8) ACKNOWLEDGMENTS

The author thanks his colleagues in the A.E.I. Research Laboratory, Rugby, for advice and assistance.

#### (9) REFERENCES

- (1) DITCHFIELD, C. R.: 'Crystal-Mixer Design at Frequencies from 20000 to 60000 Mc/s', *Proceedings I.E.E.*, Paper No. 1548, November, 1953 (100, Part III, p. 365).

- (2) COHN, S. B.: 'Properties of Ridge Waveguide', *Proceedings of the Institute of Radio Engineers*, 1947, 35, p. 783.
- (3) WHINNERY, J. R., JAMIESON, H. W., and ROBBINS, T. E.: 'Coaxial-Line Discontinuities', *ibid.*, 1944, 32, p. 695.
- (4) COHN, S. B.: 'Design of Simple Broad-band Waveguide—to Coaxial Line Junctions', *ibid.*, 1947, 35, p. 920.
- (5) WHINNERY, J. R., and JAMIESON, H. W.: 'Equivalent Circuits for Discontinuities in Transmission Lines', *ibid.*, 1944, 32, p. 98.
- (6) MIHRAN, T. G.: 'Closed and Open Ridge Waveguide', *ibid.*, 1949, 37, p. 640.
- (7) SCHELKUNOFF, S. A.: 'Electromagnetic Waves' (Van Nostrand, 1943), p. 269.
- (8) JAHNKE, E., and EMDE, F.: 'Tables of Functions with Formulae and Curves' (Dover Publications, 1943) p. 206.

#### (10) APPENDICES

##### (10.1) Design of Rectangular Double-Ridge Wafer Unit with Slotted Section Filled with Glass

The wafer unit was required to have the same impedance over the frequency band as the input feeder (of double-ridge waveguide), which necessitated the same characteristic impedance at infinite frequency and the same cut-off frequency for the fundamental mode ( $H_{10}$ ).

The present example describes the design of waveguide section within the wafer to meet specified values for the impedance and cut-off frequency when the wafer is of double-ridge construction with the ridge section filled with glass—a form suggested by the need to have the semiconducting unit within a hermetically-sealed enclosure.

An estimate is made of the importance of higher-order modes, and the maximum wafer thickness is found which can be used without risk of resonances occurring within the frequency band.

As a basis for design, the cross-sectional dimensions of the air-filled input feeder are considered, and are shown in Fig. 8. The cut-off frequency for the  $H_{10}$  mode and characteristic impedance at infinite frequency are first determined.

In the method of calculating cut-off frequencies described by Cohn,<sup>2</sup> the cross-section is treated as an infinitely-wide parallel-strip transmission line short-circuited at two points. With reference to Fig. 8, the sum of admittances across XX is equated to zero to give all the  $H_{m0}$  cut-off frequencies, using the equivalent circuit of (b) for  $m$  odd and that of (c) for  $m$  even. For  $m$  odd the equation is

$$-Y_{01} \cot \theta_1 + B_c + Y_{02} \tan \theta_2 = 0$$

which may be expressed in the form

$$\cot \theta_1 - \frac{b_1}{b_2} \tan \theta_2 - \frac{B_c}{Y_{01}} = 0 \quad (1)$$

since

$$\frac{Y_{02}}{Y_{01}} = \frac{b_1}{b_2}$$

For the dimensions of Fig. 8,  $\theta_1 = 100^\circ/\lambda'_c$  and  $\theta_2 = 37.8^\circ/\lambda'_c$ , where  $\lambda'_c$  is the wavelength in free space corresponding to the  $H_{10}$  cut-off in ridge waveguide. The term  $B_c/Y_{01}$ , calculated by the method of Whinnery and Jamieson,<sup>5</sup> is found to be  $0.966/\lambda'_c$ . Substituting these values into eqn. (1) and solving for  $\lambda'_c$  gives a first root at 3.14 cm.

The characteristic impedance for the  $H_{10}$  mode is obtained from the formula derived by Cohn and modified by Mihran:<sup>6</sup>

$$Z_{0\infty} = \frac{2 \times 377}{\frac{2C_d \cos \theta_2}{\epsilon \epsilon_0} + \frac{\lambda'_c}{\pi b_2} \left( \sin \theta_2 + \frac{b_2}{b_1} \cos \theta_2 \tan \frac{\theta_1}{2} \right)} \quad (2)$$

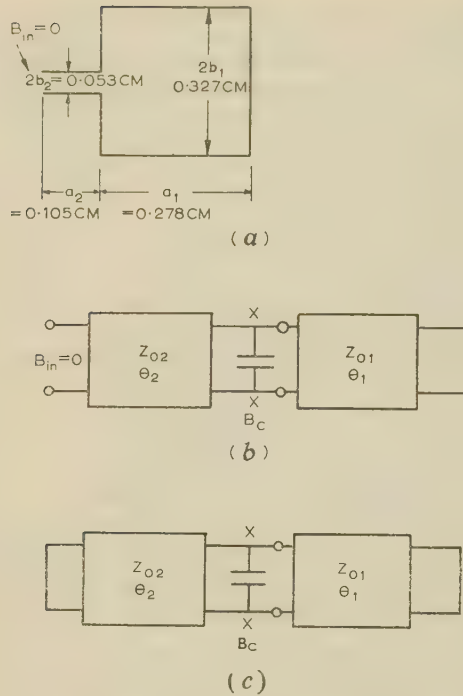


Fig. 8.—Equivalent circuit for ridge waveguide.

$$\theta_1 = a_1/\lambda_e \quad \theta_2 = a_2/\lambda'_e$$

where  $C_d$  is the discontinuity capacitance per centimetre associated with the ridge and depends on the ratio  $b_1/b_2$ . For the dimensions of Fig. 8,  $C_d$  is found, as described by Whinnery and Jamieson, to be  $0.0415\text{ pF/cm}$ .  $\epsilon_0$  is taken as  $0.0885\text{ pF/cm}$ . Eqn. (2) applied to these dimensions gives  $Z_{0\infty} = 72\Omega$ .

We now consider the effect of filling the ridge section only with glass of permittivity  $\epsilon = 5.0$ . This has the effect of increasing both the characteristic admittance and the electrical angle in the ridge section by  $\sqrt{\epsilon}$ . Eqn. (1) then becomes:

$$\cot \theta_1 - \frac{b_1}{b_2} \sqrt{\epsilon} \tan \theta'_2 - \frac{B_c}{Y_{01}} = 0 \quad (3)$$

where  $\theta'_2 = \sqrt{\epsilon} \theta_2$ .

Solving eqn. (3) in terms of  $\lambda'_c$  gives a first root at  $6.21\text{ cm}$ . In order that the solution shall give  $\lambda'_c = 3.14\text{ cm}$ , as for the air-filled ridge, it is necessary to change the ratio  $b_1/b_2$ , and it is found that this is required to be  $1.40$ . It will be seen from eqn. (2) that, if  $b_1/b_2$  is maintained constant as  $b_2$  is varied, the characteristic impedance  $Z_{0\infty}$  may be altered without changing the cut-off wavelength.

Eqn. (2) is used to give the value of  $2b_2$  corresponding to  $Z_{0\infty} = 72\Omega$ . The value of  $C_d$  is now that corresponding to a ratio of  $1.40$   $b_1/b_2$  and  $\theta_2$  is replaced by  $\theta'_2$ . The required value of  $2b_2$  is thus found to be  $0.122\text{ cm}$ , and, from the ratio,  $2b_1 = 0.172\text{ cm}$ .

We now consider higher modes which may be propagated in such a waveguide.

The  $H_{20}$  mode cut-off wavelength  $\lambda'_{c20}$  is obtained, neglecting discontinuity capacitance, by the first root of the equation

$$-\tan \theta_1 + \frac{1}{\sqrt{\epsilon}} \frac{b_2}{b_1} \tan \theta'_2$$

and is found to be  $0.98\text{ cm}$ .

The  $H_{30}$  mode cut-off wavelength  $\lambda'_{c30}$  is obtained, again

neglecting discontinuity capacitance, by the third root of the equation

$$\cot \theta_1 - \sqrt{\epsilon_1} \frac{b_1}{b_2} \tan \theta_2 = 0$$

which is found to be  $0.622\text{ cm}$ . It is thus seen that the  $H_{30}$  mode is not propagated in the frequency band  $24-40\text{ Gc/s}$ .

If the waveguide is without asymmetry, even-order modes will not be launched and therefore trouble from modes of higher order than the fundamental would appear unlikely.

In order to avoid the possibility of resonance effects within the crystal wafer, it is desirable to make its thickness less than a half-wavelength at the highest frequency in the band to be covered, i.e. that corresponding to  $7.5\text{ mm}$ .

This critical thickness is given, for the  $H_{10}$  mode, by

$$t = \frac{\lambda}{2\sqrt{[1 - (\lambda/\lambda_c)^2]}}$$

Substituting  $\lambda = 0.75\text{ cm}$  and  $\lambda'_c = 3.14\text{ cm}$  gives  $t = 0.385\text{ cm}$ .

Similarly, for the  $H_{20}$  mode, the critical thickness is found to be  $0.58\text{ cm}$ , which is a larger value. The figure corresponding to the  $H_{10}$  mode is therefore the value to be adopted.

In practice, a hole normal to the axis of the waveguide is required in the glass-filled slot to allow for insertion of the semi-conducting element, but the effect of neglecting this in the calculations is probably not serious. The actual impedance would, however, be rather higher and the cut-off wavelength slightly less than that calculated.

### (10.2) Three-Stage Video Choke

The video output line from the waveguide mount was required to incorporate a choke such that the power absorbed in this line would not exceed 10% of the power in the waveguide for any frequency in the band  $7.5-11.5\text{ mm}$  and for mismatch on the output cable between  $0.33$  and  $3.00$ .

It was decided that a 3-stage coaxial choke would be employed for this purpose and made an integral part of the crystal mount. Each stage of the choke is  $\lambda/4$  long at mid-band and the dimensions eventually chosen led to the equivalent circuit shown in Fig. 9. The properties of this circuit are discussed below.

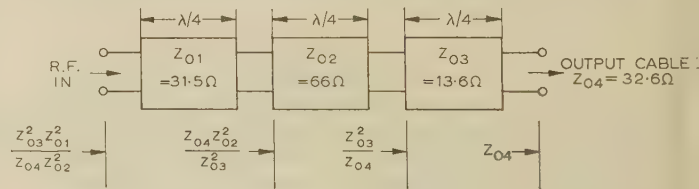


Fig. 9.—Equivalent circuit at mid-band for 3-stage video choke.

We consider the effect at mid-frequency and the extremes of the band in turn of both the matched condition at the cable and mismatches of  $0.33$  and  $3.00$ .

$\lambda = 9.5\text{ mm}$

$$(a) \text{ Matched Condition } Z_{in} = \frac{Z_{03}^2 Z_{01}^2}{Z_{04} Z_{02}} = 1.30\Omega$$

$$(b) \text{ 3 : 1 Mismatch } Z_{in} = \frac{Z_{03}^2 Z_{01}^2}{3 Z_{04} Z_{02}} = 0.43\Omega$$

$$(c) \text{ 1 : 3 Mismatch } Z_{in} = \frac{3 Z_{03}^2 Z_{01}^2}{Z_{04} Z_{02}} = 3.90\Omega$$



For frequencies other than mid-band, the formula used for  $\lambda/4$  sections does not apply. It is then necessary to consider the impedance at successive planes from the output cable to the r.f. input to the choke, using the Smith impedance diagram. The results obtained by this means for 7.5 and 11.5 mm are as follows:

$\lambda = 7.5 \text{ mm}$	
(a) Matched Condition	$Z_{in} = 1.89 + 16.2j \Omega$
(b) 3 : 1 Mismatch	$Z_{in} = 0.85 + 18.0j \Omega$
(c) 1 : 3 Mismatch	$Z_{in} = 4.73 + 16.1j \Omega$
$\lambda = 11.5 \text{ mm}$	
(a) Matched Condition	$Z_{in} = 1.89 - 17.6j \Omega$
(b) 3 : 1 Mismatch	$Z_{in} = 0.95 - 18.0j \Omega$
(c) 1 : 3 Mismatch	$Z_{in} = 5.35 - 16.7j \Omega$

The maximum input resistance ( $5.35 \Omega$ ) which occurs in the worst condition represents a power loss of only  $5.35/(72 + 5.35)\%$  i.e.  $6.9\%$ , assuming the crystal matches the ridge-waveguide impedance of  $72 \Omega$ .

### (10.3) Design of Radial Section of Choke for Coaxial Crystal Holder

The design of the radial section of the choke used in the coaxial crystal holder is described below.

We consider uniform cylindrical waves in a non-dissipative medium bounded by two cylinders  $\rho = a$  and  $\rho = b$ , where  $b > a$ . The condition which applies to the radial part of the choke is that the impedance at  $a$  is zero when that at  $b$  is infinite,

looking from  $a$  to  $b$ . The problem is to find the value of  $b$  for a given value of  $a$ .

Using the notation of Schelkunoff<sup>7</sup> the requirement of infinite impedance at  $b$  leads to the following expression for the input impedance:

$$Z_{\rho}(a) \propto \frac{N_0(\beta a)J_1(\beta b) - J_0(\beta a)N_1(\beta b)}{N_1(\beta a)J_1(\beta b) - J_1(\beta a)N_1(\beta b)}$$

For  $Z_{\rho}(a) = 0$ ,  $N_0(\beta a)J_1(\beta b) - J_0(\beta a)N_1(\beta b) = 0$

or  $J_0(\beta a)/N_0(\beta a) = J_1(\beta b)/N_1(\beta b)$ .

Solutions to this equation are given by Jahnke and Emde<sup>8</sup> for varying values of the ratio  $b/a$ .

The first root is given by

$$\beta a = \frac{0.5}{k-1} \pi(1 + \alpha)$$

or  $1 + \alpha = 1.1(k-1)$

by substituting  $\beta = \frac{2\pi\sqrt{\epsilon}}{\lambda}$  and taking  $\lambda = 1.0 \text{ cm}$ ,  $a = 0.114 \text{ cm}$ ,  $\epsilon = 5.8$  (for mica).

The value of  $k$  which satisfies the above equation is found to be  $1.805$ , giving  $b = 0.206 \text{ cm}$ .

An approximation to this solution is obtained by assuming that  $(b-a) = \lambda/4$  for a plane wave travelling in the medium of permittivity  $\epsilon$ . For the case considered, this would be  $0.25/\sqrt{5.8} \text{ cm}$ , i.e.  $0.104 \text{ cm}$ , giving  $b = (0.114 + 0.104) \text{ cm}$ , i.e.  $0.218 \text{ cm}$ .

## SWITCHING ON-OFF TYPE FILAMENT EMISSION REGULATOR

By A. F. NAGY, M.E., M.Sc., Graduate, and H. B. NIEMANN, B.E.

(Communication received 14th March, 1961.)

Ionization gauges, small spectrometers and similar devices are being widely used in rocket and satellite-borne experiments to measure pressure, temperature, density and composition of the upper atmosphere. For the proper operation of these instruments the filament emission current must be kept constant over a wide range of ambient conditions, and to achieve this a filament regulator is generally necessary. A number of transistorized series-type regulators have been described,<sup>1,2</sup> and such regulators have been successfully used in this laboratory. However, these circuits are inefficient, as a large fraction of the power from the d.c. supply is lost (dissipated) in the series transistor, thus increasing the energy requirements of the supply and also creating a secondary problem in heat dissipation. In certain applications—especially in rocket and satellite instrumentation where maximum efficiency is required—a more efficient circuit is preferable. A switching-type regulator was therefore developed, as it has been pointed out<sup>3</sup> that when transistors are operated in an on-off manner the power dissipated in the controlling transistor is only a small fraction of the peak load power, whereas under linear operation the dissipation is

equal to or greater than the load power. Such a filament regulator is described.

### DESCRIPTION OF THE CIRCUIT

The typical beam current for Bayard-Alpert type ionization gauges used in high-altitude research is of the order of  $100 \mu\text{A}$ . Using this value as a guide, a switching-type filament regulator was designed. Fig. 1 is the circuit diagram of this regulator. It is basically an asymmetric free-running multivibrator with controllable on-off periods. The thermal time-constant of the filament is large (of the order of seconds), and so a frequency of about  $1 \text{ kc/s}$  was found to be more than sufficient to avoid fluctuations in the emission, and at the same time it was not so high as to decrease the efficiency appreciably.

The operation of the circuit can be described as follows: Transistors  $T_4$ ,  $T_5$  and  $T_6$  make up the emitter-coupled multivibrator. The filament of the device to be regulated is used as the common emitter resistor. Transistors  $T_5$  and  $T_6$  are coupled together in order to handle the power requirements of the filament ( $6-8 \text{ W}$ ). To obtain maximum battery economy the power supply is made up of the following: five high-current-capacity silver cells in series, making a total of  $7.5 \text{ V}$  providing the power

Mr. Nagy and Mr. Niemann are at the Space Physics Research Laboratory, University of Michigan, U.S.A.

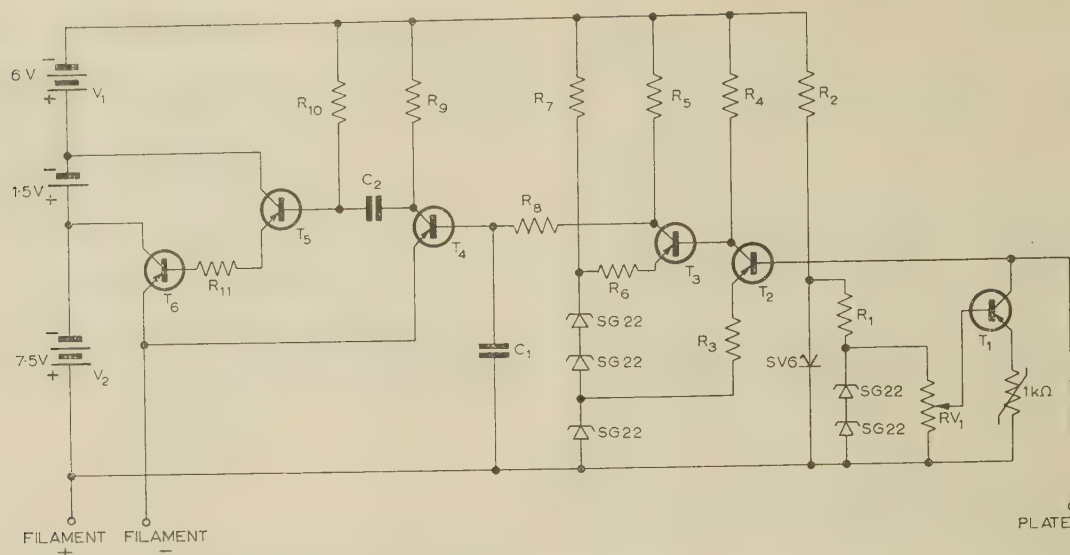


Fig. 1.—Circuit diagram of regulator.

$R_1$ : 1 k $\Omega$	$R_6$ : 80 $\Omega$	$R_{11}$ : 10 $\Omega$	$T_1$ : 2N328
$R_2$ : 1.2 k $\Omega$	$R_7$ : 1 k $\Omega$		$T_2, T_3$ : 2N329
$R_3$ : 560 $\Omega$	$R_8$ : 1 k $\Omega$		$T_4, T_5$ : 2N671
$R_4$ : 39 k $\Omega$	$R_9$ : 1.2 k $\Omega$		$T_6$ : 2N456
$R_5$ : 820 $\Omega$	$R_{10}$ : 15 k $\Omega$		
	$C_1$ : 0.3 $\mu$ F		
	$C_2$ : 0.2 $\mu$ F		

for the filament and a 6V mercury battery connected in series with it to give a total of 13.5V to supply the lower current requirements of the rest of the circuit. The  $R_{10}C_2$  combination sets the fixed 'off' time of the  $T_5$  and  $T_6$  section, whereas the variable 'on' time is determined by the  $R_8C_1$  combination and the potential at the collector of  $T_3$ . This potential is set by  $T_3$  and  $T_2$ , which are connected as conventional common-emitter amplifiers. To obtain maximum sensitivity, the base current of  $T_2$  is the algebraic difference between the current from the constant-current supply  $T_1$  and the emission current of the device to be regulated. The voltage divider  $RV_1$  permits adjustment in the emission level of the filament.

Extensive temperature tests have been carried out, and these established that the only component requiring temperature compensation is the transistor  $T_1$  of the reference supply. It has been found<sup>4</sup> that temperature drifts in silicon transistors, properly biased and operating at temperatures below 80°C, are due primarily to changes in the base-emitter voltage drop  $V_{be}$ . These changes are stable with time and are a linear function of temperature. Thus they can be compensated by positive temperature-coefficient resistors. This was done in our circuit by connecting a 1 k $\Omega$  Sensistor in series with the emitter of transistor  $T_1$ . With this compensation, the variation in the emission current was less than 1% up to temperatures of 60°C. Further tests have also indicated that the emission current stays constant, to within 1% when  $V_1$  changes from 2.5 to 7.5 V, and within 4% when the filament supply  $V_2$  changes from 7.0 to 9.0 V. The overall efficiency of the regulator was found to be 90–95%, depending on the operating conditions. If the collector of  $T_6$  is raised to the same voltage as the collector of  $T_5$ , the circuit will operate satisfactorily but with a decreased efficiency. This decrease in efficiency is due to the incomplete saturation of transistor  $T_6$  and the resulting collector dissipation. This regulator has been used with an ionization gauge operating over a pressure range of  $10^{-4}$ – $10^{-6}$  mm Hg, and resulted in an emission-current regulation well within 1%.

#### CONCLUSION

The circuit described was specifically developed for one particular model of ionization gauge, but only slight changes were found necessary when it was used with gauges having different filaments. The present design requires a gauge beam current of 100  $\mu$ A or more for optimum operation. However, when regulation at lower beam currents is required, an increase in the number of stages in the amplifier section of the regulator was found to provide satisfactory operation down to about 10  $\mu$ A. Below this value, a more complex d.c. amplifier stage would be necessary for stable operation.

This on-off type filament regulator has proved to be a very reliable and efficient device. Its main advantage over the series-type regulator is the increased efficiency, which is obtained without undue increase in circuit complexity. Thus, where efficiency is of prime importance, it will undoubtedly find wide application.

#### ACKNOWLEDGMENTS

The work was supported by the U.S. Department of the Army Signal Corps Supply Agency (Contract No. DA-36-039-sc-78131) and was carried out under the directorship of N. W. Spencer.

#### REFERENCES

- (1) HOLMES, J. C.: 'Emission Current Regulator for Rocket-Borne Radio-Frequency Mass Spectrometer', *Review of Scientific Instruments*, 1957, 28, p. 290.
- (2) BENTON, H. B.: 'Small Lightweight Ionization Gauge Control Circuit', *ibid.*, 1959, 30, p. 887.
- (3) BRIGHT, R. L.: 'Junction Transistors Used as Switches', *Transactions of the American I.E.E.*, 1955, 74, Part I, p. 111.
- (4) MATZEN, W. T., and BAIRD, J. R.: 'Differential Amplifier Features D-C Stability', *Electronics*, 1959, 32, p. 60.



## AN OUTPUT PREDICTION SYSTEM TO IMPROVE THE PERFORMANCE OF ON-OFF AND SATURATING CONTROL SYSTEMS

By J. MILLS, M.Eng.Sc., Graduate.

(The paper was first received 4th July, 1960, and in revised form 24th April, 1961.)

## SUMMARY

When a second-order on-off or saturating control system is subject to large step inputs, the best performance that can be achieved is to bring the error and its first derivative simultaneously to zero in the shortest possible time; there is then no overshoot. This response requires a single change of the output of the on-off component at the proper time before the error reaches zero. A proposal is made to achieve this response for all magnitudes of step input using a linear network and a relay in the feedback path of the control system. The proposal applies to linear and non-linear systems of second order with viscous damping, and to some higher-order systems.

## LIST OF SYMBOLS

$r$  = Input signal.  
 $c$  = Output signal.  
 $e$  = Error =  $r - c$ .  
 $b$  = 'Ideal' feedback signal.  
 $b_a$  = Actual feedback signal.  
 $a_t$  = Actuating signal =  $r - b$ .  
 $t$  = Time.  
 $v$  =  $de/dt$ .  
 $r'$  = Normalized input =  $r/\tau K$ .  
 $c'$  = Normalized output =  $c/\tau K$ .  
 $e'$  = Normalized error =  $e/\tau K$ .  
 $b'$  = Normalized feedback =  $b/\tau K$ .  
 $t'$  = Normalized time =  $t/\tau$ .  
 $v'$  = Normalized error rate =  $v/K$ .  
 $s$  = Laplace variable.  
 $R(s)$ ,  $C(s)$ , etc. = Laplace transforms of  $r$ ,  $c$ , etc.  
 $K$  = Gain constant.  
 $\tau$  = Time-constant.  
 $H(s)$  = Feedback transfer function.

## (1) INTRODUCTION

In their simplest form, on-off control systems, such as relay servo-mechanisms or servo-mechanisms with torque limitation, frequently suffer from large overshoots following sudden changes of input signal. This is because in a simple relay servo-mechanism the motor torque is not reversed until the error becomes zero, and since the velocity cannot be changed instantaneously the servo-mechanism overshoots. If the motor torque is reversed at the right time, before the error becomes zero, it is possible to bring the error and its first derivative to zero simultaneously, so that for a second-order system no overshoot will occur. Motor-torque reversal in this manner is described as optimum switching<sup>1</sup>.

A number of proposals<sup>1-6</sup> have been made for systems which achieve optimum switching. These vary in complexity of the input signals and the type of servo-mechanism for which they are suitable. The simplest of them use non-linear velocity feedback, requiring a tachometer and a diode function generator,

and achieve optimum switching for step inputs. The system proposed in this paper, referred to as the *output prediction system*, achieves optimum switching for any magnitude of step input signal. The only non-linear device which must be added to the servo-mechanism is a relay; no tachometer is required.

## (2) THE OUTPUT PREDICTION SYSTEM

Using the output prediction system, a servo-mechanism is operated in two modes: the large and small error modes. When the input signal velocities and accelerations are small enough to be within the power capabilities of the servo-mechanism, the error will be small. A relay servo-mechanism under such conditions will either oscillate continuously at fairly high frequency and small amplitude, or will have a small dead zone of error, and a saturating servo-mechanism will operate in its linear range. Linear networks designed by linear or describing-function theory are used to achieve satisfactory performance in the small-error mode. The output prediction system achieves optimum switching for step inputs. To do this, a simple network is inserted by a relay in the feedback path of the servo-mechanism. The output of this network, at any instant, is a prediction of the future position where the motor would come to rest if the torque reversal were made at that instant. The proper time for torque reversal is when the output of the network is equal to the input signal, because the motor will then come to rest at the correct position.

## (2.1) Analysis of On-Off Servo-Mechanism

The output prediction system is described in terms of its application to a control system represented, for large errors, by the diagram of Fig. 1. A simple relay servo-mechanism can be

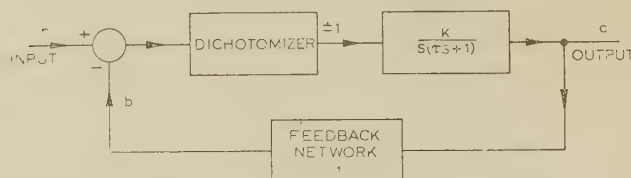


Fig. 1.—Block diagram of on-off control system.

represented in this manner. The box labelled 'dichotomizer' represents the relay or other switching device, or the torque limiting action. For the dichotomizer it is postulated that if the input is positive the output is  $-1$ , and if the input is negative the output is  $+1$ .

This system can be conveniently studied using phase-plane analysis. Its performance for a dichotomizer output of  $+1$  is given by

$$(\tau/K)(d_2c/dt^2) + (1/K)(dc/dt) = 1 \quad (1)$$

and from this, using normalized values, it can be shown that

$$e' = -v' + \log_e(1 + v') + d \quad (2)$$

Written contributions on papers published without being read at meetings are invited for consideration with a view to publication.  
 Mr. Mills is a Lecturer in Electrical Engineering in the University of Western Australia

where  $d$  is a constant of integration. Similarly, for a dichotomizer output of  $-1$ ,

$$e' = -v' - \log_e (1 - v') + d \quad (3)$$

Each of these equations is a family of curves, all of similar shape but displaced from one another in a direction parallel to the  $e'$  axis, as shown in Fig. 2. The curves through the origin are obtained by making  $d$  zero.

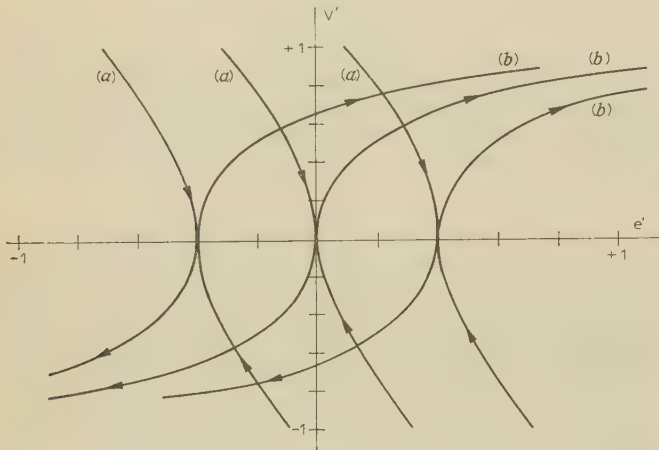


Fig. 2.—Phase-plane trajectories.

$$(a) \quad e' = -v' + \log_e (1 + v') + d$$

$$(b) \quad e' = -v' - \log_e (1 - v') + d$$

Suppose that the system is initially at rest with  $r$ ,  $c$ ,  $e$ , and  $v$  all zero. If a step-function input of magnitude  $r_0$  is applied the error becomes  $r_0$ . This may be normalized by substituting  $r'_0$  for  $r_0/\tau K$ . Without any prediction, i.e. with direct feedback, the behaviour of the system is as shown in Fig. 3. The dichotomizer output changes when  $e'$  becomes zero. With proper

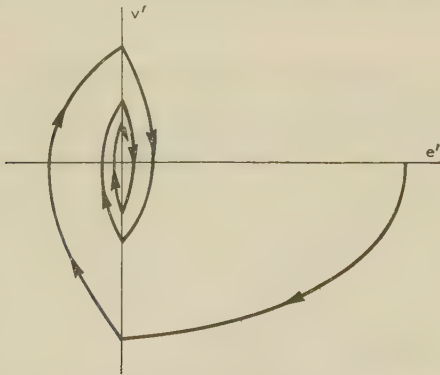


Fig. 3.—Phase-plane trajectories for on-off control system without output prediction.

mizer output changes when  $e'$  becomes zero. With proper prediction of the output, the change takes place before  $e'$  becomes zero on the trajectory which passes through the origin (Fig. 4).

Referring to Fig. 4, the trajectory through the point  $e' = r'_0$ ,  $v' = 0$  is

$$e' = r'_0 - v' + \log_e (1 + v') \quad (4)$$

The trajectory which passes through the origin is

$$e' = -v' - \log_e (1 - v') \quad (5)$$

The point  $(e'_s, v'_s)$  where the change should take place is on both

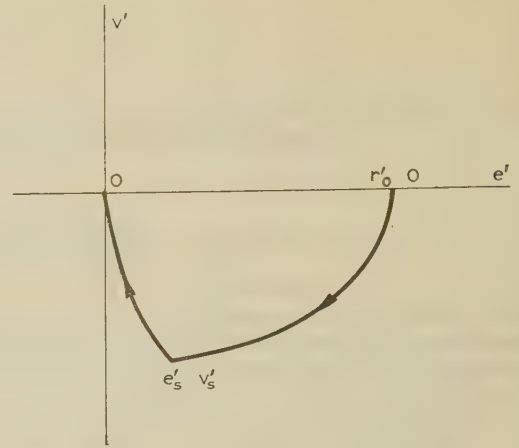


Fig. 4.—Phase-plane trajectories for on-off control system with output prediction.

these trajectories, and so these values can be substituted in eqns (4) and (5). Making this substitution, and subtracting eqn. (5) from eqn. (4) gives

$$r'_0 = -\log_e (1 - v'_s) - \log_e (1 + v'_s)$$

$$= -\log_e [1 - (v'_s)^2] \quad (6)$$

Now, from the solution of the differential equation we have along the first trajectory,

$$v' = -1 + \exp(-t') \quad (7)$$

where  $t'$  is the normalized time from the point  $(r'_0, 0)$ . Substituting this in eqn. (6) for the particular values  $v'_s$ ,  $t'_s$  at the change point  $(e'_s, v'_s)$ ,

$$r'_0 = -\log_e [2 \exp(-t'_s) - \exp(-2t'_s)]$$

$$= -\log_e [\exp(-t'_s) - \log_e [2 - \exp(-t'_s)]]$$

$$= t'_s - \log_e [1 - \exp(-t'_s)] \quad (8)$$

Now it is required that the feedback signal  $b$  should equal  $r$  at time  $t_s$  for all values of  $r_0$ . This condition requires that

$$b' = t' - \log_e [2 - \exp(-t')] \quad (9)$$

## (2.2) Synthesis of the Feedback Network

To produce a feedback signal which is a satisfactory approximation to  $b$ , a network is inserted in the feedback path. The input to this network, expressed in Laplace-transform form, is  $C(s)$ . Its transform function,  $H(s)$ , operating on  $C(s)$ , is required to produce a signal,  $B_a(s)$ , whose inverse transform  $b_a$ , approximates to  $b$ . It is not possible to produce  $b$  exactly by a network with a finite number of components, but a good approximation can be obtained with a very simple network. The input signal to the feedback block  $c$  is given by

$$c' = t' - 1 - \exp(-t') \quad (10)$$

This follows from the solution of eqn. (1). If  $b'$  is approximated by a function of the form

$$b'_a = t' \times \text{constant terms} + \text{exponential functions of } t'$$

then, with certain restrictions,  $H(s)$  can be realized using lumped passive network.

The simplest function of this type to give an approximation to  $b'$  is

$$b'_a = t' - p[1 - \exp(-t')]$$



where  $p$  is a constant. However, except when  $p = 1$  and  $b'_a = c'$  this does not lead to a passive network, as proved below. The next simplest function for  $b'_a$  is

$$b'_a = t' - p[1 - \exp(-t')] - q[1 - \exp(-nt')] \quad (11)$$

where  $p$ ,  $q$ , and  $n$  are constants. This leads to a realizable network provided that

$$p + qn = 1 \quad (12)$$

The restriction of eqn. (12) also means that the first derivatives  $b'$  and  $b'_a$  are equal at  $t = 0$ . Since the exponential terms in (11) are significant for small values of  $t'$  and not for large values, it is reasonable to expect that if one or more derivatives of  $b'$  and  $b'_a$  are equal for  $t = 0$  a good approximation will result. If in addition to eqn. (12) the further condition

$$n - np - nq = 1 \quad (13)$$

is imposed, the approximation has the correct second derivative  $b'' = 0$ , and the choice of network parameters is simplified. From eqns. (12) and (13),

$$p = \frac{n-2}{n-1} \quad q = \frac{1}{n(n-1)}$$

If  $n$  is given by  $n = 1/(1 - \log_e 2) = 3.259$ , the approximation has the correct value as  $t'$  tends to infinity. However, this is not the best value, as is shown in Fig. 5. If a value of  $n = 3.5$

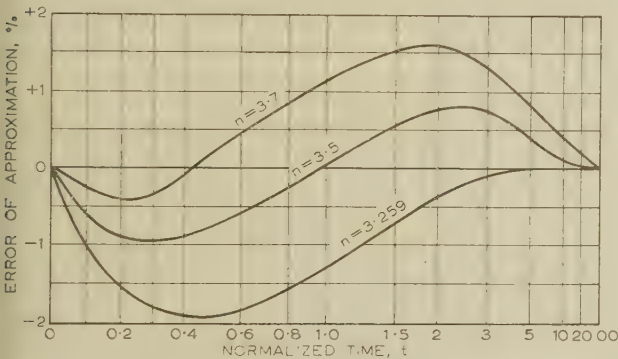


Fig. 5.—Error of approximation to ideal feedback signal.

chosen, the approximation is within 1% for all values of  $t'$  from zero to infinity.

It is now necessary to synthesize a network which will give  $b_a$  as its output when its input is  $c$ . It is convenient here to use Laplace-transform analysis. Since the Laplace variable  $s$  has the dimensions of  $T^{-1}$  it may be normalized by putting  $s' = sT$ . Taking the Laplace transform of  $b'_a$  and rearranging,

$$B'_a(s') = \frac{s'^2(1 - p - qn) + s'(n + 1 - pn - qn) + n}{s'^2(s' + 1)(s' + n)}$$

With the restrictions of eqns. (11) and (12) this becomes

$$B'_a(s') = \frac{2s' + n}{s'^2(s' + 1)(s' + n)}$$

so

$$C'(s') = \frac{1}{s'^2(s' + 1)}$$

$$H'(s') = B'_a(s')/C'(s') = \frac{2s' + n}{s' + n}$$

in actual values,

$$H(s) = \frac{2s + n/\tau}{s + n/\tau} \quad (14)$$

Had the  $s'^2$  term in  $B'(s')$  not been made zero the transfer function  $H(s)$  would have had an  $s^2$  term in the numerator, and would not have been physically realizable with a passive network.

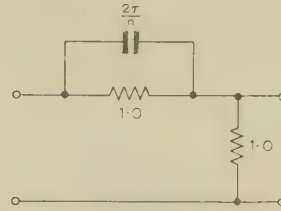


Fig. 6.—Prediction network.

The transfer function of the network shown in Fig. 6 is

$$\frac{1}{2} \frac{2s + n/\tau}{s + n/\tau}$$

This network can be used for the prediction, and the gain of 2 required with it can be obtained in effect by attenuating the  $r$  signal. Choosing a value of 3.5 for  $n$  gives a capacitance of  $0.57\tau$ , where  $\tau$  is the system time-constant. Thus for any second-order on-off control system the network component values can be immediately determined when the time-constant is known. Indeed, it may well be simpler to determine the best value of capacitance experimentally than to attempt to measure the time-constant of a system.

### (3) EXPERIMENTAL RESULTS

To test the proposed system an ideal second-order system was studied on an analogue computer, and a relay servo-mechanism was built and tested to show the effects of departure from the ideal. The parameters of the ideal and practical systems were similar. The system chosen for study had relatively low damping and was therefore markedly oscillatory without prediction.

Results of the computer study are shown in Fig. 7. These

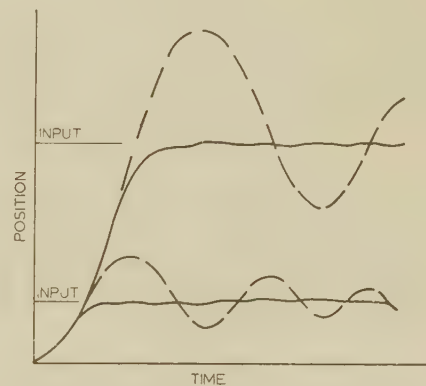


Fig. 7.—System response to step-function input.

— With output prediction.  
--- Without output prediction.

comprise the step-function response for two input magnitudes with and without output prediction. The small oscillations which can be seen after the output has reached the desired value are not at the switching frequency. The switching frequency is much higher, and the visible oscillations are lightly damped oscillations excited by the small residual error, the system operating in a quasi-linear manner. These eventually die out.

The relay servo-mechanism used for the test was built up from a 2-phase servo-motor controlled by a microswitch-relay

combination. This combination had an operating time delay of about 15 ms, and because of this, a stabilizing network was necessary in the forward path to reduce the limit cycle amplitude in the small-error mode. This network was disconnected when the predictor network was in use. A circuit diagram of the servo-mechanism is shown in Fig. 8, and results of tests are

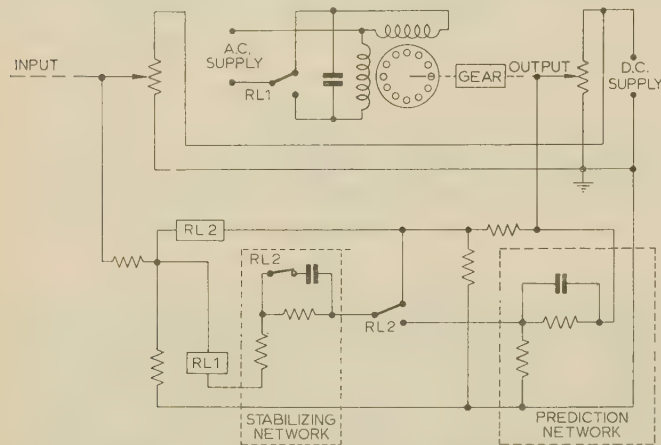


Fig. 8.—Experimental relay servo-mechanism.

RL1 Main relay (polarized).  
RL2 Prediction relay, operates when error exceeds a fixed small magnitude.

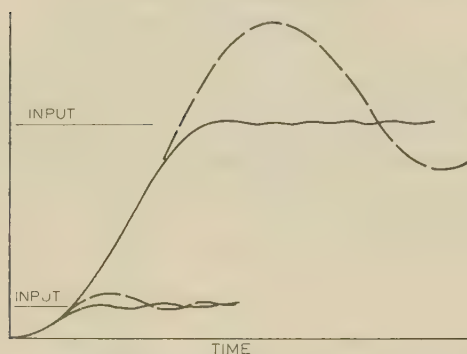


Fig. 9.—Response of experimental relay servo-mechanism.

— With output prediction.  
--- Without output prediction.

shown in Fig. 9. The small oscillations here are the steady oscillations of the system. These tests demonstrate the practicability of the proposal even when the actual control system departs somewhat from the ideal mathematical model, the departures being the relay-operating time delay and the non-linearity of the motor torque/speed relation.

#### (4) GENERAL APPLICATION OF THE SYSTEM

The output prediction system can be applied to any control system which can be represented by the block diagram of Fig. 1. In common with other proposals for optimum switching it is useful for non-linear systems and also for systems of order higher than the second, provided that the extra time-constants are small compared with the time required to respond to a step input. If the extra time-constants are not small, no system which provides only one torque reversal before the error becomes zero will give satisfactory response. Bogner and Kazda<sup>7</sup> have shown that for a system described by an  $n$ th order differential equation,  $n - 1$  torque reversals are necessary to bring the error and all its derivatives to zero simultaneously.

The output prediction system has limitations which do not apply to some of the more complex systems. It is, in general terms, limited to systems with inputs which are either slowly changing or consist of step functions of any magnitude, successive steps being sufficiently far apart for the system to come to rest after each step. One input which the output prediction system will not follow satisfactorily in the large-error mode is a ramp function, but there are many control systems for which this is not important.

Non-linear or higher-order systems must be studied individually to determine a suitable prediction network. The input and desired output of the prediction network can be found either by analysis or experiment, as shown by the above analysis of a second-order linear system. These input and desired output voltages will be determined as functions of time. Network synthesis from time functions, with the techniques available at present, is not straightforward. Guillemin<sup>8</sup> and Truxal<sup>9</sup> describe possible methods. These require the input and output to be approximated as a series of steps, straight-line segments, parabolae or higher-order segments. These approximate representations can then be transformed to the frequency domain, the ratio of the transforms being the required transfer function. However, this transfer function is not in the form of a rational algebraic function of frequency, and a further approximation is necessary to bring it to a form physically realizable by a network. A suitable approximation is not easy to find, nor is it simple to assess the resulting error in the time function.

A more satisfactory method for the present purpose is to approximate the network input and output time functions as the sum of a number of exponential terms, together with terms in  $t$ ,  $t^2$ , etc. By a proper choice of coefficients these expressions can be made to yield physically realizable networks without further approximation. To simplify the network the output approximation should contain all the terms in  $t$ ,  $t^2$ , etc., in the input, and exponential terms with the same indices as those in the input. As few extra exponential terms as possible should be added to complete the approximation. This form of the output approximation will ensure that most of the poles in the Laplace transform of the output will be cancelled by the poles in the input, leaving only the poles due to the extra exponential terms in the transfer function. Some restriction on the coefficients will be necessary to restrict the number of zeros in the transfer function, and these restrictions are best found by analysis for each system. The approximation of a function as the sum of a number of exponential terms can be carried out by the graphical method described by Kimbark<sup>10</sup> or the numerical method described by Buckingham.<sup>11</sup>

This method of designing the prediction network has two advantages. First, it leads to the simplest possible network which will give an approximation of the required accuracy, and secondly, the errors in the approximation are immediately apparent.

#### (5) CONCLUSIONS

A very simple proposal has been made for achieving optimum switching for on-off control systems subject to step inputs. The proposal has been tested by an analogue computer study and by tests on a relay servo-mechanism.

#### (6) ACKNOWLEDGMENTS

The author would like to express his appreciation of the encouragement and advice given by Professor A. R. Billings and Mr. K. W. Taplin of the Electrical Engineering Department of the University of Western Australia.



## (7) REFERENCES

- 1) UTTLEY, A. M., and HAMMOND, P. H.: 'The Stabilization of On-Off Controlled Servomechanisms', in 'Automatic and Manual Control'. Ed. A. Tustin (Butterworths, 1951), p. 285.
- 2) HOPKIN, A. M.: 'A Phase Plane Approach to the Compensation of Saturating Servomechanisms', *Transactions of the American I.E.E.*, 1951, **70**, Part I, p. 631.
- 3) NEISWANDER, R. S., and MACNEAL, R. H.: 'Optimization of Non-Linear Control Systems by means of Non-Linear Feedback', *ibid.*, 1953, **72**, Part II, p. 262.
- 4) NEISWANDER, R. S.: 'An Experimental Treatment of Non-Linear Servomechanisms', *ibid.*, 1956, **73**, Part II, p. 308.
- 5) DIESEL, J. W.: 'Extended Switching Criterion for Second Order Saturated Servomechanisms', *ibid.*, 1957, **76**, Part II, p. 388.
- (6) COALES, J. F., and NOTON, A. R. M.: 'An On-Off Servomechanism with Predicted Change-over', *Proceedings I.E.E.*, Paper No. 1895 M, August, 1955 (**103 B**, p. 449).
- (7) BOGNER, I., and KAZDA, L. F.: 'An Investigation of the Switching Criteria for Higher Order Contactor Servomechanisms', *Transactions of the American I.E.E.*, 1954, **73**, Part II, p. 118.
- (8) GUILLEMIN, E. A.: 'Synthesis of Passive Networks' (Wiley, 1957).
- (9) TRUXAL, J. G.: 'Automatic Feedback Control System Synthesis' (McGraw-Hill, 1955).
- (10) KIMBARK, E. W.: 'Power System Stability' (Wiley, 1956), Vol. 3, p. 47.
- (11) BUCKINGHAM, R. A.: 'Numerical Methods' (Pitman, 1957), p. 329.

## THE PLACE OF FORMAL STUDY IN THE POST-GRADUATE TRAINING OF AN ELECTRICAL ENGINEER

By N. N. HANCOCK, M.Sc.Tech., and P. L. TAYLOR, M.A., Associate Members.

*This paper, a summary of which is given below, was first received 19th November, 1960, and in revised form 6th January, 1961. It was published individually in February, 1961, was read before THE INSTITUTION 2nd March, and the NORTH-WESTERN CENTRE 14th March, 1961, and was republished in October, 1961, in Part A of the PROCEEDINGS (page 435). Reprints of the paper and discussion (3539 Hancock and Taylor), price 2s. each (post free) will be available towards the end of December.*

The paper examines the need for a period of formal post-graduate study by electrical engineers who will be concerned with research and development work in industry, as an integral part of their training. It is concluded that the need is real, and that study should be deferred for a year after graduation. Study courses can with advantage be organized co-operatively by an academic institution and local industry, and should be held at the academic institution. The possibilities of a full-time full-session course, a full-time course lasting about one term, and

a part-time course are considered. The advantages, both educational and practical, are discussed and it is concluded that the national and industrial need is best met by the full-time one-term course. The problems this involves for the academic institution are considered, particularly in the recruitment of part-time lecturers from industry and the granting to them of some official status within the academic institution. The conclusions are illustrated by reference to a course with which the authors are concerned.

## MONOGRAPHS PUBLISHED INDIVIDUALLY

Summaries are given below of monographs which have been published individually, price 2s. each (post free). Applications quoting the serial numbers as well as the authors' names, and accompanied by a remittance, should be addressed to the Secretary. For convenience, books of five vouchers, price 10s., can be supplied.

**An Invariant Stability Factor and its Physical Significance.** Monograph No. 468 E.

S. VENKATESWARAN, M.A.

Relationships between the maximum power gain and the internal loop gain of a general linear two-port network are developed. A new stability factor is defined from the maximum-gain potentiality of the network without external feedback, and is physically identifiable as the modulus of the internal loop loss (the inverse of loop gain) at maximum available power gain where this is finite. Several theorems on this loop gain show the relationships between the new stability factor, Stern's stability factor and the author's 'performance factor'.

Though the earlier factors may be obtained by constraints on the internal loop gain, they are shown not to be exactly related to the internal loop gain of the two-port network at maximum power gain; also, they are not exact invariants in matrix environments save in exceptional cases. The new stability factor is an exact invariant for all its values in the possible matrix environments, demarcates the regions of potential instability and absolute stability, and is directly related to the maximum available power gain of the two-port network, when this gain is finite.

**The Signal/Noise Gain of Ideal Receiving Arrays.** Monograph No. 470 E.

V. G. WELSBY, Ph.D.

A study is made of the theoretical signal/noise gain of an ideal strip transducer; this gain is the actual signal/noise ratio compared with that for a 'point' receiver (i.e. one whose dimensions are small compared with the wavelength at the lowest significant frequency). The results are not restricted to narrow-band systems and relate generally to noise fields which may be non-isotropic and have non-uniform frequency spectra. The theory is used to investigate the correlation between the noise outputs of the various sections of a subdivided transducer, and it is shown that, at least in the narrow-band case, the usual assumption of negligible correlation is generally justified in practice. Multiplicative systems are also considered, and it is shown that, in certain circumstances, the overall signal/noise ratio of such a system may be better than that of either of its component groups.

The results obtained are also generally applicable to ideal radio receiving arrays.

**The Generation of Pulse-Like Functions by means of Lumped Equivalents of Delay Lines.** Monograph No. 471 E.

N. B. CHAKRABORTI.

A method for realizing pulse-like time functions by means of 4-terminal networks developed on the basis of equivalence to delay lines is presented. Illustrative arrangements based on this method for generating pulses of the forms  $\sin t$ ,  $\sin^2 t$ ,  $\sin^3 t$ , etc., are described. A method of synthesis of networks for generating specified pulse forms is also suggested. Some experimental results are presented.

**The Conductivity of Oxide Cathodes. Part 12—Influence of Strontium Ion Migration on Matrix Conductivity.** Monograph No. 473 E.

G. H. METSON, M.C., D.Sc., Ph.D., M.Sc., B.Sc.(Eng.).

The donor element in the oxide matrix is now regarded as strontium

metal, and in the present Part its movement in an electric field is considered. It is shown experimentally that the donor is positively ionized, can be chemically isolated by solution in a platinum cathode core, is mobile in an electric field at temperatures above 550° K, and is incapable of diffusion in a concentration gradient below 800° K. Excessive concentration of the positive ion is shown to give rise to a dramatic increase in matrix resistivity. It is finally concluded that there exists an optimum donor concentration at which the conductivity of the matrix is at a maximum.

**The Evaluation of the Response of Single-Valued Non-Linearities to Several Inputs.** Monograph No. 474 M.

D. P. ATHERTON, B.Eng.

The transform method for evaluating the coefficients of the various terms in the output autocorrelation function of a non-linearity with input consisting of a sinusoidal signal and Gaussian noise is considered. Solutions, all of which involve confluent hypergeometric functions, are given for a few analytically defined non-linear characteristics. A short table of these functions is also given to facilitate computation. A new expression for evaluating the coefficients, a double integral involving the non-linear characteristic and the moments of the sinusoidal and Gaussian input signals, is derived. A graphical method of solution applicable to any single-valued non-linearity is given, and a comparison made, with experimental and theoretical results. Extension of the technique to several uncorrelated input signals of any known amplitude probability density distribution is shown to be possible.

**An Investigation of Some Waveguide Structures for the Propagation of Circular TE Modes.** Monograph No. 476 E.

J. B. DAVIES, M.A., M.Sc., Ph.D.

An analysis is given of various waveguide structures that support circular transverse electric modes. These structures are examined with a view to their application to mode filters and bends in circular low-loss waveguide systems.

Circular waveguide is examined in which narrow longitudinal circumferential slots are cut in the waveguide wall. Particular attention is given to longitudinally slotted guide, in which the  $H_{01}$  mode has a lower cut-off frequency than the  $E_{11}$  mode. A mode filter is described which transmits only the  $H_{01}$ ,  $H_{11}$ , and  $H_{21}$  modes.

Circular waveguide, with an outer conducting wall and an inner coaxial layer of closely spaced longitudinal conductors, is studied as found capable of supporting an  $H_0$  mode of free-space wavelength much greater than the outer guide diameter. It is also found, in principle, to support slow waves of the  $H_1$ ,  $H_2$ , . . . type at any frequency.

An analysis is given of curved circular waveguide with small longitudinal and circumferential surface reactances that can with advantage be varied around the waveguide circumference. Application of the analysis to waveguide with shallow longitudinal slots shows that, for suitable diameter and slot dimensions, the  $H_0$  mode can be transmitted through slightly curved guide of any length with substantially no mode conversion. Uniform longitudinal slots in curved waveguide will restrict mode conversion, over a band of frequencies, to the  $H_0$  mode, the conversion being small for large bending radius. The proposed application of these small-diameter slotted waveguides is to relatively compact bends, with bending radius as little as five times the guide diameter. Although the wall conduction losses are increased by the slots, and by the operation close to cut-off, the overall loss in a bend should be small.

The longitudinally slotted curved waveguide may be difficult to construct but it appears to provide a means of rapidly negotiating bends with little attenuation or contamination of the  $H_{01}$ .



# INDEX TO VOLUME 108, PART B

1961

## ABBREVIATIONS

- Address, lecture or paper
- Discussion on a paper.
- Abstract of paper or address.

## A

- ACKROYD, R. T., HOUSTOUN, J., LYNN, J. W., and MANN, E. Electrical analogue for heat waves in an exothermic medium. (P), 33.
- Activity of weak radioactive sample. (See Radioactive.)
- ADDRESSES.
- AYERS, C., as chairman of North-Western Utilization Group. 24.
- BECK, H. V., as chairman of Cambridge Electronics and Measurements Group. 142.
- GILL, W. E., as chairman of East Midland Centre. 137.
- GOFORD, R., as chairman of Southern Centre. 21.
- HALL, E. S., as chairman of Rugby Sub-Centre. 23.
- JONES, F., as chairman of South Midland Centre. 140.
- MACLAREN, Sir HAMISH D., as President. 1.
- PICKEN, D. A., as chairman of Mersey and North Wales Centre. 19.
- STEWART, J., as chairman of Scottish Electronics and Measurement Group. 343.
- TERRONI, T. B. D., as chairman of Electronics and Communications Section. 15.
- erial, high-gain television transmitting, use of, in populous area. G. D. MONTEATH, G. H. MILLARD and D. J. WHYTHE, (P), 65.
- radiation patterns, prediction of, from near-field measurements. J. BROWN and E. V. JULL, (P), 635.
- survey of terrestrial radioactivity. D. WILLIAMS and H. BISBY, (P), 403.
- erials. H. PAGE, (P), 473.
- of variable spacing, scatter observations at 3 480 Mc/s with. R. W. MEADOWS, (P), 349.
- , receiving, applied to reradiation of an electromagnetic horn. D. MIDGLEY, (P), 645.
- irborne microwave refractometer. (See Refractometer.)
- ircraft, future of electrics and electronics in. Lord CALDECOTE, (P), 143; (D), 150.
- alkaline-earth metals. (See Metals.)
- lloys, platinum, of alkaline-earth metals, work function measurements on. H. BATEY, (P), 468.
- merican, German and British measuring equipment, comparison of. A. H. BALL and W. NETHERCOT, (P), 273.
- mplifier, audio-frequency, for high-precision voltage measurement. S. HARKNESS and F. J. WILKINS, (P), 319; (D), 337.
- , electron-beam parametric, for the 200 Mc/s region. G. O. CHALK, (P), 125.
- analogue-computer (discrete) compensation of sampled-data control systems. T. GLUCHAROFF, (P), 167; (D), 176.
- computer, electronic, for coal transportation problem. E. G. ANDERSON, (P), 43.
- , electrical, for heat waves in an exothermic medium. R. T. ACKROYD, J. HOUSTOUN, J. W. LYNN and E. MANN, (P), 33.
- NDERSON, E. G. Electronic analogue computer for a coal transportation problem. (P), 43.
- NSLOW, N. G. V. Back-scatter sounding in operation of h.f. broadcast services. (D), 372.
- rgon, krypton and xenon, comparison of, as admixtures in neon glow-discharge reference tubes. F. A. BENSON and G. P. BURDETT, (P), 501; (D), 507.
- RNOLD, A. H. M.
- Current transformers. (D), 337.
- High-precision voltage measurement. (D), 337.
- Precision measurement of capacitance. (D), 337.
- SHWELL, G. E., HARGREAVES, J., and PRESSEY, B. G. (See PRESSEY.)
- STERAKI, J. D., and BERESFORD, A. N. (See BERESFORD.)

Astronomy, radio. (See Radio.)

ATKINS, W. T. J. Theory of time-delay networks. (P), 500.

Audio-frequency amplifier. (See Amplifier.)

—current transformers. (See Transformers.)

Automatic landing. (See Landing.)

—plotter. (See Plotter.)

Automation, effects of. C. AYERS, (A), 24.

Avalanche devices, circuit applications of. G. M. ETTINGER, (P), 563.

AYERS, C. Address as chairman of North-Western Utilization Group. 24.

Azimuth, measurements of energy distribution in. W. C. BAIN, (P), 241.

## B

Back-scatter sounding, usefulness of, in the operation of h.f. broadcasting services. E. D. R. SHEARMAN, (P), 361; (D), 372.

BAIN, W. C.

Directional observations on delayed signals on an ionospheric forward-scatter circuit. (P), 253.

Studies of ionospheric forward scattering using measurements of energy distribution in azimuth. (P), 241.

BALL, A. H., and NETHERCOT, W. Radio interference from ignition systems. (P), 273.

Banana-tube colour-television display system. P. SCHAGEN, (P), 577; (D), 630; B. A. EASTWELL and P. SCHAGEN, (P), 587; (D), 630; H. HOWDEN, (P), 596; (D), 630; K. G. FREEMAN, (P), 604; (D), 630; R. N. JACKSON, (P), 613; (D), 630; K. G. FREEMAN and B. R. OVERTON, (P), 624; (D), 630.

Band compression, television. (See Television.)

BARKER, R. H. Discrete analogue-computer compensation of sampled-data control systems. (D), 176.

BARNES, R. C. M., and COOKE-YARBOROUGH, E. H. (See COOKE-YARBOROUGH.)

BATEY, H. Work function measurements on the platinum alloys of the alkaline-earth metals. (P), 468.

B.B.C. sound broadcasting 1939-60. (P), 279.

— television 1939-60. E. L. E. PAWLEY, (P), 375.

BECK, H. V. Address as chairman of Cambridge Electronics and Measurements Group. 142.

BEDDOES, M. P. Television band compression by contour interpolation. (D), 634.

BELL, D. A. Television band compression by contour interpolation. (D), 360.

BENSON, F. A., and BURDETT, G. P. Comparison of argon, krypton and xenon as admixtures in neon glow-discharge reference tubes. (P), 501; (D), 508.

BERESFORD, A. N., and ASTERAKI, J. D. Problem of improving the British instrument landing system localizer for automatic landing. (P), 59.

BHATTACHARYYA, B. P. Describing-function expressions for sine-type functional non-linearity in feedback control systems. (P), 529.

BIGGS, A. J. Photo-electric beam-index colour-television tube and system. (D), 522.

BILLINGS, A. R., and LLOYD, D. J. Correlator with Hall multipliers for analysis of vocoder control systems. (D), 238.

BISBY, H., and WILLIAMS, D. (See WILLIAMS.)

Bolometers, transverse-film, in rectangular waveguides, design and performance of. J. A. LANE and D. M. EVANS, (P), 133.

BRAY, W. J. Standardization of international microwave radio-relay systems. (P), 180.

Bridges, transformer ratio-arm, choosing of. W. H. P. LESLIE, (P), 539.

Broadcast services, h.f., usefulness of back-scatter sounding in operation of. E. D. R. SHEARMAN, (P), 361; (D), 372.

BROWN, B. M. Discrete analogue-computer compensation of sampled-data control systems. (D), 177.

BROWN, J. Precision instruments for coaxial line measurements (D), 493.

- BROWN, J., and JULL, E. V. Prediction of aerial radiation patterns from near-field measurements. (P), 635.
- BUCHANAN, W. H.  
Banana-tube colour-television display system. (D), 631.  
Photo-electric beam-index colour-television tube and system. (D), 523.
- BURDETT, G. P., and BENSON, F. A. (See BENSON.)
- BURTNYK, N., and MCLEISH, C. W. (See MCLEISH.)

## C

- CALDECOTE, Lord. Future of electrics and electronics in aircraft. (P), 143; (D), 152.
- Calibration of standard current transformers up to 20kc/s. J. J. HILL, (P), 333; (D), 337.
- Capacitance, precision measurement of. (D), 337.
- CAPE, B. Electrics and electronics in aircraft. (D), 151.
- CARTER, A. H. Electrics and electronics in aircraft. (D), 151.
- Cathode, pressed-oxide nickel-matrix, below apertured electrodes. A. SANDOR, (P), 97.
- Cathodes, miniature hollow, emission from. A. SANDOR, (P), 90.
- Cavity, cylindrical, with radial vanes, analysis of. A. SINGH and R. A. RAO, (P), 550.
- , travelling-wave, analysis of. N. KARAYIANIS and C. A. MORRISON, (P), 545.
- Centre, Sub-Centre and Group chairmen's addresses. 19, 137.
- CHALK, G. O. Electron-beam parametric amplifier for the 200 Mc/s region. (P), 125.
- Channelling [telecommunication]. T. B. D. TERRONI, (A), 15.
- CHERRY, E. M. Third-harmonic tuning of e.h.t. transformers. (P), 227.
- CHRISTIANSEN, W. N., LABRUM, N. R., MCALISTER, K. R., and MATHEWSON, D. S. Crossed-grating interferometer: a new high-resolution radio telescope. (P), 48.
- Circuit applications of avalanche devices. G. M. ETTINGER, (P), 563.
- design, advantages of silicon transistors in. M. K. MCPHUN, (P), 570.
- for reducing the exciting current of inductive devices. D. L. H. GIBBINGS, (P), 339.
- Coal transportation problem, electronic analogue computer for. E. G. ANDERSON, (P), 43.
- Coaxial line measurements up to 4Gc/s, precision instruments for. D. WOODS, (P), 490; (D), 493.
- COHEN, E., and JENKINS, R. O. Gas-discharge tubes. (D), 510.
- Colour television. (See Television.)
- Connector system, coaxial, for precision r.f. measuring instruments and standards. D. WOODS, (P), 205.
- Contour interpolation, television band compression by. D. GABOR and P. C. J. HILL, (P), 303; (D), 360, 634.
- Control system, self-optimizing non-linear. J. L. DOUCE and R. E. KING, (P), 441.
- systems, on-off and saturating, output prediction system to improve performance of. J. MILLS, (P), 667.
- COOKE-YARBOROUGH, E. H., and BARNES, R. C. M. Rapid methods for ascertaining whether the activity of a weak radioactive sample exceeds a predetermined level. (P), 153; (D), 166.
- COOPER, A.  
Current transformers. (D), 337.  
High-precision voltage measurement. (D), 337.  
Precision measurement of capacitance. (D), 337.
- CORBETT, B. D. Activity of weak radioactive sample. (D), 164.
- Corona- and precipitation-interference. (See Interference.)
- Correlator employing Hall multipliers for analysis of vocoder control systems. (D), 237.
- Crossed-grating interferometer. (See Interferometer.)
- CRUICKSHANK, A. J. O. Discrete analogue-computer compensation of sampled-data control systems. (D), 178.
- Crystal detectors to cover the frequency band 26–40Gc/s. H. V. SHURMER, (P), 659.
- Palace television transmitting station. G. D. MONTEATH, G. H. MILLARD and D. J. WHYTHE, (P), 65.
- Current, decaying turn-off, storage time of transistor with. D. M. TAUB, (P), 344.

## D

- DAGLISH, H. N. Electron emission from cold magnesium oxide. (P), 103.
- DANIELS, H. B. Self-optimizing non-linear filter, predictor and simulator. (D), 438.
- Delayed signals on an ionospheric forward-scatter circuit, direction observations on. W. C. BAIN, (P), 253.
- DENNIS, J. A., and LOOSEMORE, W. R. (See LOOSEMORE.)
- Describing-function expressions for non-linearity in feedback control systems. B. P. BHATTACHARYYA, (P), 529.
- Design processes for electronic equipment. H. V. BECK, (A), 142.
- Direction-finding, h.f., application of interferometer to. C. V. MCLEISH and N. BURTNYK, (P), 495.
- Directional couplers, use of coupled transmission lines as. R. KOKK, (P), 120.
- observations on delayed signals on an ionospheric forward scatter circuit. W. C. BAIN, (P), 253.
- Discrete analogue-computer compensation. (See Analogue.)
- Display system, banana-tube. (See Banana-tube.)
- DOUCE, J. L., and KING, R. E. Self-optimizing non-linear control system. (P), 441.
- DOUCE, J. L., and LEARY, B. G. Random pulse generator with variable mean rate. (P), 524.

## E

- EASTWELL, B. A., and SCHAGEN, P. Development of the banana tube. (P), 587; (D), 632.
- ECKERSLEY, P. P. Electrics and electronics in aircraft. (D), 151.
- EDWARDS, Sir GEORGE. Electrics and electronics in aircraft. (D), 151.
- EGELSTAFF, P. A., HAY, H. J., HOLT, G., RAFFLE, J. F., and PICKLE, J. R. Phase control of rotors at high spinning speeds. (P), 2.
- Electrical analogue. (See Analogue.)
- determination of moisture in paper. (See Paper.)
- engineering. (See Engineering.)
- Electricity, effects of, on human beings. D. A. PICKEN, (A), 19.
- Electrics and electronics in aircraft, future of. Lord CALDECOTE, (P), 143; (D), 150.
- Electrodes, apertured, pressed-oxide nickel-matrix cathode below. A. SANDOR, (P), 97.
- Electrodynamical multiplier. (See Multiplier.)
- Electromagnetic horn. (See Horn.)
- Electron-beam parametric amplifier. (See Amplifier.)
- emission from cold magnesium oxide. H. N. DAGLISH, (P), 103.
- Electronic analogue. (See Analogue.)
- equipment, design processes for. H. V. BECK, (A), 142.
- plotter. (See Plotter.)
- Electronics and Communications Section: chairman's address. T. B. D. TERRONI, 15.
- in aircraft. (See Aircraft.)
- , industrial, new look in. E. S. HALL, (A), 23.
- , the engineer and reliability. J. STEWART, (A), 343.
- Emission from miniature hollow cathodes. A. SANDOR, (P), 90.
- Energy distribution in azimuth, measurements of. W. C. BAIN, (P), 241.
- losses in hydrogen-filled thyratron, measurement of. H. de KNIGHT and J. LORD, (P), 455.
- Engineer, telecommunication, and the background in which he works. R. GOFORD, (A), 21.
- , the, electronics and reliability. J. STEWART, (A), 343.
- Engineering, electrical, in the Royal Navy. Sir HAMISH D. MACLAREN, (P), 1.
- Equivalent source e.m.f. and equivalent available power in signal generator calibration. D. WOODS, (P), 37.
- ETTINGER, G. M. Circuit applications of avalanche devices. (P), 563.
- EVANS, D. M., and LANE, J. A. (See LANE.)
- Exciting current of inductive devices. (See Inductive.)
- Exothermic medium, heat waves in an. (See Heat.)

## F

- Feedback control systems, describing-function expressions for non-linearity in. B. P. BHATTACHARYYA, (P), 529.



errite, formula for loss in. L. LEWIN, (P), 25.  
 field-strength survey at 59 Mc/s, mobile field radio derived from. D. R. W. THOMAS, (P), 264.  
 filament emission regulator. A. F. NAGY and H. B. NIEMANN, (P), 665.  
 filter, predictor and simulator which optimizes itself by a learning process. D. GABOR, W. P. L. WILBY and R. WOODCOCK, (P), 422; (D), 436.  
 —, self-optimizing non-linear. J. K. LUBBOCK, (P), 439.  
 flux intensity in high-power nuclear reactors. W. R. LOOSEMORE and J. A. DENNIS, (P), 413.  
 GORD, L. H., and RAYNER, G. H. (See RAYNER.)  
 forward-scatter circuit, ionospheric, directional observations on, delayed signals on. W. C. BAIN, (P), 253.  
 GRASER, H. J., and REECE, W. V. P. Automatic electronic Nyquist plotter. (P), 535.  
 FREEMAN, K. G. Circuits for the banana-tube colour-television display system. (P), 604; (D), 632, 633.  
 FREEMAN, K. G., and OVERTON, B. R. Banana-tube colour-television display system. (P), 624; (D), 632.  
 frequency band 26–40 Gc/s, crystal detectors to cover. H. V. SHURMER, (P), 659.  
 —, modulated continuous-wave ranging system. (D), 238.  
 —, range 30–1 250 Mc/s, measurements in. I. A. HARRIS, (P), 651.  
 ROOME, D. S., MCCONNELL, G. J., and LANE, J. A. (See LANE.)

## G

GABOR, D., and HILL, P. C. J. Television band compression by contour interpolation. (P), 303; (D), 360, 634.  
 GABOR, D., WILBY, W. P. L., and WOODCOCK, R. Universal non-linear filter, predictor and simulator which optimizes itself by a learning process. (P), 422; (D), 438.  
 GARDNER, Sir GEORGE. Electrics and electronics in aircraft. (D), 151.  
 GIBBINGS, D. L. H. Circuit for reducing the exciting current of inductive devices. (P), 339.  
 GILL, W. E. Address as chairman of East Midland Centre. 137.  
 glow-discharge tubes, neon, comparison of argon, krypton and xenon as admixtures in. F. A. BENSON and G. P. BURDETT, (P), 501; (D), 507.  
 GLUCHAROFF, T. Discrete analogue-computer compensation of sampled-data control systems. (P), 167; (D), 178.  
 GOFORD, R. Address as chairman of Southern Centre. 21.  
 GRAHAM, R., JUSTICE, J. W. H., and OXENHAM, J. K. Progress report on the development of a photo-electric beam-index colour-television tube and system. (P), 511; (D), 523.

## H

HALL, E. S. Address as chairman of Rugby Sub-Centre. 23.  
 Hall multipliers, correlator employing. (D), 237.  
 HAMER, R. Radio-frequency interference in multi-channel telephony f.m. radio systems. (P), 75.  
 HAMMERTON, T. G.  
 Current transformers. (D), 338.  
 High-precision voltage measurement. (D), 338.  
 Precision measurement of capacitance. (D), 338.  
 HARGREAVES, J., PRESSEY, B. G., and ASHWELL, G. E. (See PRESSEY.)  
 HARKNESS, S., and WILKINS, F. J. Design of audio-frequency amplifier for high-precision voltage measurement. (P), 319; (D), 338.  
 HARRIS, I. A. Design of noise generator for measurements in the frequency range 30–1 250 Mc/s. (P), 651.  
 HAY, H. J., HOLT, G., RAFFLE, J. F., PICKLES, J. R., and EGELSTAFF, P. A. (See EGELSTAFF.)  
 heat waves in an exothermic medium, electrical analogue for. R. T. ACKROYD, J. HOUSTOUN, J. W. LYNN and E. MANN, (P), 33.  
 HENDERSON, J. G. Electrodynamic multiplier using torque balance. (P), 465.  
 HILL, J. J. Techniques for the calibration of standard current transformers up to 20 kc/s. (P), 333; (D), 338.  
 HILL, J. J., and MILLER, A. P. Design and performance of high-precision audio-frequency current transformers. (P), 327; (D), 338.

HILL, P. C. J., and GABOR, D. (See GABOR.)  
 HITCHCOCK, R. J. Back-scatter sounding in operation of h.f. broadcast services. (D), 373.  
 HOLMES, J. N., and SHEARME, J. N. Correlator with Hall multipliers for analysis of vocoder control systems. (D), 237.  
 HOLT, G., RAFFLE, J. F., PICKLES, J. R., EGELSTAFF, P. A., and HAY, H. J. (See EGELSTAFF.)  
 Horizon, radio-wave propagation oversea within and beyond the. F. A. KITCHEN, W. R. R. JOY and E. G. RICHARDS, (P), 257.  
 Horn, electromagnetic, reradiation of. D. MIDGLEY, (P), 645.  
 HOUSTOUN, J., LYNN, J. W., MANN, E., and ACKROYD, R. T. (See ACKROYD.)  
 HOWDEN, H. Mechanical and manufacturing aspects of the banana-tube colour-television display system. (P), 596; (D), 632.  
 Human beings, effects of electricity on. D. A. PICKEN, (P), 19.  
 Hybrid ring circuits used in radio astronomy. (See Radio.)  
 HYMAN, A. J., and LAIT, J. Frequency-modulated continuous-wave ranging system. (D), 239.

## I

Ignition systems, radio interference from. A. H. BALL and W. NETHERCOT, (P), 273.  
 Inductive devices, circuit for reducing exciting current of. D. L. H. GIBBINGS, (P), 339.  
 Industrial electronics. (See Electronics.)  
 Instrument landing system localizer. (See Landing.)  
 Instruments and standards, precision r.f. measuring, coaxial connector system for. D. WOODS, (P), 205.  
 —, precision, for coaxial line measurements up to 4 Gc/s. D. WOODS, (P), 490; (D), 493.  
 Interference, corona- and precipitation-, in v.h.f. reception. H. PAGE, (P), 469.  
 —, probabilities of, with mobile field radio derived from a field-strength survey at 59 Mc/s. D. R. W. THOMAS, (P), 264.  
 —, radio-frequency. (See Radio-frequency.)  
 Interferometer, application of, to h.f. direction-finding. C. W. MCLEISH and N. BURTYNYK, (P), 495.  
 —, crossed-grating: a new high-resolution radio telescope. W. N. CHRISTIANSEN, N. R. LABRUM, K. R. MCALISTER and D. S. MATHEWSON, (P), 48.  
 Inverters, silicon-controlled rectifier. R. H. MURPHY and K. P. P. NAMBIAR, (P), 556.  
 Ionospheric forward-scatter circuit, directional observations on delayed signals on. W. C. BAIN, (P), 253.  
 ISAACS, A. Banana-tube colour-television display system. (D), 631.

## J

JACKSON, R. N. Colorimetry of the banana-tube colour-television display system. (P), 613; (D), 633.  
 JAMES, F. H. Effects of parasitic modulation on the accuracy of measurement of the Q-factor of a resonator. (P), 316.  
 JAMES, I. J. P. Banana-tube colour-television display system. (D), 631.  
 JENKINS, R. O., and COHEN, E. (See COHEN.)  
 JESTY, L. C.  
 Banana-tube colour-television display system. (D), 631.  
 Photo-electric beam-index colour-television tube and system. (D), 522.  
 JONES, F., as chairman of South Midland Centre. 140.  
 JONES, F. E. Photo-electric beam-index colour-television tube and system. (D), 521.  
 JOWETT, J. K. S. Back-scatter sounding in operation of h.f. broadcast services. (D), 372.  
 JOY, W. R. R., RICHARDS, E. G., and KITCHEN, F. A. (See KITCHEN.)  
 JULL, E. V., and BROWN, J. (See BROWN.)  
 JUSTICE, J. W. H., OXENHAM, J. K., and GRAHAM, R. (See GRAHAM.)

## K

KARAYIANIS, N., and MORRISON, C. A. Analysis of the travelling-wave cavity. (P), 545.

- KAY, L. Frequency-modulated continuous-wave ranging system. (D), 238.
- KING, R. E., and DOUCE, J. L. (See DOUCE.)
- KITCHEN, F. A., JOY, W. R. R., and RICHARDS, E. G. Factors influencing 3 cm radio-wave propagation oversea within and beyond the radio horizon. (P), 257.
- KNIGHT, H. de B., and LORD, J. Measurement of energy losses in a hydrogen-filled thyatron in modulator duty. (P), 455.
- KOIKE, R. Use of coupled transmission lines as directional couplers. (P), 120.
- Krypton. (See under Argon.)

## L

- LABRUM, N. R., McALISTER, K. R., MATHEWSON, D. S., and CHRISTIANSEN, W. N. (See CHRISTIANSEN.)
- LAIT, J., and HYMAN, A. J. (See HYMAN.)
- LAKE, R. Gas-discharge tubes. (D), 508.
- Landing system localizer for automatic landing. A. N. BERESFORD and J. D. ASTERAKI, (P), 59.
- LANE, J. A., and EVANS, D. M. Design and performance of transverse-film bolometers in rectangular waveguides. (P), 133.
- LANE, J. A., FROOME, D. S., and McCONNELL, G. J. Construction and performance of an airborne microwave refractometer. (P), 398.
- Learning process, filter which optimizes itself by. D. GABOR, W. P. L. WILBY and R. WOODCOCK, (P), 422; (D), 436.
- LEARY, B. G., and DOUCE, J. L. (See DOUCE.)
- LEE, E. M. Precision instruments for coaxial line measurements. (D), 493.
- LESLIE, W. H. P. Choosing transformer ratio-arm bridges. (P), 539.
- LEWIN, L.  
Formula for loss in a ferrite. (P), 25.  
Precision instruments for coaxial line measurements. (D), 493.
- LLOYD, D. J., and BILLINGS, A. R. (See BILLINGS.)
- Long distances, v.l.f. waves propagated over. (See Waves.)
- LOOSEMOORE, W. R., and DENNIS, J. A. Continuous measurement of thermal-neutron flux intensity in high-power nuclear reactors. (P), 413.
- LORD, A. V.  
Banana-tube colour-television display system. (D), 630.  
Photo-electric beam-index colour-television tube and system. (D), 522.
- LORD, J., and KNIGHT, H. de B. (See KNIGHT.)
- Loss in a ferrite, formula for. L. LEWIN, (P), 25.
- LUBBOCK, J. K. Self-optimizing non-linear filter. (P), 439.
- LYNCH, A. C.  
Current transformers. (D), 337.  
High-precision voltage measurement. (D), 337.  
Precision instruments for coaxial line measurements. (D), 493.  
Precision measurement of capacitance. (D), 337.
- LYNN, J. W., MANN, E., ACKROYD, R. T., and HOUSTOUN, J. (See ACKROYD.)

## M

- McALISTER, K. R., MATHEWSON, D. S., CHRISTIANSEN, W. N., and LABRUM, N. R. (See CHRISTIANSEN.)
- McCONNELL, G. J., LANE, J. A., and FROOME, D. S. (See LANE.)
- MACLAREN, Sir HAMISH D. Address as President. 1.
- MCLEISH, C. W., and BURTNKY, N. Application of the interferometer to h.f. direction-finding. (P), 495.
- MCLEOD, T. S., and YALLUP, A. E. Electrical determination of moisture in paper. (P), 449.
- McPHERSON, J. W. Electrics and electronics in aircraft. (D), 152.
- McPHUN, M. K. Advantages of silicon transistors in circuit design. (P), 570.
- Magnesium oxide, cold, electron emission from. H. N. DAGLISH, (P), 103.
- MANN, E., ACKROYD, R. T., HOUSTOUN, J., and LYNN, J. W. (See ACKROYD.)
- MARSHALL, C. A. Banana-tube colour-television display system. (D), 631.
- MATHEWSON, D. S., CHRISTIANSEN, W. N., LABRUM, N. R., and McALISTER, K. R. (See CHRISTIANSEN.)

- MAURICE, R. D. A. Photo-electric beam-index colour-television tube and system. (D), 520.
- MEADOWS, R. W. Tropospheric scatter observations at 3480 Mc, with aerials of variable spacing. (P), 349.
- Mean rate, variable, random pulse generator with. J. L. DOUCE and B. G. LEARY, (P), 524.
- Measurement of capacitance. (See Capacitance.)
- of energy. (See Energy.)
- of flux intensity. (See Flux.)
- of Q-factor of a resonator. (See Resonator.)
- of voltage. (See Voltage.)
- of work function. (See Work.)
- Measurements in frequency range 30–1250 Mc/s. (See Frequency.)
- , coaxial line. (See Coaxial.)
- , near-field. (See under Aerial radiation.)
- Measuring instruments and standards. (See Instruments.)
- MERRIMAN, J. H. H. Back-scatter sounding in operation of h.f. broadcast services. (D), 373.
- Metals, alkaline-earth, work function measurements on platinum alloys of. H. BATEY, (P), 468.
- Microwave radio-relay systems, international, standardization of. W. J. BRAY, (P), 180.
- refractometer, airborne. J. A. LANE, D. S. FROOME and G. J. McCONNELL, (P), 398.
- spectroscopy. D. J. MILLEN, (P), 111.
- MIDGLEY, D. Theory of receiving aerials applied to the reradiation of an electromagnetic horn. (P), 645.
- MILLARD, G. H., WHYTHE, D. J., and MONTEATH, G. D. (See MONTEATH.)
- MILLEN, D. J. Microwave spectroscopy. (P), 111.
- MILLER, A. P., and HILL, J. J. (See HILL.)
- MILLS, J. Output prediction system to improve performance of on-off and saturating control systems. (P), 667.
- Mobile field radio. (See Radio.)
- Modulation, parasitic, effects of, on accuracy of measurement of the Q-factor of a resonator. F. H. JAMES, (P), 316.
- Modulator duty, energy losses in hydrogen-filled thyatron for. H. de B. KNIGHT and J. LORD, (P), 455.
- Moisture in paper, electrical determination of. T. S. MCLEOD and A. E. YALLUP, (P), 449.
- Monographs published individually. 136, 239, 348, 471, 575, 672.
- MONTEATH, G. D., MILLARD, G. H., and WHYTHE, D. J. Use of high-gain transmitting aerial in a populous area. (P), 65.
- MORRIS, P. A. C. Back-scatter sounding in operation of h.f. broadcast services. (D), 373.
- MORRISON, C. A., and KARAYIANIS, N. (See KARAYIANIS.)
- Multiplier, electrodynamic, using torque balance. J. G. HENDERSON, (P), 465.
- MURPHY, R. H., and NAMBIAR, K. P. P. Design basis for silicon-controlled rectifier parallel inverters. (P), 556.

## N

- NAGY, A. F., and NIEMANN, H. B. Switching on-off type filament emission regulator. (P), 665.
- NAMBIAR, K. P. P., and MURPHY, R. H. (See MURPHY.)
- Neon glow-discharge tubes. (See Glow-discharge.)
- NETHERCOT, W., and BALL, A. H. (See BALL.)
- NIEMANN, H. B., and NAGY, A. F. (See NAGY.)
- Noise generator for measurements in the frequency range 30–1250 Mc/s. I. A. HARRIS, (P), 651.
- Non-linearity in feedback control systems, describing-function expressions for. B. P. BHATTACHARYYA, (P), 529.
- Nuclear reactors, measurement of flux intensity in. W. R. LOOSEMOORE and J. A. DENNIS, (P), 413.
- Nyquist plotter, automatic electronic. H. J. FRASER and W. V. REECE, (P), 535.

## O

- Output prediction system to improve performance of on-off and saturating control systems. J. MILLS, (P), 667.
- Oversea radio-wave propagation. (See Radio-wave.)



VERTON, B. R., and FREEMAN, K. G. (See FREEMAN.)  
 OXENHAM, J. K., GRAHAM, R., and JUSTICE, J. W. H. (See GRAHAM.)

## P

AGE, H.  
 Aerials. (p), 473.  
 Back-scatter sounding in operation of h.f. broadcast services. (d), 373.  
 Suppression of corona- and precipitation-interference in v.h.f. reception. (p), 469.  
 Paper, electrical determination of moisture in. T. S. MCLEOD and A. E. YALLUP, (p), 449.  
 Papers published individually. 136, 239, 471.  
 Parasitic modulation. (See Modulation.)  
 PASK, G. Self-optimizing filter, predictor and simulator. (d), 437.  
 PAWLEY, E. L. E.  
 B.B.C. sound broadcasting 1939-60. (p), 279.  
 B.B.C. television 1939-60. (p), 375.  
 Phase control of rotors. (See Rotors.)  
 — variation of v.l.f. waves propagated over long distances. B. G. PRESSEY, G. E. ASHWELL and J. HARGREAVES, (p), 214.  
 PHILLIPS, G. J.  
 Back-scatter sounding in operation of h.f. broadcast services. (d), 373.  
 Banana-tube colour-television display system. (d), 631.  
 Photo-electric beam-index colour-television tube and system. R. GRAHAM, J. W. H. JUSTICE and J. K. OXENHAM, (p), 511; (d), 520.  
 PICKLES, D. A. Address as chairman of Mersey and North Wales Centre. 19.  
 PICKLES, J. R., EGELSTAFF, P. A., HAY, H. J., HOLT, G., and RAFFLE, J. F. (See EGELSTAFF.)  
 Platinum alloys. (See Alloys.)  
 Potter, automatic electronic. H. J. FRASER and W. V. P. REECE, (p), 535.  
 Power, equivalent available, in signal-generator calibration, concept of. D. WOODS, (p), 37.  
 Precision measurement of capacitance. (d), 337.  
 Prediction of aerial radiation patterns. (See Aerial.)  
 President's Address. Sir HAMISH D. MACLAREN, 1.  
 Pressed-oxide nickel-matrix cathode. (See Cathode.)  
 PRESSEY, B. G., ASHWELL, G. E., and HARGREAVES, J. Phase variation of very-low-frequency waves propagated over long distances. (p), 214.  
 PROGRESS REVIEWS  
 Aerials. H. PAGE, (p), 473.  
 B.B.C. sound broadcasting 1939-60. E. L. E. PAWLEY, (p), 279.  
 B.B.C. television 1939-60. E. L. E. PAWLEY, (p), 375.

## Q

Q-factor of a resonator, measurement of. F. H. JAMES, (p), 316.

## R

Radial vanes. (See Vanes.)  
 Radiation patterns, aerial. (See Aerial.)  
 Radioactive sample, weak, methods for ascertaining activity of. E. H. COOKE-YARBOROUGH and R. C. M. BARNES, (p), 153; (d), 164.  
 Radioactivity, terrestrial, aerial survey of. D. WILLIAMS and H. BISBY, (p), 403.  
 Radio astronomy, r.f. switching circuits and hybrid ring circuits used in. F. G. SMITH, (p), 201.  
 — frequency interference in multi-channel telephony f.m. radio systems. R. HAMER, (p), 75.  
 — interference from ignition systems. A. H. BALL and W. NETHERCOT, (p), 273.  
 — interference measuring sets: comparison of American, German and British equipment. A. H. BALL and W. NETHERCOT, (p), 273.  
 —, mobile field, probabilities of interference with, derived from a field-strength survey at 59 Mc/s. D. R. W. THOMAS, (p), 264.  
 — relay systems, microwave, standardization of. W. J. BRAY, (p), 180.  
 — telescope, high-resolution. W. N. CHRISTIANSEN, N. R. LABRUM, K. R. MCALISTER and D. S. MATHEWSON, (p), 48.

— wave propagation over sea within and beyond the radio horizon, factors influencing. F. A. KITCHEN, W. R. R. JOY and E. G. RICHARDS, (p), 257.  
 RAFFLE, J. F., PICKLES, J. R., EGELSTAFF, P. A., HAY, H. J., and HOLT, G. (See EGELSTAFF.)  
 Random pulse generator with variable mean rate. J. L. DOUCE and B. G. LEARY, (p), 524.  
 Ranging system, frequency-modulated continuous-wave. (d), 238.  
 RAO, R. A., and SINGH, A. (See SINGH.)  
 RAYNER, G. H., and FORD, L. H. Precision measurement of capacitance. (d), 338.  
 REECE, W. V. P., and FRASER, H. J. (See FRASER.)  
 REES, D. Gas-discharge tubes. (d), 508.  
 Refractometer, airborne microwave. J. A. LANE, D. S. FROOME and G. J. MCCONNELL, (p), 398.  
 Reradiation of electromagnetic horn. (See Horn.)  
 Resonator, measurement of Q-factor of. F. H. JAMES, (p), 316.  
 R. F. switching circuits. (See Switching.)  
 RICHARDS, E. G., KITCHEN, F. A., and JOY, W. R. R. (See KITCHEN.)  
 ROBERTS, J. D. Self-optimizing non-linear filter, predictor and simulator. (d), 438.  
 Rotors, phase control of, at high spinning speeds. P. A. EGELSTAFF, H. J. HAY, G. HOLT, J. F. RAFFLE and J. R. PICKLES, (p), 26.  
 ROWE, R. P. Gas-discharge tubes. (d), 508.  
 Royal Navy, electrical engineering in. Sir HAMISH D. MACLAREN, (p), 1.  
 RUDD, D. A. Index colour-television tube and system. (d), 522.  
 RUSSELL, J. L. Self-optimizing non-linear filter, predictor and simulator. (d), 438.  
 RUSSELL, K. A. Banana-tube colour-television display system. (d), 631.

## S

Sampled-data control systems, discrete analogue-computer compensation of. T. GLUCHAROFF, (p), 167; (d), 176.  
 SANDOR, A.  
 Emission from miniature hollow cathodes. (p), 90.  
 Pressed-oxide nickel-matrix cathode below apertured electrodes. (p), 97.  
 Scatter (tropospheric) observations at 3480 Mc/s with aerials of variable spacing. R. W. MEADOWS, (p), 349.  
 Scattering, ionospheric forward, using measurements of energy distribution in azimuth. W. C. BAIN, (p), 241.  
 SCHAGEN, P. Banana-tube display system. (p), 577; (d), 632.  
 SCHAGEN, P., and EASTWELL, B. A. (See EASTWELL.)  
 Self-optimizing non-linear control system. J. L. DOUCE and R. E. KING, (p), 441.  
 — non-linear filter. J. K. LUBBOCK, (p), 439.  
 SERBY, J. E. Electrics and electronics in aircraft. (d), 151.  
 SETTELEN, M. Electrics and electronics in aircraft. (d), 152.  
 SHARPE, J. Photo-electric beam-index colour-television tube and system. (d), 521.  
 SHEARMAN, E. D. R. Usefulness of back-scatter sounding in the operation of h.f. broadcast services. (p), 361; (d), 374.  
 SHEARME, J. N., and HOLMES, J. N. (See HOLMES.)  
 SHURMER, H. V. Crystal detectors to cover the frequency band 26-40 Gc/s. (p), 659.  
 Signal-generator calibration, concept of equivalent source e.m.f. and equivalent available power in. D. WOODS, (p), 37.  
 Silicon-controlled rectifier parallel inverters, design basis for. R. H. MURPHY and K. P. P. NAMBIAR, (p), 556.  
 — transistors. (See Transistors.)  
 SINGH, A., and RAO, R. A. Analysis of a cylindrical cavity with radial vanes. (p), 550.  
 SMITH, F. G. R.F. switching circuits and hybrid ring circuits used in radio astronomy. (p), 201.  
 SMITH, J. Gas-discharge tubes. (d), 508.  
 Sound broadcasting 1939-60. E. L. E. PAWLEY, (p), 279.  
 Spectroscopy, microwave. D. J. MILLEN, (p), 111.  
 Spinning speeds, high, phase control of rotors at. P. A. EGELSTAFF, H. J. HAY, G. HOLT, J. F. RAFFLE and J. R. PICKLES, (p), 26.  
 Standardization of international microwave radio-relay systems. W. J. BRAY, (p), 180.

- Standards, measuring instruments and. (*See* Instruments.)  
 Storage time of a transistor. (*See* Transistor.)  
 STEWART, J. Address as chairman of Scottish Electronics and Measurement Group. 343.  
 Switching circuits, r.f., and hybrid ring circuits used in radio astronomy. F. G. SMITH, (P), 201.  
 — on-off type filament emission regulator. A. F. NAGY and H. B. NIEMANN, (P), 665.

## T

- TAUB, D. M. Storage time of transistor with decaying turn-off current. (P), 344.  
 TAYLOR, DENIS. Activity of weak radioactive sample. (D), 165.  
 TAYLOR, W. K. Self-optimizing non-linear filter, predictor and simulator. (D), 437.  
 Telecommunication engineer. R. GOFORD, (A), 21.  
 Telecommunications: some modern developments. W. E. GILL, (A), 137.  
 Telephone service, growth of. F. JONES, (A), 140.  
 Telephony (multi-channel) f.m. radio systems, radio-frequency interference in. R. HAMER, (P), 75.  
 Television band compression by contour interpolation. D. GABOR and P. C. J. HILL, (P), 303; (D), 360, 634.  
 —, B.B.C., 1939-60. E. L. E. PAWLEY, (P), 375.  
 — (colour-) banana-tube display system. (*See* Banana-tube.)  
 — (colour-) tube and system. R. GRAHAM, J. W. H. JUSTICE and J. K. OXENHAM, (P), 511; (D), 520.  
 — (high-gain) transmitting aerial, use of, in a populous area. G. D. MONTEATH, G. H. MILLARD and D. J. WHYTE, (P), 65.  
 Terrestrial radioactivity. (*See* Radioactivity.)  
 TERRONI, T. B. D. Address as chairman of Electronics and Communications Section. 15.  
 Third-harmonic tuning. (*See* Tuning.)  
 THOMAS, D. R. W. Interference with mobile field radio derived from a field-strength survey at 59 Mc/s. (P), 264.  
 THOMPSON, G. V. E. Electrics and electronics in aircraft. (D), 151.  
 Thyatron, hydrogen-filled, measurement of energy losses in. H. de B. KNIGHT, (P), 455.  
 Time-delay networks, theory of. W. T. J. ATKINS, (P), 500.  
 TIZARD, R. H. Self-optimizing non-linear filter, predictor and simulator. (D), 436.  
 Torque balance, electrodynamic multiplier using. J. G. HENDERSON, (P), 465.  
 Transformer ratio-arm bridges, choosing of. W. H. P. LESLIE, (P), 539.  
 Transformers, audio-frequency current, design and performance of. J. J. HILL and A. P. MILLER, (P), 327; (D), 337.  
 —, e.h.t., third-harmonic tuning of. E. M. CHERRY, (P), 227.  
 —, standard current, calibration of, up to 20 kc/s. J. J. HILL, (P), 333.  
 Transistor with decaying turn-off current, storage time of. D. M. TAUB, (P), 344.  
 Transistors, silicon, advantages of, in circuit design. M. K. MCPHUN, (P), 570.  
 Transmission lines used as directional couplers. R. KOIKE, (P), 120.  
 Travelling-wave cavity, analysis of. N. KARAYIANIS and C. A. MORRISON, (P), 545.  
 Tropospheric scatter. (*See* Scatter.)  
 TROTTER, R. D. Activity of weak radioactive sample. (D), 165.  
 Tuning, third-harmonic, of e.h.t. transformers. E. M. CHERRY, (P), 227.  
 TUSTIN, A. Self-optimizing non-linear filter, predictor and simulator. (D), 438.

## V

- Vanes, radial, cylindrical cavity with. A. SINGH and R. A. RAO, (P), 550.  
 V.H.F. reception, suppression of corona- and precipitation-interference in. H. PAGE, (P), 469.  
 Vocoder control signals, correlator applied to analysis of. (D), 23.  
 Voltage measurement, high-precision, audio-frequency amplifier for. S. HARKNESS and F. J. WILKINS, (P), 319; (D), 337.

## W

- WALDRON, R. A. Waveguide modes. (P), 236.  
 WARD, G. M. Gas-discharge tubes. (D), 508.  
 Waveguide modes. R. A. WALDRON, (P), 236.  
 Waveguides, rectangular, design and performance of transverse-field bolometers in. J. A. LANE and D. M. EVANS, (P), 133.  
 Waves, v.l.f., propagated over long distances, phase variation of. B. G. PRESSEY, G. E. ASHWELL and J. HARGREAVES, (P), 214.  
 WESTCOTT, J. H. Discrete analogue-computer compensation of sampled-data control systems. (D), 176.  
 WESTON, G. F. Gas-discharge tubes. (D), 507.  
 WHITE, E. L. C. Photo-electric beam-index colour-television tube and system. (D), 521.  
 WHYTE, D. J., MONTEATH, G. D., and MILLARD, G. H. (*See* MONTEATH.)  
 WILBY, W. P. L., WOODCOCK, R., and GABOR, D. (*See* GABOR.)  
 WILKINS, F. J., and HARKNESS, S. (*See* HARKNESS.)  
 WILLIAMS, D., and BISBY, H. Aerial survey of terrestrial radioactivity. (P), 403.  
 WILLSHAW, W. E. Gas-discharge tubes. (D), 508.  
 WILSON, H. M. Electrics and electronics in aircraft. (D), 151.  
 WOODCOCK, R., GABOR, D., and WILBY, W. P. L. (*See* GABOR.)  
 WOODFORD, C. G. A. Electrics and electronics in aircraft. (D), 151.  
 WOODS, D.  
 Coaxial connector system for precision r.f. measuring instruments and standards. (P), 205.  
 Concept of equivalent source e.m.f. and equivalent available power in signal-generator calibration. (P), 37.  
 Precision instruments for coaxial line measurements up to 4 Gc/s. (P), 490; (D), 493.  
 Work function measurements on the platinum alloys of the alkaline earth metals. H. BATEY, (P), 468.

## X

- Xenon. (*See under* Argon.)

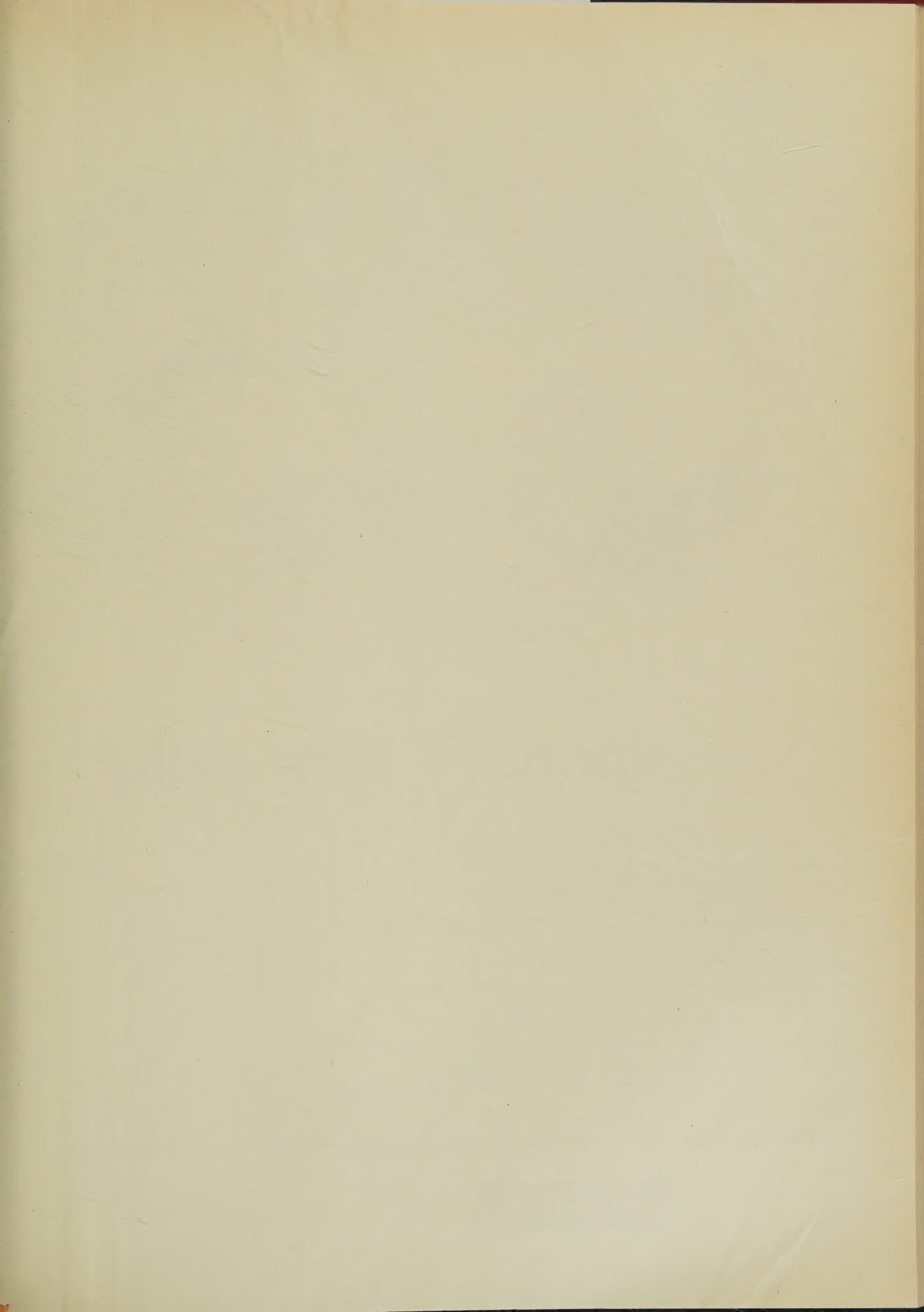
## Y

- YALLUP, A. E., and MCLEOD, T. S. (*See* MCLEOD.)

## Z

- ZEFFERT, H. Electrics and electronics in aircraft. (D), 151.











# plan with Plannair

Make Plannair a member of your own design team. Many manufacturers requiring temperature control by planned air movement are realising the need to consider this special problem at an early stage—and are calling in Plannair, the air movement specialists, to sit in on their first planning meetings.

The strength of Plannair lies in the ability of its design engineers to solve complex air movement problems and to design blowers which will provide the right amount of air in the right place for temperature control in specific projects. Size, weight and performance are the prime considerations and these are skilfully balanced in every designed-for-purpose Plannair Blower.

**Plannair Limited, Windfield House, Leatherhead, Surrey Tel : Leatherhead 4091**





# PROCEEDINGS OF THE INSTITUTION OF ELECTRICAL ENGINEERS

Part B. ELECTRONIC AND COMMUNICATION ENGINEERING (INCLUDING RADIO ENGINEERING), NOVEMBER 1961

## CONTENTS

The Banana-Tube Display System .....	P. SCHAGEN, Ph.D.	577
Development of the Banana Tube .....	B. A. EASTWELL, B.Sc., and P. SCHAGEN, Ph.D.	587
Mechanical and Manufacturing Aspects of the Banana-Tube Colour-Television Display System .....	H. HOWDEN	596
Circuits for the Banana-Tube Colour-Television Display System .....	K. G. FREEMAN, B.Sc.	604
Colorimetry of the Banana-Tube Colour-Television Display System .....	R. N. JACKSON	613
Appraisal of the Banana-Tube Colour-Television Display System .....	K. G. FREEMAN, B.Sc., and B. R. OVERTON, B.Sc.	624
Discussion on the above six Papers .....		630
Discussion on 'Television Band Compression by Contour Interpolation' .....		634
The Prediction of Aerial Radiation Patterns from Near-Field Measurements ...	JOHN BROWN, D.Sc.(Eng.), and E. V. JULL, B.Sc., Ph.D.	635
A Theory of Receiving Aerials applied to the Reradiation of an Electromagnetic Horn .....	D. MIDGLEY, B.Sc.(Eng.), Ph.D.	645
The Design of a Noise Generator for Measurements in the Frequency Range 30-1 250 Mc/s .....	I. A. HARRIS	651
Crystal Detectors to cover the Frequency Band 26-40 Gc/s .....	H. V. SHURMER, M.Sc., Ph.D.	659
Switching On-Off Type Filament Emission Regulator (Communication) .....	A. F. NAGY, M.E., M.Sc., and H. B. NIEMANN, B.E.	665
An Output Prediction System to improve the Performance of On-Off and Saturating Control Systems .....	J. MILLS, M.Eng.Sc.	667
The Place of Formal Study in the Post-Graduate Training of an Electrical Engineer (Summary).	N. N. HANCOCK, M.Sc.Tech., and P. L. TAYLOR, M.A.	671
Monographs published individually .....		672

*Papers for the Proceedings.*—An author who supplies an outline of a paper he proposes to submit for the *Proceedings* may apply to the Secretary for a free copy of The Institution's Handbook for Authors. This gives particulars of a number of requirements—including maximum acceptable length—compliance with which is essential. See page ad 38 in the advertisement section.

*Declaration on Fair Copying.*—Within the terms of the Royal Society's Declaration on Fair Copying, to which The Institution subscribes, material may be copied from issues of the *Proceedings* (prior to 1949, the *Journal*) which are out of print and from which reprints are not available. The terms of the Declaration and particulars of a Photocopying Service afforded by the Science Museum Library, London, are published in the *Journal* from time to time.

*Bibliographical References.*—It is requested that bibliographical reference to an Institution paper should always include the serial number of the paper and the month and year of publication, which will be found at the top right-hand corner of the first page of the paper. This information should precede the reference to the Volume and Part.

*Example.*—SMITH, J.: 'Reflections from the Ionosphere', *Proceedings I.E.E.*, Paper No. 5001 E, December, 1960 (102 B, p. 1234).

## THE BENEVOLENT FUND

During the last few years the amount received from subscriptions and donations has been insufficient to meet the cost of grants and management charges. The deficiency is met by making encroachments on capital funds. This may one day prove to be disastrous unless it is checked. Will you help to ensure that the income from subscriptions exceeds outgoings?

Subscriptions, preferably under Deed of Covenant, and Donations may be sent by post to

THE HONORARY SECRETARY

THE INCORPORATED BENEVOLENT FUND OF THE INSTITUTION OF  
ELECTRICAL ENGINEERS, SAVOY PLACE, W.C.2

or may be handed to one of the Local Honorary Treasurers of the Fund.

*Though your gift may be small, please do not hesitate to send it.*



### LOCAL HON. TREASURERS OF THE FUND:

EAST MIDLAND CENTRE .....	L. Adlington	NORTHERN IRELAND CENTRE .....	G. H. Moir, J.P.
IRISH BRANCH .....	A. Harkin, M.E.	SCOTTISH CENTRE .....	R. H. Dean, B.Sc.Tech.
MERSEY AND NORTH WALES CENTRE .....	D. A. Picken	SOUTH MIDLAND CENTRE .....	H. M. Fricke
TEES-SIDE SUB-CENTRE .....	W. K. Harrison	RUGBY SUB-CENTRE .....	P. G. Ross, B.Sc.
NORTH-EASTERN CENTRE .....	R. G. Scotson	SOUTHERN CENTRE .....	J. E. Brunnen
NORTH MIDLAND CENTRE .....	E. C. Walton, Ph.D., B.Eng.	WESTERN CENTRE (BRISTOL) .....	A. H. McQueen
SHEFFIELD SUB-CENTRE .....	F. Seddon	WESTERN CENTRE (CARDIFF) .....	E. W. S. Watt
NORTH-WESTERN CENTRE .....	E. G. Taylor, B.Sc.(Eng.)	WEST WALES (SWANSEA) SUB-CENTRE .....	O. J. Mayo
NORTH LANCASHIRE SUB-CENTRE .....	H. Charnley	SOUTH WESTERN SUB-CENTRE .....	W. E. Johnson

Members are asked to bring to the notice of the Court of Governors any deserving cases of which they may have knowledge.